DETERMINATION OF THE PHYSICAL PROPERTIES OF SEVERAL MULTIPHASE LUBRICANTS AND THEIR THEORETICAL PERFORMANCE IN HYDRODYNAMICALLY LUBRICATED BEARINGS

A THESIS

Presented to

The Faculty of the Graduate Division

by

Henry Grady Rylander

In Partial Fulfillment

of the Requirements for the Degree

Doctor of Philosophy in the

School of Mechanical Engineering

Georgia Institute of Technology

August, 1964

DETERMINATION OF THE PHYSICAL PROPERTIES OF SEVERAL MULTIPHASE LUBRICANTS AND THEIR THEORETICAL PERFORMANCE IN HYDRODYNAMICALLY LUBRICATED BEARINGS

Approved:

Chairman

Date approved by Chairman: 9/1/64

DETERMINATION OF THE PHYSICAL PROPERTIES OF SEVERAL MULTIPHASE LUBRICANTS AND THEIR THEORETICAL PERFORMANCE IN HYDRODYNAMICALLY LUBRICATED BEARINGS

A THESIS

Presented to

The Faculty of the Graduate Division

by

Henry Grady Rylander

In Partial Fulfillment

of the Requirements for the Degree

Doctor of Philosophy in the

School of Mechanical Engineering

Georgia Institute of Technology

August, 1964

ACKNOWLEDGMENTS

The author wishes to acknowledge the financial assistance afforded him by the National Science Foundation, the Ford Foundation and TRACOR, Incorporated, and to express his gratitude to these groups for providing assistance. The advice and counsel of Professor Venton L. Doughtie which has led the author to continue research and study has been a great help and is greatly appreciated.

Deep appreciation is extended to Dr. J. P. Vidosic for his able direction and supervision of the author's graduate study and research. The author is also grateful to Dr. J. P. Vidosic and the members of the committee, Dr. C. W. Gorton and Dr. C. E. Stoneking for their guidance and motivation throughout the author's study of Mechanical Engineering at the Georgia Institute of Technology.

The assistance, suggestions and facilities provided by Dr. K. G. Picha and the staff of the School of Mechanical Engineering are deeply appreciated.

July 4, 1964 H. Grady Rylander

TABLE OF CONTENTS

LIST OF TABLES

LIST OF ILLUSTRATIONS

NOMENCLATURE

A	Area, $in.^2$
A_t	Viscosity coefficient, $\frac{lb\text{-}sec}{in.^2}$
B	Elemental body force, lb
B'	Length of bearing grid in x-direction, in.
B_t	Viscosity coefficient, $\frac{lb\text{-}sec}{in.^2}$
C	A constant, variable dimensions
c	Bearing radial clearance, in.
C_v	Specific heat at constant volume, $\frac{in.\text{-}lb}{lb\text{-}degR}$
$\frac{D}{Dt}$	Total derivative with respect to time
d	Diameter, in.
E	Modulus of elasticity in tension and compression, psi
e	Base of natural logarithms
e'	Journal eccentricity, in.
F	Friction force, lb
f	Coefficient of friction, dimensionless
G	Modulus of elasticity in shear, psi
g	Acceleration of gravity, $\frac{in.}{sec^2}$
h	Film thickness, in.
h_p	Particle size, in.
K	Heat conductivity coefficient, $\frac{in.\text{-}lb\text{-}in.}{in.\text{-}degR\text{-}sec}$

K_m	Bulk modulus, psi
k	Location of variable in the x-direction, in.
L	Number of grid stations in the x-direction, dimensionless
L'	Width of bearing grid, center line of bearing to outer edge, in.
ℓ	Bearing width, in.
M	Mixture ratio by weight, dimensionless
m	Location of variable in the y-direction, in.
N	Particle concentration number, dimensionless
N'	Angular velocity of journal, rps
n	Exponent for polytropic gas law, dimensionless
n'	Direction perpendicular to surface, dimensionless
P	Elemental surface force, lb
p	Fluid pressure, psi
p'	Bearing pressure on projected area, psi
$\overline{p}$	Arithmetic mean pressure, psi
Q	Heat, in.-lbs
Q_c	Conduction Heat, in.-lb
Q_f	Friction heat, in.-lb
Q'	Fluid weight-flow-rate, $\frac{lb}{sec}$
q	Heat flux, $\frac{in.-lb}{lb\text{-}deg\ R}$
R	Gas constant, $\frac{in.-lb}{lb\text{-}deg\ R}$
R_o	Flow ratio, $\frac{lb\ of\ lubricant}{lb\ of\ air}$, dimensionless
r	Journal radius, in.

$\vec{S}$	Displacement vector, in.
S_o	Sommerfeld number $= \frac{\mu N'}{p'} \left(\frac{r}{c}\right)^2$, dimensionless
T	Temperature, deg. R
T'	Temperature, deg. F
T_q	Torque, in.-lb
t	Time, sec
U	Surface velocity, $\frac{in.}{sec}$
u	Velocity in x-direction, $\frac{in.}{sec}$
V	Volume or Elemental volume, in.^{3}
v	Velocity component in y-direction, $\frac{in.}{sec}$
W	Work, $\frac{in.-lb}{sec}$
W_f	Weight, lb
W_t	Total work, $\frac{in.-lb}{sec}$
W'	Load capacity, lb
$\vec{w}$	Velocity vector, $\frac{in.}{sec}$
w	Velocity component in the z-direction, $\frac{in.}{sec}$
X	Body force in x-direction, lb
x	Dimension in the x-direction, in.
Y	Body force in the y-direction, lb
y	Dimension in the y-direction, in.
Z	Body force in the z-direction, lb
z	Dimension in the z-direction, in.
α	A constant, or defined where used in text
β	A constant, or defined where used in text
γ	A constant, or defined where used in text

ζ	Elongation in the z-direction, in.
η	Elongation in the y-direction, in.
μ	Absolute viscosity, reyns $(\frac{\text{lb-sec}}{\text{in.}^2})$
ξ	Elongation in the x-direction, in.
π	3.14159..., dimensionless
ρ	Mass density $\frac{\text{lb-sec}^2}{\text{in.}^4}$
σ	Normal stress, psi
$\overline{\sigma}$	Arithmetic mean of normal stress, psi
τ	Shear stress, psi
τ_p	Shear stress of particle, psi
φ	A constant, or defined where used in text

SUMMARY

This investigation was undertaken for the purpose of extending the design methods for hydrodynamic bearings using multiphase lubricants. These multiphase lubricants were obtained from mixtures of solid, liquid, and gas constituents.

Hydrodynamic design theories were developed for compressible and incompressible lubricant mixtures. Solutions of the non-linear, coupled, partial differential equations for the temperature and pressure distribution in these bearings were obtained by the use of numercial analysis and a large digital computer. These solutions not only provided a means for design with hydrodynamic multiphase lubricants but also provided a means for extended study of single phase lubricants with variable boundary conditions.

Three separate experimental programs were conducted to obtain the physical properties of several multiphase lubricant mixtures and to obtain some verification of the design theories in an actual bearing. The compressibility of gas-lqiuid and gas-solid mixtures was obtained in a piston compressor. Measurements of density, viscosity, and phase equilibrium conditions were obtained as functions of the mixture ratio, temperature, and pressure in a constant volume test cylinder. Actual bearing tests were made in a universal bearing test machine with liquid and liquid-solid mixtures.

The scope of the compressibility tests was quite limited in that the only results sought were values of the exponent n as used in the equation of state

$$pV^n = \text{constant.}$$

With air-oil mixtures the value of n varied from 1.34 for air to 1.62 for a ratio of 14 pounds of oil to one pound of air. Tests with air-molybdenum disulfide and air-Teflon mixtures produced a value of $n = 1.34$ for all weight ratios of solid to air up to 0.016.

Liquid-gas mixtures of the "incompressible" type were produced by forcing gas into the liquid under pressure. The gas was absorbed by the liquid with large changes in the viscosity of the liquid and only negligible changes in the density of the liquid. A paraffinic oil was used with carbon dioxide, ethane, methane, hydrogen and helium at pressures to 1000 psig and temperatures to 250F. Polyphenyl ether was tested with carbon dioxide. Accurate measurements of the viscosity, density, and weight of gas absorbed were made for a wide range of equilibrium temperatures and pressures. Liquid-gas stability tests were made with carbon dioxide gas.

Tests in an actual bearing were compared with the theoretical solutions for clean oil and liquid-solid lubricants. A close agreement was obtained between the theoretical solutions and experimental values for friction and load capacity.

Experimental values of the solid particle shear strength were determined in the test bearings. The particle shear strength was found to be a function of the shaft speed.

Design methods for the use of multiphase lubricants were outlined using the results of experimentally determined physical data combined with theoretical solutions for the friction torque, temperature distribution, load capacity, bearing eccentricity, and lubricant flow rates.

CHAPTER I

INTRODUCTION

The study of hydrodynamic lubrication has continued to grow in scope and interest since the classical experiment of Beauchamp Tower*(24) in 1883 and the formulation of the differential equation for pressure distribution by Osborne Reynolds (17) in 1886. Mathematical theory, at present, consists of various solutions based upon some form of the Navier-Stokes equations. Each of these solutions is a function of temperature and pressure. In order to avoid the very difficult problem of solutions with variable viscosity, nearly all are based upon an assumption of constant viscosity.

A very significant advance in the analysis of bearing lubrication characteristics was made by Christropherson (4) when he applied the relaxation techniques of Southwell (23), to solve an energy equation for the temperature distribution in a journal bearing. With the temperature and pressure known, Christropherson corrected the viscosity for the effects of both temperature and pressure at each station in his relaxation grid. From these hand-relaxed calculations

*Numbers within parenthesis designate references, p. 216.

for load capacity and friction force, he found that the results were almost identical to those obtained by using an average viscosity for calculations. This close agreement is certain to have come from the consideration of lightly-loaded, low-speed bearings where the pressures are low and the temperature rise is small.

Although Christropherson set the stage for future solution of many difficult partial differential equations, his methods were never widely used for analysis or design because of the tedious calculations involved in the hand-relaxation solutions. Perhaps this was fortunate as Cope (5) and others discovered that Christropherson neglected the flow work in his energy equations.

The development of high speed digital computers has greatly enhanced the relaxation technique for the solution of lubrication problems. One of the best publications of computer solutions is by Boyd (2). In this volume of journal-bearing characteristics, the computer solutions were made for constant viscosity. However, he did include one article on temperature distribution for an infinite bearing (16).

Recently, there has been an increased interest in the use of compressible lubricants such as air because of low friction at high speed, abundant and inexpensive supply, constant composition at elevated temperature, and ability to operate with small clearance. Gross (6) and Michael (8) solved the Reynolds' equation for compressible fluid lubrication of slider bearings with the aid of relaxation techniques and a digital computer. Again, they assumed constant viscosity since the viscosity variation in a gas is small for the normal range of bearing temperature rise.

The use of multiphase lubricants such as grease, air-oil mist, graphite-oil and molybdenum disulfide-oil has pushed design beyond the presently available theory. At present, only a small amount of work has been done toward theoretical bearing design with such lubricants. A small amount of work has been published on grease treated as a Bingham plastic. Milne (9), (11), and Osterle (12), (13), have been the principal investigators for most of this work. No provision has been made to correct the shear stress for the solid phase or to correct for temperature variations in any direction.

Bearing designs have always been pushed to the limit with small margins of safety. Present design needs are no exception with demands for higher loads, higher speeds, higher and lower temperatures, and lower friction. Both theoretical and practical studies show a need for lubricants with viscosities between those for liquids and gases since the liquid viscosities are approximately one thousand times the viscosity of gases. The use of solid-liquid-gas lubricant mixtures satisfies, in part, the challenge to the designer with special needs beyond the capabilities of the individual solid, liquid, or gas constituents.

Two-phase lubrication systems are now common, and three-phase systems will be used in the future; however, present bearing designs are being limited by the lack of information regarding the physical properties of multiphase lubricants and a corresponding lack of hydrodynamic theory to back up these designs. This research is directed toward filling the need for basic design information pertaining to the physical properties of multiphase lubricants and to the establishment of design theories suitable for design or analysis of bearings operating with these lubricants.

Statement of the Problem

Useful design methods normally encompass theoretical design, experimental verification and extension of theory, and experimental determination of the physical properties of all materials. The basic problem of this research is to establish useful design methods for sleeve type bearings operating with multiphase lubricants. In order to isolate the important design parameters, this problem is approached by separating the problem into the following parts:

(1) Starting with basic physical relations, derive theoretical expressions for the temperature, pressure, load, friction torque, film thickness, and lubricant flows in a journal bearing using compressible multiphase lubricant mixtures. It should be noted that some of these mixtures are non-Newtonian.

(2) Determine the density of several of these mixtures and try to establish an empirical relation to relate the density of the mixture to the density of its constituents and some function of temperature and pressure.

(3) Determine the compressibility characteristics of several multiphase lubricants and again try to relate the compressibility to the properties of each constituent and some function of temperature and pressure.

(4) Determine the viscosity of the liquid phase with absorbed gas. Establish a relationship between percent gas absorbed, viscosity, temperature, and pressure.

(5) Determine the shear characteristics of certain solid lubricants.

(6) Determine the time stability for the gas-liquid mixtures.

(7) Test the theories of part (1) above along with the physical properties of the lubricants in an actual bearing. Compare the results of theory and experiment.

(8) Derive design relations for sleeve bearings using multiphase lubricants.

CHAPTER II

THEORY OF MULTIPHASE LUBRICANTS

Formulation of Equations for Elemental Velocity and Frictional Stress

In order to determine the velocity and frictional stress in the lubricant film, it is desirable to consider an element of fluid between two plates as shown in Fig. 1.

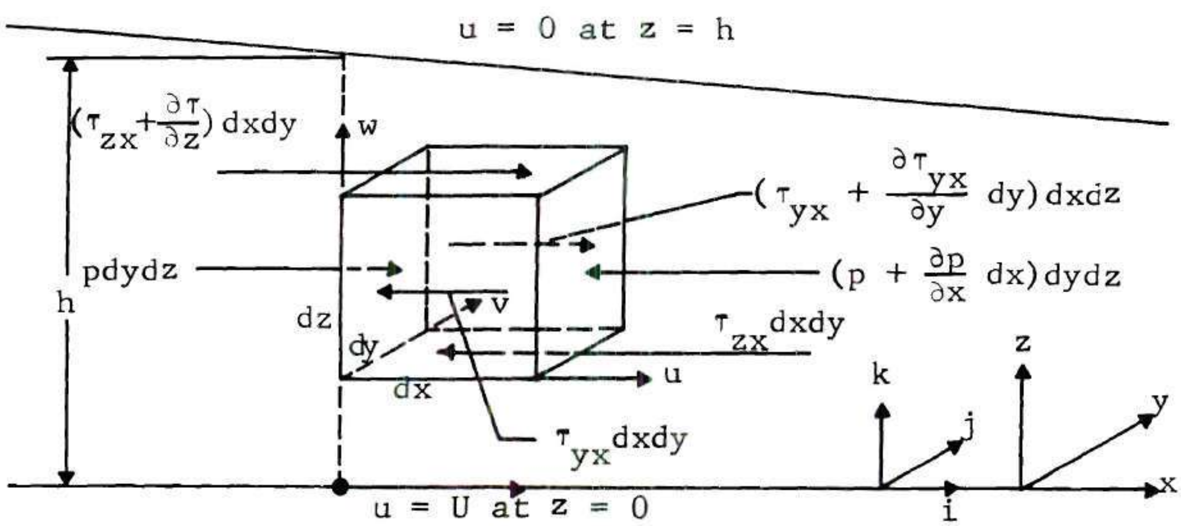

Figure 1. X-Direction Forces on a Fluid Element

All of the forces considered in the x-direction are shown on the fluid element. A similar set of forces would also occur in the y-direction and in the z-direction. These are not shown on this element for clarity.

The assumptions involved in reducing the forces in the x-direction to those shown on the fluid element of Fig.

1 are:

(1) No external body forces such as gravity act on the film.

(2) Inertia forces of all types are neglected. These include forces from acceleration in a curved flow passage and from solid particles in the fluid.

Additional assumptions used in the derivation of basic differential equations are:

(1) The pressure is constant in the z-direction. Since this dimension is very much smaller than the x and y-dimensions, the pressure would be essentially constant even with large pressure gradients.

(2) Boundary conditions are to be such that no slip occurs between the moving or fixed surfaces in contact with the liquid. Slip will occur between the solids and the bearing surfaces.

(3) Curvature of the fluid film may be neglected since the thickness of the film is very much less than the radius of curvature.

(4) Velocities in the x and y-directions are assumed to be very much larger than the velocity in the z-direction. Thus the only velocity gradients of importance are $\partial u/\partial z$ and $\partial v/\partial z$. All other velocity gradients are assumed to be negligible.

These assumptions are the ones normally made in the derivation of the basic differential equations for the theory of hydrodynamic lubrication (15). They do not conflict with the theory of compressible or non-Newtonian fluids; therefore, they should be satisfactory for multiphase lubricants. Summing the x-direction forces and equating to zero yields the following equation:

$$-\left(p + \frac{\partial p}{\partial x}\, dx\right) dydz + pdydz - \tau_{zx} dxdy + \left[\tau_{zx} + \frac{\partial \tau}{\partial z}\, dz\right] dxdy - \tau_{yx} dxdz + \left[\tau_{yx} + \frac{\partial \tau_{yx}}{\partial y}\, dy\right] dxdz = 0 \quad . \tag{2.1}$$

Adding identical terms of opposite sign and dividing by dxdydz, equation (2.1) becomes:

$$-\frac{\partial p}{\partial x} + \frac{\partial \tau_{zx}}{\partial z} + \frac{\partial \tau_{yx}}{\partial y} = 0 \quad . \tag{2.2}$$

Thus it is possible to relate the pressure gradient to two shear gradients. At this point it is necessary to consider a deviation from the classical derivations of fluid mechanics (20) in order to consider the physical properties of multiphase lubricants.

Certain physical phenomena occur which make it possible to obtain a realistic empirical expression for the shear stress. From experimental investigations, these multiphase lubricants fall into three basic classes:

(1) Newtonian Incompressible

This class of lubricants has shear stresses proportional to the rate of shear,

$$\text{thus:} \quad \tau_{zx} = \mu(T,p) \frac{\partial u}{\partial z} . \tag{2.3}$$

(2) Newtonian Compressible

This class of lubricants also (can be a mixture) has shear stresses proportional to the rate of shear but viscosity is a function of mixture, temperature, and pressure,

$$\text{thus:} \quad \tau_{zx} = \mu(M,T,p) \frac{\partial u}{\partial z} . \tag{2.4}$$

(3) Non-Newtonian

The type considered herein will be a type encountered with gas-solid and liquid-solid lubricant mixtures. Experimental investigations (7) have shown that particles smaller than the minimum film thickness will simply pass through the bearing with only slight increases in the effective viscosity of the liquid or gas phase of the lubricant (19). However, when the minimum film thickness is less than the size of the solid particles, there may be large changes in the shearing forces. For this condition the shear stress is taken as one of the following, depending upon the zone of operation:

$$\tau_{zx} = \mu(M,T,p) \frac{\partial u}{\partial z} \text{ where } h_{min} > h_p \tag{2.5}$$

or

$$\tau_{zx} = \mu(M,T,p)\ \frac{\partial u}{\partial z} \pm N\tau_p \text{ where } h_p > h_{min} \tag{2.6}$$

and N = Concentration Number

τ_p = Shear Stress of Particles.

The classification of lubricants as suggested above would also cover the rheodynamic bearings using grease considered as a Bingham plastic provided equation (2.6) is used with a test to determine whether $N\tau_p$ occurs at $\frac{\partial u}{\partial z}$ equal to zero or not. Milne (10), Osterle (12), Saibel (13), and Silbar (22) have published experimental and theoretical work on bearings using a Bingham plastic lubricant. The characteristic shear stress curves for the three classes of lubricants are given in Fig. 3.

One may observe from Fig. 3 that Class 1 and Class 2 lubricants are the same as Class 3 lubricants provided the point where $h_p = h_{min}$ is beyond the range of $\frac{\partial u}{\partial z}$. From this it is concluded that only Class 3 lubricants need be considered in the derivations.

From the theory of elasticity the general form of Hooke's law for an elastic solid body is given in matrix form by the following equation (20):

$$\begin{pmatrix} \sigma_x & \tau_{xy} & \tau_{xz} \\ \tau_{xy} & \sigma_y & \tau_{yz} \\ \tau_{xz} & \tau_{yz} & \sigma_z \end{pmatrix} = \begin{pmatrix} \overline{\sigma} & 0 & 0 \\ 0 & \overline{\sigma} & 0 \\ 0 & 0 & \overline{\sigma} \end{pmatrix} +$$

$$G \begin{pmatrix} \frac{\partial \xi}{\partial x} & \frac{\partial \xi}{\partial y} & \frac{\partial \xi}{\partial z} \\ \frac{\partial \eta}{\partial x} & \frac{\partial \eta}{\partial y} & \frac{\partial \eta}{\partial z} \\ \frac{\partial \zeta}{\partial x} & \frac{\partial \zeta}{\partial y} & \frac{\partial \zeta}{\partial z} \end{pmatrix} + G \begin{pmatrix} \frac{\partial \xi}{\partial x} & \frac{\partial \eta}{\partial x} & \frac{\partial \zeta}{\partial x} \\ \frac{\partial \xi}{\partial y} & \frac{\partial \eta}{\partial y} & \frac{\partial \zeta}{\partial y} \\ \frac{\partial \xi}{\partial z} & \frac{\partial \eta}{\partial z} & \frac{\partial \zeta}{\partial z} \end{pmatrix}$$

$$- \frac{2}{3}G \begin{pmatrix} \mathrm{div}\,\vec{S} & 0 & 0 \\ 0 & \mathrm{div}\,\vec{S} & 0 \\ 0 & 0 & \mathrm{div}\,\vec{S} \end{pmatrix} \tag{2.7}$$

where:

$$\vec{S} = \xi\vec{i} + \eta\vec{j} + \zeta\vec{k}$$

and

$$\mathrm{div}\,\vec{S} = \frac{\partial \xi}{\partial x}\,\vec{i} + \frac{\partial \eta}{\partial y}\,\vec{j}\,\frac{\partial \zeta}{\partial z}\,\vec{k}$$

$$\overline{\sigma} = \frac{1}{3}\left(\sigma_x + \sigma_y + \sigma_z\right) = -p \quad . \tag{2.8}$$

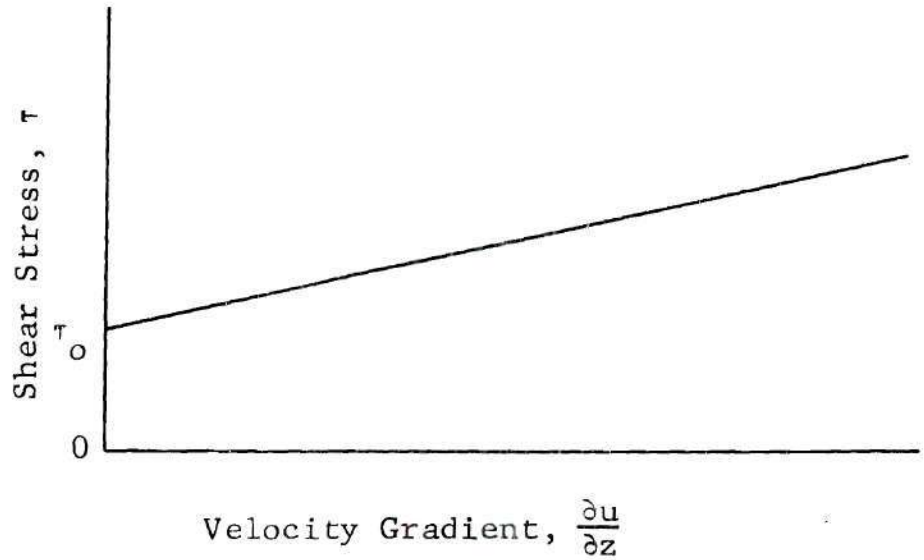

Figure 2. Characteristic Shear Stress Curve for a Bingham Plastic

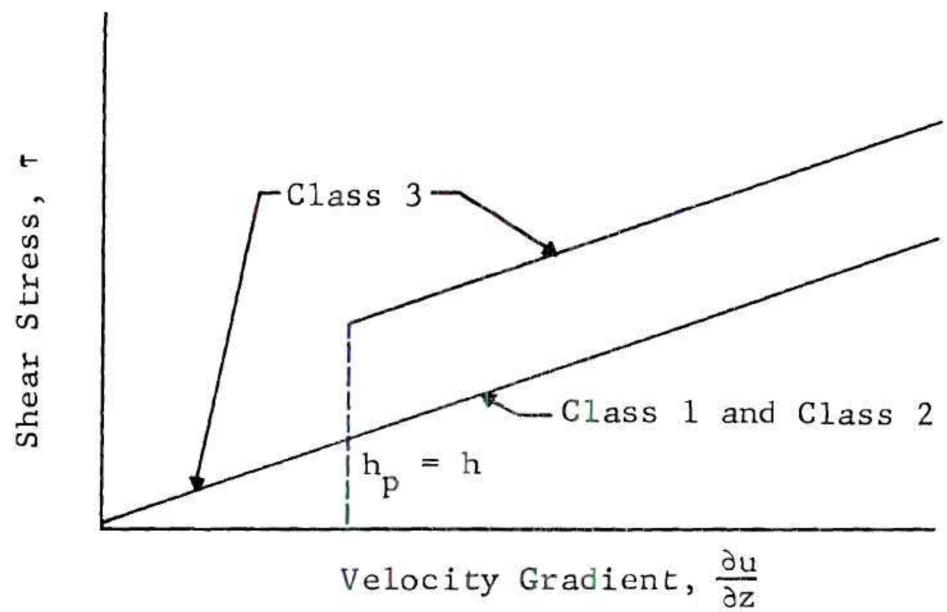

Figure 3. Characteristic Shear Stress Curve for Class 1, Class 2, and Class 3 Multiphase Lubricants.

Thus the fluid pressure is equal to the arithmetical mean of the three normal stresses. This fluid pressure is an invariant of the stress tensor.

Matrix (2.7) may be written in the form of the following equations:

$$\sigma_x = \bar{\sigma} + 2G \frac{\partial \xi}{\partial x} - \frac{2}{3} G \operatorname{div} \vec{S} \tag{2.9a}$$

$$\sigma_y = \bar{\sigma} + 2G \frac{\partial \eta}{\partial y} - \frac{2}{3} G \operatorname{div} \vec{S} \tag{2.9b}$$

$$\sigma_z = \bar{\sigma} + 2G \frac{\partial \zeta}{\partial z} - \frac{2}{3} G \operatorname{div} \vec{S} \tag{2.9c}$$

$$\tau_{xy} = G\left(\frac{\partial \eta}{\partial x} + \frac{\partial \xi}{\partial y}\right) \tag{2.10a}$$

$$\tau_{yz} = G\left(\frac{\partial \zeta}{\partial y} + \frac{\partial \eta}{\partial z}\right) \tag{2.10b}$$

$$\tau_{zx} = G\left(\frac{\partial \xi}{\partial z} + \frac{\partial \zeta}{\partial x}\right) \quad . \tag{2.10c}$$

Stokes' Law of Friction

The surface forces acting on an element of a solid depend upon the magnitude of the strain, while the surface forces acting on a liquid or gas depend upon the time rate of strain. Therefore, Hooke's law may be changed to Stokes' law by making the stresses proportional to the time rate of strain. This may be accomplished by replacing the shear modulus G(lb/in.^{2}) with the viscosity μ(lb-sec/in.^{2}), replacing the mean normal stress $\bar{\sigma}$ with the fluid pressure -p,

Page missing from thesis

Using a 2.168 inch diameter shaft operating at 3500 rpm with an oil having an average viscosity of 3.0×10^{-6} Reyns in a 1.0 inch long bearing, the torque, T_q, equals 8.83 inch-pounds with a shear stress of only 1.20 psi when the radial bearing clearance is 0.001 inch. This shear stress is much less than the shear strength of a soft solid material such as molybdenum disulfide which has a shear strength of approximately 100 psi, as used in a bearing. From this it is seen that the solid lubricant particles are not broken down until they reach an interference state where the film thickness is less than the particle size ($h<h_p$). Fig. 4 shows the steps particles must go through in order to pass through a bearing.

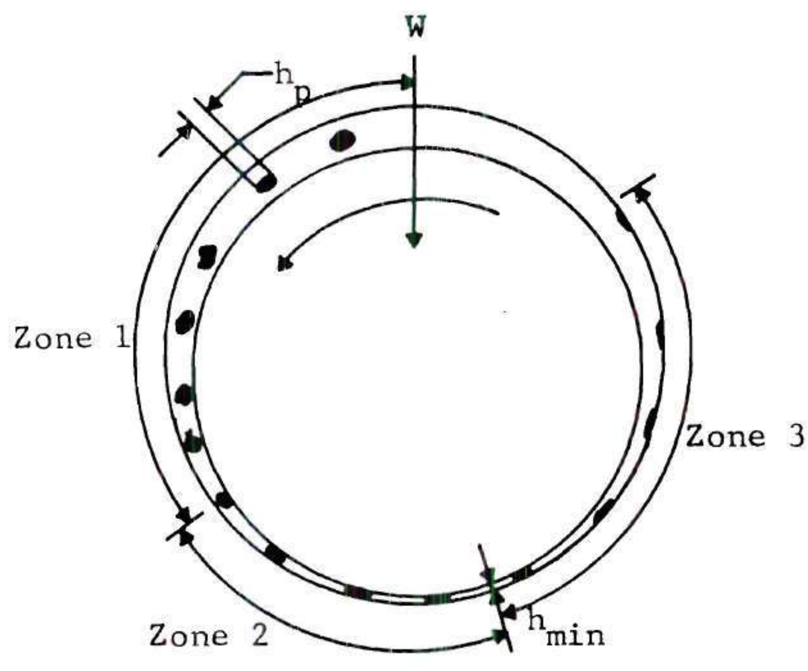

Figure 4. Illustration of Solid Particles Passing Through a Bearing

A solid lubricant will be subjected to the following processes when passing through the three bearing zones:

(1) Zone 1 ($h>h_p$) - In this zone the particles flow with the fluid, producing only small changes in the bearing friction and load capacity. A Newtonian fluid will remain Newtonian with only slight increases in effective viscosity.

(2) Zone 2 ($h_p>h$) - In this zone the solid particle is in intimate contact with both bearing surfaces and will almost instantaneously be stressed beyond the yield stress of the material. For small particle concentrations (less than 5% by weight), the shear stress may be accurately predicted by equation 2.6 when the particles are suspended in a liquid carrier.

(3) Zone 3 (particles past minimum clearance point) - In this zone the particles and fluid both lose contact when the absolute pressure falls to zero. The short zone of positive pressure will be characterized by Newtonian flow.

Applying Stoke's law to equations (2.9) and (2.10) assumes Newtonian flow, and these equations become:

$$\sigma_x = -p + 2\mu \frac{\partial u}{\partial x} - \frac{2}{3} \mu \operatorname{div} \vec{W} \tag{2.13a}$$

$$\sigma_y = -p + 2\mu \frac{\partial v}{\partial y} - \frac{2}{3} \mu \operatorname{div} \vec{W} \tag{2.13b}$$

$$\sigma_z = -p + 2\mu \frac{\partial w}{\partial z} - \frac{2}{3} \mu \operatorname{div} \vec{W} \tag{2.13c}$$

$$\tau_{xy} = \mu\left(\frac{\partial v}{\partial x} + \frac{\partial u}{\partial y}\right) \tag{2.14a}$$

$$\tau_{yz} = \mu \left(\frac{\partial w}{\partial y} + \frac{\partial v}{\partial z}\right) \tag{2.14b}$$

$$\tau_{zx} = \mu \left(\frac{\partial u}{\partial z} + \frac{\partial w}{\partial x}\right) \qquad (2.14c)$$

where:

$$\vec{W} = u\vec{i} + v\vec{j} + w\vec{k} \quad . \qquad (2.15)$$

Equations (2.13) are good for all zones of operation since they do not directly contain the shear stress, but equations (2.14) are effected by operation in zone 2.

If the pressure is subtracted from the normal stresses, the frictional components of the normal stresses σ' are

$$\sigma_x' = \sigma_x - (-p) \qquad (2.16a)$$

$$\sigma_y' = \sigma_y - (-p) \qquad (2.16b)$$

$$\sigma_z' = \sigma_z - (-p) \, . \qquad (2.16c)$$

In terms of the frictional stresses of equations (2.16), equations (2.13) become

$$\sigma_x' = \mu \left[2 \frac{\partial u}{\partial x} - \frac{2}{3} \operatorname{div} \vec{W}\right] \qquad (2.17a)$$

$$\sigma_y' = \mu \left[2 \frac{\partial v}{\partial y} - \frac{2}{3} \operatorname{div} \vec{W}\right] \qquad (2.17b)$$

$$\sigma_z' = \mu \left[2 \frac{\partial w}{\partial z} - \frac{2}{3} \operatorname{div} \vec{W}\right] \, . \qquad (2.17c)$$

In terms of equations (2.10), equations (2.14) for operations in zone 2 become

$$\tau_{xy} = \mu \left(\frac{\partial v}{\partial x} + \frac{\partial u}{\partial y}\right) \tag{2.18a}$$

$$\tau_{yz} = \mu \left(\frac{\partial w}{\partial y} + \frac{\partial v}{\partial z}\right) \tag{2.18b}$$

$$\tau_{zx} = \mu \left(\frac{\partial u}{\partial z} + \frac{\partial w}{\partial x}\right) \pm N\tau_p \ . \tag{2.18c}$$

Equations (2.18a) and (2.18b) do not contain the particle shear term since there is no shear motion of the surfaces in these directions.

If $\frac{\partial w}{\partial x}$, $\frac{\partial u}{\partial y}$, and $\frac{\partial v}{\partial x}$ are assumed negligible compared with $\frac{\partial u}{\partial z}$, the resulting stress on the element is

$$\tau_{zx} = \mu \frac{\partial u}{\partial z} \pm N\tau_p \tag{2.19}$$

$$\tau_{yx} = 0 \ . \tag{2.20}$$

Differentiation of equation (2.19) with respect to z gives

$$\frac{\partial \tau_{zx}}{\partial z} = \mu \frac{\partial^2 u}{\partial z^2} \ . \tag{2.21a}$$

Differentiation of equation (2.20) with respect to y gives

$$\frac{\partial \tau_{yx}}{\partial y} = 0 \ . \tag{2.21b}$$

Substitution of equations (2.21) into (2.2) gives

$$\frac{\partial^2 u}{\partial z^2} = \frac{1}{\mu} \frac{\partial p}{\partial x} \, . \tag{2.22}$$

Integrating equation (2.22) twice with respect to z yields

$$\frac{\partial u}{\partial z} = \frac{1}{\mu} \frac{\partial p}{\partial x} z + C_1 \tag{2.23}$$

$$u = \frac{1}{\mu} \frac{\partial p}{\partial x} \frac{z^2}{2} + C_1 z + C_2 \, . \tag{2.24}$$

Using the boundary conditions shown in Fig. 1,

$$u = U \text{ for } z = 0 \tag{2.25a}$$

and

$$u = 0 \text{ for } z = h, \tag{2.25b}$$

the constants of integration of equation (2.24) may be evaluated. Using the constants, the x-component of the velocity becomes

$$u = \frac{1}{2\mu} \frac{\partial p}{\partial x} z(z-h) + \frac{h-z}{h} U. \tag{2.26}$$

A similar analysis yields the y-component of velocity.

$$v = \frac{1}{2\mu} \frac{\partial p}{\partial y} (z-h)z \tag{2.27}$$

Equations (2.26) and (2.27) are identical to those obtained from using a Newtonian fluid. This results from using boundary conditions (2.25) which are not applicable for Coulomb type friction. Errors from this assumption are small due to the use of low particle concentrations and the fact that the particles do have velocities approximately equal to the average fluid velocity.

Differentiating equations (2.26) and (2.27) gives the velocity gradients

$$\frac{\partial u}{\partial z} = \frac{1}{2\mu}\frac{\partial p}{\partial x}(2z-h) - \frac{U}{h} , \tag{2.28}$$

$$\frac{\partial v}{\partial z} = \frac{1}{2\mu}\frac{\partial p}{\partial y}(2z-h) , \tag{2.29}$$

across the lubricant fluid.

Substitution of equation (2.28) into equation (2.19) gives the shearing stress at any point in the lubricating fluid. This shear stress is

$$\tau_{zx} = \frac{1}{2}\frac{\partial p}{\partial x}(2z-h) - \frac{\mu U}{h} \pm N\tau_p . \tag{2.30}$$

From equation (2.30), the frictional shear stress at the moving surface can be determined by evaluating this function at $z = 0$. Thus, the shearing stress at the moving surface is

$$\tau_{zx} = \frac{-h}{2}\frac{\partial p}{\partial x} - \frac{\mu U}{h} \pm N\tau_p . \tag{2.31}$$

From equation (2.31) the friction torque on a bearing journal may be calculated by integrating the radius times the differential force. Thus the torque is

$$T_q = \int^{A} r\tau_{zx}\, dA \;, \qquad (2.32)$$

where the lubricant film is thin compared to the radius.

Pressure Distribution

The Reynolds' equation is based upon a derivation using Newtonian fluids and is satisfactory for the portion of a bearing using multiphase lubricants of class 1 or class 2. Since the original derivations were based upon incompressible fluids, it is necessary to modify this derivation to make it valid for compressible Newtonian fluids.

For a class 3 lubricant considering only forces in the x direction,

$$\tau = \mu \frac{\partial u}{\partial z} \pm N\tau_p \;. \qquad (2.33)$$

Using equations (2.21) and (2.22), $\frac{\partial p}{\partial x} = \frac{\partial \tau}{\partial z}$. This expression may be integrated to obtain

$$\tau = z \frac{\partial p}{\partial x} + C_1 \;, \qquad (2.34)$$

which leads to the same type of argument Milne (9) presented and was later introduced by Pinkus and Sternlicht (15) for Bingham plastics.

If some function of the shear stress is defined as $F(\tau)$, then

$$F(\tau) = \frac{\partial u}{\partial z}. \qquad (2.35)$$

Then by placing τ from equation (2.34) into equation (2.35),

$$F\left[z\frac{\partial p}{\partial x} + C_1\right] = \frac{\partial u}{\partial z}\ . \qquad (2.36)$$

From which u may be determined by integration.

$$u = \int_0^z F\left[z\frac{\partial p}{\partial x} + C_1\right]dz + C_2 \qquad (2.37)$$

If $F(\tau) = \frac{\tau}{\mu} + K$, as indicated in Fig. 3, is substituted into equation (2.35) and differentiated with respect to z, the shear gradient in the z-direction is equal to the pressure gradient in the x-direction and also equal to $\mu\frac{\partial^2 u}{\partial z^2}$. Thus,

$$\frac{\partial \tau}{\partial z} = \frac{\partial p}{\partial x} = \mu\frac{\partial^2 u}{\partial z^2}\ . \qquad (2.38)$$

When using a Newtonian fluid

$$\tau = \mu\frac{\partial u}{\partial z}\ . \qquad (2.39)$$

$$\frac{\partial \tau}{\partial z} = \mu\frac{\partial^2 u}{\partial z^2} \qquad (2.40)$$

Equation (2.40) for Newtonian fluids is the same expression as equation (2.38) for non-Newtonian class 3 fluids.

Equations (2.38) or (2.40) are the basis for the derivation of Reynolds' partial differential equation which can be used to determine the pressure distribution for any of the three classes of lubricants discussed. A derivation of the Reynolds' equation appears in a number of published works. Of these, one of the most straightforward and easily followed derivations was presented by J. S. Ausman (1). The resulting partial differential equation is:

$$\frac{\partial}{\partial x}\left[\frac{h^3 \rho \frac{\partial p}{\partial x}}{\mu}\right] + \frac{\partial}{\partial y}\left[\frac{h^3 \rho \frac{\partial p}{\partial y}}{\mu}\right] = 6U \frac{\partial}{\partial x} [h \rho] \; . \tag{2.41}$$

With the equation of state for a perfect gas

$$\frac{p}{\rho^n} = C$$

or,

$$\rho = \frac{p^{\frac{1}{n}}}{C^{\frac{1}{n}}} \tag{2.42}$$

and with the assumption that the viscosity is not a direct function of the x and y coordinates, equation (2.41) may be written

$$\frac{\partial}{\partial x}\left[h^3 p^{\frac{1}{n}} \frac{\partial p}{\partial x}\right] + \frac{\partial}{\partial y}\left[h^3 p^{\frac{1}{n}} \frac{\partial p}{\partial y}\right] = 6\mu U \frac{\partial}{\partial x} h\rho^{\frac{1}{n}}\right] . \tag{2.43}$$

Differentiation of equation (2.43) yields

$$h^3 \left[p^{\frac{1}{n}} \frac{\partial^2 p}{\partial x^2} + \frac{\partial p}{\partial x} \frac{1}{n} p^{\left(\frac{1}{n}-1\right)} \frac{\partial p}{\partial x}\right] + 3 p^{\frac{1}{n}} \frac{\partial p}{\partial x} h^2 \frac{\partial h}{\partial x} +$$

$$h^3 \left[p^{\frac{1}{n}} \frac{\partial^2 p}{\partial y^2} + \frac{\partial p}{\partial y} \frac{1}{n} p^{\left(\frac{1}{n}-1\right)} \frac{\partial p}{\partial y}\right] + 3 p^{\frac{1}{n}} \frac{\partial p}{\partial y} h^2 \frac{\partial h}{\partial y} =$$

$$6\mu U \frac{\partial h}{\partial x} p^{\frac{1}{n}} + 6\mu U h \frac{1}{n} p^{\left(\frac{1}{n}-1\right)} \frac{\partial p}{\partial x} . \tag{2.44}$$

Dividing equation (2.44) by $h^3 p^{\left(\frac{1}{n} - 1\right)}$ gives

$$p \frac{\partial^2 p}{\partial x^2} + \frac{\left(\frac{\partial p}{\partial x}\right)^2}{n} + 3p \frac{\frac{\partial p}{\partial x} \frac{\partial h}{\partial x}}{h} + p \frac{\partial^2 p}{\partial y^2} + \frac{\left(\frac{\partial p}{\partial y}\right)^2}{n} +$$

$$3p \frac{\frac{\partial p}{\partial y} \frac{\partial h}{\partial y}}{h} = \frac{6\mu U p \frac{\partial h}{\partial x}}{h^3} + \frac{6\mu U \frac{\partial h}{\partial x}}{h^3} + \frac{6\mu U \frac{\partial p}{\partial x}}{nh^2} . \tag{2.45}$$

Collecting terms of p and its derivatives, the differential equation of pressure distribution may be written as:

$$p \left[\frac{\partial^2 p}{\partial x^2} + \frac{\partial^2 p}{\partial y^2}\right] = \left[\frac{6\mu U}{nh^2} - \frac{3p \frac{\partial h}{\partial x}}{h}\right] \frac{\partial p}{\partial x} - \left[\frac{3p \frac{\partial h}{\partial y}}{h}\right] \frac{\partial p}{\partial y} -$$

$$\frac{1}{n}\left[\left(\frac{\partial p}{\partial x}\right)^2 + \left(\frac{\partial p}{\partial y}\right)^2\right] + \frac{6\mu U p \frac{\partial h}{\partial x}}{h^3} \; . \tag{2.46}$$

Equation (2.46) is the same equation as that presented by Gross (6) for compressible lubricants.

CHAPTER III

THEORETICAL TEMPERATURE DISTRIBUTION IN THE LUBRICANT

General Energy Balance

The temperature of the lubricant film can be calculated by establishing an energy balance on a control volume. In studying this control volume, there are three methods in which energy may be transported into and out of the control volume: by conduction, by transport of fluid containing kinetic and internal energy, and by radiation. In this analysis, radiation will be neglected due to the relatively low temperatures involved.

In making this theoretical analysis it is important to realize that its usefulness depends upon the ability to obtain an accurate analysis of a hydrodynamic bearing using multiphase lubricants. General energy equations for Newtonian fluids have been developed in a number of books and papers. Of these, Sternlicht and Pinkus (15) and Schlichting (20) have outlined a method of solution which can be extended to derive an expression for the temperature distribution in a hydrodynamic bearing using a multiphase lubricant. Any useful solution must consider compressible lubricants with viscosity dependent upon temperature, pressure, rate of shear, film thickness, and phase proportions. Density must be considered as a function of pressure, temperature, and phase proportions. In order to make a meaningful solution including these variables, it is necessary to use a three dimensional analysis.

An energy balance will be made on an element of fluid of volume ΔV, where

$$\Delta V = \Delta x \Delta y \Delta z \tag{3.1}$$

of weight

$$\Delta W_f = \rho g \Delta V \ . \tag{3.2}$$

External heat added to the control volume plus mechanical energy will increase the internal energy and perform expansion work of amount dQ where

$$dQ = \Delta W_f C_v dt + pd(\Delta V) \ . \tag{3.3}$$

The term $\Delta W_f C_v dt$ is the change in internal energy, and the term $pd(\Delta V)$ is the amount of expansion work.

The quantity of heat dQ is also equal to the heat added through conduction plus the heat added by friction or shear work.

$$dQ = dQ_c + dQ_f \tag{3.4}$$

Fig. 5 shows a control volume with the frictional stresses acting on the faces perpendicular to the x-direction.

Page missing from thesis

or

$$W_{\sigma'_x} = dydz \left\{ -\sigma'_x u + \sigma'_x u + \sigma'_x \frac{\partial u}{\partial x} dx + \frac{\partial \sigma'_x}{\partial x} udx + \right.$$

$$\left. \frac{\partial \sigma'_x}{\partial x} \frac{\partial u}{\partial x} (dx)^2 \right\} \tag{3.8}$$

$$W_{\tau_{xy}} = dydz \left\{ -\tau_{xy} v + \tau_{xy} v + \tau_{xy} \frac{\partial v}{\partial x} dx + \frac{\partial \tau_{xy}}{\partial x} v\,dx + \right.$$

$$\left. \frac{\partial \tau_{xy}}{\partial x} \frac{\partial v}{\partial x} (dx)^2 \right\} \tag{3.9}$$

$$W_{\tau_{xz}} = dydz \left\{ -\tau_{xz} w + \tau_{xz} w + \tau_{xz} \frac{\partial w}{\partial x} + \frac{\partial \tau_{xz}}{\partial x} wdx + \right.$$

$$\left. \frac{\partial \tau_{xz}}{\partial x} \frac{\partial w}{\partial x} (dx)^2 \right\} . \tag{3.10}$$

If the second order differentials are neglected, and dxdydz is replaced by ΔV, the above equations become:

$$W_{\sigma'_x} = \Delta V \left[\sigma'_x \frac{\partial u}{\partial x} + u \frac{\partial \sigma'_x}{\partial x} \right] \tag{3.11}$$

$$W_{\tau_{xy}} = \Delta V \left[\tau_{xy} \frac{\partial v}{\partial x} + v \frac{\partial \tau_{xy}}{\partial x} \right] \tag{3.12}$$

$$W_{\tau_{xz}} = \Delta V \left[\tau_{xz} \frac{\partial w}{\partial x} + w \frac{\partial \tau_{xz}}{\partial x} \right] . \tag{3.13}$$

In a similar manner, the frictional work done on the other faces will be found to be

$$W_{\sigma'_y} = \Delta V\left[\sigma'_y \frac{\partial v}{\partial y} + v \frac{\partial \sigma'_y}{\partial y}\right] \tag{3.14}$$

$$W_{\tau_{yx}} = \Delta V \left[\tau_{yx} \frac{\partial u}{\partial y} + u \frac{\partial \tau_{yx}}{\partial y}\right] \tag{3.15}$$

$$W_{\tau_{yz}} = \Delta V \left[\tau_{yz} \frac{\partial w}{\partial y} + w \frac{\partial \tau_{yz}}{\partial y}\right] \tag{3.16}$$

$$W_{\sigma'_z} = \Delta V \left[\sigma'_z \frac{\partial w}{\partial z} + w \frac{\partial \sigma'_z}{\partial z}\right] \tag{3.17}$$

$$W_{\tau_{zx}} = \Delta V \left[\tau_{zx} \frac{\partial u}{\partial z} + u \frac{\partial \tau_{zx}}{\partial z}\right] \tag{3.18}$$

$$W_{\tau_{zy}} = \Delta V \left[\tau_{zy} \frac{\partial v}{\partial z} + v \frac{\partial \tau_{zy}}{\partial z}\right]. \tag{3.19}$$

The summation of equations (3.11) through (3.19) is the total work (W_t) done on the volume element by frictional stresses per unit of time.

$$W_t = \Delta V \left[\sigma'_x \frac{\partial u}{\partial x} + u \frac{\partial \sigma'_x}{\partial x} + \tau_{xy} \frac{\partial v}{\partial x} + v \frac{\partial \tau_{xy}}{\partial x}\right.$$

$$+ \tau_{xz} \frac{\partial w}{\partial x} + w \frac{\partial \tau_{xz}}{\partial x} + \sigma'_y \frac{\partial v}{\partial y} + v \frac{\partial \sigma'_y}{\partial y} + \tau_{yx} \frac{\partial u}{\partial y} +$$

$$u \frac{\partial \tau_{yx}}{\partial y} + \tau_{yz} \frac{\partial w}{\partial y} + w \frac{\partial \tau_{yz}}{\partial y} + \sigma'_z \frac{\partial w}{\partial z} + w \frac{\partial \sigma'_z}{\partial z} +$$

$$\left.\tau_{zx} \frac{\partial u}{\partial z} + u \frac{\partial \tau_{zx}}{\partial z} + \tau_{zy} \frac{\partial v}{\partial z} + v \frac{\partial \tau_{zy}}{\partial z}\right] \tag{3.20}$$

Mechanical Energy

A portion of the frictional energy of equation (3.20) will go to mechanical energy which will not increase the temperature of the fluid in the control volume. In order to determine the mechanical energy, the equations of motion will be used. These equations are:

$$\rho \frac{Du}{Dt} = X - \frac{\partial p}{\partial x} + \left(\frac{\partial \sigma_x'}{\partial x} + \frac{\partial \tau_{xy}}{\partial y} + \frac{\partial \tau_{xz}}{\partial z}\right) \tag{3.21}$$

$$\rho \frac{Dv}{Dt} = Y - \frac{\partial p}{\partial y} + \left(\frac{\partial \tau_{xy}}{\partial x} + \frac{\partial \sigma_y'}{\partial y} + \frac{\partial \tau_{yz}}{\partial z}\right) \tag{3.22}$$

$$\rho \frac{Dw}{Dt} = Z - \frac{\partial p}{\partial z} + \left(\frac{\partial \tau_{xz}}{\partial x} + \frac{\partial \tau_{yz}}{\partial y} + \frac{\partial \sigma_z'}{\partial z}\right). \tag{3.23}$$

Body forces X, Y, and Z are assumed as negligible. Multiplying the above equations by ΔV and by their respective velocities, u, v, and w and summing the three gives:

$$\rho\Delta V\left[u \frac{Du}{Dt} + v \frac{Dv}{Dt} + w \frac{Dw}{Dt}\right] + \Delta V\left[u \frac{\partial p}{\partial x} + v \frac{\partial p}{\partial y} + w \frac{\partial p}{\partial z}\right]$$

$$= u\Delta V\left[\frac{\partial \sigma_x'}{\partial x} + \frac{\partial \tau_{xy}}{\partial y} + \frac{\partial \tau_{xz}}{\partial z}\right] + v\Delta V\left[\frac{\partial \tau_{xy}}{\partial x} + \frac{\partial \sigma_y'}{\partial y} + \frac{\partial \tau_{yz}}{\partial z}\right]$$

$$+ w\Delta V\left[\frac{\partial \tau_{xz}}{\partial x} + \frac{\partial \tau_{yz}}{\partial y} + \frac{\partial \sigma_z'}{\partial z}\right] . \tag{3.24}$$

The first group of terms on the left-hand side of equation (3.24) is the time rate of change of the kinetic energy. The second group of terms is the time rate of change of pressure energy. Since both of these terms are mechanical energy, they do not contribute to the temperature of the fluid element. Subtracting the right-hand side of equation (3.24) from equation (3.20) gives the quantity of energy (DQ_f/Dt) converted into internal energy and compression work in the element.

$$\frac{DQ_f}{Dt} = \Delta V\left[\sigma'_x \frac{\partial u}{\partial x} + \tau_{xy}\frac{\partial v}{\partial x} + \tau_{xz}\frac{\partial w}{\partial x} + \sigma'_y \frac{\partial v}{\partial y} + \tau_{yx}\frac{\partial u}{\partial y} + \tau_{yz}\frac{\partial w}{\partial y} + \sigma'_z \frac{\partial w}{\partial z} + \tau_{zx}\frac{\partial u}{\partial z} + \tau_{zy}\frac{\partial v}{\partial z}\right] \tag{3.25}$$

In terms of equations (2.17) and (2.18) equation (3.25) becomes

$$\frac{DQ_f}{Dt} = \mu\Delta V\left[2\left[\left(\frac{\partial u}{\partial x}\right)^2 + \left(\frac{\partial v}{\partial y}\right)^2 + \left(\frac{\partial w}{\partial z}\right)^2 - \frac{1}{3}\frac{\partial u}{\partial x}\operatorname{div}\vec{W} - \frac{1}{3}\frac{\partial u}{\partial y}\operatorname{div}\vec{W} - \frac{1}{3}\frac{\partial w}{\partial z}\operatorname{div}\vec{W}\right] + \frac{\partial v}{\partial x}\frac{\partial u}{\partial y} + \left(\frac{\partial v}{\partial x}\right)^2 + \left(\frac{\partial w}{\partial x}\right)^2 + \frac{\partial w}{\partial x}\frac{\partial u}{\partial z} \pm \frac{\partial w}{\partial x}\frac{1}{\mu}N\tau_p + \left(\frac{\partial u}{\partial y}\right)^2 + \frac{\partial u}{\partial y}\frac{\partial v}{\partial x} + \frac{\partial w}{\partial y}\frac{\partial v}{\partial z} + \left(\frac{\partial w}{\partial y}\right)^2 + \frac{\partial u}{\partial z}\frac{\partial w}{\partial x} + \left(\frac{\partial u}{\partial z}\right)^2 \pm \frac{\partial u}{\partial z}\frac{1}{\mu}N\tau_p + \left(\frac{\partial v}{\partial z}\right)^2 + \frac{\partial v}{\partial z}\frac{\partial w}{\partial y}\right]. \tag{3.26}$$

Substituting $\operatorname{div}\vec{W} = \frac{\partial u}{\partial x} + \frac{\partial v}{\partial y} + \frac{\partial w}{\partial z}$ and collecting terms, equation (3.26) becomes

$$\frac{DQ_f}{Dt} = \mu\Delta V\Big[2\Big[\Big(\frac{\partial u}{\partial x}\Big)^2 + \Big(\frac{\partial v}{\partial y}\Big)^2 + \Big(\frac{\partial w}{\partial z}\Big)^2\Big] - \frac{2}{3}\Big[\frac{\partial u}{\partial x} + \frac{\partial v}{\partial y} + \frac{\partial w}{\partial z}\Big]\Big[\frac{\partial u}{\partial x} + \frac{\partial v}{\partial y} + \frac{\partial w}{\partial z}\Big] + \Big[\Big(\frac{\partial u}{\partial y}\Big)^2 + \Big(\frac{\partial v}{\partial x}\Big)^2 + \Big(\frac{\partial w}{\partial y}\Big)^2 + \Big(\frac{\partial v}{\partial z}\Big)^2 + \Big(\frac{\partial w}{\partial x}\Big)^2\Big] + 2\,\frac{\partial v}{\partial x}\frac{\partial u}{\partial y} + 2\,\frac{\partial w}{\partial y}\frac{\partial v}{\partial z} + 2\,\frac{\partial u}{\partial z}\frac{\partial w}{\partial x} \pm \frac{\partial w}{\partial x}\frac{1}{\mu}N\tau_p \pm \frac{\partial u}{\partial z}\frac{1}{\mu}N\tau_p\Big], \tag{3.27}$$

which is the heat added by friction per unit of time, and may be written

$$\frac{DQ_f}{Dt} = \mu\Delta V\Big[2\Big[\Big(\frac{\partial u}{\partial x}\Big)^2 + \Big(\frac{\partial v}{\partial y}\Big)^2 + \Big(\frac{\partial w}{\partial z}\Big)^2\Big] + \Big[\frac{\partial v}{\partial x} + \frac{\partial u}{\partial y}\Big]^2 + \Big[\frac{\partial w}{\partial y} + \frac{\partial v}{\partial z}\Big]^2 + \Big[\frac{\partial u}{\partial z} + \frac{\partial w}{\partial x}\Big]^2 - \frac{2}{3}\Big[\frac{\partial u}{\partial x} + \frac{\partial v}{\partial y} + \frac{\partial w}{\partial z}\Big]^2 + \frac{1}{\mu}N\tau_p\Big[\Big|\frac{\partial w}{\partial x}\Big| + \Big|\frac{\partial u}{\partial z}\Big|\Big]\Big] \tag{3.28}$$

where the absolute value of the coulomb friction terms $\frac{\partial w}{\partial x}$ and $\frac{\partial u}{\partial z}$ insures the addition of this quantity of heat to the element irrespective of the direction of the motion causing this friction.

Heat Added by Conduction

Fourier's equation of heat flux equates the heat flux (q) crossing an area A to the temperature gradient in the direction perpendicular to the surface of the area times a proportionality constant. Thus:

$$\frac{dQ_c}{ADt} = q = - K \frac{\partial T}{\partial n'} , \tag{3.29}$$

where K = thermal conductivity

n' = dimension in direction perpendicular to the surface.

The heat flow in the x-direction at station x in an element would be

$$\left.\frac{DQ_c}{Dt}\right|_x = - K \frac{\partial T}{\partial x} dydz , \tag{3.30}$$

and at station (x+dx)

$$\left.\frac{DQ_c}{Dt}\right|_{x+dx} = - \left[-K \frac{\partial T}{\partial x} + \frac{\partial}{\partial x}\left(K \frac{\partial T}{\partial x}\right) dx\right]dydz. \tag{3.31}$$

The heat gain by conductive flow in the x-direction along the space interval dx may be obtained by subtracting equation (3.31) from equation (3.30). The heat gain is:

$$\frac{DQ_{cx}}{Dt} = \frac{\partial}{\partial x}\left(K \frac{\partial T}{\partial x}\right) dx\ dydz = \Delta V \frac{\partial}{\partial x}\left(K \frac{\partial T}{\partial x}\right). \tag{3.32a}$$

The heat gains in the y and z - directions are respectively

$$\frac{DQ_{cy}}{Dt} = \Delta V \frac{\partial}{\partial y}\left(K \frac{\partial T}{\partial y}\right), \tag{3.32b}$$

and

$$\frac{DQ_{cz}}{Dt} = \Delta V \frac{\partial}{\partial z}\left(K \frac{\partial T}{\partial z}\right). \tag{3.32c}$$

Summing equations (3.32) gives the total heat added to the element by conduction per unit of time. The total heat gain is:

$$\frac{DQ_c}{Dt} = \Delta V \left[\frac{\partial}{\partial x}\left(K \frac{\partial T}{\partial x}\right) + \frac{\partial}{\partial y}\left(K \frac{\partial T}{\partial y}\right) + \frac{\partial}{\partial z}\left(K \frac{\partial T}{\partial z}\right)\right]. \tag{3.33}$$

Dissipation of Total Heat

The total heat added to the element from equation (3.33) will do compression work and increase the internal energy of the element. This total is:

$$\frac{DQ}{\Delta V Dt} = \frac{p}{\Delta V} \frac{D(\Delta V)}{Dt} + \frac{g\rho}{\Delta V} \frac{D(C_v T)}{Dt} . \tag{3.34}$$

If it is assumed that

$$\frac{1}{\Delta V} \frac{D(\Delta V)}{Dt} = \rho \frac{D \frac{1}{\rho}}{Dt} , \tag{3.35}$$

and

$$\frac{p}{\Delta V} \frac{D(\Delta V)}{dt} = \rho p \frac{D \frac{1}{\rho}}{Dt} . \tag{3.36}$$

Taking the total derivative of $\frac{1}{\rho}$ as indicated

$$\rho p \frac{D \frac{1}{\rho}}{Dt} = \rho p \left[\frac{\partial \frac{1}{\rho}}{\partial x} \frac{dx}{dt} + \frac{\partial \frac{1}{\rho}}{\partial y} \frac{dy}{dt} + \frac{\partial \frac{1}{\rho}}{\partial z} \frac{dz}{dt}\right] \tag{3.37}$$

and noting that

$$\frac{dx}{dt} = u; \ \frac{dy}{dt} = v; \ \frac{dz}{dt} = w. \tag{3.38}$$

In a similar manner taking the total derivative of $C_v T$,

$$g\rho \frac{D(C_v T)}{Dt} = g\rho \left[u \frac{\partial(C_v T)}{\partial x} + v \frac{\partial(C_v T)}{\partial y} + w \frac{\partial(C_v T)}{\partial z}\right] \tag{3.39}$$

Substitution of equations (3.37), (3.38), and (3.39) into equation (3.34) gives the dissipation of total heat,

$$\frac{DQ}{\Delta V Dt} = g\rho\left[u \frac{\partial(C_v T)}{\partial x} + v \frac{\partial(C_v T)}{\partial y} + \right.$$

$$\left. w \frac{\partial(C_v T)}{\partial z}\right] + \rho p \left[u \frac{\partial \frac{1}{\rho}}{\partial x} + v \frac{\partial \frac{1}{\rho}}{\partial y} + w \frac{\partial \frac{1}{\rho}}{\partial z}\right]. \tag{3.40}$$

The general energy equation for this type of multiphase lubricant under steady laminar flow conditions is obtained by equating the right side of equation (3.40), which is the total heat dissipation, to the sum of the right side of equations (3.28) and (3.33) which are the heat added by friction and the heat added by conduction. Thus the general energy equation is:

$$g\rho \left[u \frac{\partial(C_v T)}{\partial x} + v \frac{\partial(C_v T)}{\partial y} + w \frac{\partial(C_v T)}{\partial z}\right] + \rho p \left[u \frac{\partial \frac{1}{\rho}}{\partial x} + v \frac{\partial \frac{1}{\rho}}{\partial y} + w \frac{\partial \frac{1}{\rho}}{\partial z}\right] = \left[\frac{\partial}{\partial x}\left(K \frac{\partial T}{\partial x}\right) + \frac{\partial}{\partial y}\left(K \frac{\partial T}{\partial y}\right) + \frac{\partial}{\partial z}\left(K \frac{\partial T}{\partial z}\right)\right] + \mu\left[2\left[\left(\frac{\partial u}{\partial x}\right)^2 + \left(\frac{\partial v}{\partial y}\right)^2 + \left(\frac{\partial w}{\partial z}\right)^2\right] + \left[\frac{\partial v}{\partial x} + \frac{\partial u}{\partial y}\right]^2 + \left[\frac{\partial w}{\partial y} + \frac{\partial v}{\partial z}\right]^2 + \left[\frac{\partial u}{\partial z} + \frac{\partial w}{\partial x}\right]^2 - \frac{2}{3}\left[\frac{\partial u}{\partial x} + \frac{\partial v}{\partial y} + \frac{\partial w}{\partial z}\right]^2 + \frac{1}{\mu} N \tau_p \left[\left|\frac{\partial w}{\partial x}\right| + \left|\frac{\partial u}{\partial z}\right|\right]\right]. \qquad (3.41)$$

CHAPTER IV

SOLUTION OF COUPLED PARTIAL DIFFERENTIAL EQUATIONS BY FINITE - DIFFERENCES

Form of Equations for Temperature and Pressure Distribution

A lubricant film is so thin compared to the other two dimensions that many of the terms in equation (3.41) are negligible. One of the best discussions of the relative importance of these terms is given by Cope (5) in which he gives calculated values of the magnitudes of terms for a set of representative conditions. Pinkus and Sternlicht (15) also give a good discussion of the order of magnitude of these terms in the first chapter of their book. The use of multiphase lubricants of the type suggested does not invalidate their order analysis. Using the original assumptions stated in the derivation of the velocity and frictional stresses, the following terms are either constant or negligible:

w(velocity in z-direction) -- negligible

$$C_v = \text{constant}$$

$$K = \text{constant}$$

$$\frac{\partial u}{\partial x};\ \frac{\partial v}{\partial y};\ \frac{\partial w}{\partial z}\ \text{-- negligible}$$

$$\frac{\partial v}{\partial x};\ \frac{\partial u}{\partial y};\ \frac{\partial w}{\partial y};\ \frac{\partial w}{\partial x}\ \text{-- negligible}$$

Using these assumptions and rearranging terms, equation (3.41) becomes

$$K\left(\frac{\partial^2 T}{\partial x^2} + \frac{\partial^2 T}{\partial y^2} + \frac{\partial^2 T}{\partial z^2}\right) = \rho g C_v\left[u\,\frac{\partial T}{\partial x} + v\,\frac{\partial T}{\partial y}\right] +$$

$$\rho p\left[u\,\frac{\partial \frac{1}{\rho}}{\partial x} + v\,\frac{\partial \frac{1}{\rho}}{\partial y}\right] - \mu\left[\left(\frac{\partial u}{\partial z}\right)^2 + \left(\frac{\partial v}{\partial z}\right)^2\right] -$$

$$N\tau_p\left|\frac{\partial u}{\partial z}\right|, \qquad (4.1)$$

where

$$T = T(x,y,z)$$

$$p = p(x,y)$$

$$\rho = \left(\frac{p}{C^*}\right)^{\frac{1}{n}}$$

$$\mu = \mu(M,T,p) ,$$

and C_v, K, C* and n denote constants. In order to solve equation (4.1) for T it is necessary to solve equation (2.46) for p. This equation which must be solved for p has the following form:

$$p\left[\frac{\partial^2 p}{\partial x^2} + \frac{\partial^2 p}{\partial y^2}\right] = \left[\frac{6\mu U}{nh^2} - \frac{3p\,\frac{\partial h}{\partial x}}{h}\right]\frac{\partial p}{\partial x} - \left[\frac{3p\,\frac{\partial h}{\partial y}}{h}\right]\frac{\partial p}{\partial y} -$$

$$\frac{1}{n}\left[\left(\frac{\partial p}{\partial x}\right)^2 + \left(\frac{\partial p}{\partial y}\right)^2\right] + \frac{6\mu U\ p\ \frac{\partial h}{\partial x}}{h^3}\ . \tag{2.46}$$

Equation (4.1) which is to be solved for temperature, T, varies with three dimensions, x, y, and z. The pressure function of equation (2.46) varies with two dimensions, x and y. These two equations are coupled by terms involving the viscosity, μ, a function of temperature and pressure which appears in both equations (4.1) and (2.46).

In addition to the set of coupled partial differential equations, these equations are nonlinear for two reasons. The viscosity contains temperature and pressure as exponential functions, and the derivatives of the velocity components u and v, which are functions of viscosity and in turn temperature and pressure, also appear as second-power terms.

Method of Solution

The problem of solving these non-linear partial differential equations is first replaced by a similar problem of solving the respective equations when written in finite-difference form. This substitution has the effect of substituting a set of n algebraic equations in n unknowns for the original equations. The partial derivatives in equation (4.1) and (2.46) are approximated by finite differences which in turn are substituted into the differential equations to form the difference equations.

A three-dimensional mesh is superimposed over the temperature field by passing planes perpendicular to the x-axis and the y-axis and parallel to the boundary in the z-direction. In general, the z-boundary is not perpendicular to the z-axis due to the converging-diverging wedge. The intersections of the planes form mesh points which define physical locations for values of temperature.

These n difference-equations are implicit; that is, $T(x,y,z)$ is in terms of $f\left(e^{T(x,y,z)}\right)$. It is therefore necessary to employ a special procedure to solve for improved values of T. This is done by setting an initial value for the viscosity at all points which is held fixed at these values until improved values of T are obtained by iterating the n difference equations. Now the viscosity is recalculated for each point using the improved values of T; then it is again fixed while the iterative process is repeated until the values of the temperature change little from one viscosity-temperature iteration to the next.

In the method of solution outlined above, it is necessary to have a pressure distribution and a set of boundary values for temperature. Boundary values of pressure are known and are exact. These values represent the lubricant supply pressure and the pressure surrounding the bearing. The initial pressure distribution within the bearing is made by assuming a set of pressures. The accuracy of the original set of assumed pressure values has been found to be of little importance since the pressure functions are rapidly convergent. Therefore, a constant value of pressure is set initially at all points in the bearing and is modified after the temperature distribution is calculated. A procedure similar to the one used for calculating the temperature distribution is used with the values of pressure recalculated until there is little change from one iteration to the next.

Temperature boundary values are used to control the thermodynamic process. The lubricant inlet temperature is preset and remains at a fixed value for all (2,y,z) points in the y-z plane at x-station 2. Temperature and pressure symmetry about the y-axis centerline is assumed. Therefore, no temperature gradient exists in the y-direction along the centerline of the bearing. Since only half of the bearing is studied due to this symmetry, temperatures are reflected to the outside of the bearing centerline so as to maintain no temperature gradient toward the other half of the bearing. A similar temperature reflection is made along the outside edge of the bearing in order to set up a zero temperature gradient in the y-direction along the outer edge.

Temperatures at the two bearing surfaces namely, z=0 and z=h, are varied to satisfy different operating conditions. Constant temperatures at these surfaces would produce heat sinks or sources, and a zero temperature gradient at these surfaces would produce adiabatic conditions. Adiabatic conditions normally yield bearing temperatures which are too high and thus can be used as an upper limit.

Temperatures at the end of the film in the x-direction are reflected to give a zero temperature gradient in the x-direction. These temperatures are in the zone where the lubricant film is ruptured.

The values of the temperature and the pressure are modified in alternate order until there is little change in the values from one viscosity-temperature-pressure iteration to the next. The resulting temperature and pressure distributions are assumed to be the mathematical solution of the difference equations (3). Experimental and direct solutions are compared with these in a later section.

Temperature Equation in Finite-Differences

In this section equation (4.1) will be transformed into a set of difference equations which can be solved by an iterative process. Starting with equation (4.1) which is:

$$K\left(\frac{\partial^2 T}{\partial x^2} + \frac{\partial^2 T}{\partial y^2} + \frac{\partial^2 T}{\partial z^2}\right) = g\rho C_v\left[u\,\frac{\partial T}{\partial x} + v\,\frac{\partial T}{\partial y}\right]$$

$$+ \rho p\left[u\,\frac{\partial \frac{1}{\rho}}{\partial x} + v\,\frac{\partial \frac{1}{\rho}}{\partial y}\right] - \mu\left[\left(\frac{\partial u}{\partial z}\right)^2 + \left(\frac{\partial v}{\partial z}\right)^2\right] -$$

$$N\tau_p\left|\frac{\partial u}{\partial z}\right| . \qquad (4.1)$$

At this point the right side of this equation will be denoted by RHS to reduce the amount of writing. Equation (4.1) now becomes

$$\frac{\partial^2 T}{\partial x^2} + \frac{\partial^2 T}{\partial y^2} + \frac{\partial^2 T}{\partial z^2} = \frac{1}{K}\,(\mathrm{RHS})\,. \qquad (4.2)$$

Writing the second-order partial derivatives as finite central differences:

$$\frac{\partial^2 T}{\partial x^2} = \frac{T(x+\Delta x,y,z)+T(x-\Delta x,y,z)-2T(x,y,z)}{(\Delta x)^2}$$

$$\frac{\partial^2 T}{\partial y^2} = \frac{T(x,y+\Delta y,z)+T(x,y-\Delta y,z)-2T(x,y,z)}{(\Delta y)^2}$$

$$\frac{\partial^2 T}{\partial z^2} = \frac{T(x,y,z+\Delta z)+T(x,y,z-\Delta z)-2T(x,y,z)}{(\Delta z)^2}$$

Substituting these expressions into equation (4.2) yields the following expression:

$$T(x,y,z)\left[\frac{-2}{(\Delta x)^2} - \frac{2}{(\Delta y)^2} - \frac{2}{(\Delta z)^2}\right] + \frac{T(x+\Delta x,y,z)}{(\Delta x)^2}$$

$$+\, T\,\frac{(x-\Delta x,y,z)}{(\Delta x)^2} + T\,\frac{(x,y+\Delta y,z)}{(\Delta y)^2} + T\,\frac{(x,y-\Delta y,z)}{(\Delta y)^2}$$

$$+\, T\,\frac{(x,y,z+\Delta z)}{(\Delta z)^2} + T\,\frac{(x,y,z-\Delta z)}{(\Delta z)^2} = \frac{1}{K}\,(\mathrm{RHS})\;.$$

This equation can now be solved for T(x,y,z).

$$T(x,y,z) = \left[\frac{(\Delta x \Delta y \Delta z)^2}{2\,(\Delta y \Delta z)^2 + 2\,(\Delta x \Delta z)^2 + 2\,(\Delta x \Delta y)^2}\right]$$

$$\left[\frac{T(x+\Delta x,y,z) + T\,(x-\Delta x,y,z)}{(\Delta x)^2} + \frac{T(x,y+\Delta y,z) + T(x,y-\Delta y,z)}{(\Delta y)^2}\right.$$

$$\left. + \frac{T(x,y,z+\Delta z) + T\,(x,y,z-\Delta z)}{(\Delta z)^2} - \frac{1}{K}\,(RHS)\right] \qquad (4.3)$$

A simplification of equation (4.3) can be made by multiplying through by $(\Delta x \Delta y \Delta z)^2$. Thus

$$T(x,y,z) = \left[\frac{1}{2\,(\Delta y \Delta z)^2 + 2\,(\Delta x \Delta z)^2 + 2\,(\Delta x \Delta y)^2}\right]$$

$$\Big\{(\Delta y \Delta z)^2 \left[T\,(x+\Delta x,y,z) + T\,(x-\Delta x,y,z)\right] +$$

$$(\Delta x \Delta z)^2 \left[T\,(x,y+\Delta y,z) + T\,(x,y-\Delta y,z)\right] +$$

$$(\Delta x \Delta y)^2 \left[T\,(x,y,z+\Delta z) + T\,(x,y,z-\Delta z)\right]$$

$$- \frac{(\Delta x \Delta y \Delta z)^2}{K}\,(RHS)\Big\} \qquad (4.4)$$

Equation (4.4) is the expression for the temperature at a point expressed in terms of the RHS and the temperature of the six surrounding points.

The expression for RHS is given by

$$\text{RHS} = g\rho C_v \left[u \frac{\partial T}{\partial x} + v \frac{\partial T}{\partial y}\right] + \rho p \left[u \frac{\partial \frac{1}{\rho}}{\partial x} + v \frac{\partial \frac{1}{\rho}}{\partial y}\right] -$$

$$\mu \left[\left(\frac{\partial u}{\partial z}\right)^2 + \left(\frac{\partial v}{\partial z}\right)^2\right] - N\tau_p \left| \frac{\partial u}{\partial z} \right| . \qquad (4.5)$$

The first term of the right member is

$$g\rho C_v \left(u \frac{\partial T}{\partial x} + v \frac{\partial T}{\partial y}\right) .$$

This term contains the lubricant density, ρ, which shall be determined by one of the following means:

(a) Primarily Liquid Lubricant

For liquid lubricants, the Bulk Modulus, K_m, is defined from the equation

$$K_m = \frac{dp}{dV/V} \qquad (4.6)$$

or from equation (4.6)

$$dV = \frac{Vdp}{K_m} . \qquad (4.7)$$

The density of a liquid is also effected by temperature as per the following equation:

$$\rho_1 = \rho_{T_o} - \alpha \left(T_1 - T_o\right) . \qquad (4.8)$$

From equation (4.7) the density is

$$\rho = \frac{\rho_1 V}{V-dV} = \frac{\rho_1 V}{V-\frac{Vdp}{K_m}} = \frac{\rho_1 K_m}{K_m-dp} \qquad (4.9)$$

where dp is the change in pressure from the ρ_1 conditions of temperature and pressure. Substituting equation (4.8) into equation (4.9) gives the following expression for the density of the liquid:

$$\rho = \left[\rho_{520} - \alpha \quad (T-520)\right] \frac{K_m}{K_m - p + 15} . \qquad (4.10)$$

(b) Primarily Compressible Lubricant

In this case the equation of state for a perfect gas is assumed. The resulting equation for density is the same as equation (2.42).

$$\frac{P}{(\rho)^n} = C^*$$

or,

$$\rho = \frac{(p)^{\frac{1}{n}}}{(C^*)^{\frac{1}{n}}} = \left[\frac{(P)}{C^*}\right]^{\frac{1}{n}} . \qquad (4.11)$$

The first-order partial derivatives of temperature and pressure with respect to x and y expressed in finite-difference form are:

$$\frac{\partial T}{\partial x} = \frac{T(x+\Delta x,y,z)-T(x-\Delta x,y,z)}{2\,\Delta x}$$

$$\frac{\partial T}{\partial y} = \frac{T(x,y+\Delta y,z)-T(x,y-\Delta y,z)}{2\Delta y}$$

$$\frac{\partial p}{\partial x} = \frac{p(x+\Delta x,y)-p(x-\Delta x,y)}{2\Delta x}$$

$$\frac{\partial p}{\partial y} = \frac{p(x,y+\Delta y)-p(x,y-\Delta y)}{2\Delta y}$$

From equations (2.26) and (2.27) the expressions for u and v are:

$$u = \frac{1}{2\mu}\frac{\partial p}{\partial x}z(z-h) + \frac{h-z}{h}U$$

$$v = \frac{1}{2\mu}\frac{\partial p}{\partial y}(z-h)\ z.$$

Substituting the first partial derivatives of the pressure in finite-difference form, the expressions for u and v become

$$u = \frac{1}{2\mu}\left[\frac{p(x+\Delta x,y)-p(x-\Delta x,y)}{2\Delta x}\right]z(z-h) + \frac{(h-z)}{h}U \tag{4.12}$$

$$v = \frac{1}{2\mu}\left[\frac{p(x,y+\Delta y)-p(x,y-\Delta y)}{2\Delta y}\right](z-h)z \tag{4.13}$$

where

$$\mu = \left(A_t e^{-\alpha T(x,y,z)} + B_t\right)\ e^{\gamma p(x,y)} \tag{4.14}$$

and A_t, B_t, α, and γ are constants.

The first term of the right member of equation (4.5) may now be written in finite-difference form.

$$\text{First term} = g\rho C_v\left(u\frac{\partial T}{\partial x} + v\frac{\partial T}{\partial y}\right) \tag{4.15}$$

Selecting the ρ for a compressible lubricant, equation (4.15) becomes

$$\text{First Term} = \left[\frac{p(x,y)}{C^*}\right]^{\frac{1}{n}} C_v g \left\{\frac{1}{2\mu}\left[\frac{p(x+\Delta x,y)-p(x-\Delta x,y)}{2\Delta x}\right]\right.$$

$$\left[z(z-h) + \frac{(h-z)}{h}U\right]\left[\frac{T(x+\Delta x,y,z)-T(x-\Delta x,y,z)}{2\Delta x}\right]$$

$$+\frac{1}{2\mu}\left[\frac{p(x,y+\Delta y)-p(x,y-\Delta y)}{2\Delta y}\right]\left[(z-h)z\right]$$

$$\left.\left[\frac{T(x,y+\Delta y,z)-T(x,y-\Delta y,z)}{2\Delta y}\right]\right\} . \tag{4.16}$$

The second term of the right member of equation (4.5) is

$$\rho p \left[u \frac{\partial \frac{1}{\rho}}{\partial x} + v \frac{\partial \frac{1}{\rho}}{\partial y}\right]$$

where

$$\frac{1}{\rho} = \left[\frac{p(x,y)}{C^*}\right]^{-\frac{1}{n}} \quad \text{for compressible lubricants.}$$

When the lubricant is primarily liquid, the second term is taken as zero since the $\frac{\partial \frac{1}{\rho}}{\partial x}$ and $\frac{\partial \frac{1}{\rho}}{\partial y}$ are very small. For the compressible lubricant,

$$\frac{\partial \frac{1}{\rho}}{\partial x} = -\frac{1}{n}\left[\frac{p(x,y)}{C^*}\right]^{(-1-n)/n}\left[\frac{1}{C^*}\frac{\partial p(x,y)}{\partial x}\right] ,$$

$$\frac{\partial \frac{1}{\rho}}{\partial y} = - \frac{1}{n} \left[\frac{p(x,y)}{C^*}\right]^{(-1-n)/n} \left[\frac{1}{C^*} \frac{\partial p(x,y)}{\partial y}\right] ,$$

In finite-difference form these derivatives are

$$\frac{\partial \frac{1}{\rho}}{\partial x} = \frac{-1}{C^* n} \left[\frac{p(x,y)}{C^*}\right]^{(-1-n)/n} \left[\frac{p(x+\Delta x,y)-p(x-\Delta x,y)}{2\Delta x}\right]$$

$$\frac{\partial \frac{1}{\rho}}{\partial y} = - \frac{1}{C^* n} \left[\frac{p(x,y)}{C^*}\right]^{(-1-n)/n}$$

$$\left[\frac{p(x,y+\Delta y)-p(x,y-\Delta y)}{2\Delta y}\right] .$$

The second term of the right member of equation (4.5) may now be written in finite-difference form.

$$\text{Second Term} = \left[\frac{p(x,y)}{C^*}\right]^{\frac{1}{n}} \left[p(x,y)\right]\left[\frac{-1}{C^* n}\right]\left[\frac{p(x,y)}{C^*}\right]^{(-1-n)/n}$$

$$\left[\left\{\frac{1}{2\mu}\left[\frac{p(x+\Delta x,y)-p(x-\Delta x,y)}{2\Delta x}\right]\left[z(z-h)\right]\right.\right.$$

$$\left. + \frac{(h-z)}{h} U\right\}\left[\frac{p(x+\Delta x,y)-p(x-\Delta x,y)}{2\Delta x}\right]$$

$$\left. + \left\{\frac{1}{2\mu}\left[\frac{p(x,y+\Delta y)-p(x,y-\Delta y)}{2\Delta y}\right]^2\left[(z-h)z\right]\right\}\right] \qquad (4.17)$$

The third term of the right member of equation (4.5) is

$$\mu\left[\left(\frac{\partial u}{\partial z}\right)^2 + \left(\frac{\partial v}{\partial z}\right)^2\right] .$$

Taking u and v from equations (2.26) and (2.27), respectively, the following partial derivatives may be calculated:

$$\frac{\partial u}{\partial z} = \frac{1}{2\mu}\frac{\partial p}{\partial x}(2z-h) - \frac{1}{2}\frac{\partial p}{\partial x}\left(z^2-zh\right)\mu^{-2}\frac{\partial \mu}{\partial z} - \frac{U}{h}$$

$$\frac{\partial v}{\partial z} = \frac{1}{2\mu}\frac{\partial p}{\partial y}(2z-h) - \frac{1}{2}\frac{\partial p}{\partial y}\left(z^2-zh\right)\mu^{-2}\frac{\partial \mu}{\partial z}.$$

Since $\mu = \left(A_t e^{-\alpha T(x,y,z)} + B_t\right)e^{\gamma p(x,y)}$, the finite-difference form of the partial derivative of μ with respect to z is given by

$$\frac{\partial \mu}{\partial z} = \frac{1}{2\Delta z}\left[\left(A_t e^{-\alpha T(x,y,z+\Delta z)} + B_t\right)e^{\gamma p(x,y)}\right.$$

$$\left. - \left(A_t e^{-\alpha T(x,y,z-\Delta z)} + B_t\right)e^{\gamma p(x,y)}\right] .$$

The third term of the right member of equation (4.5) may now be written in finite difference form.

$$\text{Third Term} = \mu\left\{\frac{1}{2\mu}\left[\frac{p(x+\Delta x,y)-p(x-\Delta x,y)}{2\Delta x}\right]\right.$$

$$\left(\left[2z-h\right] - \left[z^2-zh\right]\mu^{-1}\left[\frac{1}{2\Delta z}\left[\left(A_t e^{-\alpha T(x,y,z+\Delta z)}\right.\right.\right.\right.$$

$$\left. + B_t\right)e^{\gamma p(x,y)} - \left(A_t e^{-\alpha T(x,y,z-\Delta z)} + B_t\right)$$

Page missing from thesis

(4.4), the following expression for the temperature at a point expressed in terms of the temperature of the six surrounding points is:

$$T(x,y,z) = \left[\frac{1}{2(\Delta y\Delta z)^2 + 2(\Delta x\Delta z)^2 + 2(\Delta x\Delta y)^2}\right]$$

$$\Big[(\Delta y\Delta z)^2\left[T(x+\Delta x,y,z) + T(x-\Delta x,y,z)\right]$$

$$+ (\Delta x\Delta z)^2\left[T(x,y+\Delta y,z) + T(x,y-\Delta y,z)\right]$$

$$+ (\Delta x\Delta y)^2\left[T(x,y,z+\Delta z) + T(x,y,z-\Delta z)\right]$$

$$\frac{-(\Delta x\Delta y\Delta z)^2}{K}\Bigg[\left[\frac{p(x,y)}{C^*}\right]^{\frac{1}{n}} C_v g\Big\{\frac{1}{2}\Big[\Big(A_t e^{-\alpha T(x,y,z)}$$

$$+ B_t\Big)e^{\gamma p(x,y)}\Big]^{-1}\left[\frac{p(x+\Delta x,y)-p(x-\Delta x,y)}{2\Delta x}\right]$$

$$\left[z(z-h) + \frac{(h-z)}{h}U\right]\left[\frac{T(x+\Delta x,y,z)-T(x-\Delta x,y,z)}{2\Delta x}\right]$$

$$+ \frac{1}{2}\Big[\Big(A_t e^{-\alpha T(x,y,z)} + B_t\Big)e^{\gamma p(x,y)}\Big]^{-1}$$

$$\left[\frac{p(x,y+\Delta y)-p(x,y-\Delta y)}{2\Delta y}\right]\Big[(z-h)z\Big]\left[\frac{T(x,y+\Delta y,z)-T(x,y-\Delta y,z)}{2\Delta y}\right]\Big\}$$

$$+ \frac{[p(x,y)]^{\frac{1}{n}}}{C^*}\Big[p(x,y)\Big]\left[\frac{-1}{C^* n}\right]\left[\frac{p(x,y)}{C^*}\right]^{(-1-n)/n}$$

$$\left[\left\{\frac{1}{2}\left[\left(A_t e^{-\alpha T(x,y,z)} + B_t\right) e^{\gamma p(x,y)}\right]^{-1}\right.\right.$$

$$\left[\frac{p(x+\Delta x,y)-p(x-\Delta x,y)}{2\Delta x}\right] z(z-h) + \frac{(h-z)}{h} U\Big\}$$

$$\left[\frac{p(x+\Delta x,y)-p(x-\Delta x,y)}{2\Delta x}\right] + \left\{\frac{1}{2}\left[\left(A_t e^{-\alpha T(x,y,z)}\right.\right.\right.$$

$$\left.\left.+ B_t\right) e^{\gamma p(x,y)}\right]^{-1} (z-h) z\Big\} \left[\frac{p(x,y+\Delta y)-p(x,y-\Delta y)}{2\Delta y}\right]^2 \Big]$$

$$-\left[\left(A_t e^{-\alpha T(x,y,z)} + B_t\right) e^{\gamma p(x,y)}\right] \left\{\frac{1}{2}\left[\left(A_t e^{-\alpha T(x,y,z)}\right.\right.\right.$$

$$\left.\left.+ B_t\right) e^{\gamma p(x,y)}\right]^{-1} \left[\frac{p(x+\Delta x,y)-p(x-\Delta x,y)}{2\Delta x}\right]$$

$$\Big(\left[2z-h\right] - \left[z^2 - zh\right] \Big[\left(A_t e^{-\alpha T(x,y,z)} + B_t\right)$$

$$e^{\gamma p(x,y)}\Big]^{-1} \left[\frac{1}{2\Delta z} \left[\left(A_t e^{-\alpha T(x,y,z+\Delta z)}\right.\right.\right.$$

$$\left. + B_t\right) e^{\gamma p(x,y)} - \left(A_t e^{-\alpha T(x,y,z-\Delta z)} + B_t\right)$$

$$e^{\gamma p(x,y)}\Big]\Big]\Big) - \frac{U}{h}\Big\}^2 - \left[\left(A_t e^{-\alpha T(x,y,z)} + B_t\right)\right.$$

$$e^{\gamma p(x,y)}\Big] \left\{\frac{1}{2}\left[\left(A_t e^{-\alpha T(x,y,z)} + B_t\right) e^{\gamma p(x,y)}\right]^{-1}\right.$$

$$\left[\frac{p(x,y+\Delta y)-p(x,y-\Delta y)}{2\Delta y}\right] \Big(\left[2z-h\right] - \left[z^2 - zh\right]$$

$$\left[\left(A_t e^{-\alpha T(x,y,z)} + B_t\right) e^{\gamma p(x,y)}\right]^{-1} \left[\frac{1}{2\Delta z}\right]$$

$$\left[\left(A_t e^{-\alpha T(x,y,z+\Delta z)} + B_t\right) e^{\gamma p(x,y)}\right.$$

$$\left. - \left(A_t e^{-\alpha T(x,y,z-\Delta z)} + B_t\right) e^{\gamma p(x,y)}\right]\Big)\Big\}^2$$

$$-N \; \tau_p \; \Bigg| \; \frac{1}{2}\left[\left(A_t e^{-\alpha T(x,y,z)} + B_t\right) e^{\gamma p(x,y)}\right]^{-1}$$

$$\left[\frac{p(x+\Delta x,y) - p(x-\Delta x,y)}{2\Delta x}\right] \Big\{ \left[2z-h\right] - \left[z^2 - zh\right]$$

$$\left[\left(A_t e^{-\alpha T(x,y,z)} + B_t\right) e^{\gamma p(x,y)}\right]^{-1} \left[\frac{1}{2\Delta z}\right]$$

$$\left[\left(A_t e^{-\alpha T(x,y,z+\Delta z)} B_t \; e^{\gamma p(x,y)}\right.\right.$$

$$\left. - \left(A_t e^{-\alpha T(x,y,z-\Delta z)} + B_t\right) e^{\gamma p(x,y)}\right]\Big\} - \frac{U}{h} \; \Bigg| \; \Bigg] \Bigg] \; . \qquad (4.20)$$

Equation (4.20) above has been derived in terms of central differences and will converge rapidly if the heat conduction Laplacian part of this differential equation predominates. The energy dissipation terms converge best using forward differences if they are the predominate terms. In order to make a comparison between these two methods, the first term of equation (4.5) was changed to forward differences and a solution obtained for $T(x,y,z)$ using this combination method.

Changing the first term on the right side of equation (4.5) to forward differences yields this form:

$$\text{First term} = \rho C_v \left\{ \left[u \, \frac{T(x,y,z)-T(x-\Delta x,y,z)}{\Delta x} \right] \right.$$

$$\left. \left[v \, \frac{T(x,y,z)-T(x,y-\Delta y,z)}{\Delta y} \right] \right\} . \qquad (4.21)$$

Substituting this term with others previously obtained for RHS of equation (4.5) in equation (4.4) gives the following expression:

$$T(x,y,z) = \left[\frac{1}{2(\Delta y \Delta z)^2 + 2(\Delta x \Delta z)^2 + 2(\Delta x \Delta y)^2} \right]$$

$$\left\{ (\Delta y \Delta z)^2 \left[T(x+\Delta x,y,z) + T(x-\Delta x,y,z) \right] + \right.$$

$$(\Delta x \Delta z)^2 \left[T(x,y+\Delta y,z) + T(x,y-\Delta y,z) \right]$$

$$+ (\Delta x \Delta y)^2 \left[T(x,y,z+\Delta z) + T(x,y,z-\Delta z) \right]$$

$$- \frac{(\Delta x \Delta y \Delta z)^2}{K} \left[\left[\rho C_v \right] \left[u \, \frac{T(x,y,z)-T(x-\Delta x,y,z)}{\Delta x} \right. \right.$$

$$\left. + v \, \frac{T(x,y,z)-T(x,y-\Delta y,z)}{\Delta y} \right] + \text{Second Term}$$

$$\left. \left. - \text{Third Term} - \text{Fourth Term} \right] \right\} . \qquad (4.22)$$

Equation (4.22) may now be solved for T(x,y,z).

$$T(x,y,z) = \left\{\frac{1}{1 + \frac{(\Delta x \Delta y \Delta z)^2}{K}\left[\rho \frac{C_v u}{\Delta x} + \rho \frac{C_v v}{\Delta y}\right]}\right\}$$

$$\left[\frac{1}{2(\Delta y \Delta z)^2 + 2(\Delta x \Delta z)^2 + 2(\Delta x \Delta y)^2}\right]$$

$$\left\{(\Delta y \Delta z)^2\left[T(x+\Delta x,y,z)+T(x-\Delta x,y,z)\right]\right.$$

$$+(\Delta x \Delta z)^2\left[T(x,y+\Delta y,z)+T(x,y-\Delta y,z)\right]$$

$$+(\Delta x \Delta y)^2\left[T(x,y,z+\Delta z)+T(x,y,z-\Delta z)\right]$$

$$-\frac{(\Delta x \Delta y \Delta z)^2}{K}\left[\left[\rho C_v\right]\left[\frac{-uT(x-\Delta x,y,z)}{\Delta x}\right.\right.$$

$$\left.\frac{-vT(x,y-\Delta y,z)}{\Delta y}\right] + \text{Second Term}$$

$$\left.\left.- \text{Third Term} - \text{Fourth Term}\right]\right\} . \qquad (4.23)$$

Pressure Equation in Finite-Differences

Equation (2.46) may be used to calculate the pressure distribution in the bearing by changing the partial derivatives to finite-differences. The resulting algebraic set of equations may be solved for the pressure at all points within the bearing. Since it is assumed that no pressure variation exists in the z-direction due to the thin film, the requirements for pressure variation are only two-dimensional.

Equation (2.46) is

$$p\left[\frac{\partial^2 p}{\partial x^2} + \frac{\partial^2 p}{\partial y^2}\right] = \left[\frac{6\mu U}{nh^2} - \frac{3p\,\frac{\partial h}{\partial x}}{h}\right]\frac{\partial p}{\partial x}$$

$$- \left[\frac{3p\,\frac{\partial h}{\partial y}}{h}\right]\frac{\partial p}{\partial y} - \frac{1}{n}\left[\left(\frac{\partial p}{\partial x}\right)^2 + \left(\frac{\partial p}{\partial y}\right)^2\right]$$

$$+ \frac{6\mu U p\,\frac{\partial h}{\partial x}}{h^3} \,. \tag{2.46}$$

The differentials of equation (2.46) may be expressed by the following linear finite-difference approximations:

$$\frac{\partial p}{\partial x} = \frac{p(k+1,m)-p(k-1,m)}{2\Delta x} \tag{4.24}$$

$$\frac{\partial p}{\partial y} = \frac{p(k,m+1)-p(k,m-1)}{2\Delta y} \tag{4.25}$$

$$\frac{\partial^2 p}{\partial x^2} = \frac{p(k+1,m)-2p(k,m)+p(k-1,m)}{(\Delta x)^2} \tag{4.26}$$

$$\frac{\partial^2 p}{\partial y^2} = \frac{p(k,m+1)-2p(k,m)+p(k,m-1)}{(\Delta y)^2} \,, \tag{4.27}$$

where $p(k,m) = p(k\Delta x, m\Delta y)$. Substituting equations (4.24), (4.25), (4.26), and (4.27) into equation (2.46) yields

$$p(k,m)\left[\frac{p(k+1,m)-2p(k,m)+p(k-1,m)}{(\Delta x)^2}\right.$$

$$\left.+\frac{p(k,m+1)-2p(k,m)+p(k,m-1)}{(\Delta y)^2}\right] =$$

$$\left[\frac{6\mu U}{nh^2}-\frac{3p(k,m)\frac{\partial h}{\partial x}}{h}\right]\left[\frac{p(k+1,m)-p(k-1,m)}{2\Delta x}\right]$$

$$\frac{-3p(k,m)\frac{\partial h}{\partial y}}{h}\left[\frac{p(k,m+1)-p(k,m-1)}{2\Delta y}\right]$$

$$-\frac{1}{n}\left[\left[\frac{p(k+1,m)-p(k-1,m)}{2\Delta x}\right]^2+\left[\frac{p(k,m+1)-p(k,m-1)}{2\Delta y}\right]^2\right]$$

$$+\frac{6\mu Up(k,m)\ \frac{\partial h}{\partial x}}{h^3}\ . \tag{4.28}$$

Multiplying as indicated in equation (4.28) results in the following equation:

$$\frac{p(k,m)p(k+1,m)}{(\Delta x)^2}-\frac{2[p(k,m)]^2}{(\Delta x)^2}+\frac{p(k,m)p(k-1,m)}{(\Delta x)^2}$$

$$+\frac{p(k,m)p(k,m+1)}{(\Delta y)^2}-\frac{2[p(k,m)]^2}{(\Delta y)^2}$$

$$+\frac{p(k,m)p(k,m-1)}{(\Delta y)^2}=\frac{6\mu Up(k+1,m)}{2nh^2\Delta x}$$

$$- \frac{6\mu U p(k-1,m)}{2nh^2 \Delta x} - \frac{3p(k,m)\frac{\partial h}{\partial x}\, p(k+1,m)}{2h\Delta x}$$

$$+ \frac{3p(k,m)\frac{\partial h}{\partial x}\, p(k-1,m)}{2h\Delta x} - \frac{3p(k,m)\frac{\partial h}{\partial y}\, p(k,m+1)}{2h\Delta y}$$

$$+ 3p(k,m)\ \frac{\partial h}{\partial y}\ p(k,m-1)/2h\Delta y$$

$$- \frac{[p(k+1,m)]^2 - p(k+1,m)p(k-1,m) + [p(k-1,m)]^2}{4n(\Delta x)^2}$$

$$- \frac{[p(k,m+1)]^2 - 2(k,m+1)p(k,m-1) + [p(k,m-1)]^2}{4n(\Delta y)^2}$$

$$+ \frac{6\mu U p(k,m)\frac{\partial h}{\partial x}}{h^3}\ . \tag{4.29}$$

Collecting like powers of p, equation (4.29) becomes

$$- [p(k,m)]^2 \left[\frac{2}{(\Delta x)^2} + \frac{2}{(\Delta y)^2}\right] + p(k,m)\left[\frac{p(k+1,m)}{(\Delta x)^2}\right.$$

$$+ \frac{p(k-1,m)}{(\Delta x)^2} + \frac{p(k,m+1)}{(\Delta y)^2} + \frac{p(k,m-1)}{(\Delta y)^2}$$

$$+ \frac{3\frac{\partial h}{\partial x}\, p(k+1,m)}{2h\Delta x} - \frac{3\frac{\partial h}{\partial x}\, p(k-1,m)}{2h\Delta x} + \frac{3\frac{\partial h}{\partial y}\, p(k,m+1)}{2h\Delta y}$$

$$\left. - \frac{3\frac{\partial h}{\partial y}\, p(k,m-1)}{2h\Delta y} - \frac{6\mu U\frac{\partial h}{\partial x}}{h^3}\right] - \frac{6\mu U p(k+1,m)}{2nh^2 \Delta x}$$

$$+ \frac{6\mu U p(k-1,m)}{2nh^2 \Delta x} + \frac{[p(k+1,m)]^2 - 2p(k+1,m)p(k-1,m) + [p(k-1,m)]^2}{4n(\Delta x)^2}$$

$$+ \frac{[P(k,m+1)]^2 - 2p(k,m+1)p(k,m-1) + [p(k,m-1)]^2}{4n(\Delta y)^2}$$

$$= 0 \ . \qquad (4.30)$$

Let $\alpha = \frac{2}{(\Delta x)^2} + \frac{2}{(\Delta y)^2}$ and divide equation (4.30) by $-\alpha$.

Equation (4.30) now becomes

$$[p(k,m)]^2 - p(k,m)\Big[\frac{p(k+1,m)}{\alpha(\Delta x)^2} + \frac{p(k-1,m)}{\alpha(\Delta x)^2} + \frac{p(k,m+1)}{\alpha(\Delta y)^2} +$$

$$+ \frac{p(k,m-1)}{\alpha(\Delta y)^2} + \frac{3\frac{\partial h}{\partial x}\, p(k+1,m)}{2\alpha h \Delta x} - \frac{3\frac{\partial h}{\partial x}\, p(k-1,m)}{2\alpha h \Delta x}$$

$$+ \frac{3\frac{\partial h}{\partial y}\, p(k,m+1)}{2\alpha h \Delta y} - \frac{3\frac{\partial h}{\partial y}\, p(k,m-1)}{2\alpha h \Delta y} - \frac{6\mu U \frac{\partial h}{\partial x}}{\alpha h^3}\Big]$$

$$- \Big[\frac{6\mu U p(k+1,m)}{2\alpha n h^2 \Delta x} + \frac{6\mu U p(k-1,m)}{2\alpha n h^2 \Delta x}$$

$$+ \frac{[p(k+1,m)]^2 - 2p(k+1,m)\ p(k-1,m) + [p(k-1,m)]^2}{4\alpha n(\Delta x)^2}$$

$$+ \frac{[p(k,m+1)]^2 - 2p(k,m-1)p(k,m+1) + [p(k,m-1)]^2}{4\alpha n(\Delta y)^2}\Big] \qquad (4.31)$$

Equation (4.31) is in the form of a quadratic in terms of p(k,m) if the pressure of the surrounding points is considered as a constant. For cylindrical bearings running without shaft deflection there is no gradient in the film in the y-direction. Therefore, $\frac{\partial h}{\partial y} = 0$. In order to simplify the writing of this equation, let

$$C_1 = \left[\frac{p(k+1,m)}{\alpha(\Delta x)^2} + \frac{p(k-1,m)}{\alpha(\Delta x)^2} + \frac{p(k,m+1)}{\alpha(\Delta y)^2} + \frac{p(k,m-1)}{\alpha(\Delta y)^2} + \right.$$

$$\left. + \frac{3\frac{\partial h}{\partial x}\, p(k+1,m)}{2\alpha h\Delta x} - \frac{3\frac{\partial h}{\partial x}\, p(k-1,m)}{2\alpha h\Delta x} - \frac{6\mu U\frac{\partial h}{\partial x}}{\alpha h^3}\right]$$

and

$$C_2 = \left[- \frac{3\mu U p(k+1,m)}{\alpha n h^2 \Delta x} + \frac{3\mu U p(k-1,m)}{\alpha n h^2 \Delta x}\right.$$

$$+ \frac{[p(k+1,m)]^2 - 2p(k+1,m)p(k-1,m) + [p(k-1,m)]^2}{4\alpha n(\Delta x)^2}$$

$$\left. + \frac{[p(k,m+1)]^2 - 2p(k,m+1)p(k,m-1) + [p(k,m-1)]^2}{4\alpha n(\Delta y)^2}\right] .$$

Substituting C_1, C_2 and $\frac{\partial h}{\partial y} = 0$ in equation (4.31) gives

$$[p(k,m)]^2 - C_1 p(k,m) - C_2 = 0 . \qquad (4.32)$$

Equation (4.32) can now be solved for p(k,m). The pressure at a point expressed in terms of the four surrounding pressure points is

$$p(k,m) = \frac{C_1 \pm \sqrt{(C_1)^2 + 4C_2}}{2} , \qquad (4.33)$$

or

$$p(k,m) = \frac{C_1 + \sqrt{(C_1)^2 + 4C_2}}{2} . \qquad (4.34)$$

The other root of equation (4.33) provides a trivial solution for the pressure distribution.

Errors in Finite-Difference Approximations

Equation (4.20) for temperature and equation (4.34) for pressure are not exact solutions of the differential equations involved since the partial derivatives have been approximated by finite-differences. To determine the maximum error in approximating the first-order partial derivative of T with respect to x, consider the following Taylor's series expansions with a remainder term:

$$T(x,+\Delta x,y,z) = T\,(x,y,z) + \Delta x \,\frac{\partial T(x,y,z)}{\partial x}$$

$$+ \frac{(\Delta x)^2}{2}\,\frac{\partial^2 T(x,y,z)}{\partial x^2} + \frac{(\Delta x)^3}{3!}\,\frac{\partial^3 T(x_1,y,z)}{\partial x^3} ,$$

where

$$x<x_1<(x+\Delta x) ,$$

$$T(x-\Delta x,y,z) = T(x,y,z) - \Delta x \frac{\partial T(x,y,z)}{\partial x} + \\ + \frac{(\Delta x)^2}{2} \frac{\partial^2 T(x,y,z)}{\partial x^2} - \frac{(\Delta x)^3}{3!} \frac{\partial^3 T(x_2,y,z)}{\partial x^3}$$

where

$$(x-\Delta x)<x_2<x .$$

If $T(x-\Delta x,y,z)$ is subtracted from $T(x+\Delta x,y,z)$ and the terms rearranged, the result is

$$\left| \frac{T(x+\Delta x,y,z)-T(x-\Delta x,y,z)}{2\Delta x} - \frac{\partial T(x,y,z)}{\partial x} \right| \leqq$$

$$\frac{(\Delta x)^2}{6} \left| \frac{\partial^3 T(x_3,y,z)}{\partial x^3} \right|$$

where x_3 is a suitable number in the range $(x-\Delta x)<x_3<(x+\Delta x)$. Since the left member of the inequality represents the absolute value of the difference between the finite-difference approximation and the partial derivative, the maximum error involved in approximating the first-order partial derivative of T with respect to x is given by

$$\text{Error}_1 < \frac{(\Delta x)^2}{6} \left| \frac{\partial^3 T(x_3,y,z)}{\partial x^3} \right| . \tag{4.35}$$

A similar analysis can be made for the partial of T and p with respect to x, y, or z.

When the second-order partial derivative is approximated, the maximum error involved may again be found by considering the following Taylor series expansion with remainder term:

$$T(x+\Delta x,y,z) = T(x,y,z) + \Delta x \frac{\partial T(x,y,z)}{\partial x}$$

$$+ \frac{(\Delta x)^2}{2} \frac{\partial^2 T(x,y,z)}{\partial x^2} + \frac{(\Delta x)^3}{3!} \frac{\partial^3 T(x,y,z)}{\partial x^3} + \frac{(\Delta x)^4}{4!} \frac{\partial^4 T(x_1,y,z)}{\partial x^4},$$

where

$$x<x_1<(x+\Delta x) \quad ,$$

$$T(x-\Delta x,y,z) = T(x,y,z) - \Delta x \frac{\partial T(x,y,z)}{\partial x}$$

$$+ \frac{(\Delta x)^2}{2} \frac{\partial^2 T(x,y,z)}{\partial x^2} - \frac{(\Delta x)^3}{3!} \frac{\partial^3 T(x,y,z)}{\partial x^3}$$

$$+ \frac{(\Delta x)^4}{4!} \frac{\partial^4 T(x_2,y,z)}{\partial x^4} \quad ,$$

where

$$(x-\Delta x) < x_2 < x \ .$$

Adding T $(x+\Delta x,y,z)$ and $T(x-\Delta x,y,z)$ and rearranging terms results in the following:

$$\left| \frac{T(x+\Delta x,y,z)+T(x-\Delta x,y,z)-2T(x,y,z)}{(\Delta x)^2} \right.$$

$$\left. - \frac{\partial^2 T(x,y,z)}{\partial x^2} \right| \leqq \frac{(\Delta x)^2}{12} \left| \frac{\partial^4 T(x_3,y,z)}{\partial x^4} \right|$$

where x_3 is a suitable number in the range $(x-\Delta x)<x_3<(x+\Delta x)$. The left side of this inequality is the absolute value of the difference between the finite-difference approximation and the partial derivative. Thus, the maximum error involved in approximating the second-order partial derivative of T with respect to x is

$$\text{Error}_2 = \frac{(\Delta x)^2}{12} \left| \frac{\partial^4 T(x_3,y,z)}{\partial x^4} \right| . \qquad (4.36)$$

A similar analysis can be made for the second-order partial derivatives of T and p with respect to x, y, or z.

The maximum errors as defined by equations (4.35) and (4.36) vary with the size of the increment, Δx. If a smaller increment is selected, $(\Delta x)^2$ is reduced and the maximum error is correspondingly reduced. In most of the solutions for T and p, $\Delta x = 0.1$, $\Delta y = 0.1$, and Δz varied with the x-coordinate of the mesh point. Average values of Δz were approximately 0.0002.

CHAPTER V

EXPERIMENTAL INVESTIGATIONS

Theoretical studies of bearing performance mean little to a designer if the physical properties of the lubricants are unknown. Some of the physical properties must be evaluated in actual bearings; others may be determined by isolated tests. From the many possible physical properties to be studied, certain ones were selected for specific determination in order to supply data for theoretical studies of the important design parameters in hydrodynamically lubricated journal bearings. It should be noted that the solution of equations (4.23) and (4.34) for temperature and pressure require the following list of physical properties of the lubricant:

C_v, Specific heat at constant volume.

K, Thermal conductivity coefficient.

n, Exponent for polytropic gas law.

μ, Absolute viscosity.

ρ, Density.

τ_p, Shear strength of particles.

Of these, C_v and K are sufficiently well known over the normal range of operation to permit good design accuracy, but values of n, μ, ρ, and τ_p are not available for multiphase lubricant mixtures. Actual bearing performance is most affected by the viscosity of the liquid and by the shear strength of the solid particles; therefore these quantities must be accurately determined. The exponent, n, is used to establish the density of highly compressible mixtures.

Final experimental investigations were made in a full-size bearing test machine. From these tests, it was possible to determine the accuracy of theoretical solutions and determine the shear strength of several solids when used in a bearing.

The experimental investigations were separated into three independent test programs. Each of these tests required apparatus and instrumentation peculiar to the physical quantity under investigation.

Instrumentation and Equipment

Compressibility Apparatus

Several experimental methods were considered for determining the compressibility of the highly compressible lubricants. These included tests using shock waves, bouncing pistons, and compressors. Of these, the compressor test was selected because apparatus was readily available.

A modified variable-compression C.F.R. (Combustion Fuel Research) engine manufactured by the Waukesha Motor Company was used as a compressor. Engine specifications were:

Bore	= 3.24 inches
Stoke	= 4.50 inches
Displacement	= 37.4 cu. in.
C. F. R. Model	= 11-34.

During those tests, the engine was electrically driven through a V-belt drive at speeds of 582 and 888 rpm. Fig. 6 shows the over-all test apparatus. This figure shows the oil pump connected to a Reeves Vari-Speed Motor-drive, model D75758. A Racine Seco Piston Pump, Model 80-LAM was used. This pump is a positive displacement pump capable of delivering three gallons per minute at 500 psia and 1750 rpm. The oil was pumped through a spray nozzle into the engine intake manifold.

A slightly different arrangement was used to test gas-solid lubricants. Solid particles of lubricant dust were suspended in a moving gas stream by using a dust generator as shown in Fig. 7. Two gas streams were necessary, one to blow from the bottom to the top in order to fluff the dust, and another tangential gas jet to rotate the dust-laden gas as in a cyclone dust trap. The fine dust particles suspended in the gas stream at the center of this dust generator were taken out of the center of the top of the dust generator. Heavy masses of particles which were stuck together would be thrown to the outside and fall back to the bottom for another cycle. A mechanical vibrator

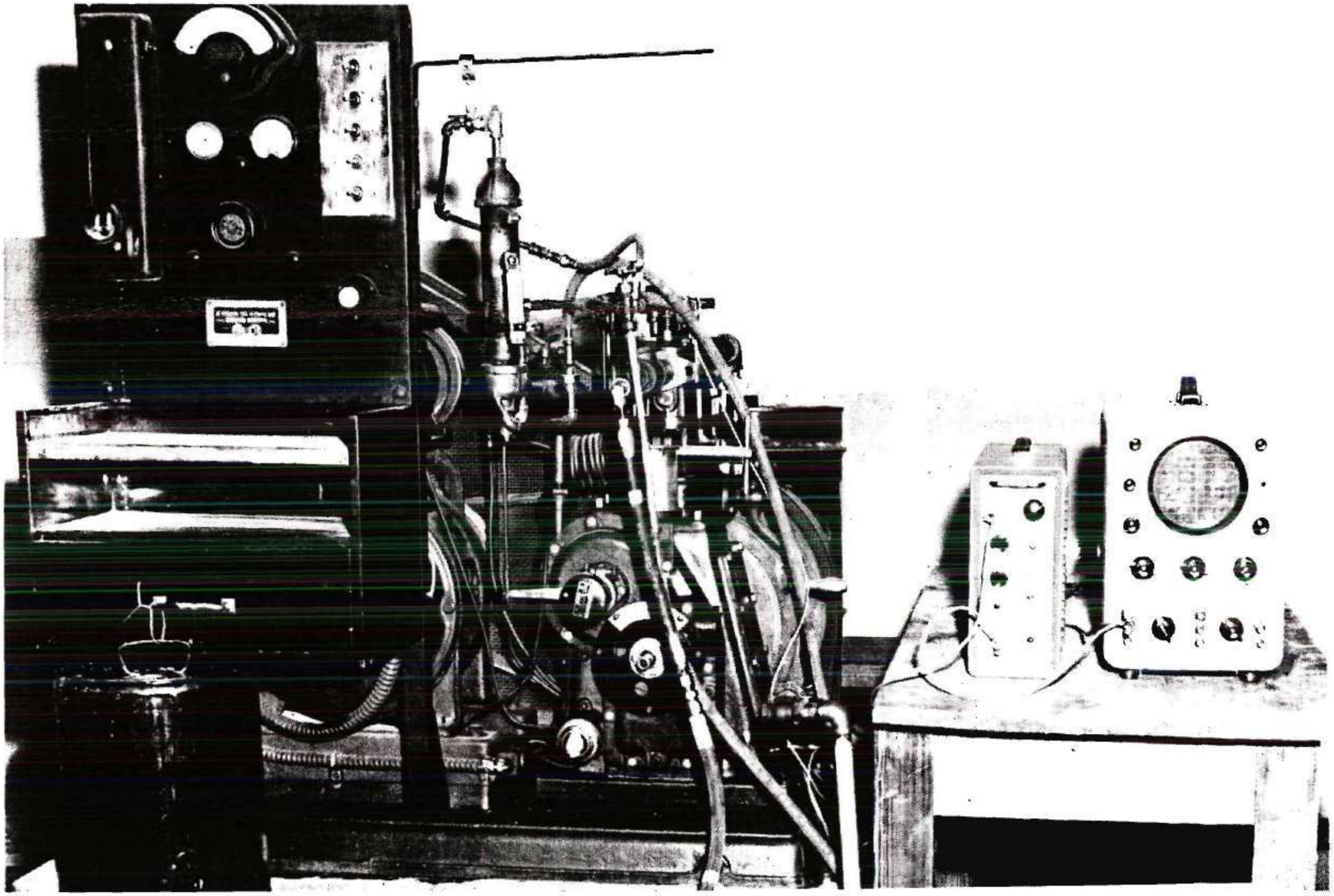

Figure 6. Compression Test Apparatus

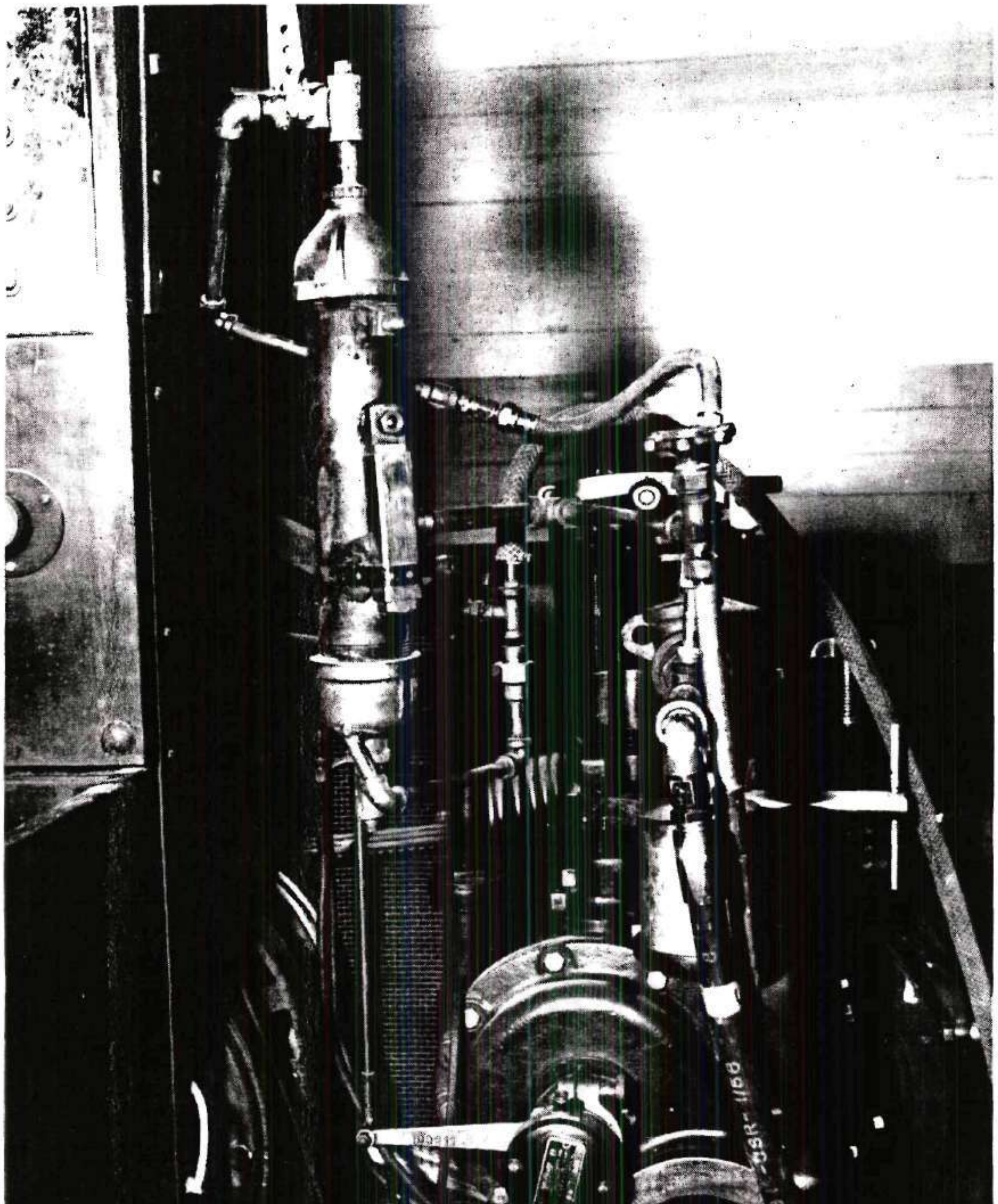

Figure 7. Dust Generator

was attached to the dust generator to keep the bottom gas stream from channeling through the dust bed.

Cylinder pressure was measured by an electric strain gage pressure transducer made by Statham Instruments Incorporated. Specifications for this model are:

Nominal Bridge Resistance = 350 ohms

Range, 0-300 psia

Compensated Temperature Range, -65 to 250°F

Full Scale Output = 56 millivolts at 7 volts

Non-linearity and Hysteresis = $\pm$ 0.75% of full scale.

Model PA-208TC.

This pressure transducer was mounted in the bouncing-pin port of the compressor cylinder sleeve. Output from the transducer was fed through a Sanborn Carrier Preamplifier, model 350-1100, into one channel of a Hewlett Packard dual channel oscilloscope, model 122A. Timing marks were made on the oscilloscope screen by feeding the output from a Hewlett Packard Electronic Counter, model 522B, into the other channel of the oscilloscope. A photoelectric attachment reflectively picked up marks on the compressor flywheel. These trace fluctuation marks can be seen on the scope pictures shown in Fig. 8. The compressor volume was accurately determined from the timing marks recorded with the pressure.

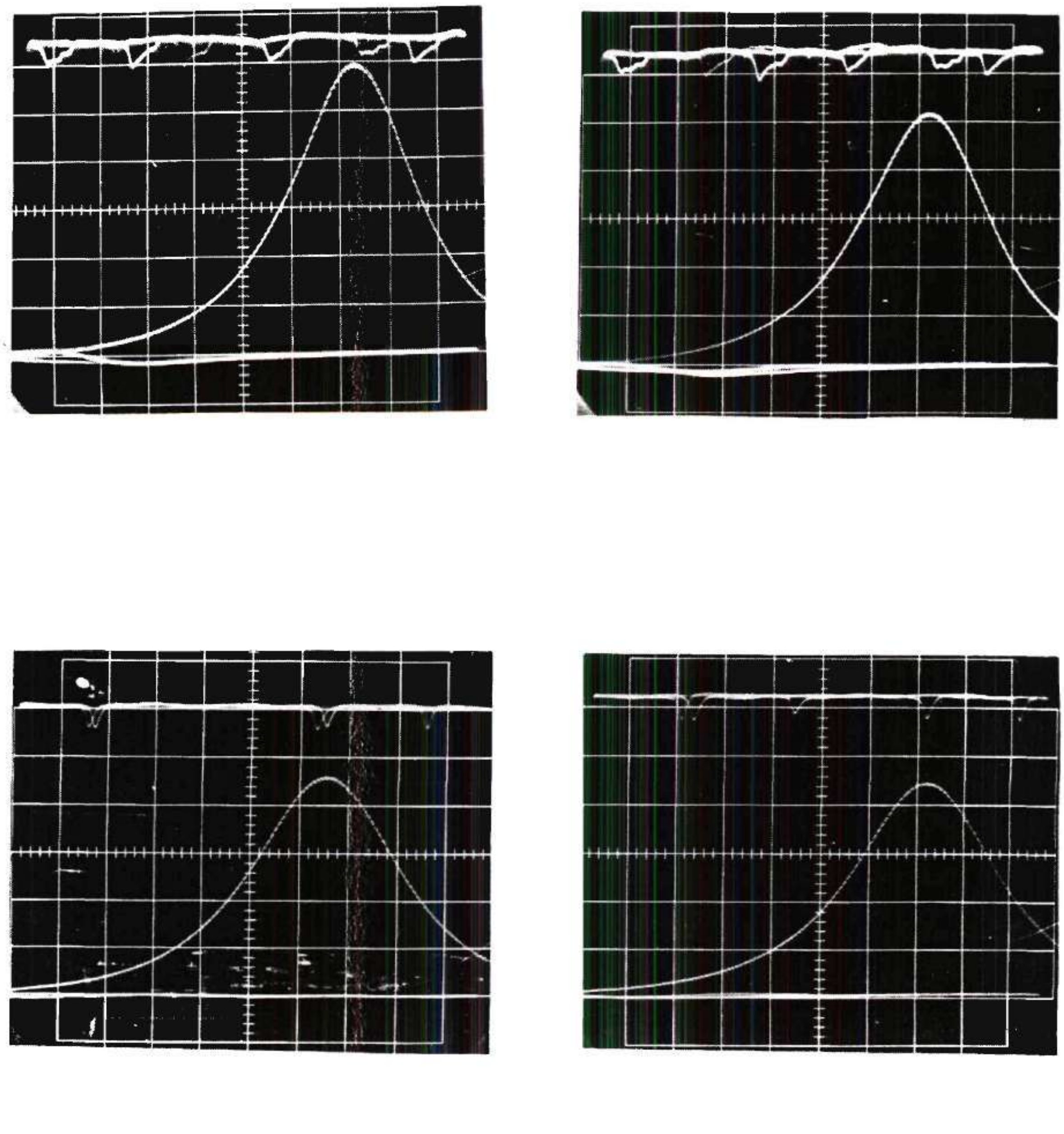

Figure 8. Oscilloscope Record of Pressure

Gas Absorption Apparatus

Earlier tests on gas-liquid solutions (18) pointed out the need for accurate data on the viscosity. Experimental apparatus used to measure the density, viscosity, and amount of gas absorbed is shown in Fig. 9 and Fig. 10. This apparatus consists of a controlled temperature box with a circulating system, volume measurement system, pressure measurement system, and viscosity measurement system. Fig. 11 shows a schematic diagram of this system with the location of valves and sensing devices.

The entire apparatus was designed to hold a constant temperature from 20 to 300 degrees Fahrenheit, sustain internal pressures from a vacuum to one thousand psig, and to circulate gas through the liquid. Data were taken for several three-phase and two-phase lubricants; therefore, it was necessary to circulate and handle each of these lubricants in this system.

The visual cell shown was the last of several designs used to measure the volume of the liquid-solid phase. Electrical probes and a mercury displacement system were found much more difficult to read accurately than a direct visual measurement of the liquid level. A direct reading Griffin and George Ltd. cathatometer, model number 7156, was used to measure the liquid level to 0.001 centimeter. The visual cell was machined from a 10-inch long, 4-inch diameter stainless steel bar which was bored out to a 2-inch internal

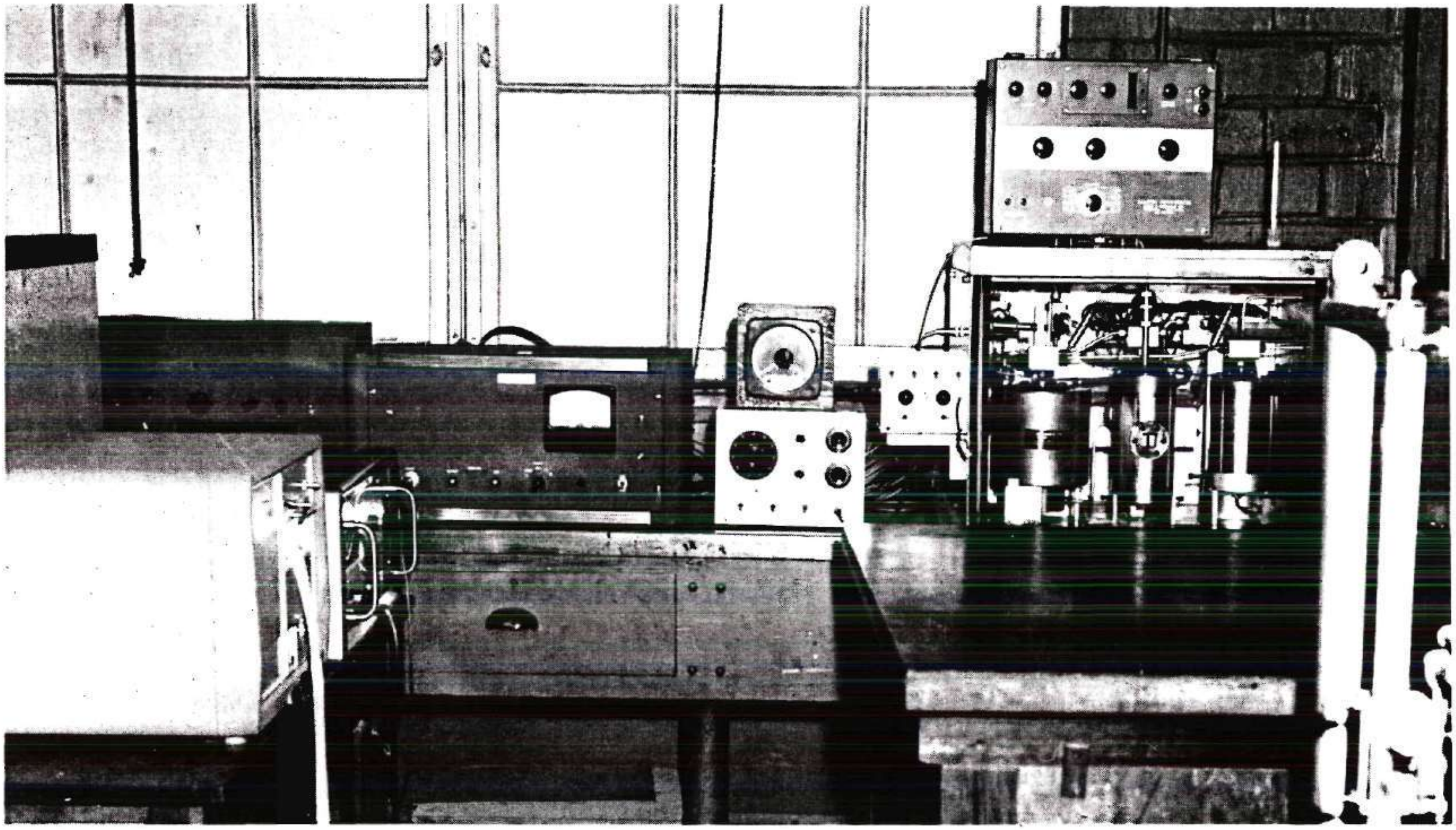

Figure 9. General View of Gas Absorption Apparatus

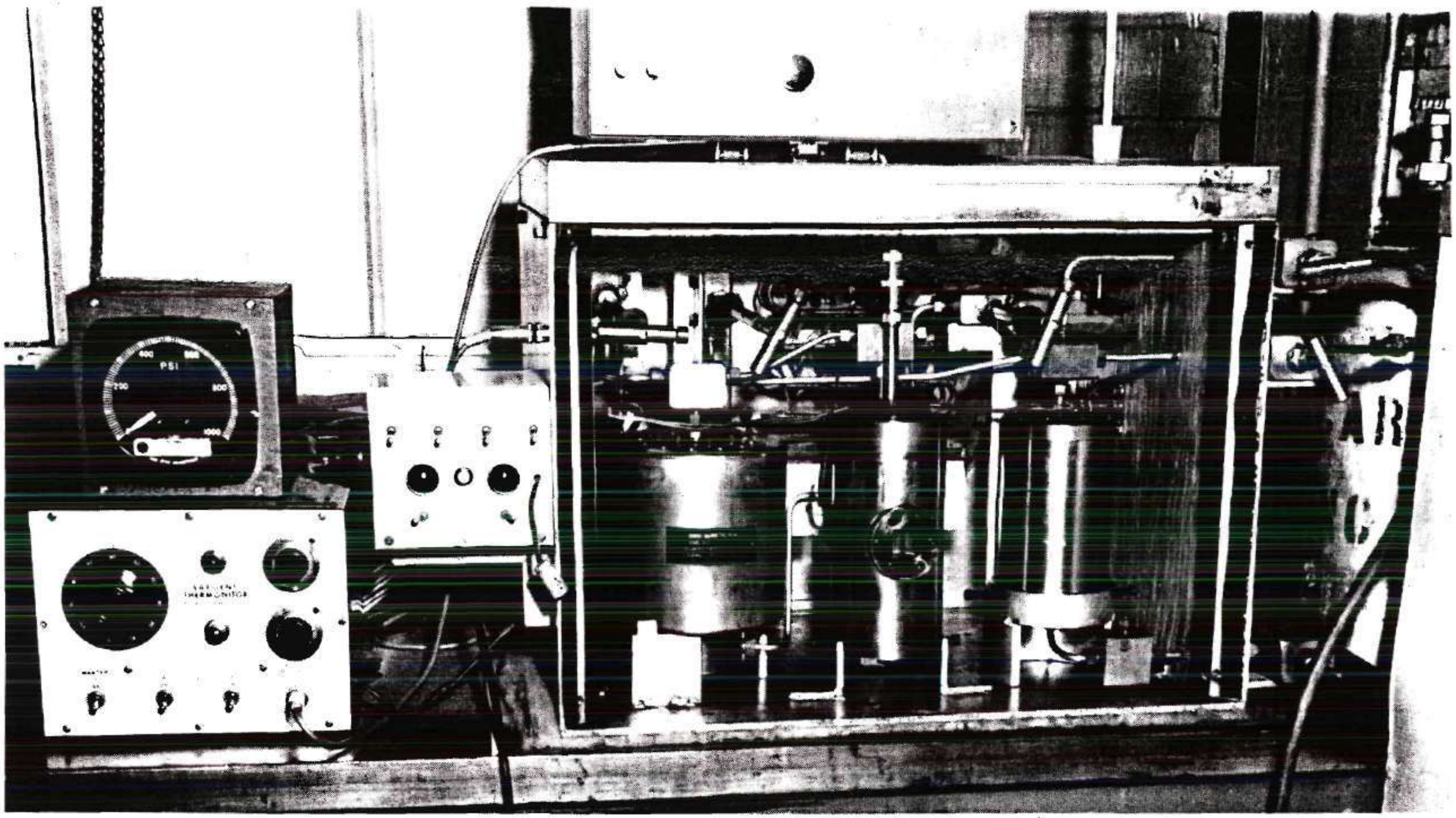

Figure 10. Close-Up of Gas Absorption Apparatus

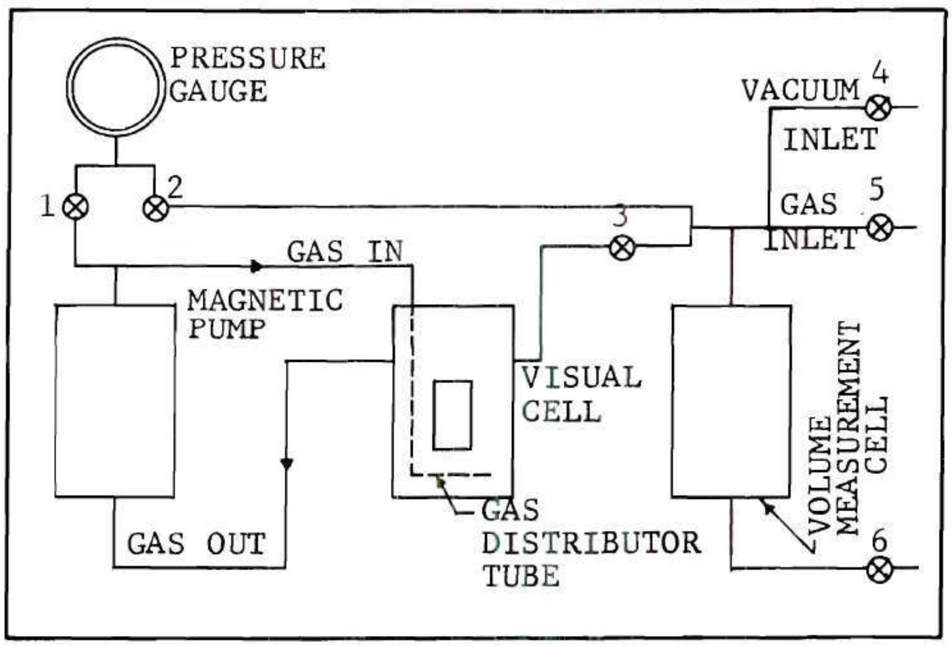

Figure 11. Schematic Drawing of Gas Absorption Apparatus

diameter. A circular tempered glass window 2.00 inches in diameter and 1/2-inch thick was attached to the cell with eight 1/4-inch bolts and an O-ring seal. The top closure carried the Bendix Ultraviscoson probe and the gas-distributor tube and was sealed to the cell with another O-ring.

Gas was circulated by a Coleman Instrument Company magnetic pump, model number 200. Since leakage could not be tolerated, a pump of this type was a necessity. Pumping rate and stroke were variable through an external control box. System pressure was monitored by a Taber Instrument Company, 350 ohm, Teledyne, pressure transducer and was read on a Taber Instrument Company pressure indicator, model 216. The same transducer was valved to either side of the system, so that good relative data were obtained, but this valving introduced a small volume transfer from one side of the volume measurement system to the other; thereby the data reduction was complicated.

Heating and cooling inside the box were controlled by a Sargent, model S, Thermonitor Controller connected to a 150-watt control heater. The 500-watt base heater was controlled by a variable transformer. Cooling was obtained by circulating a refrigerant through the tubed heat exchanger. Cold water was sufficient for most of these tests. When cooling was required, the control heater was used to maintain constant temperature in the box. A small circulating fan inside the box helped to maintain a uniform temperature distribution.

Viscosity was continuously measured by a Bendix Ultraviscoson viscometer which was comprised of a small probe and an electric analog computer. The analog computer was designed and constructed specifically for these tests by modifying the Bendix design. A direct output was available from a meter in the instrument, but this meter was not used to obtain data because of poor accuracy. The electrical output from the computer was fed into a Hewlett Packard, model 405 AR, automatic D.C. digital voltmeter which continuously monitored the output voltage. Data from this voltmeter were recorded on a Hewlett Package model 561B digital recorder. Calibrating fluids with known viscosities were used to obtain a relation between voltage output and fluid viscosity.

The Bendix probe is of particular interest due to its small size and ability to accurately measure viscosity over a wide range (0.1 centipoise to 50,000 centipoise). Samples as small as 4 cubic centimeters may be accurately investigated. A magnetostrictive transducer is used to vibrate a probe at 28 kilocycles per second. The special magnetostrictive alloy probe extends from the center of a thin diaphragm seal at the end of the probe housing. When the probe is immersed in a liquid, the vibrating metal strip forms shear stresses with the liquid which radiate into the liquid. Thus vibrations from the metal strip are damped by the elastic and dissipative properties of the test liquid.

The viscometer operated by measuring the attenuation, as a function of time, of the elastic wave which is magnetostrictively induced in the metal strip of the probe. Maximum vibration amplitude of the probe is 1/2 micron. These vibrations decay to zero at a rate proportional to $e^{-\alpha t}$, where α is the damping factor of the liquid. Maximum errors in the viscosity measurements are less than 3 percent when the instrument is properly calibrated.

Two temperatures were measured. A thermocouple 1/2-inch inside the visual cell was read on a Leeds and Northrup potentiometer, catalog number 8686. Air temperature inside the insulated box was measured with a thermometer.

Bearing Test Machine

This machine was designed to study lubricants and bearings with unidirectional loading. Since this machine had to serve as a multipurpose tester, it was necessary to use additional instrumentation and a more accurate means of loading than that required for a load-friction device. A general view of the test machine is shown in Fig. 12 and Fig. 13. Schematic drawings of this machine are shown in Fig. 14 and Fig. 15.

The test journal was supported by two stationary

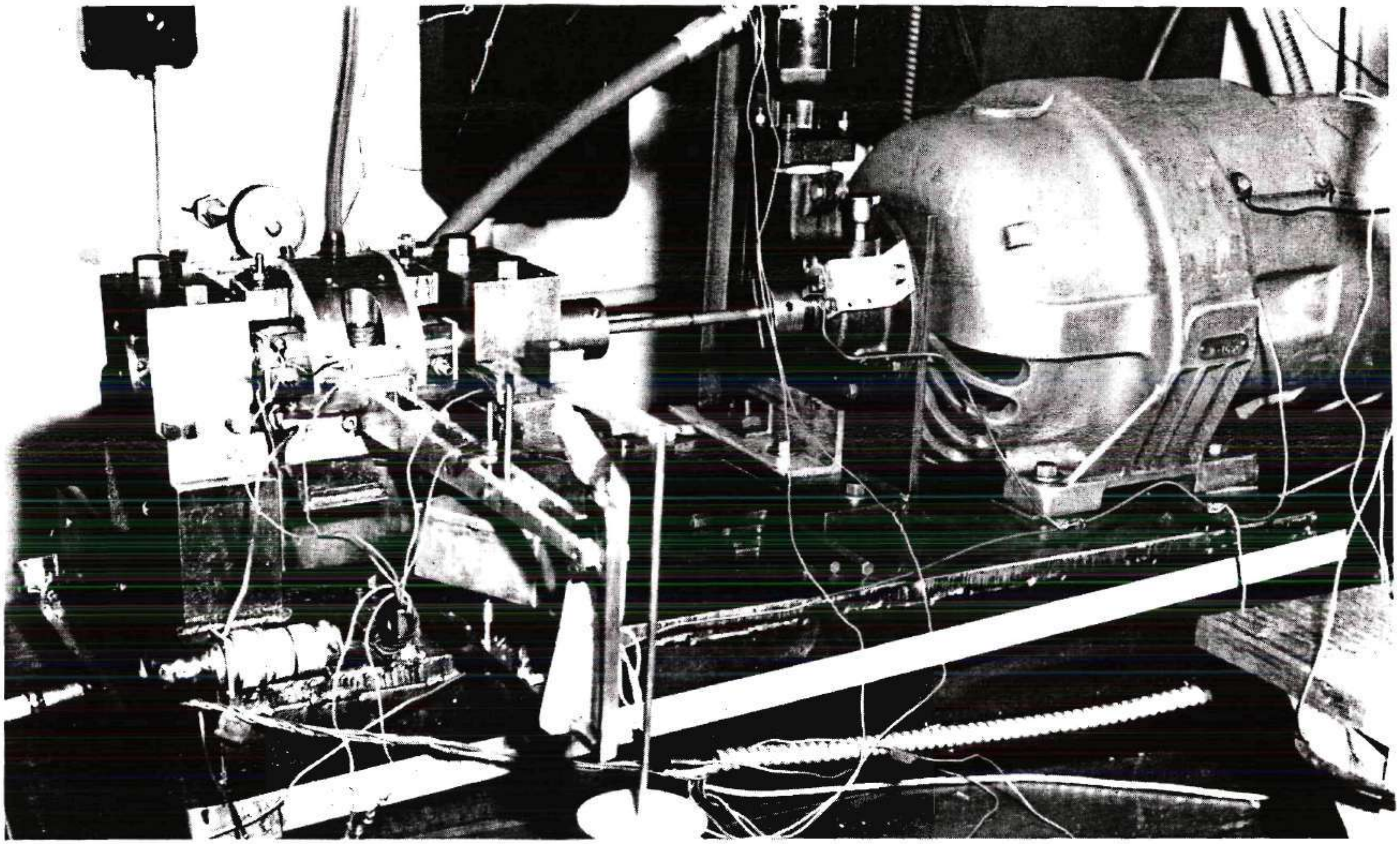

Figure 12. Bearing Test Machine

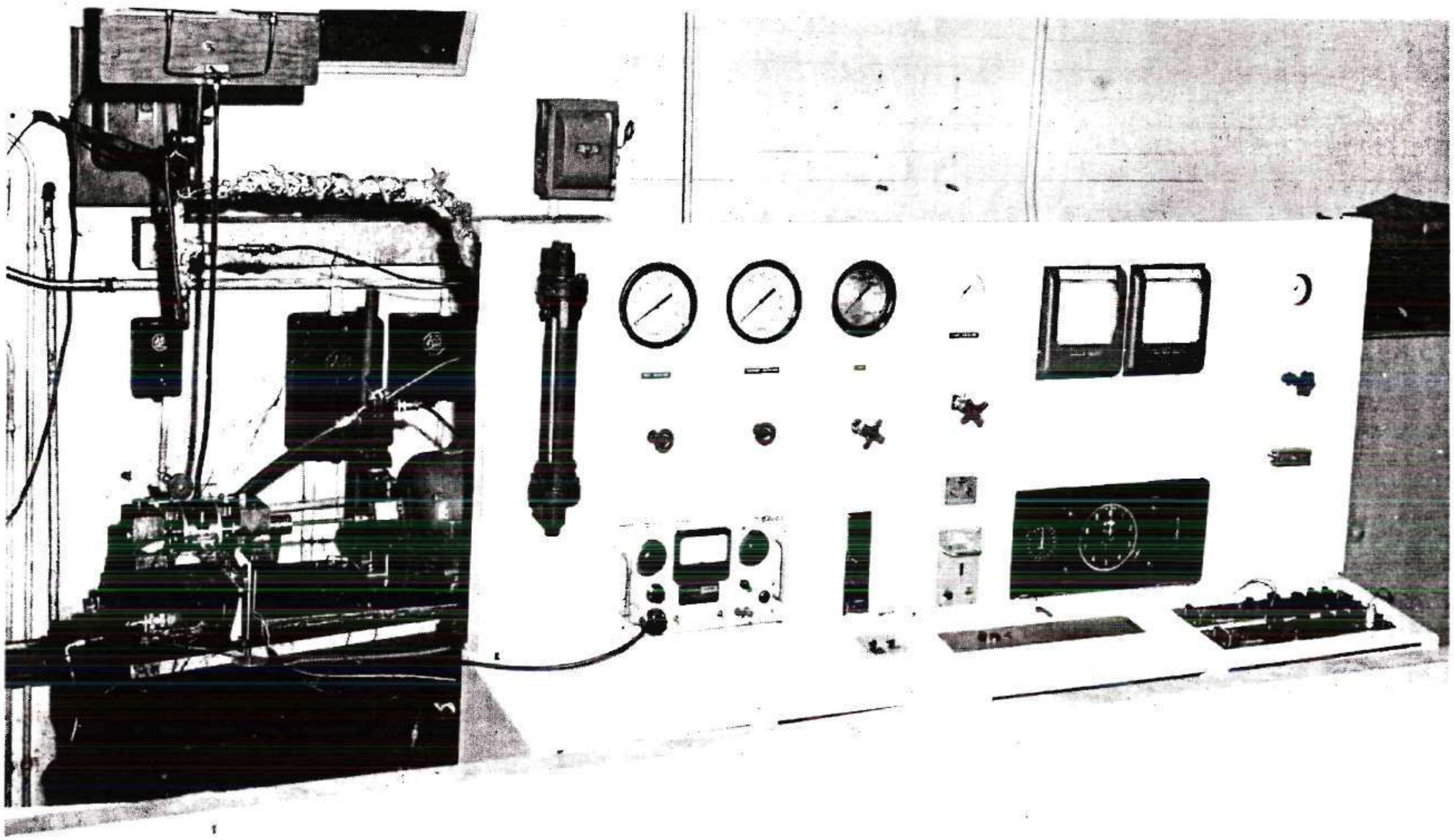

Figure 13. Instrumentation and Controls

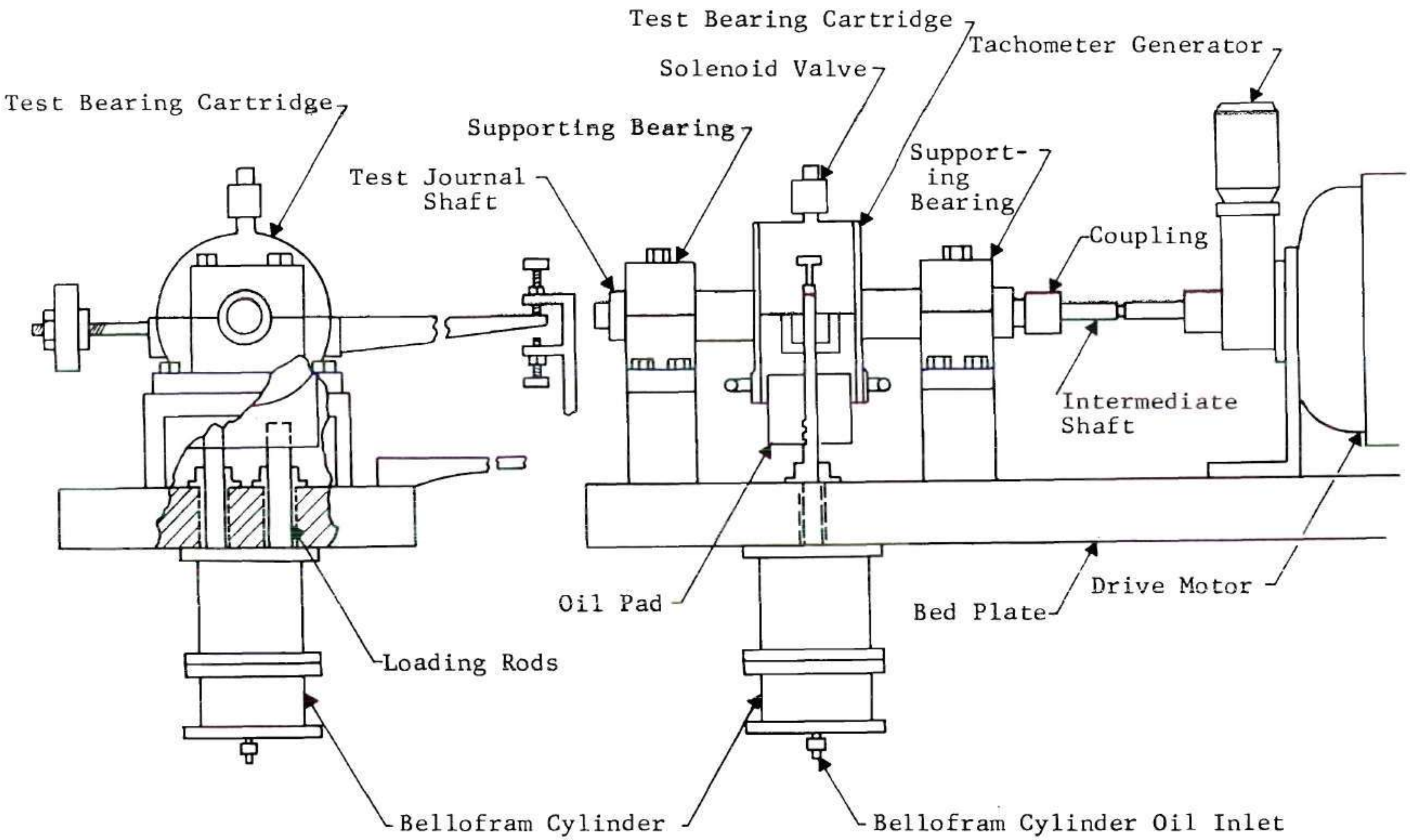

Figure 14. Schematic Diagram of Bearing Test Machine

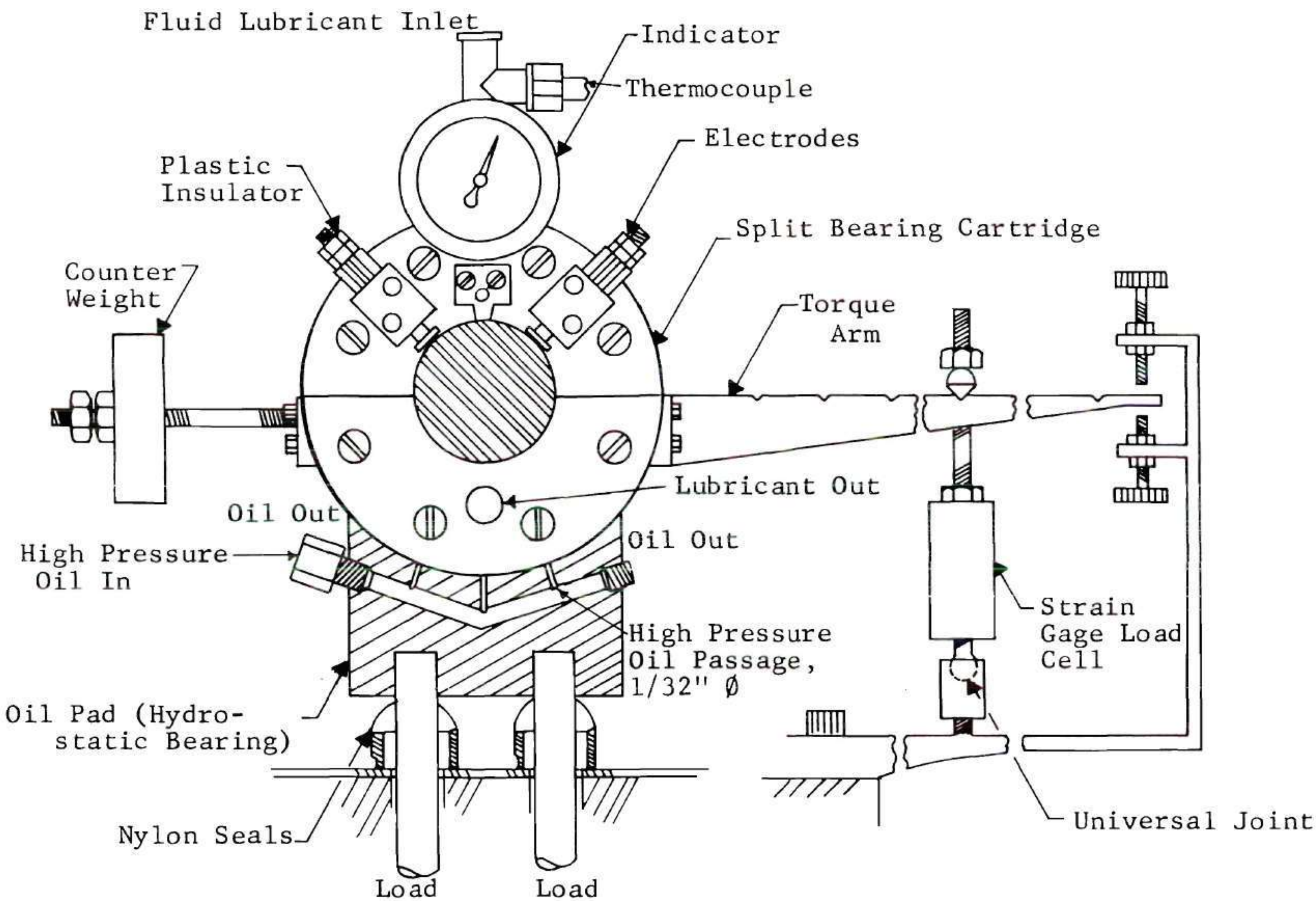

Figure 15. Schematic Diagram of Test Bearing Housing

force-fed journal bearings identical to the test bearing. A 5-horsepower Louis Allis Type E. G. Adjusto-Speed drive was direct-coupled to the test shaft with a small intermediate shaft. Excellent speed control was obtained by an electronic governor which permitted operation at any speed between 330 rpm and 3550 rpm.

Radial load was applied to the test bearing through a hydrostatic bearing between the test bearing housing and a cylindrical loading saddle. This loading saddle or oil pad is shown in Fig. 16 with the test bearing housing. High pressure oil enters through six 1/32-inch diameter holes on the curved, ground, saddle surfaces, forming a hydrostatic flotation film between the saddle and the bearing cartridge. This hydrostatic bearing provides an essentially frictionless connection between the test bearing cartridge and the load, in order to permit the measurement of friction torque. Experiments by Potts (14) indicate that a coefficient of friction of the order of 10^{-6} is to be expected for this type of bearing. This amount of torque is negligible compared to the test bearing friction.

A "bellofram" hydraulic load cylinder located as shown in Fig. 14 was used to load the test bearing. The first design used a hydraulic piston, but friction within this unit produced inaccuracies in the radial load calculations and it was later abandoned for a much better design. The bellofram is essentially frictionless with all of the advantages of hydraulic loading. Load calibration tests with strain gages on the lifing rods shown in Fig. 14, proved the radial load to be directly proportional to the oil pressure in the bellofram load cell. A calibration curve for this load cell is shown in Fig. 49.

Friction torque was measured by the resistive force required to prevent the bearing housing from rotating. The force measurement cell was mounted between a stationary beam extension of the frame and the torque arm as shown on Fig. 14. Provision was made for measuring a wide variation in torque by moving the force cell to various radial positions along the torque arm. The force cell was an elastic steel ring of rectangular cross section with four Baldwin SR-4 strain gages bonded to the internal and external surfaces by epoxy resin adhesive. A universal joint was used in the connecting link to the support beam to prevent bending strains due to non-colinear forces across the force cell.

The four gage bridge of the load cell was connected to a Sanborn strain gage amplifier which supplied an A.C. carrier voltage to the bridge. The direct current voltage output of the Sanborn amplifier was fed to a Varian Model G-11A, null-balance, strip chart recorder, type B1 input. This instrumentation provided a continuous torque reading.

The test bearing housing is shown on Fig. 16 with a schematic diagram on Fig. 15. This housing was split at the horizontal center line such that the test bearing could be

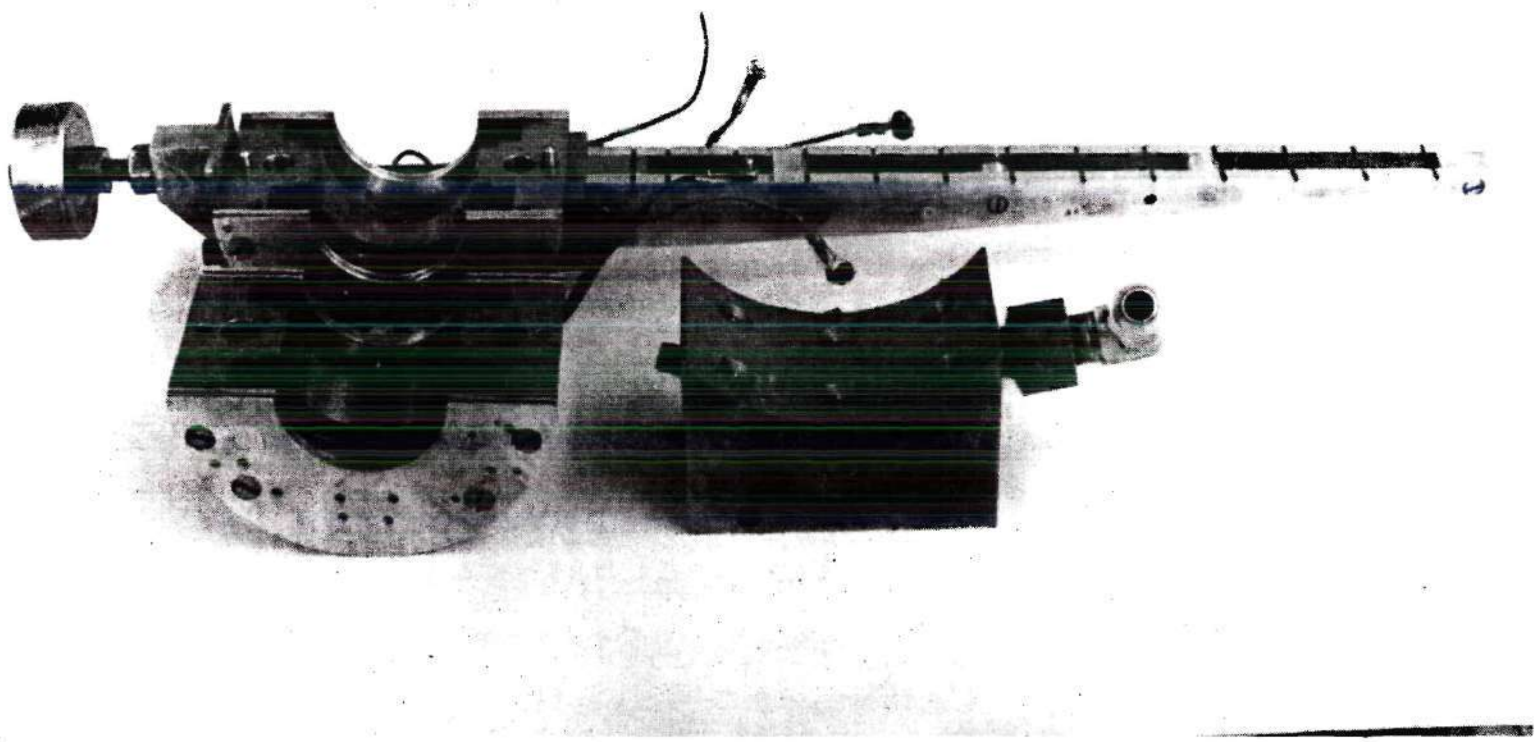

Figure 16. Test Bearing Housing and Oil Pad

replaced or inspected without removing the lower half of the housing. Both the torque arm and the counterbalance were attached to the lower half along with the drain lines and thermocouples. This design feature made the upper half free of instrumentation with only the oil inlet line complicating the replacement of a bearing. Two 5/8-inch diameter bolts were used to fasten the upper bearing cap to the lower half. The lubricant entered through a 1/4-inch diameter radial center hole in the upper half and drained out two identical exits on the two side covers. Spiral groove oil seals were used on each side of the test bearing to provide a minimum of friction. When the shaft was rotated, air was drawn through these seals to keep the oil inside the housing. Operating properly, these seals only require enough torque to shear the air film between the shaft and seal.

Automotive type, steel backed, strip bearings were tightly fitted into each half of the housing. A slight crush of approximately 0.003 inch on the diameter assured conformance of the strip bearing to the cylindrical base of the housing. A thermocouple junction for reading the test bearing temperature was spring-loaded against the outside surface at the center of the lower half bearing. Several test bearings were drilled so as to solder a thermocouple junction near the active bearing surface. Readings from these thermocouples were only slightly higher than readings from the back side of the shell. Since soldering to the shell produced some distortion of the bearing surface, this practice was exchanged for the spring loaded thermocouple.

Temperature readings for the bearing, oil in, oil out, housing, and the room were fed to a Datex stepping switch and from there to a Varian Model G-11A strip-chart recorder with a type T2 input chassis. Each thermocouple was read on the chart as programmed by the Datex stepping switch. All temperatures could be read in three seconds.

Shaft speed was measured by a Model 6 Standard Electric Time Company Chrono-Tachometer. This unit provided a continuous reading as well as a revolution count over one-tenth of a minute.

A proximity meter, capacitance gage made by the Robertshaw-Fulton Controls Company was used with four probes to measure the film thickness. This instrument was designed to accurately measure to one-millionth of an inch. It was found that the extreme sensitivity could not be fully utilized due to thermal expansion of the housing, shaft, and probes. Two perpendicular coordinates of radial displacement were measured at each of two positions on each side of the test bearing. These probes were also used to determine the radial clearance between the shaft and bearing.

Test Procedure

Lubricant Compressibility

The C. F. R. compressor was first set for a compression ratio of 6.76 to one so that the 300 psig maximum pressure rating of the pressure transducer would not be exceeded. All experimental investigations were conducted at this compression ratio. In order to make this setting, the clearance volume was determined by volumetric oil measurement. The head-space micrometer was set at zero for this volume measurement, then reset to obtain the desired compression ratio.

Calibration of the pressure transducer was obtained by static tests and checked dynamically from the results of air compression. A standard setting was 40 psi pressure per centimeter deflection on the oscilloscope screen. Very good reproducibility was obtained.

The following test procedure was used for all tests:

1. Turn on electronic equipment and allow 30 minutes to become stabilized.
2. Start compressor and check jacket water temperature until stabilized.
3. Check the pressure calibration and adjust to standard if necessary.
4. Start injection of lubricant (solid or liquid) into the air intake.
5. Photograph the pressure time curve displayed on the oscilloscope.

6. Measure the weight of lubricant flowing per unit of time.
7. Record barometric pressure, the wet and dry bulb air temperatures, the temperature of the lubricant, rpm of the compressor, jacket temperature, air flow rate, and lubricant flow rate.
8. A photographic negative was developed and projected on a calibrated screen to obtain readings of volume and pressure in the cylinder.

Test variables included the weight ratio of lubricant to air, the drop size, the liquid viscosity, speed of compression, and cylinder jacket temperature. Since liquid was much easier to control than solids, most of the testing was done on oil injected into air. The lubricant flow rate was difficult to control with solid lubricants; whereas, oil could be pumped by a metering pump with very close control.

Gas Absorption

Prior to the actual tests, volume measurements were obtained for each section of the apparatus. These measurements were made by filling the section with measured volumes of liquid. Best results were obtained by putting a vacuum on the system; then a valve was opened to the liquid so that it would be drawn into the system. The volume measurements were needed for the calculations using p-V-T (pressure-volume-temperature) relations. Calculated volumes checked the measured volumes closely.

A liquid sample of known weight was charged into the visual cell after it was cleaned and dried. The vacuum pump was then started and allowed to run until no signs of bubbles were visible through the sight glass. Leaks into the system were normally detected at this stage when bubbles continued to pass through the liquid.

The viscosity measuring system was checked for the dead oil viscosity against the viscosity supplied by the manufacturer and confirmed by tests in a Saybolt apparatus. The oil volume was measured by reading the oil level through the sight glass with the cathatometer. A reference mark on the visual cell served as a reference for all readings and was used to calculate the oil volume using the area of the oil column in the visual cell.

For each experimental run, the temperature of the test apparatus was allowed to maintain equilibrium. Several hours were normally required for thermal equilibrium and overnight runs were even better. Gas was charged into the system from a gas cylinder into the volume measurement cell. For this operation, valves 1, 3, 4, and 6 as shown in Fig. 11 were closed, and valves 5 and 2 were opened. Pressure readings were observed until the desired charge was obtained in the volume measurement cell. At this point, valve 5 was closed and all temperatures and pressures recorded.

From the p-V-T relations the weight of gas charged into the volume measurement cell was obtained.

Gas was admitted to the oil from the charge in the volume measurement cell by first closing valve 2; then valve 1 was opened; then valve 2 was partially opened until the desired pressure was obtained in the visual cell. At this point, valve 2 was closed; then the magnetic pump was started and adjusted to pump small amounts of the gas through the distributor tube to bubble through the oil. Pressure and viscosity were continuously monitored to determine equilibrium conditions. As long as gas was being absorbed, the pressure would continue to decrease. This process normally required 30 minutes for good equilibrium, but tests with very viscous liquids required longer times at low temperatures. When equilibrium was reached, the magnetic circulating pump was turned off; then all readings of pressure, temperature, liquid level, and viscosity were made. In order to valve the pressure transducer back to the volume measurement cell, it was necessary to close valve 1 and open valve 2. This process allowed a small volume of gas to be transferred from the visual cell back into the volume measurement cell side of the system. The same volume was involved in an exchange of gas into the visual cell system when charging. Even though these volumes were small, they did represent appreciable weights relative to the amount of gas absorbed and must be considered in the calculations.

The amount of gas absorbed by the oil was obtained by calculating the weight of gas remaining above the liquid and in the volume measurement cell after absorption. This weight of gas was subtracted from the original weight of gas in the volume measurement cell. Since this small amount of gas was obtained by subtraction, it was necessary to obtain accurate data and make exacting calculations using gas compressibility factors for real gases. A digital computer was used to reduce the data. This program is shown in the Appendix, Section C.

Additional gas was admitted into the volume measurement cell in order to obtain higher pressures in the visual cell. The same process of valving and measurement was used for a recharge as in the first charge outlined above; however, the calculations must take into account the weight of gas already in the system from previous runs. Any error in measurement or leak in the system will be amplified in the results; thus it is necessary to pump down the system at the end of each test and check the oil volume to be certain no liquid was lost in the test cycle.

Gas leak tests were made at the highest equilibrium pressures in the test cycle. The system was allowed to rest for several hours while pressure readings were recorded for the visual cell. Leaks could be detected by decreasing pressures. Any run with appreciable leakage values was voided.

Bearing Performance

Test programs using the bearing test machine were arranged so as to obtain a maximum of machine running time on each bearing and shaft combination. Each test series was started with a new bearing and new shaft position. This same combination of shaft and bearing was used for only one type of solid lubricant because of the effect of the embedded lubricant.

Calibration of the bearing torque measuring instrumentation was obtained by using a dummy shaft fitted with ball bearings to fit the support bearing housings. With the dummy shaft in place, the counterweight was adjusted to give a zero reading on the torque measuring load cell. Errors caused by the ball bearing friction were minimized by applying torque in the clockwise direction then reversing to a counterclockwise direction. Torque readings were equalized for the two directions by adjusting the counterbalance location. After obtaining a zero position, a torque calibration curve was obtained by applying a known torque to the housing by using weights. This calibration curve is shown in Fig. 48, Appendix E. Electrical zeros could be obtained throughout the test series by depressing the torque arm, in order to release the force on the load cell. The electrical "calibrate" was used to reset the gain during the course of a run.

Bearing radial clearance was obtained in several ways. Direct measurements of the bearing inside diameter and shaft diameter gave the clearance by subtraction. Another method which was simple and accurate used a strip of non-resilient plastic wire sold under the name "Plastigage." This material was placed between the bearing and shaft on one side of the bearing; then the bearing cap was tightened so that the plastic strip was flattened. The width of the flattened strip was measured and gave accurate bearing clearances when used with a good calibration of the plastic wire. Since there were variations in clearance at different circumferential locations around the bearing, a theoretical clearance was obtained by running the bearing full of oil without load. Sufficient data were recorded to calculate the bearing clearance by using the Petroff equation (2.11). Direct readings of the clearance were made by using the Robertshaw-Fulton proximity meter.

Independent calibrations were made on the other instrumentation including all pressure gages, load cylinder, torque load cell, tachometer, proximity meter, torque recorder, and temperature recorder. All instruments were periodically checked to maintain good accuracy.

A few tests involved dry bearings using gas-solid lubrication. These tests were conducted on bearings with large clearances ($c/r = 0.0015$). All other tests were run first with clean oil to get a bearing calibration; then the lubricant was changed to multiphase and the same tests repeated. The following steps were used as standard test procedure:

1. Turn on lubricant heater and agitator.
2. Start the support bearing oil pump.
3. Turn on all electronic instrumentation.
4. Start circulating test bearing lubricant.
5. Start pump to hydrostatic bearing on the oil pad.
6. Start drive motor and bring shaft speed to 500 rpm.
7. Start load pump with low pressure setting; then adjust for proper load.
8. Bring shaft speed up to desired speed and wait for equilibrium temperature on the test bearing.
9. Check calibration and zero setting on all electronic instrumentation.
10. Read data when equilibrium temperature is established in order to obtain bearing temperature, bearing housing temperature, lubricant inlet temperature, lubricant outlet temperature, ambient temperature, torque, shaft speed, load, lubricant supply pressure, lubricant flow rate, and pressure on the oil pad.

After a complete series of tests on a bearing, it was removed for inspection. If the shaft or bearing showed signs of wear, the clearance was rechecked. Solid lubricants sometimes pack in the converging wedge between the lubricant supply point and the minimum clearance point. The degree of packing was noted. This conditions was sometimes observed as a decrease in bearing clearance.

CHAPTER VI

DISCUSSION OF RESULTS

Multiphase Lubricants

Results pertaining to the physical properties of multiphase lubricants from the three independent test programs will be discussed separately. The relation between these physical properties and bearing performance will be discussed later as it pertains to the pressure distribution, load capacity, temperature, friction, and lubricant flow rate.

Compressible

The scope of this experimental program was quite limited in that the only results sought were values of the exponent n as used in the equation of state,

$$pV^n = \text{constant}.$$

For an adiabatic process (that process involving no heat transfer) n has the value of 1.40 for air. For an isothermal process (constant temperature), n is one. For an isopiestic process (constant pressure), n has a value of zero. Air was used as the gas phase for all by phase compression tests. In selecting a piston compressor, the process was preselected and was closely approximated by the adiabatic process.

In these investigations, n was found to have an average value of 1.34 for the compression of air without additives. This value is close to the value of 1.40 for adiabatic compression. Leakage from the cylinder and heat transfer to and from the cylinder walls all contribute to this deviation from the adiabatic theoretical value of n.

Fig. 17 shows a typical logarithmic plot of pressure versus volume. Note the good straight line approximation. The deviations from a straight line approximation may be attributed to leakage past the valves and piston rings at the extremities of the curves. Speed of compression and cylinder temperature had little effect upon the slope of the curves. Crankshaft speeds of 582 rpm and 888 rpm were used. The cylinder head jacket cooling water temperature was varied from 66F to 160F without noticeable effects on the slope of the p-V curves. Even with the good straight line approximations as shown in Fig. 17, there was considerable scatter in the values of n as shown in Fig. 18. This scatter was attributed to unsteady oil flow rates in and out of the test cylinder since the instrumentation was much more accurate than indicated by the variations in slope. Oil flow rate from the pump was quite steady, but it would accumulate in the cylinder before being discharged. Typical data is shown in Table 2.

Most of the testing used oil-air mixtures since the oil flow rate was easy to regulate and the drop sizes were easily varied by changing spray nozzles. The difference in drop size was only measured in a qualitative manner with an

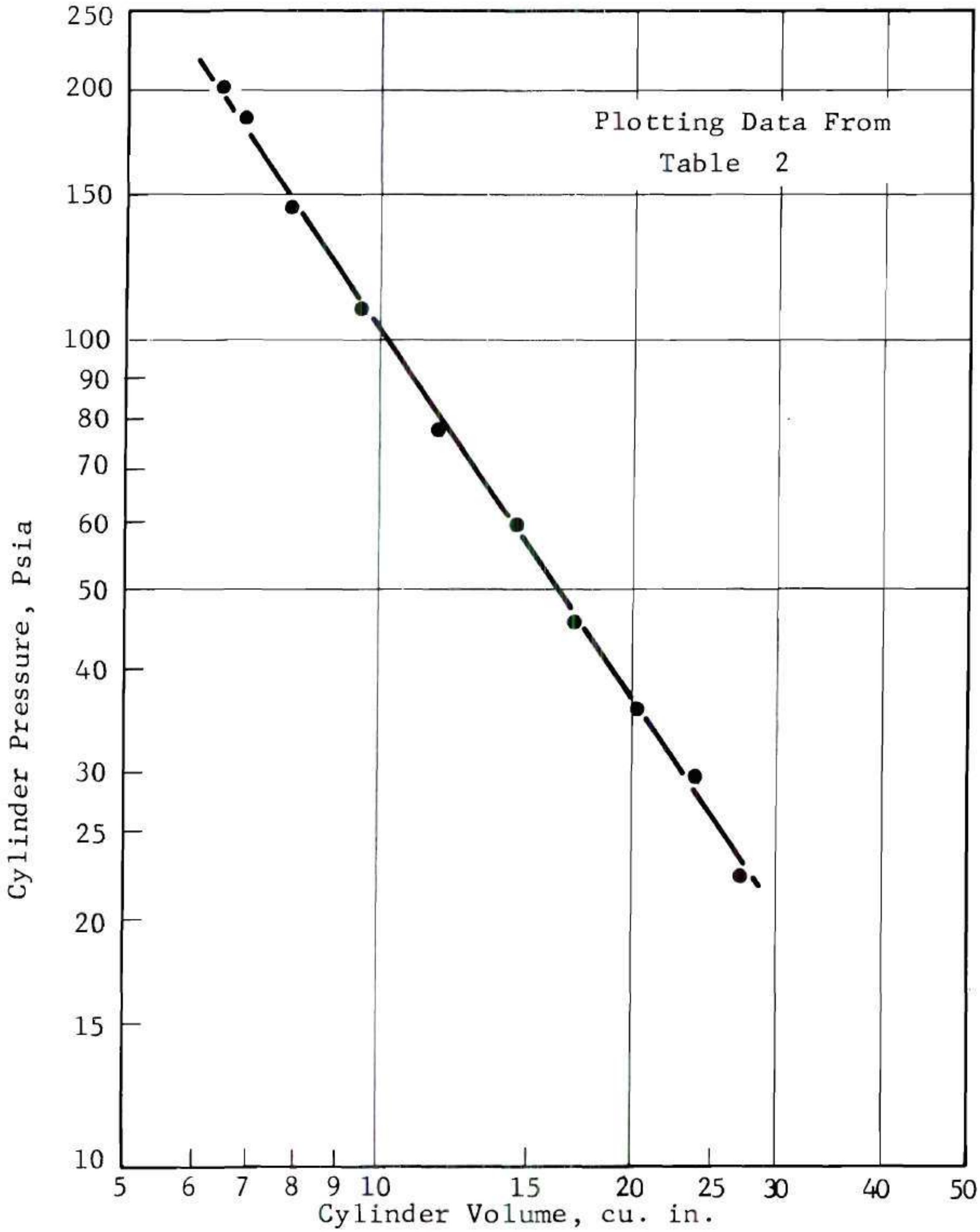

Figure 17. Typical Logarithmic Plot of Pressure vs. Volume

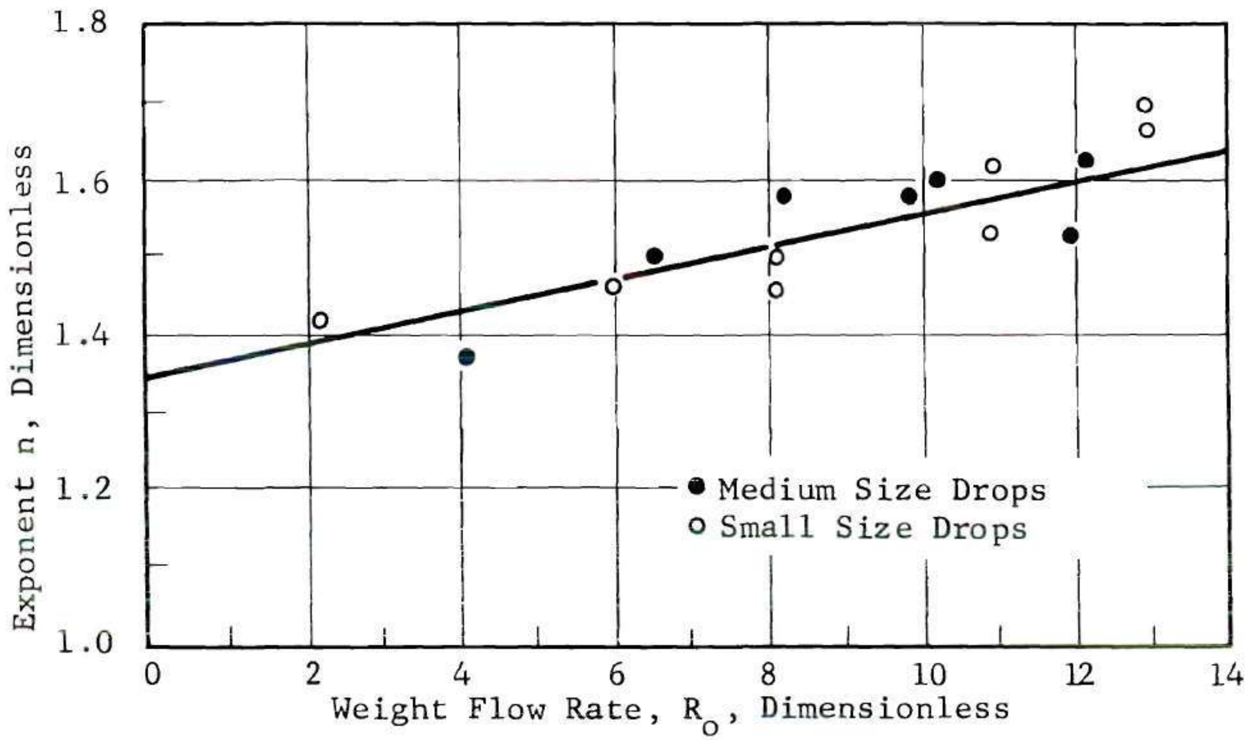

Figure 18. Plot of n vs. R_o for SAE 10 Weight Oil as a Function of Drop Sizes M and S

appreciable visual difference between the small and medium drop sizes. No noticeable difference could be detected between the slopes for medium and small drops of oil as shown in Fig. 18.

Oil viscosity was varied from 47 centistokes to 83 centistokes at 100F over a flow range of values for R_o from zero to 14. The results of these tests were the same as those shown in Fig. 18, thereby indicating that no noticeable effect is produced by changing the viscosity. Other variations gave very similar data which is little different from these curves. The following summary of tests followed by a brief comment as to the results is sufficient to impart most of the useful information relative to the experiments:

1. Air-oil mixtures tested with varying rate of oil flow ratios, R_o.
   (a) Exponent n is a function of R_o. (See Fig. 18.)
   (b) Changing compressor speed from 582 rpm to 888 rpm had no effect.
   (c) Cylinder jacket water temperature variations produced no effect.
   (d) Oil droplet size variations produced no effect.
   (e) Oil viscosity variations produced no effect.
2. Air-molybdenum disulfide mixtures tested with a ratio of molybdenum disulfide flow to air, R_o, of 0.016.

   Exponent n = 1.34 which is the same as for air.

3. Air-Teflon mixtures tested with a ratio of Teflon flow to air, R_o, of 0.016.
   No valid data could be obtained due to the instability of the pressure versus time curves caused by collection of Teflon within the cylinder of the compressor.

All data observed could be well approximated by a straight line. The deviations from this line are attributed to instrumentation errors and errors in the data reduction starting with a film record of an oscilloscope trace. The line representing average values of the exponent n has the following equation:

$$n = 0.021\ R_o + 1.34. \qquad (6.1)$$

Tests with air-Teflon were inconclusive due to an accumulated collection of Teflon within the cylinder of the compressor. In the planning stage of these experiments, it was feared that oil and solid powder would collect within the cylinder so that steady flow data with a fixed compression ratio would be impossible to obtain. Teflon powder proved to be the only lubricant which would not flow through the test cylinder.

This experimental test program was not extended because it was considered to be sufficiently complete to supply data for theoretical hydrodynamic bearing calculations using highly compressible lubricant mixtures. The usual flow rates for journal bearings lubricated with air-oil mist are approximately 0.1 pound of oil per pound of air. These tests covered a range up to 14.0 pounds of oil per pound of air. The flow rate for molybdenum disulfide was also extended to 0.016 pounds of molybdenum disulfide per pound of air as compared to the usual flow rates of 0.001 pound of solid per pound of air.

The density of these highly compressible mixtures may be obtained by using values of the exponent n from equation (6.1) in equation (2.42). The constant in this equation can be determined by using the known density of the gas phase.

Gas-Liquid

The results of the highly compressible gas-liquid tests were discussed as "compressible" lubricants. This discussion will be confined to the "incompressible" gas-liquid type of lubricant mixture. For each particular gas and liquid combination, there will be a definite amount of gas in solution with the liquid at equilibrium conditions. The gas phase, which may be miscible or immiscible in the liquid, can have an appreciable effect on the viscosity of the liquid, even in small amounts.

Oil type A was selected to test the relative solubility of different gases. Section A of the Appendix lists the physical properties of all lubricants tested as specified by the manufacturer. Some of the specifications are quite vague as this information is all that is normally supplied. Oil Type A is a paraffinic base petroleum oil without additives. This oil was purchased directly from the refinery in order to eliminate the effects produced by various additives. The various gases tested included Freon-22, carbon dioxide, ethane, methane, hydrogen, and helium. Freon-22 was used as a check against data already published (18) and is not included with this material. All viscosity data as shown on the curves are the average values and are expected to be accurate within the three percent as specified by Bendix with the exception of the polyphenyl ether data which are the result of only two tests.

Typical gas-liquid viscosity and equilibrium curves for carbon dioxide-oil mixtures are shown in Figs. 19 and 20. Additional curves for other gas-liquid combinations are shown in the Appendix, Section B. Viscosity of the liquid phase was always decreased when gas was absorbed by the liquid, but the percent decrease was very dependent upon the type of gas. Oil type A with two percent carbon dioxide shows a 30 percent decrease in viscosity at 100F. The same oil shows a decrease of 43 percent with ethane under the same conditions. However, at 200 degrees F, both of these gases produced less effect upon the viscosity; the ethane produced only 28 percent decrease, and the carbon dioxide produced a 31 percent decrease. It should be noted that the ethane produced more effect upon the viscosity at lower temperatures, but at the higher temperatures the carbon dioxide produced the largest effect.

Of the liquid lubricants tested, the viscosity of poly-

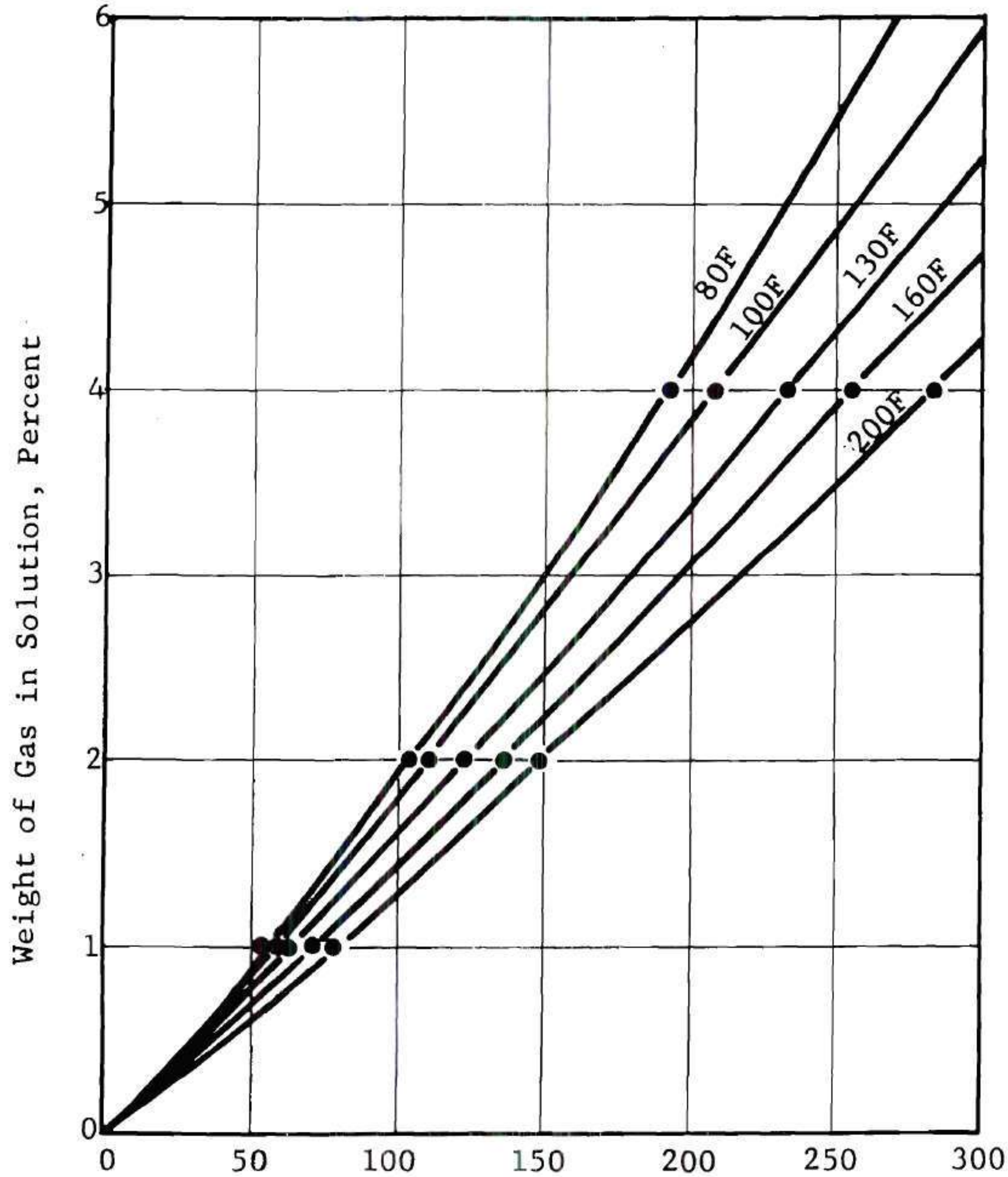

Figure 19. Gas Solubility in Oil Type A for Equilibrium Conditions with Carbon Dioxide

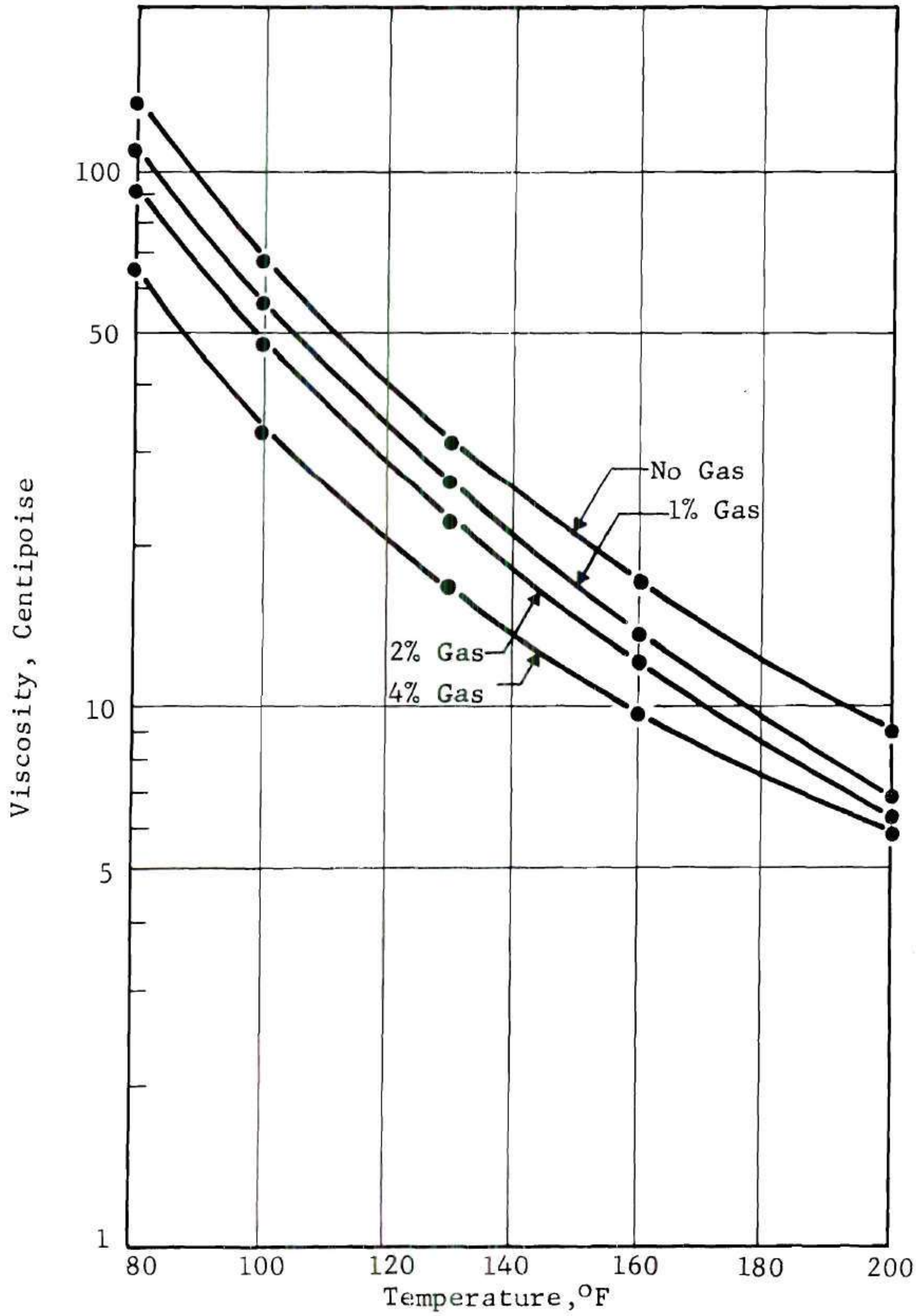

Figure 20. Viscosity vs. Temperature for Carbon Dioxide-Oil Type A System

phenyl ether was most effected by gas absorption. At 160F the polyphenyl ether had a viscosity of 160 centipoise, but the absorption of four percent gas reduced this viscosity to 49 centipoise. The polyphenyl ether was difficult to test in that it was too viscous to pour into the test chamber at room temperature; it was too thick to bubble gas through at temperatures below 140F, and it was subject to carryover with bubbles of gas into the pump chamber.

Oil type B was a popular brand of SAE 30 grade oil in an unused condition. Oil type C was the same oil after use in an automobile engine for 1750 miles of normal driving. This same oil which had a viscosity of 92 centipoise at 100F had a viscosity of only 47 centipoise at 100F after use. When put under a vacuum at absolute pressures less than one millimeter of mercury for 24 hours, the used oil viscosity increased to 50 centipoise at 100F. After cycling to temperatures above 220F, the used oil was subjected to gas absorption. The absorbed gas produced less effect upon the viscosity of the used oil, type C, than on the same oil in a new condition as type B. At a temperature of 220F, the new and used oils had practically the same viscosity with four percent carbon dioxide in solution.

Saturation pressures required to force a given amount of gas into solution varied greatly for the different combinations of gas and liquid. Measurable amounts of hydrogen and helium could not be forced into solution with the oils tested at pressures below 1000 psig. At pressures up to 1000 psig, no effect upon the oil viscosity could be detected. At the higher pressures, a slight increase in viscosity was expected due to the pressure effect upon the viscosity, but the slight absorption of helium and hydrogen apparently offset the pressure effect. Table 1 below shows the pressure required to put two percent of gas into solution in oil type A at a temperature of 100F.

Table 1. Pressure for Two Percent Solution at 100F in Oil Type A

Gas	Pressure, psia
Helium	Greater than 1000
Hydrogen	Greater than 1000
Methane	470
Carbon Dioxide	115
Ethane	105

All of the gases were less soluble at higher temperature. Fig. 19 for carbon dioxide and oil type A is typical for all combinations of liquid and gas investigated. At 200 psia, 4.2 percent gas will go into solution at 80F, but only 2.8 percent gas will go into solution at 200F. The solubility of gas in polyphenyl ether was effected less than the other oils by increasing temperatures.

Mechanical mixtures are always subject to instability by a separation of the mixture components. The stability of two liquid lubricants with carbon dioxide in solution is shown on Figs. 21 and 22. Oil type A with 4.0 percent carbon dioxide in solution at 200 psig and 101.5F temperature was subjected to a sudden release of pressure to atmospheric conditions. Time measurement was started when the pressure was released with viscosity measurements recorded at 1/10 minute intervals. Only the values at one minute intervals are plotted on Fig. 21 since they are quite representative of all values. This test continued for 227 minutes before the oil gradually returned to a viscosity near 65 centipoise which is the viscosity of this oil without gas in solution. During this period, 2270 data recordings were made without evidence of any sudden changes in viscosity or density.

The application of a vacuum to the oil greatly changed the shape of the viscosity-time curve. These test results for the same oil are also plotted on Fig. 21. The oil at 92F with 4.1 percent gas in solution at 200 psig pressure was suddenly subjected to a vacuum. The pressure was reduced to less than one inch of mercury absolute in approximately six minutes. After twenty minutes, the viscosity had reached 85 centipoise. Continuation of the test for 120 minutes brought the oil up to 89 centipoise which is the viscosity of this oil without gas in solution.

Fig. 22 shows the stability of a carbon dioxide-polyphenyl ether mixture which was initially saturated with

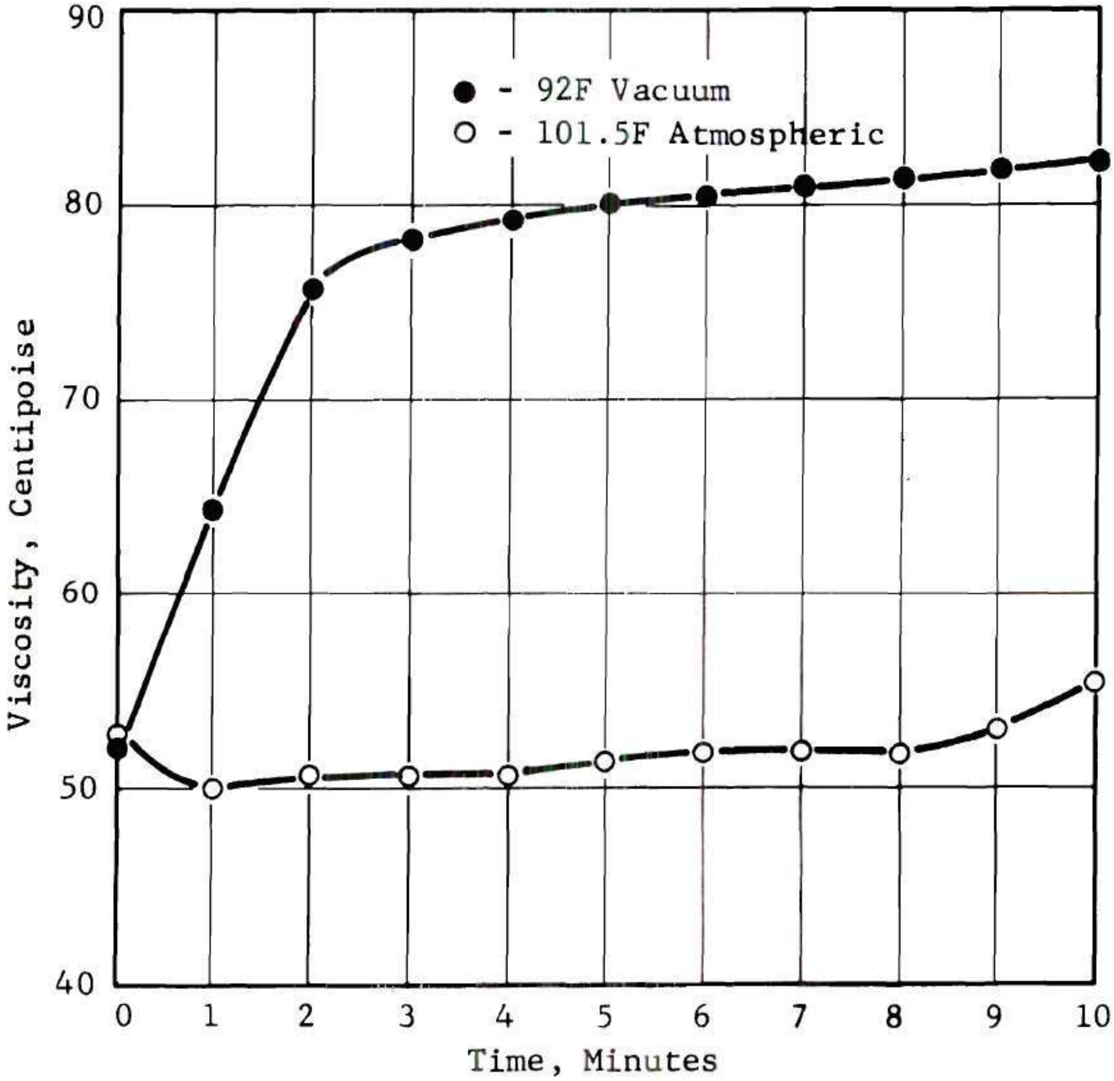

Figure 21. Stability of Carbon Dioxide-Oil Type A Mixtures

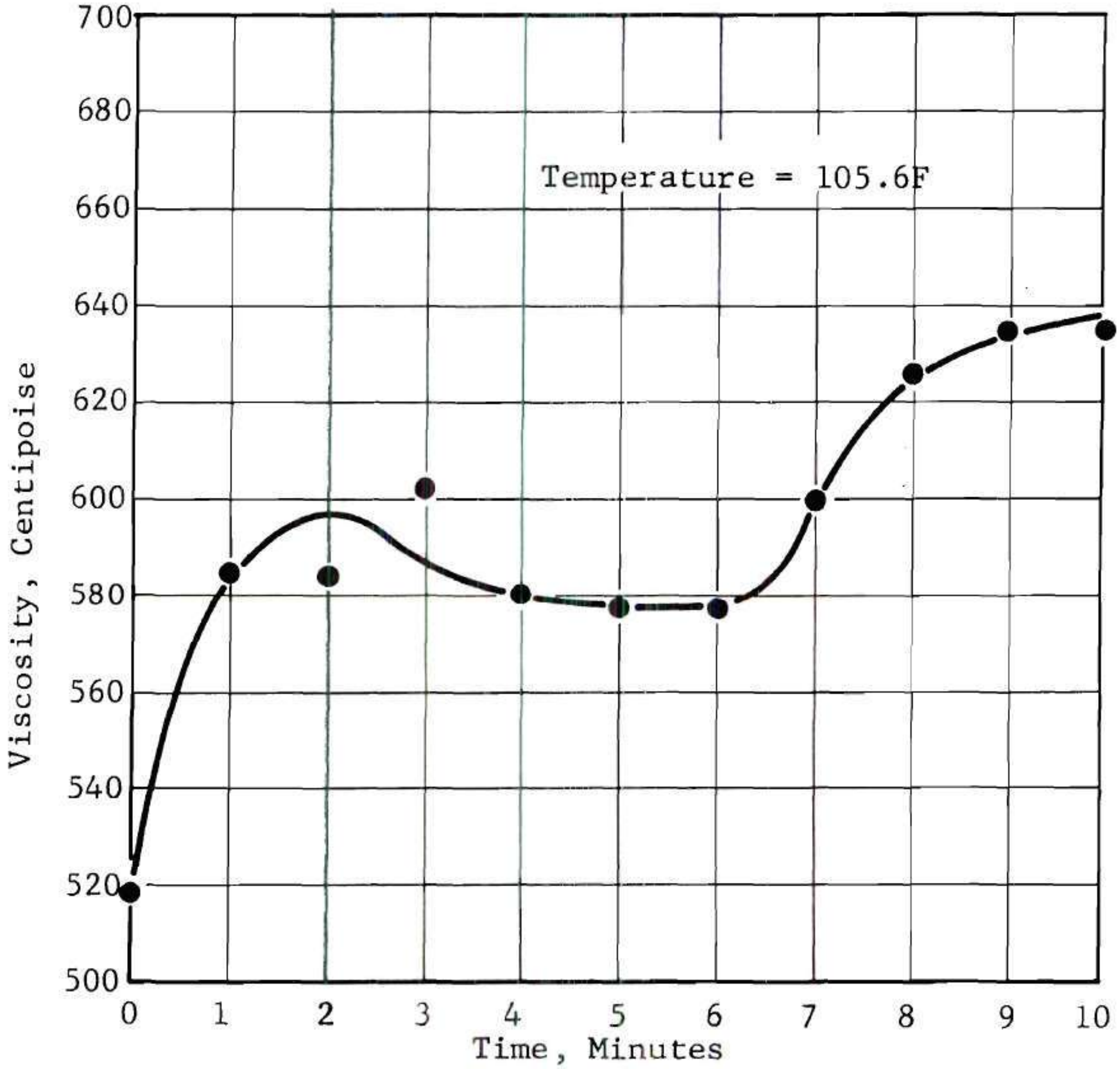

Figure 22. Stability of Carbon Dioxide-Polyphenyl Ether Mixtures

carbon dioxide at 200 psig pressure and a temperature of 112.3F. The 200 psig charging pressure forced 1.6 percent gas into solution with the decrease in viscosity from 1675 centipoise to the initial 519 centipoise. At time equal to zero, the pressure was suddenly reduced to atmospheric pressure. During the first minute, the viscosity rose to 585 centipoise; then it oscillated slightly about the 590 centipoise value for the next six minutes before starting a gradual increase back to the 1675 centipoise value at the end of 16 hours. Again, the data values were recorded at 1/10 minute intervals, but only the values at the minute intervals were plotted on Fig. 22. The choice of a curve path between these points was arbitrary since there was a possibility of about three percent error in this range of viscosity.

Tests at higher temperature and pressure did not show any radical changes in the time required for measurable changes in viscosity to occur. In hydrodynamic lubrication, the lubricant flows through the bearing in a fraction of a second. Any change in viscosity which occurs over a period of minutes will not effect the performance of a pressure fed hydrodynamic bearing. For these reasons, the experimental findings do not indicate any change in bearing performance due to lubricant instability during the time required for a lubricant to flow through a pressure fed hydrodynamic bearing.

Density variations of the mixtures relative to the liquid density were small for the gas-liquid combinations tested. These values are tabulated in Table 6 of the Appendix, Section D. Higher concentrations of gas in solution reduced the density of gas-oil mixtures slightly, but the reduction in all cases was less than two percent.

Polyphenyl ether was subject to a volume expansion with increasing temperature which created decreasing density for a temperature increase, but the addition of gas up to four percent in solution did not appreciably change the density of the liquid.

Gas-Liquid-Solid

The addition of three percent molybdenum disulfide to oil type A produced only small effects upon the viscosity (Fig. 23). Mixtures of the oil and solid produced no measurable effect upon the viscosity of the oil at solid concentrations up to three percent, but a slight increase was noticed in the oil viscosity with gas in solution. The viscosity increased with temperature and gas concentration to eight percent above the gas-liquid viscosity at 200F with four percent gas in solution. Most of the difference could be due to instrumentation errors of three percent in opposite directions for the two readings.

The density of the gas-liquid-solid mixtures was not measured since this density can be calculated from the data on gas-liquid mixtures and the known density of the solids. Visual observation of the liquid level did not reveal any

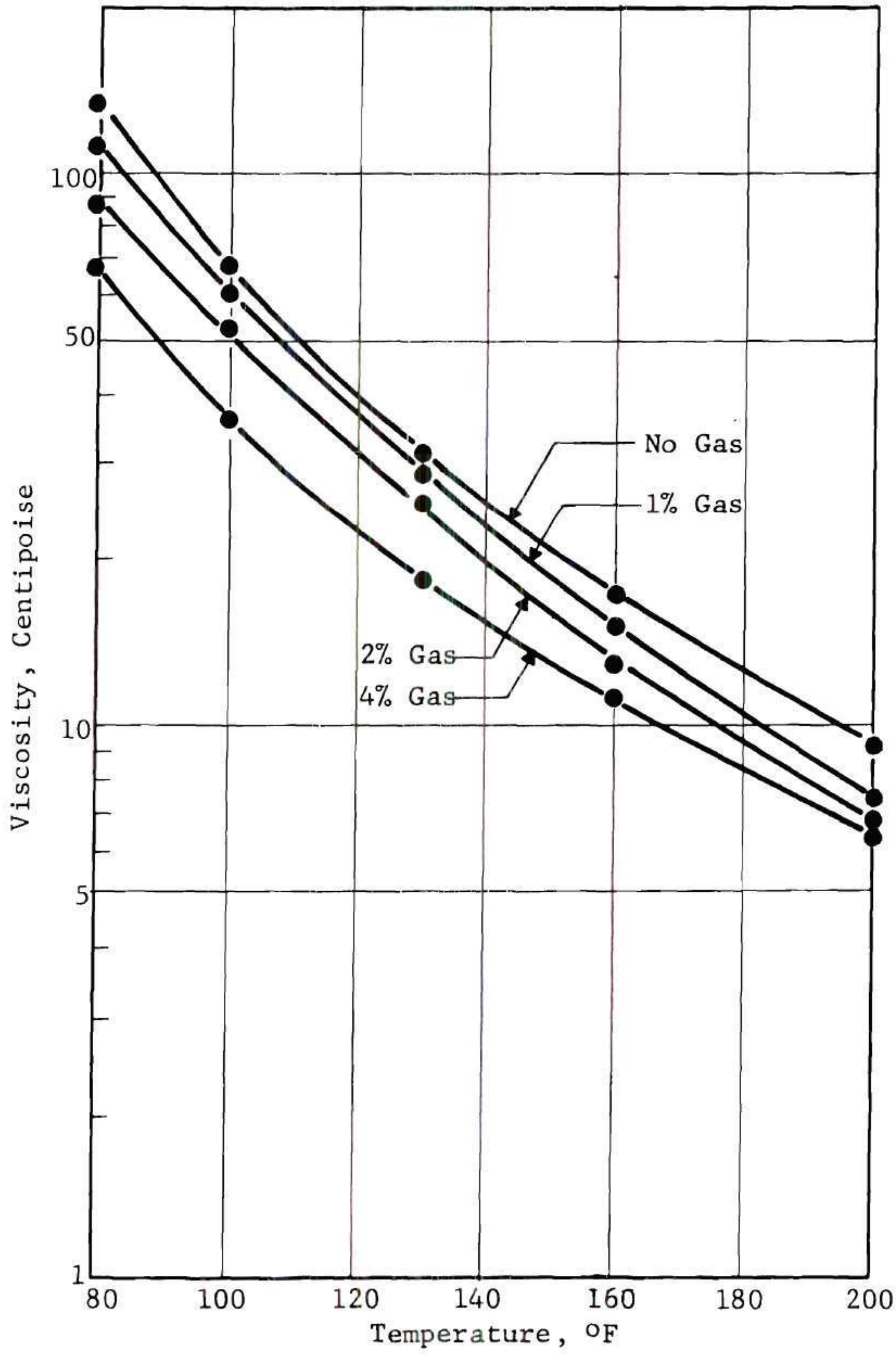

Figure 23. Viscosity vs. Temperature for Carbon Dioxide-Oil Type A-Three Percent Molybdenum Disulfide System

unusual volume changes.

Liquid-solid lubricants are not stable at any condition of temperature and pressure due to the relative density of liquid and solid plus the forces of attraction and repulsion on and between the particles. Some form of agitation is necessary to keep the solid particles dispersed throughout the liquid.

Pressure Distribution and Load Capacity

The pressure distribution in a hydrodynamic bearing is the most important single parameter in the analysis or design of this type of bearing. For most applications, pressure may be considered as a function of only two variables (x and y as used in this research) because of the extremely small dimensions across the film in the z-direction. Basic design parameters which depend upon the pressure distribution are:

a) The load capacity.

b) The oil flow to and from the bearing.

c) The viscosity of the lubricant.

d) The temperature distribution.

e) The coefficient of friction.

f) The location of the shaft center relative to the bearing.

g) The location of the lubricant supply.

Equations (4.20) and (4.34) for the temperature and pressure at a point were derived in a very general manner to permit maximum flexibility in the study of the significant parameters of all kinds of boundary conditions and all types of lubricant. With these equations it was possible to study the behavior of a theoretical lubricant under a great variety of conditions. First, some solutions were made on bearings by using conventional lubricants to show the effects of certain boundary conditions; then solutions were made for a number of multiphase lubricants in the same bearing operating under the same conditions as the conventional lubricants.

Several complete listings of pressure values are included in the Appendix, Section C. These are only a few of the set of more than a hundred different pressure distributions calculated for this research to bring out certain points of interest.

Fig. 24 shows a typical pressure distribution from the center of the bearing to the outer edge for a bearing with an eccentricity ratio (e'/c) of 0.40. These calculations are for a constant temperature of 620 R at the bearing wall which was arbitrarily selected as the next station radially outward from the surface of the bearing. Oil was supplied at a constant temperature of 600 R and a constant pressure of 50 psia at the station $x = 0$. This bearing has a relatively low ℓ/d ratio resulting in the rapid decrease in pressure from the center to the outer edge. The maximum pressures of 465 psia are low for hydrodynamic bearings and can be easily obtained in an actual bearing with a minimum film thickness of 0.0006

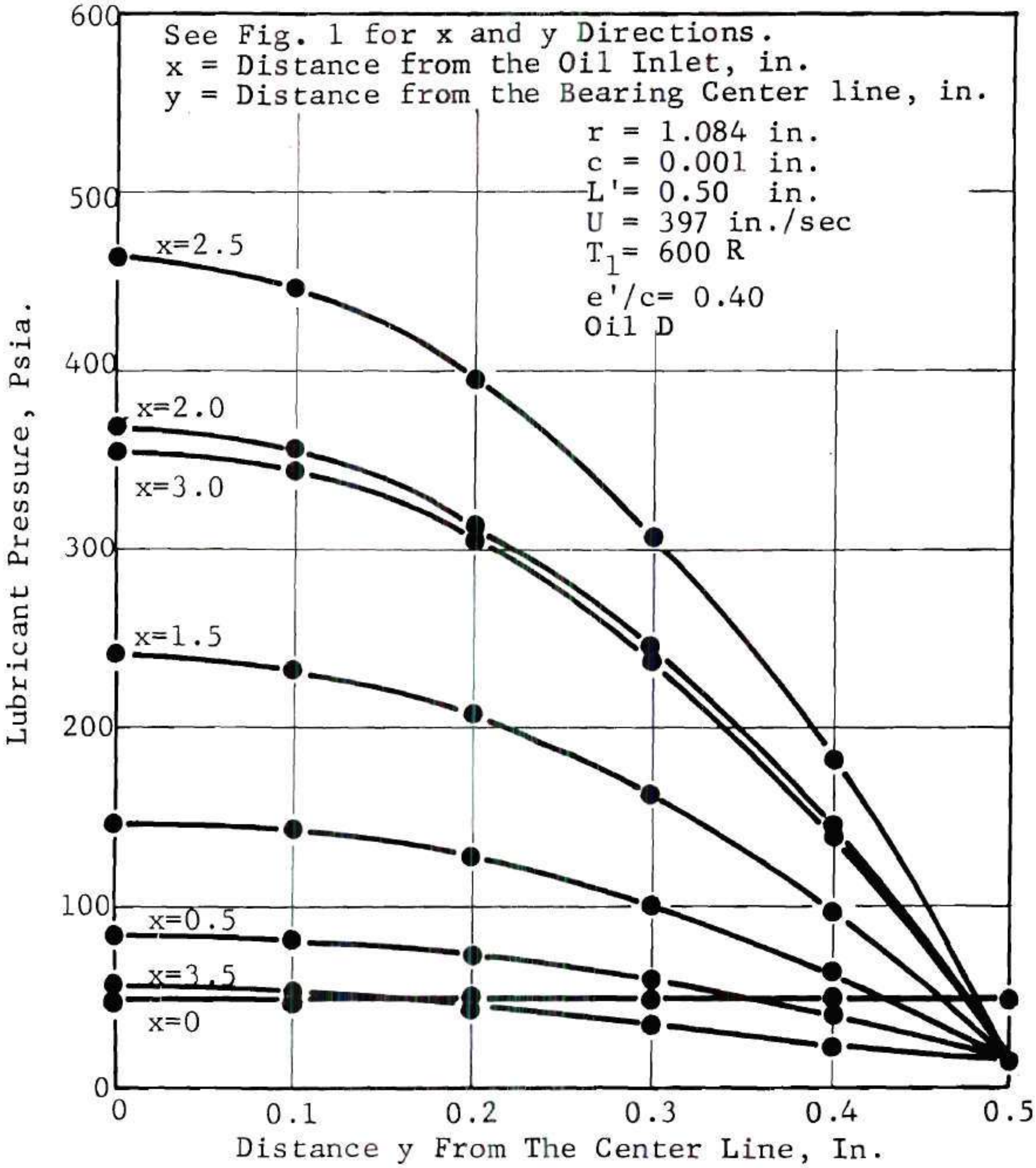

Figure 24. Typical Pressure Distribution in the y-Direction for Oil D

inches and a surface velocity of 397 in./sec.

A contrast in the effects of boundary conditions is shown in Fig. 25 for a bearing operating with an eccentricity ratio of 0.90. The only difference between the two curves for pressure is the condition placed upon the surface of the bearing. For the curve marked "adiabatic," no heat was removed from the lubricant during the cycle. For the other curve, the bearing wall temperature was maintained at 620R. The extremely high pressure of 53,000 psia shown on this curve is not realistic for an actual bearing for several reasons. First, the minimum film thickness of 0.0001 inch would not be maintained uniformly due to inaccuracies in machining, distortion of the surfaces due to the high loads, and surface distortion due to thermal stresses. In addition, the pressure coefficient α would decrease below the value of 4.36×10^{-5} used in these calculations.

By changing to adiabatic conditions, the maximum pressures are reduced to 13,000 psia for the same bearing. Pressures of this magnitude are often encountered in hydrodynamic bearings, but extremely small surface irregularities and solids in the lubricant become highly significant at these small values of film thickness. For boundary conditions such that the lubricant receives heat, the maximum pressure in the bearing would be reduced below those for the adiabatic conditions. These changes in pressure from one set of boundary conditions to another are due to the variation in the viscosity

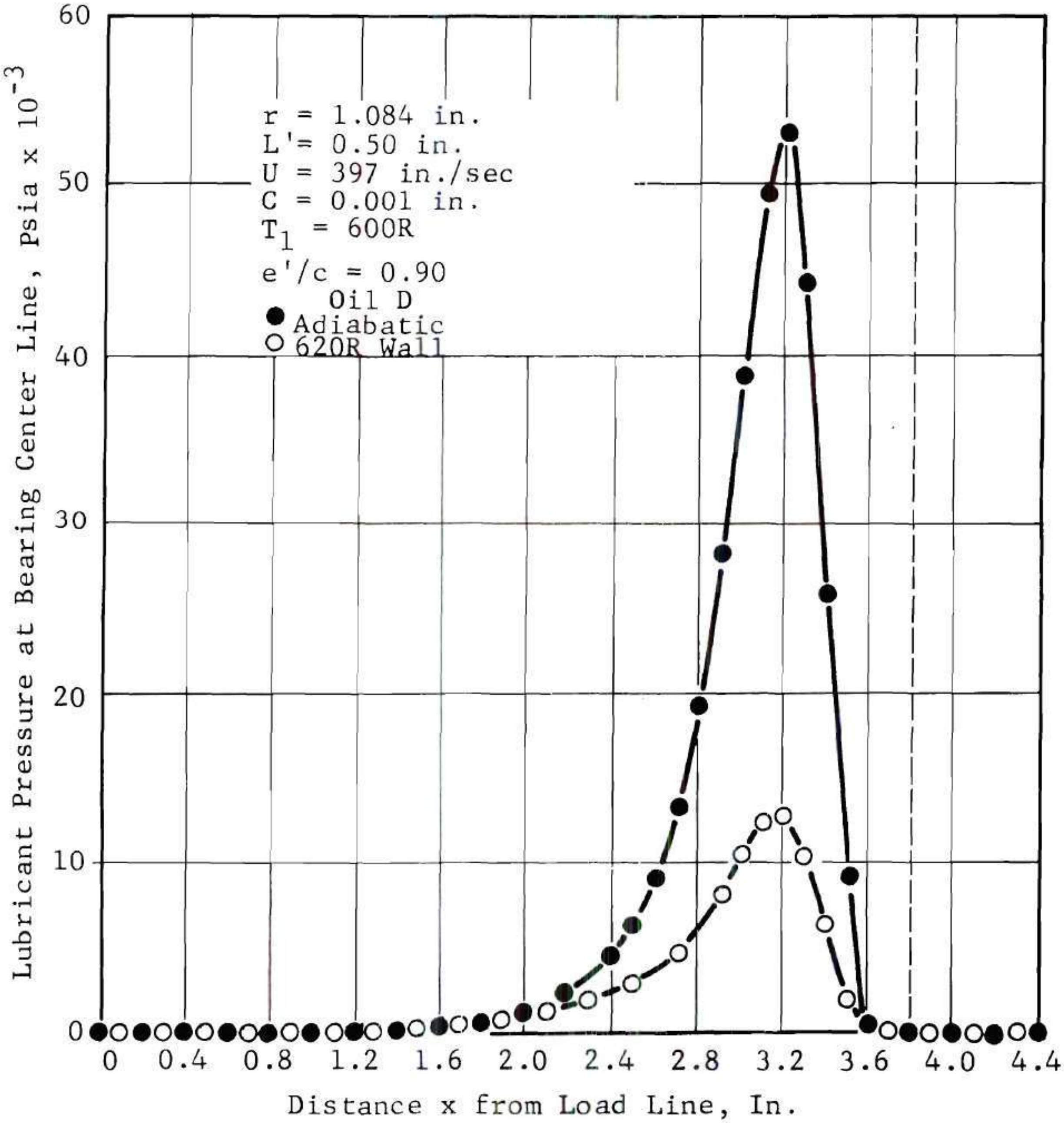

Figure 25. Pressure Distribution for Oil D with 0.90 Eccentricity Ratio

with changing oil temperatures.

The load capacity of a bearing can be determined directly from the pressure distribution. Curves such as the ones shown on Fig. 26 are used extensively for the determination of the load capacity by selecting an eccentricity ratio and reading a corresponding value of the Sommerfeld number. From the Sommerfeld number, the load capacity can be calculated if an average viscosity is known. There are several limitations to the use of a curve like this one. One of the limitations is the requirement that the lubricant must have a constant density. Another limitation is the determination of an average viscosity. The use of an average temperature will not give an average viscosity due to the exponential relation between viscosity and temperature. If an accurate load capacity is desired, it is necessary to solve for the pressure distribution in the bearing at the specified eccentricity ratio.

The relative load capacity for the two bearing conditions as shown on Fig. 25 is 13,700 pounds for the constant wall temperature and 3990 pounds for the adiabatic condition. At lower eccentricity ratios, the load capacities for these two boundary conditions would be closer together due to the decrease in the temperature rise in the adiabatic bearing.

For the multiphase lubricants, it is necessary to classify the lubricant, then select a method to determine the load capacity. The liquid-gas and liquid-solid lubricants which are predominately liquid and fall into the imcompressible

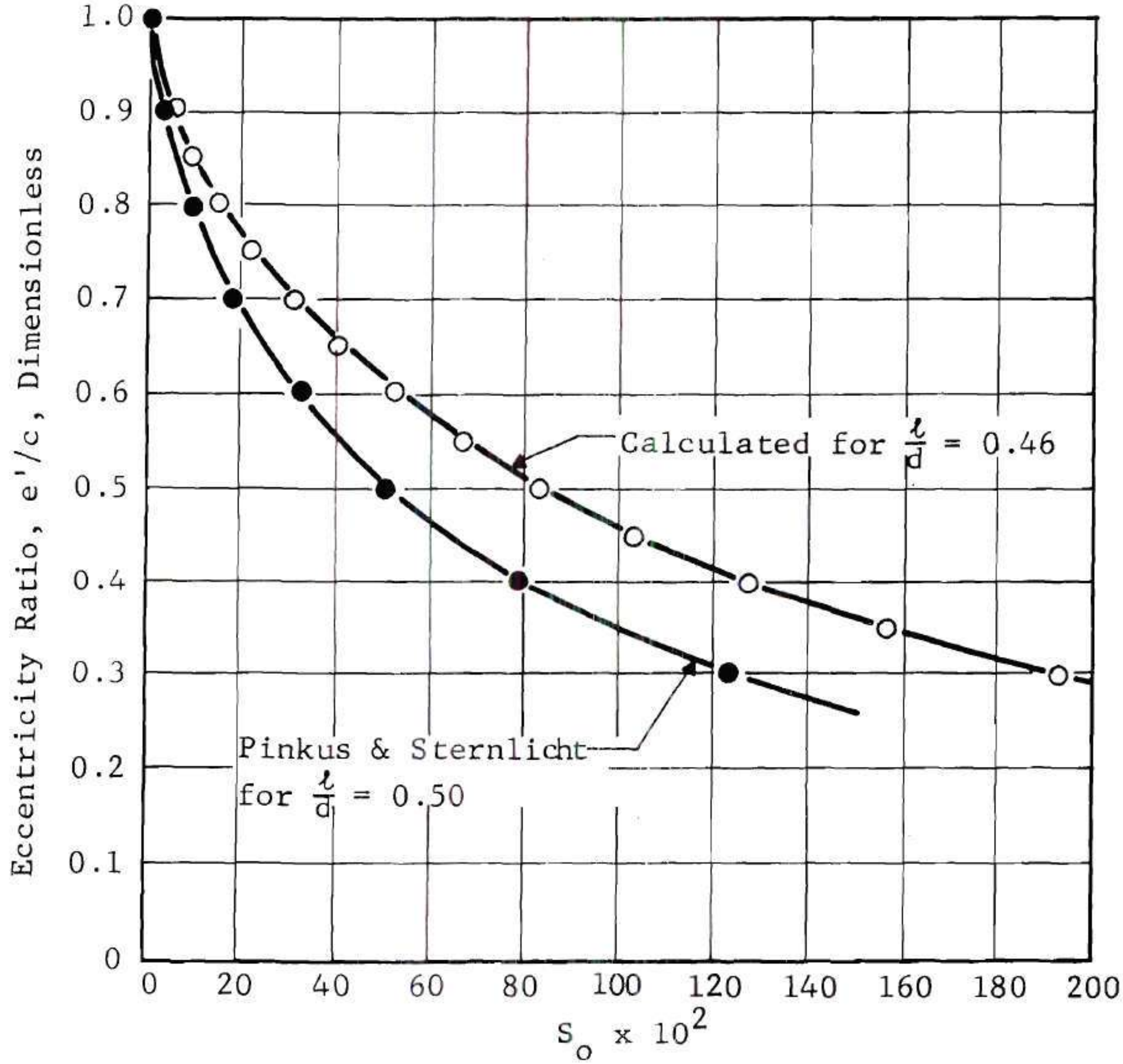

Figure 26. Bearing Eccentricity as a Function of the Sommerfeld Number

class will behave like oil, and the same method of calculation used for oil may be applied in most cases. If adiabatic operation is used, the higher operating temperatures of the liquid-solid lubricants must be considered.

The highly compressible lubricants have much lower load capacities. If air were used in the bearing selected for the pressure distribution curves shown on Fig. 25 in the place of oil D, the pressure curves would remain below the supply pressure, and the load capacity would be negative. However, at very high speeds, these compressible lubricants are attractive due to their low viscosity and high temperature stability. Fig. 27 shows the relation between the bearing eccentricity and the Sommerfeld number for $n = 1.4$. Two points for $n = 1.7$ are shown. Other values of eccentricity are the same as for $n = 1.4$ at Sommerfeld numbers below 5.0. A comparison between Fig. 26 and Fig. 27 shows the eccentricity ratio of the compressible lubricants to be appreciably below the eccentricity ratio of the incompressible lubricants at the same Sommerfeld number. The data for Fig. 27 is for high speed (3970 in./sec) operation with gas and multiphase compressible lubricants. Even at these high speeds, the load capacity of this bearing, which is the same size bearing as the one used for oil (Fig. 25), is only 42 pounds.

Temperature Distribution

The ability to calculate an accurate temperature distribution in the lubricant film is of prime importance for

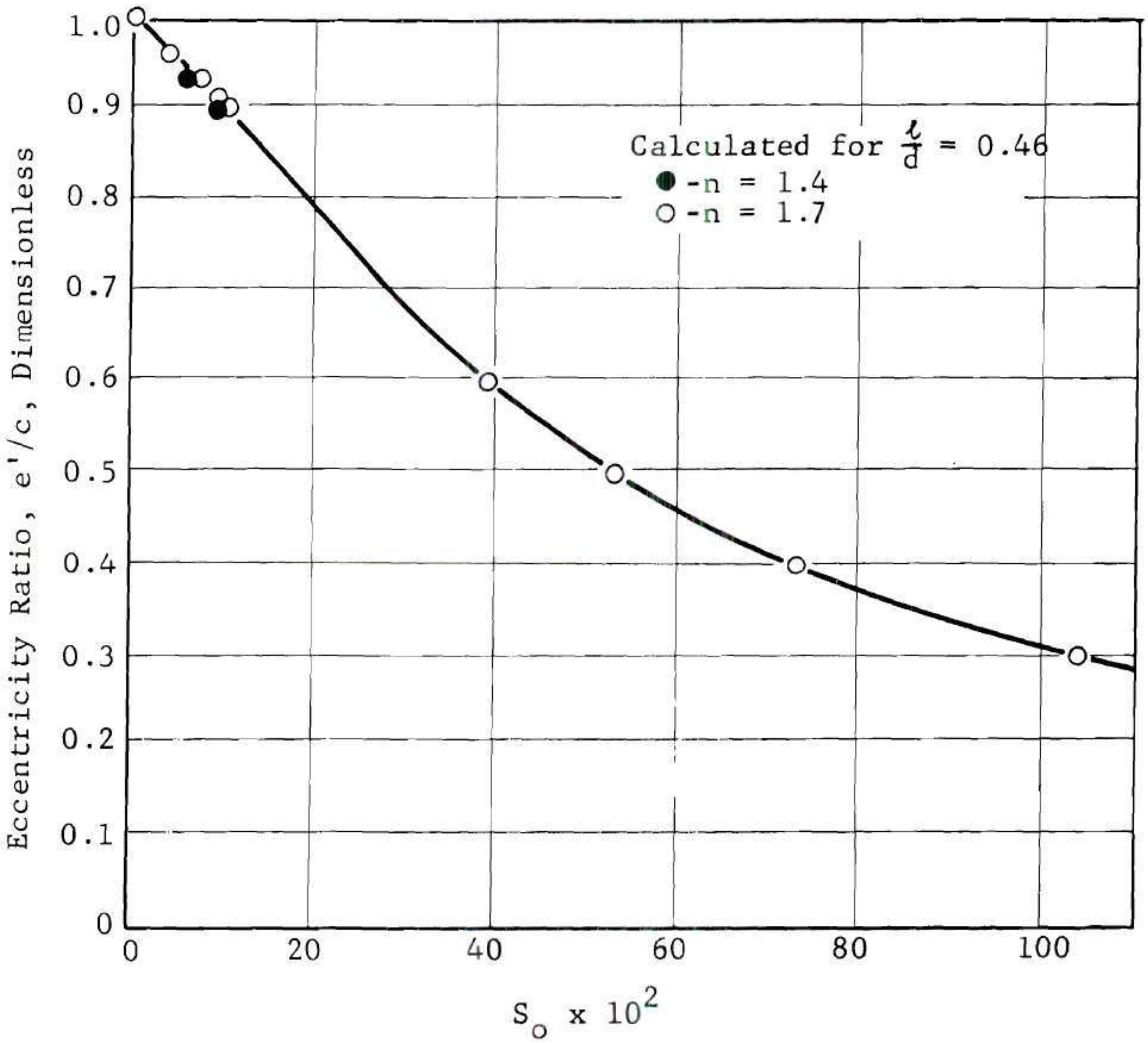

Figure 27. Bearing Eccentricity as a Function of The Sommerfeld Number for Compressible Lubricants

bearing design studies because the viscosity is exponentially related to temperature. Fig. 28 shows a typical temperature distribution curve across the lubricant film for an eccentricity ratio of 0.40, constant bearing wall temperature of 620 R, and an oil supply temperature of 600 R. Oil temperature at the shaft surface varied from 600 R to 628 R. When using multi-phase lubricants of liquid-solid and gas-solid mixtures, this temperature range is increased due to the zones of high friction.

Fig. 29 shows the temperature distribution along the center line of the bearing (y=0) at the third z-station for the same bearing and operating conditions as shown in Fig. 25 for pressure distribution. Note the sharp rise in the lubricant temperature for adiabatic operation from the 2.0-inch x-station to the minimum film thickness at the 3.2-inch x-station. Film temperatures shown for adiabatic operation are in question beyond the 3.7-inch x-station where film rupture takes place. The importance of bearing cooling is demonstrated at the 2.6-inch x-station where the temperature curve breaks sharply upward for adiabatic conditions and begins to decrease for conditions with a constant wall temperature.

No curves are shown for the temperature distribution across the oil film for adiabatic conditions because the variation is too small (two degrees F) to plot relative to the large temperature variations in the x-direction. Temperature variations in the y-direction are small (approximately one degree F) for all adiabatic conditions and constant wall

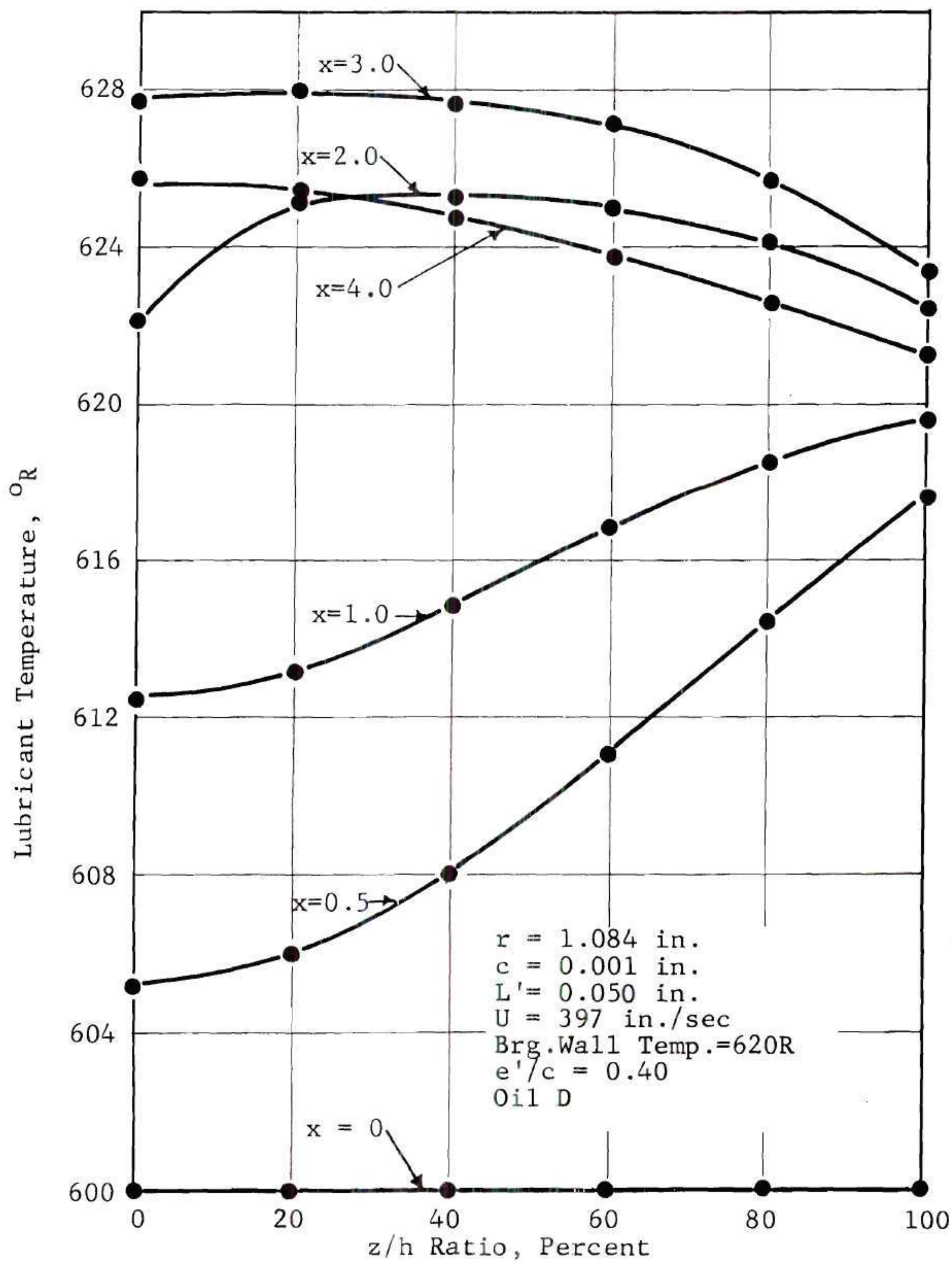

Figure 28. Typical Temperature Across the Oil Film for Constant Wall Temperature

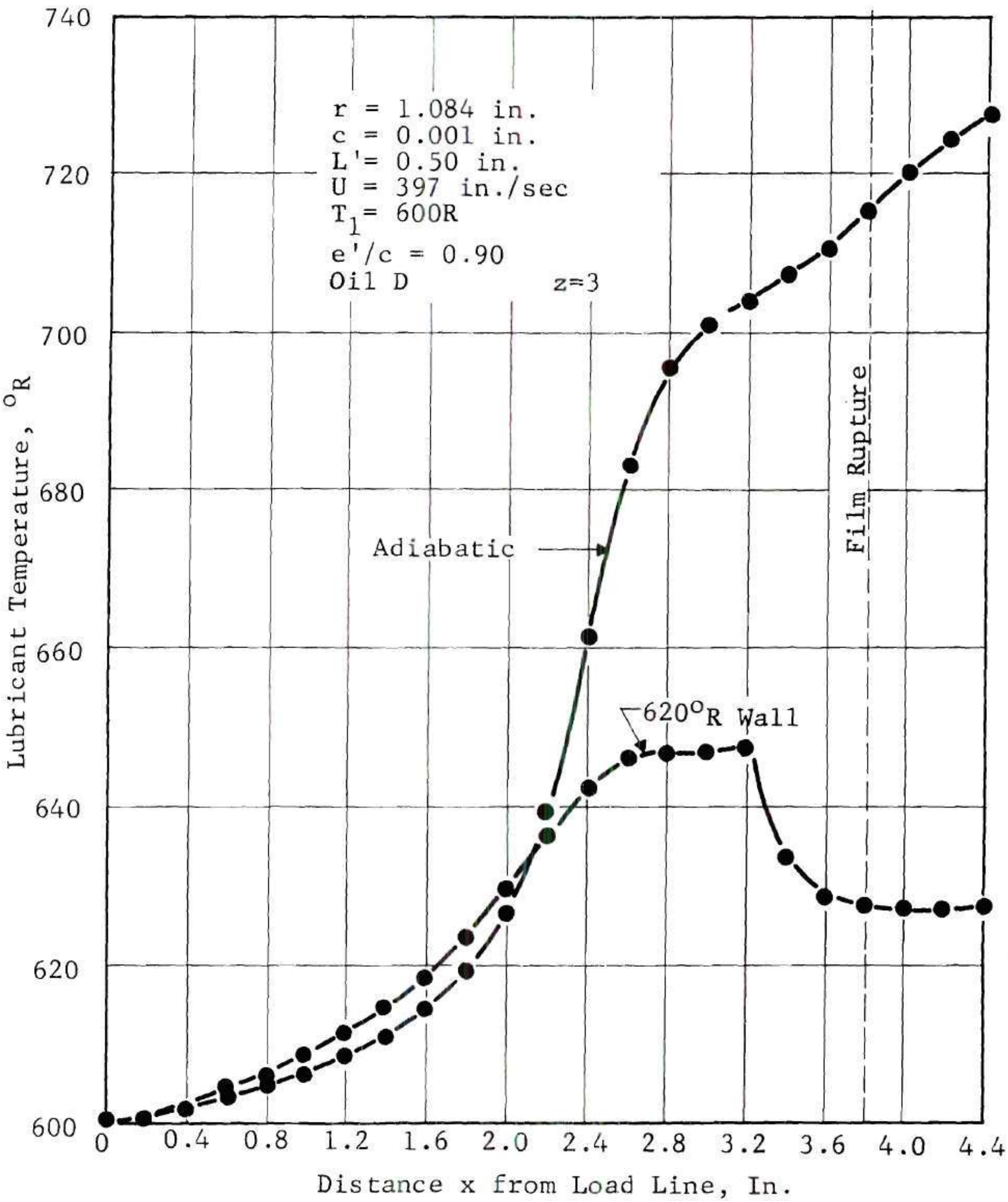

Figure 29. Temperature Distribution in the x-Direction for Oil D with 0.90 Eccentricity Ratio

temperature conditions. Temperature distributions as tabulated in the Appendix, Section C for adiabatic operation show this small variation in the y and z-directions.

Bearing Friction

All bearings operate with friction which causes a power loss and heating in the bearing. The normal function of the lubricant is to reduce the friction, prevent wear, and cool the bearing. Unfortunately, minimum friction occurs at a point where wear may occur and cooling is difficult and the bearing factor of safety is near one.

Figure 30 shows the friction factor expected for lightly loaded bearings. The friction of oil lubricated bearings in this range may be closely approximated by the Petroff equation (2.11). Highly loaded bearings would be represented by the curve shown on Fig. 31. When operating at low Sommerfeld numbers, the bearing may "seize" with very high friction. The point at which seizure occurs is dependent upon many factors such as the type of lubricant, the material of shaft and bearing, and the surface roughness. One way to reduce the Sommerfeld number for seizure is to use a multiphase lubricant of the liquid-solid type. Small amounts of solid molybdenum disulfide or Teflon will give good protection from seizure.

Friction factors determined both experimentally and analytically are shown on Figs. 30, 31, 32, and 33. In order to calculate the coefficient of friction, the pressure distribution and the temperature distribution must be determined.

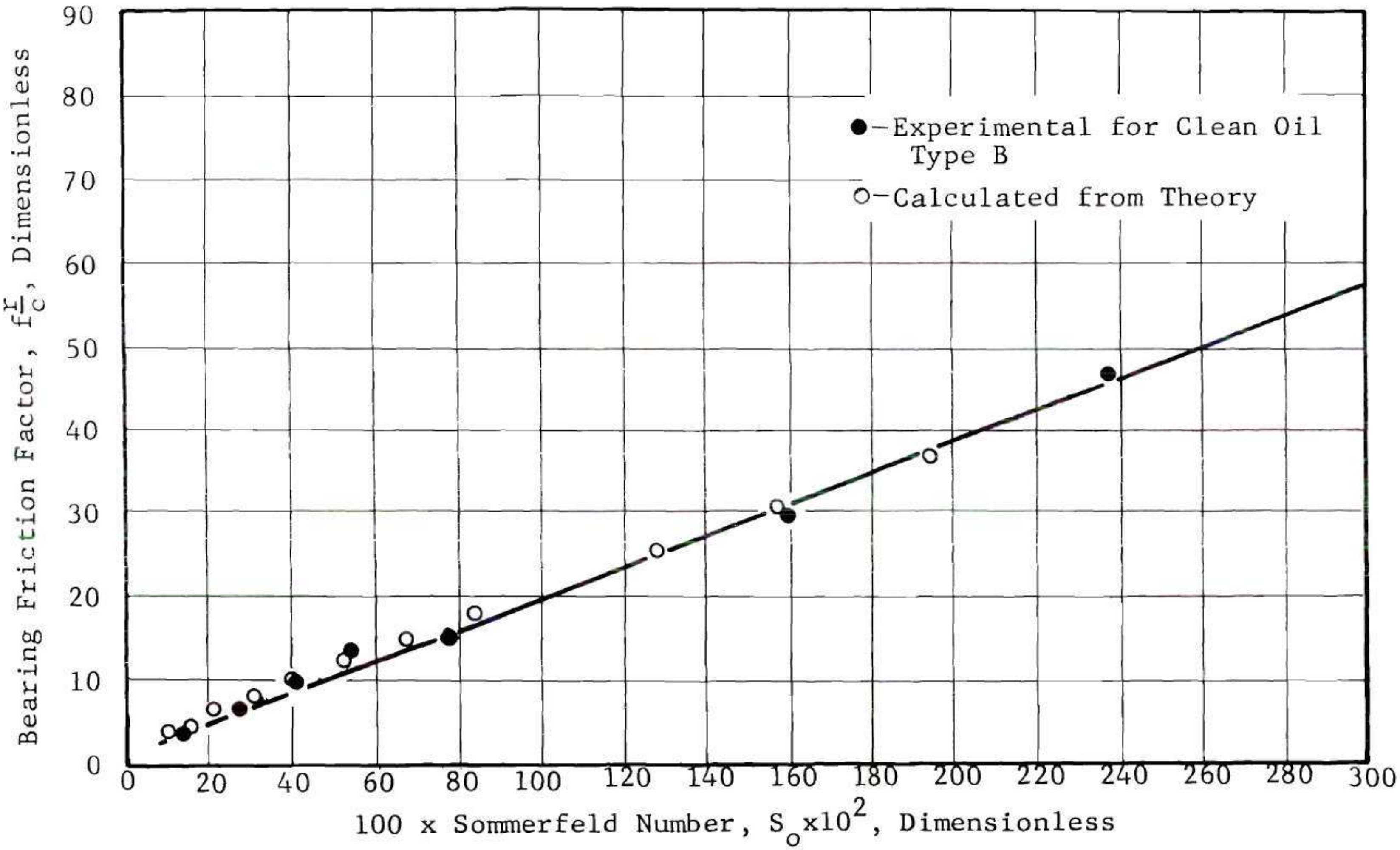

Figure 30. Bearing Friction as a Function of the Sommerfeld Number for Clean Oil

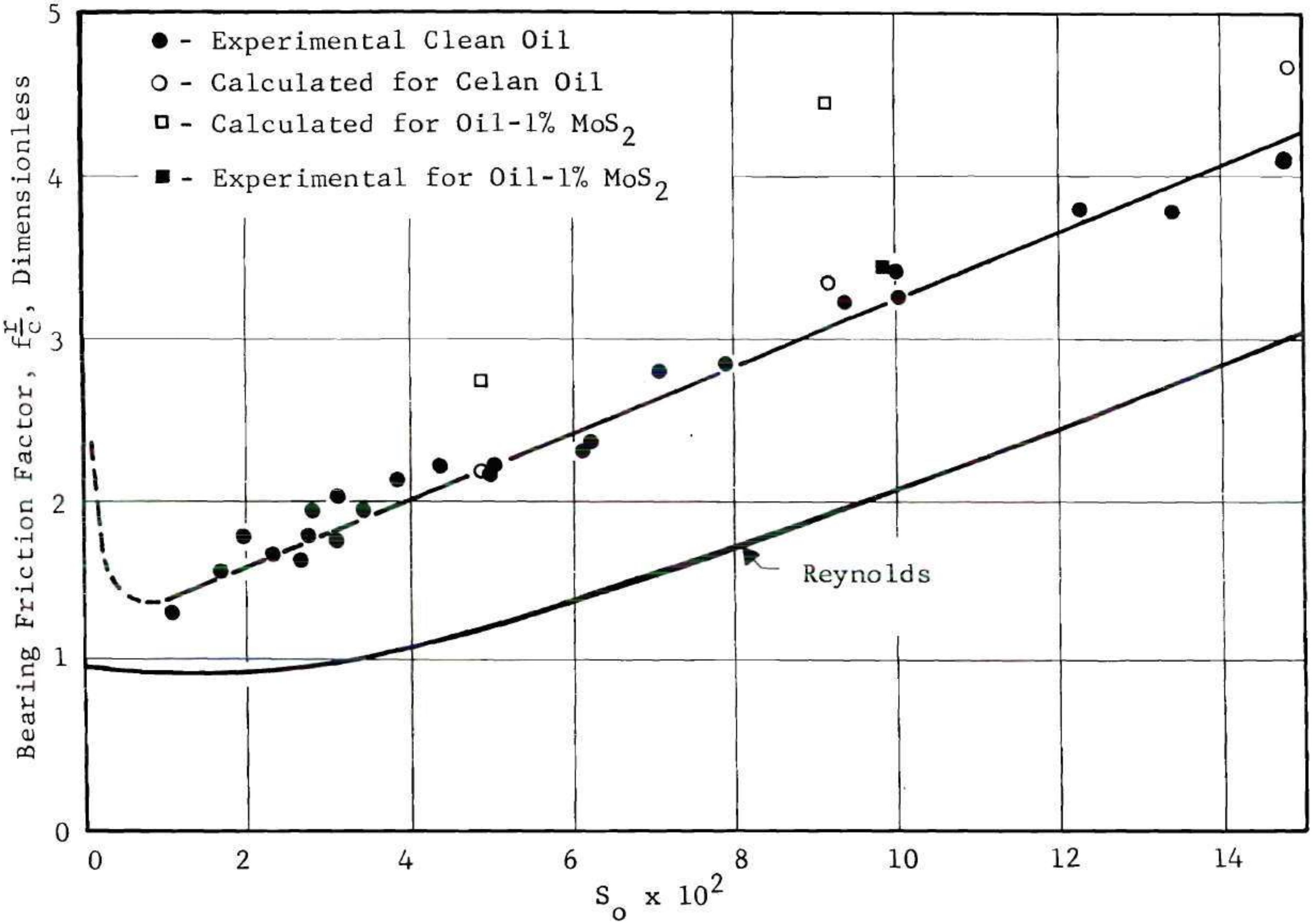

Figure 31. Bearing Friction Curve

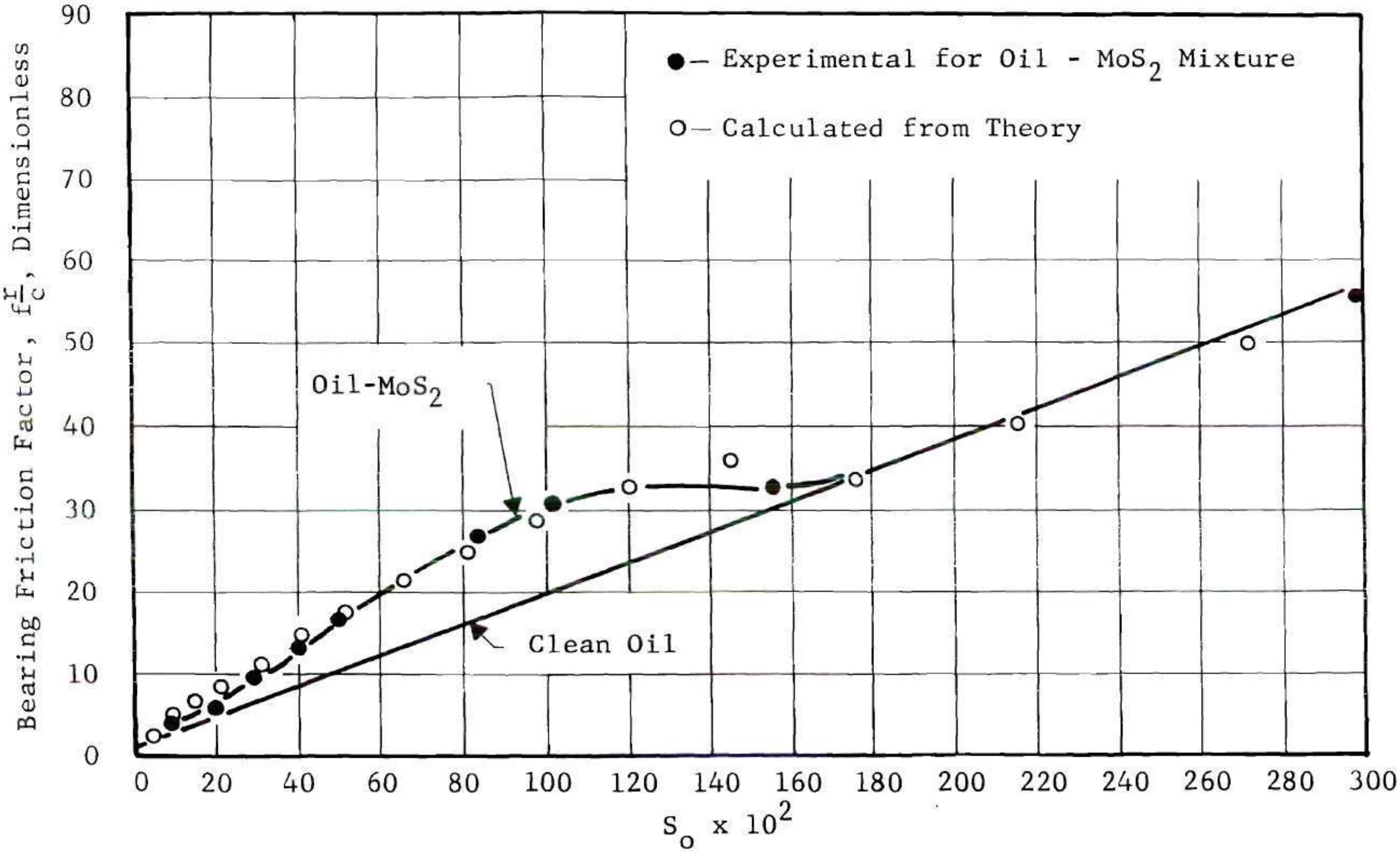

Figure 32. Bearing Friction as a Function of the Sommerfeld Number for Oil Type B with One Percent MoS_2 Powder

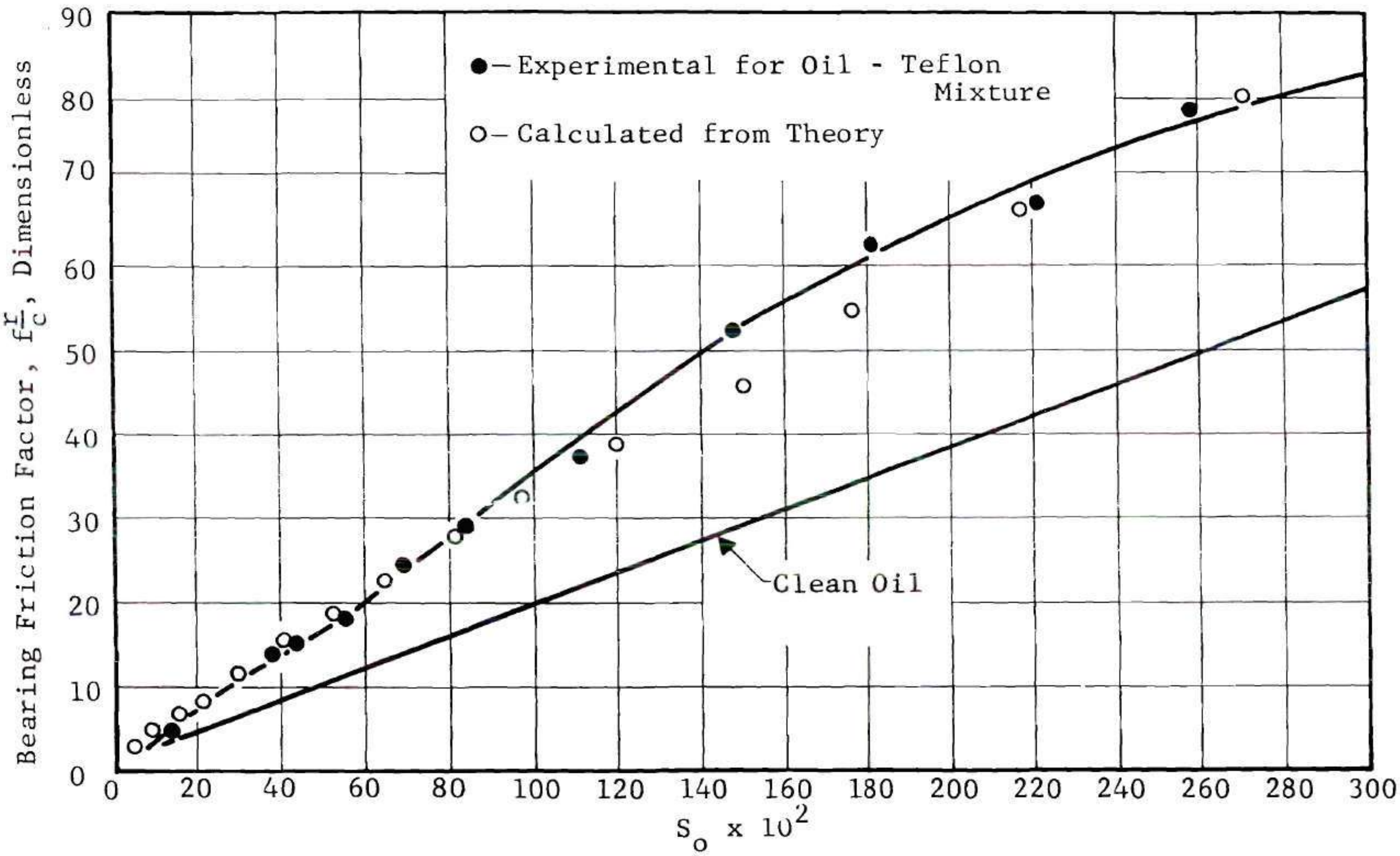

Figure 33. Bearing Friction as a Function of the Sommerfeld Number for Oil Type B with One Percent Teflon Powder.

From these values, the shear stress can be calculated by using equation (2.31) and the friction torque calculated from equation (2.32).

At high loads (Fig. 31), experimental variations are expected unless the tests are run at low speeds and small temperature rises in the lubricant. As the speeds go up, the average oil temperature is not an accurate means of predicting the average oil viscosity to use in calculating the Sommerfeld number. When bearings are to be designed for Sommerfeld numbers below 20, accurate calculations of the temperature and pressure distribution and the friction should be made instead of using average chart values.

Figs. 32 and 33 show the results of multiphase lubricants of the liquid-solid type. A general characteristic of this type of lubricant is the relatively large mid-range increase in friction above the friction of the liquid phase alone. At low Sommerfeld numbers, the friction of the liquid-solid lubricant returns to a value near that of the liquid only. The film thickness of the lubricant and the friction increase with increasing Sommerfeld numbers until the minimum film thickness exceeds the diameter of the solid particles. At this point, the friction curves for liquid-solid lubricants return to the curve for clean oil.

A very good representation of the experimental curve for the oil-molybdenum disulfide mixture (Fig. 32) is obtained by using the theory of multiphase lubricants developed in

Chapter II. The shear stress of the solid molybdenum disulfide particles is found to be 116 psi as loaded in this bearing with oil type A. The friction factors for oil-Teflon mixtures shown on Fig. 33 are considerably higher than the friction factors for the oil-molybdenum disulfide mixtures at Sommerfeld numbers above 1.00. A shear stress of 100 psi is used in the calculation of the theoretical points shown on Fig. 33, but the friction factor is low in the mid-range, indicating that a higher stress will give better results in this range.

A Teflon particle size of 24 microns corresponds closely to the measured and purchased size of these particles. The molybdenum disulfide particles used in the calculations are 17.8 microns in diameter, but they were purchased as 7 micron particles. Some of these particles measured 18 microns on a filar microscope, but many were smaller than 18 microns. This discrepency in size is not easily explained. The most likely possibility is that a large number of the particles are of the 18 micron size even though the average particle size may be considerably less than 18 microns.

The calculated values of friction for Figs. 32 and 33 are for shaft surface speeds of 170 inches per second which is about the average speed used in the experimental investigations. If the shaft speed is increased above 170 inches per second, the calculated friction falls below the experimental values; and if the shaft speed is decreased, the friction falls above the experimental values. This indicates that another term is needed in the derivation of the theoretical friction which is a function of velocity. The derivations of Chapter II have only the one constant stress term added for the solid particles as a first approximation to this problem. If the shear stress of the particles is modified for speed, a relatively good solution should result at all speeds. This investigation was not extended to investigate additional velocity effects upon the particle shear.

Lubricant Flow Rates

In bearing design, the lubricant flow rate is quite important in many cases. For incompressible fluids, there is a minimum flow requirement in order to keep the bearing full of fluid. When this minimum flow is not supplied, the bearing is said to be in an "oil starved" condition. Bearings operating with an occasional drop of oil or bearings operating with a wick are usually in the starved condition. A starved bearing will not have the clearance space full of lubricant. This condition is to be avoided if possible because of the indeterminate decrease in load capacity. The clearance volume in the diverging flow passage past the point of minimum film thickness is a region which is an exception to the full flow requirement. A bearing is not considered as starved if this low pressure region is not full of oil.

Fluid pressures of any appreciable magnitude below absolute zero cannot be obtained in a liquid due to its in-ability to carry tension stresses. For this reason, the regions of a bearing which are theoretically below absolute zero pressure are considered as discontinuous with a rupture in the lubricant film. All liquid shear stresses were neglected in this region.

The side leakage or side flow can be calculated from the pressure and temperature distribution using equation (2.27) to calculate the velocity. By multiplying the velocity by the flow area, a volume flow is determined. The product of the volume flow and the exit density gives the weight flow. Flow in the y-direction is calculated for each x-station and summed over the boundary for total side flow.

Some of the oil supplied to a bearing is not lost by side leakage. This oil is carried through the minimum clearance space by shear at the point where the $\frac{\partial p}{\partial x} = 0$. Equation (2.26) for the velocity u is applicable if the $\frac{\partial p}{\partial x}$ is made equal to zero. As the eccentricity ratio is increased, the "swept oil" flow is decreased. In a bearing using a pressurized oil supply, the "swept oil" is considered as lost from the bearing to compensate for the reverse flow loss at the point of supply.

Fig. 34 shows a plot of the side flow ratio (Side Flow/ Total Flow) for an oil lubricated bearing. The shape of this curve is typical for a full 360 degree bearing operating with an incompressible fluid. A decrease in the ℓ/d ratio will shift the curve up and an increase in ℓ/d will move the curve

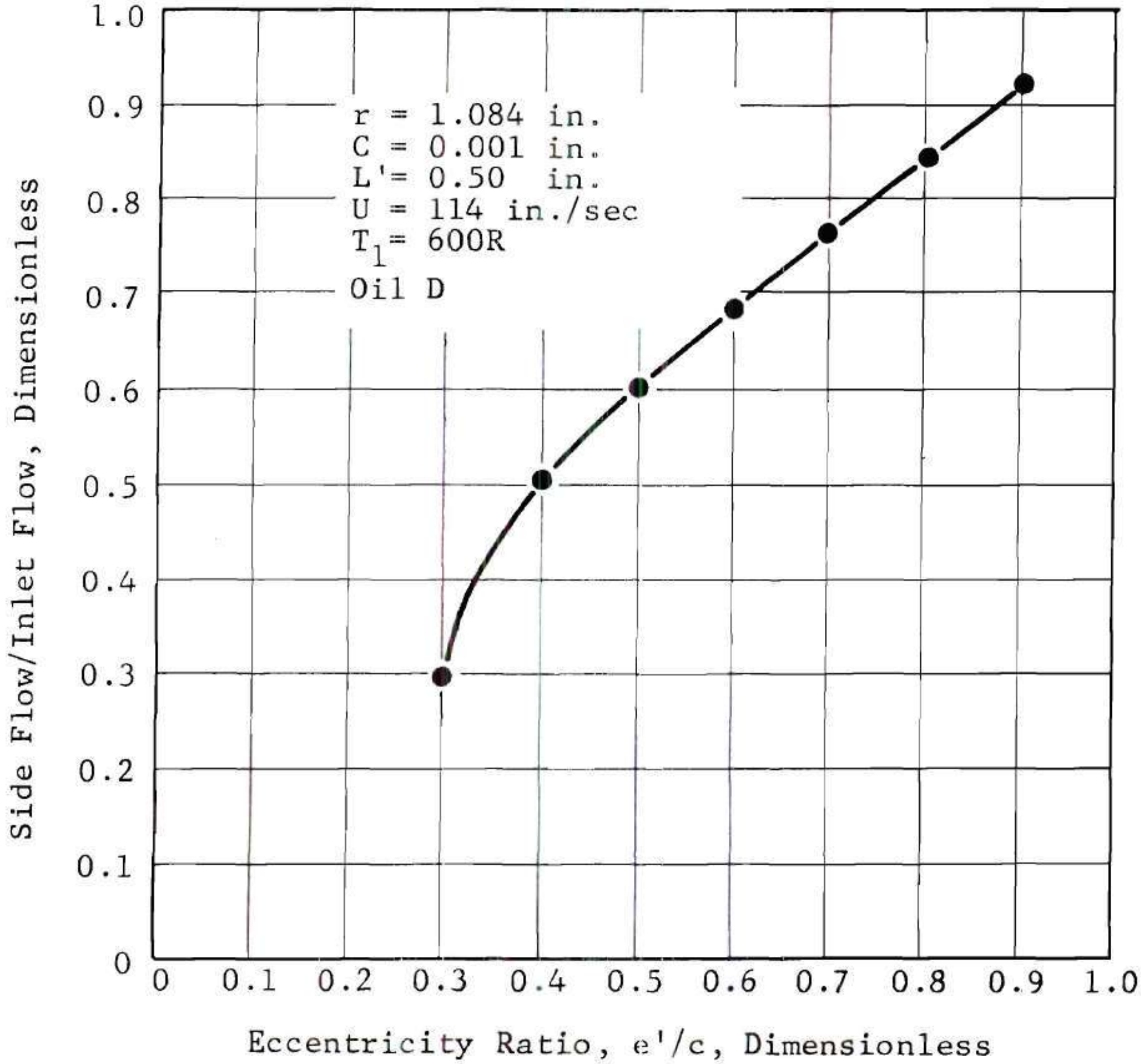

Figure 34. Lubricant Flow Ratio as a Function of the Eccentricity Ratio

down, but it will still have the same general shape for all incompressible lubricants. For compressible lubricants, the side flow is much more dependent upon the supply pressure and should be investigated for each specific design.

The use of oil grooves will increase the oil flow to a bearing and should be considered where a large amount of cooling is needed. Increasing the clearance will also increase the flow rapidly since the side flow is a function of c^3. High speed designs normally use larger clearance for reduced friction and increased flow.

Multiphase lubricants of the liquid-solid and gas-solid type may collect solid particles in the converging flow section of the bearing and restrict the flow. This flow characteristic was noticed in experimental gas-solid tests where the bearing would operate for a long period of time at a steady load and speed. This accumulation of solid could be expelled by cycling the load or speed. It should be noted, however, that some collection of solid was necessary to support high loads on a gas-solid lubricant.

CHAPTER VII

DESIGN METHODS

A specific step by step procedure for the design of a hydrodynamic bearing is impossible due to the relatively large number of choices in the design process. The following design methods are not a set of procedural steps, but instead they are a list of suggestions to make certain that important design aspects have not been neglected. These methods are applicable to the selection of a lubricant and the design of a satisfactory bearing geometry.

Many of the parameters such as the temperature, pressure and viscosity of the lubricant film are interrelated and must be considered jointly in the design process. The shaft rotational speed is normally fixed, but the surface speed is a function of the shaft diameter. If the shaft diameter is fixed, the design is reduced to the selection of a lubricant and the determination of the length, clearance, grooving and lubricant supply pressure. In many applications, there are a number of bearings which are fed from the same oil supply system. A system of this type would probably have a preset supply pressure due to the other bearings on the system. The following list of design steps is recommended for careful design.

1. Choice of Lubricant

For the selection of a lubricant, some help may be derived from a listing such as the one below.

a) Liquid lubricants -- use for high loads, moderate temperatures and speeds, and for maximum cooling.

b) Gas lubricants -- use for very high speeds, light loads, and any temperature.

c) Solid lubricants -- use for low speeds, very high to light loads, minimum cooling, and a wide range of temperature depending upon the solid and the environment.

d) Liquid-gas (incompressible) -- use where variable viscosity is desired or cannot be avoided in a liquid.

e) Gas-liquid (compressible) -- use in place of liquid where loads and cooling requirements are moderate.

f) Gas-solid -- use for any load, any speed, where relatively high friction can be tolerated, at a wide range of temperature depending upon the solid and the environment, and where only a small amount of cooling is necessary.

g) Liquid-solid -- use for high loads, low to moderate speeds, and for maximum cooling.

2. Lubricant Physical Properties

   Theoretical analysis requires the determination of the specific heat, thermal conductivity, viscosity, and density for all lubricants. For compressible lubricants, the exponent n must be determined. Equation (6.1) should be of some help. For liquid-solid and gas-solid mixtures, the concentration and the shear strength of the particles is required. Data for a number of lubricants are listed in the Appendix, Sections A and B. The lubricant stability may be important in liquid-gas systems (see Chapter VI).

3. Calculate Design Parameters

   Use the data for the lubricant from (2) above to calculate the design parameters of pressure, temperature, load, friction, lubricant flow, and eccentricity. For the solution of equations (4.20) and (4.34) for temperature and pressure, the computer solutions listed in the Appendix, Section C, are recommended. The computer solutions also give an easy way to calculate the load capacity, lubricant flows, average viscosity, average temperature, coefficient of friction, and Sommerfeld number as a function of speed, eccentricity ratio, particle shear strength, and particle concentration for any kind of boundary conditions. Adiabatic wall conditions are too conservative, and constant wall temperatures do not impose sufficiently stringent conditions.

4. Optimize Design

   Since the prime function of a bearing is to reduce the friction and wear at the point of relative motion, a minimum friction condition must be selected such that seizure and wear will not occur. This condition requires that the Sommerfeld number (Fig. 31) be reduced to a value corresponding to the maximum eccentricity ratio permissible. Fig. 26 shows a typical eccentricity plot as a function of the Sommerfeld number. Many other curves of this type are available in the literature (2), (15), (21). Considerations for some minimum cooling must be provided. The flow of lubricant must be adjusted so as to obtain the desired cooling by varying the supply pressure, changing the clearance, varying the ℓ/d ratio, or by oil grooving.

CHAPTER VIII

CONCLUSIONS

The equations derived to analyze the performance of multiphase lubricants in hydrodynamically lubricated bearings satisfactorily predicted the performance of liquid and liquid-solid lubricants when used under certain conditions. Theoretical studies of several compressible multiphase lubricants demonstrated the ability to calculate the performance of any bearing operated with any of the lubricant mixtures of solid, liquid, and gas, provided the physical properties of the lubricant were known.

From a study of the physical properties of several multiphase lubricants, the following general conclusions are made.

1. Compressible gas-solid and gas-liquid mixtures have values of the exponent n which are the same as the gas phase for the weight of solid or liquid normally used with this type of lubricant. For large amounts of liquid, equation (6.1) predicts the value of n for air.
2. The viscosity of the incompressible liquid-gas mixtures always decreases as the amount of absorbed gas increases. Large decreases in

viscosity are caused by small amounts of absorbed gas.

3. The amount of gas absorbed in a liquid at equilibrium conditions is dependent upon the type of gas, the type of liquid, and the temperature and pressure. The amount of gas absorbed increases with increasing pressure and decreases with increasing temperature.
4. The density of the incompressible liquid-gas mixtures is practically the same as for the liquid phase alone.
5. Liquid-gas mixtures in which the gas is in solution are sufficiently stable to pass through a bearing with the same physical properties as the original mixture. Applying a vacuum to the mixture greatly accelerates the return to the viscosity of the original liquid phase. For design purposes, the condition of the oil as supplied to the bearing should be used.
6. An oil used in an automobile engine does not absorb as much gas as the unused oil.
7. The addition of solid molybdenum-disulfide to an oil in amounts up to three percent by weight does not change the viscosity of the oil as measured by the Bendix Ultraviscoson viscometer.

A method for design of a bearing using multiphase lubricants of any type was developed. By using these equations, one may predict the temperature gradient through the lubricant film as well as the temperature distribution in the direction of motion. Computer programs for the design of a bearing using any of these lubricant mixtures have been assembled and run in the FORTRAN computer language. The use of computer solutions essentially allows the designer to construct his own design charts which will apply directly to his application.

CHAPTER IX

RECOMMENDATIONS FOR FUTURE INVESTIGATIONS

This investigation was limited to a few types of multiphase mixtures. The physical properties needed for bearing design should be determined for many other lubricant mixtures which offer excellent possibilities to the designer. Also of considerable importance would be a study of the undesirable mixtures with which the designer must contend, such as a liquid with solid contaminants of carbon, rust, and dirt.

The shear stress of particles in a liquid carrier was found to vary with the rate of shear. Satisfactory correlation between experimental data and theoretical calculations could only be obtained by varying the shear stress of the particles with speed. This indicates that additional terms should be added to the single constant term which was added to the fluid shear stress in the derivation of the design equations.

A study of the temperature distribution in a bearing with various amounts of cooling should be made by using the equations derived in this investigation. The expected operational temperature of a bearing is difficult to predict, but the designer would be greatly aided by some charts of expected temperature rise under certain design conditions.

APPENDICES

APPENDIX A

TABULATION OF PHYSICAL DATA FOR THE LUBRICANTS

Oil A

Gas Engine Oil (no additives)

Gravity, ^{o}API		29.0
Viscosity:	SUS at 100F	420.0
	SUS at 210F	58.7
Molecular weight		420.0
Viscosity index		94.0
Pour point, ^{o}F		20.0
Flash point, ^{o}F		425.0
Base		Paraffinic

Oil B

Pennzoil SAE 30

Specific gravity at 60F		0.88
Viscosity:	SUS at 100F	483.0
	SUS at 210F	63.0
Meets service requirements		MS,DG,DM

Oil C

Pennzoil SAE 30 (Used in VW engine 1750 miles)

This is the same oil as B but in a used condition.

Specific gravity at 60F		0.88
Viscosity:	SUS at 100F	252.0
	SUS at 210 F	62.1
Meets service requirements		MS,DG,DM

Oil D

Mathematical Model of SAE 30

Weight density, $lb/in.^3$	ρg
$\rho = 0.0307 - 0.0000132(T-520.0)$	
Viscosity, $lb - sec./in.^2$	μ
$\mu = e^{\alpha P} (Ae^{-\alpha T} + B)$	
α, temperature coefficient, $1/^oR$	0.0186
α, pressure coefficient, 1/psi	$4.36x10^{-5}$
A, viscosity coefficient, $lb - sec./in.^2$	0.260
B, viscosity constant, $lb - sec./in.^2$	$0.260x10^{-6}$
C_v, $\frac{in.-lb}{lb - deg R}$	4300
K, $\frac{in.-lb-in.}{in.-deg R-sec}$	0.0171

Polyphenyl Ether

Dow ET-54D

Specific gravity at 68F	1.2162
Viscosity, centistokes at 100F	3000
at 210F	28.4
at 400F	3.03
Flash point, ^oF	625
Fire point, ^oF	720
Pour point, ^oF	60

Teflon (powdered tetrafluoroethylene)

E. I. DuPont De Nemours	Teflon 7
Particle size (as purchased), microns	34
Screened to, microinches	950

Molybdenum Disulfide

Alpha Molykote	Microsize MoS_2 Powder
Molecular weight	160
Specific gravity	4.8 - 5.0
Melting point, ^oF	2700
Oxidizing temperature, ^oF	750
Purity, percent	98.7
Particle size, microns	7

GASES

	Carbon Dioxide	Ethane	Methane	Hydrogen	Helium
Molecular weight	44.0	30.069	16.040	2.016	4.0024
Purity, mole percent	99.2	99.6	99.35	99.15	99.3
Critical temp., ^{o}F	87.8	89.6	-115.0	-396.0	-447.0
Critical pressure, atmospheres	72.9	48.2	45.8	12.8	1.72

APPENDIX B

GRAPHICAL REPRESENTATION OF RESULTS FOR LIQUID-GAS LUBRICANTS

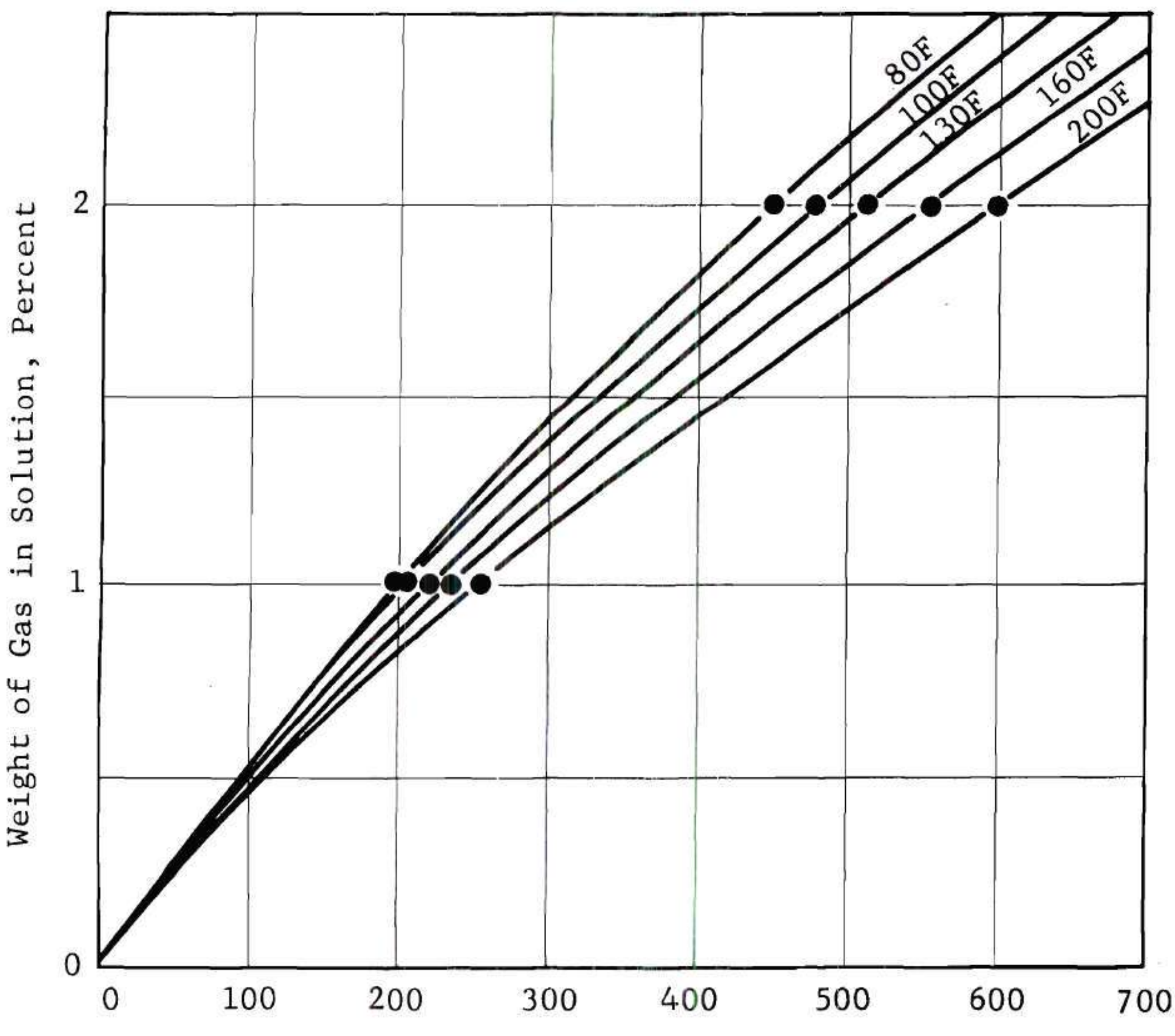

Figure 35. Gas Solubility in Oil Type A for Equilibrium Conditions with Methane

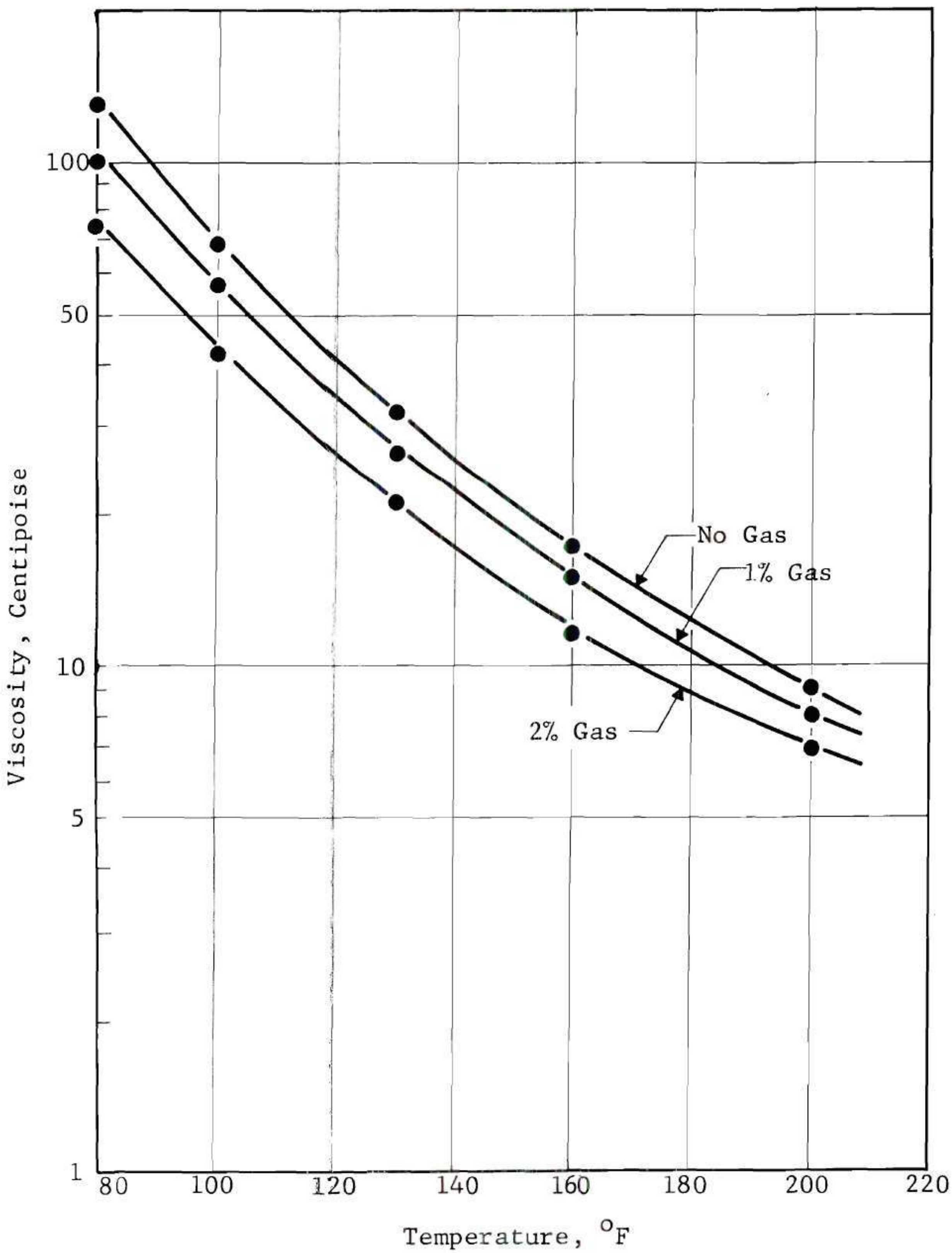

Figure 36. Viscosity vs. Temperature for Methane-Oil Type A System

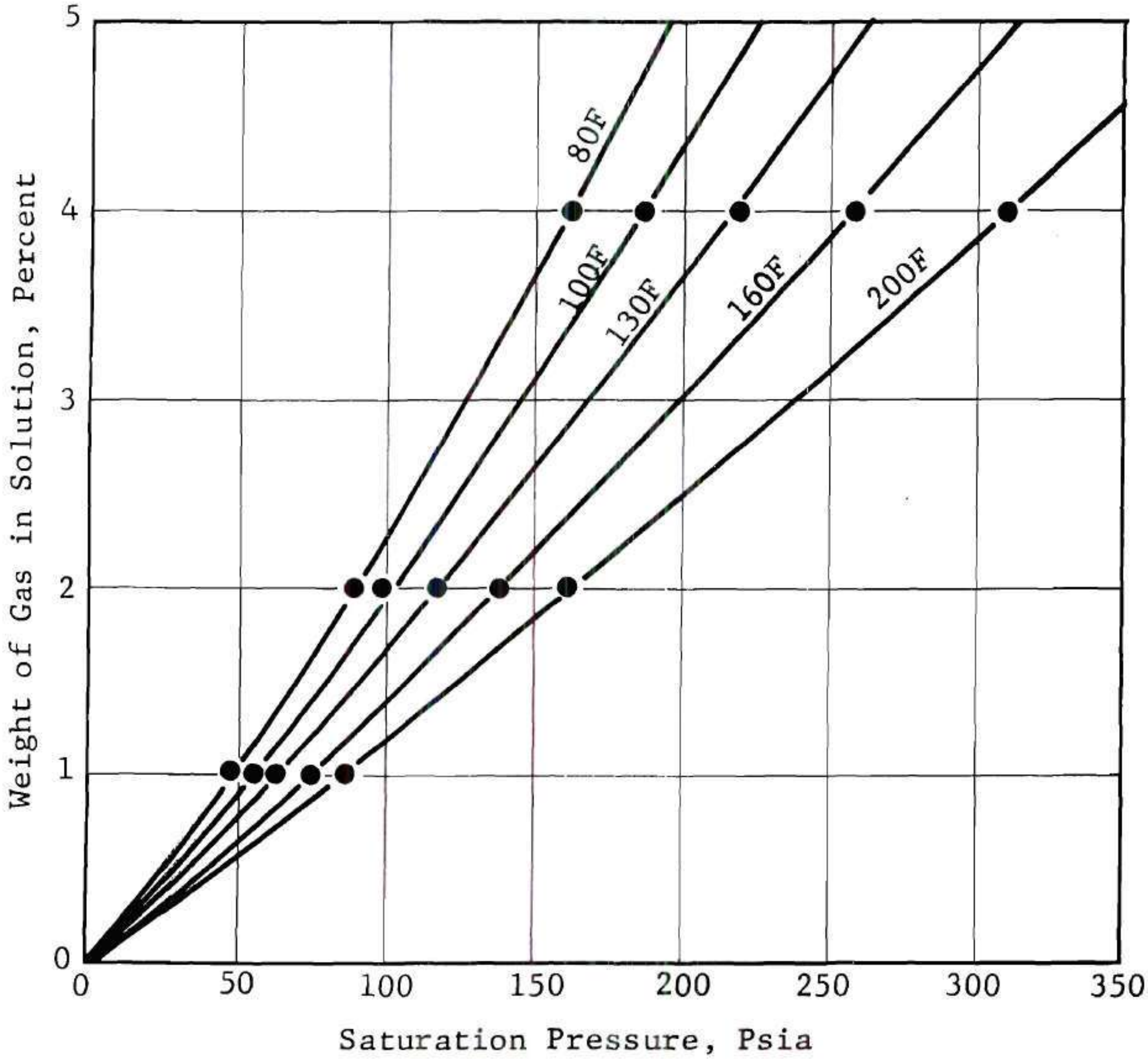

Figure 37. Gas Solubility in Oil Type A for Equilibrium Conditions with Ethane

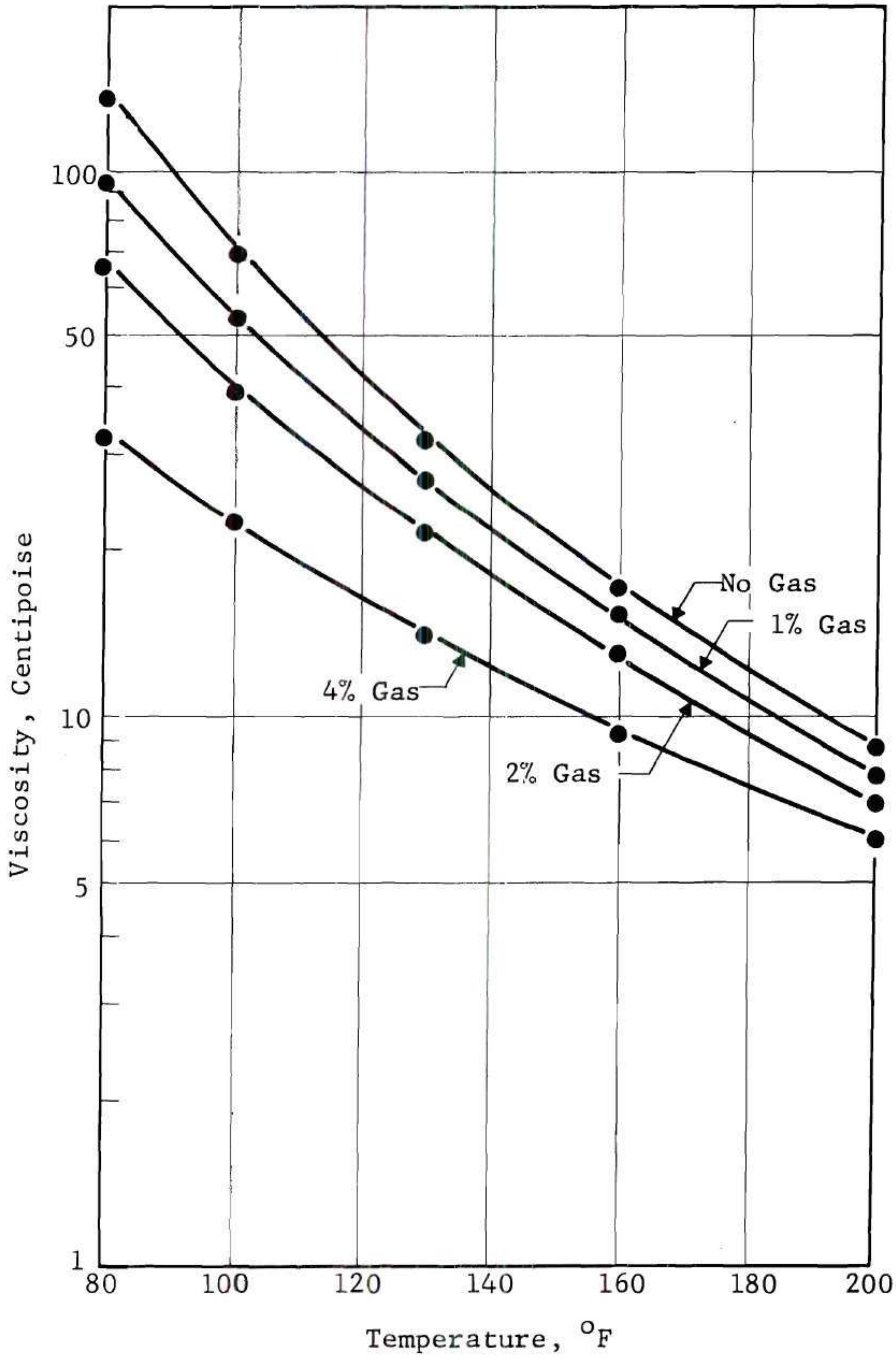

Fgiure 38. Viscosity vs. Temperature for Ethane-Oil Type A System

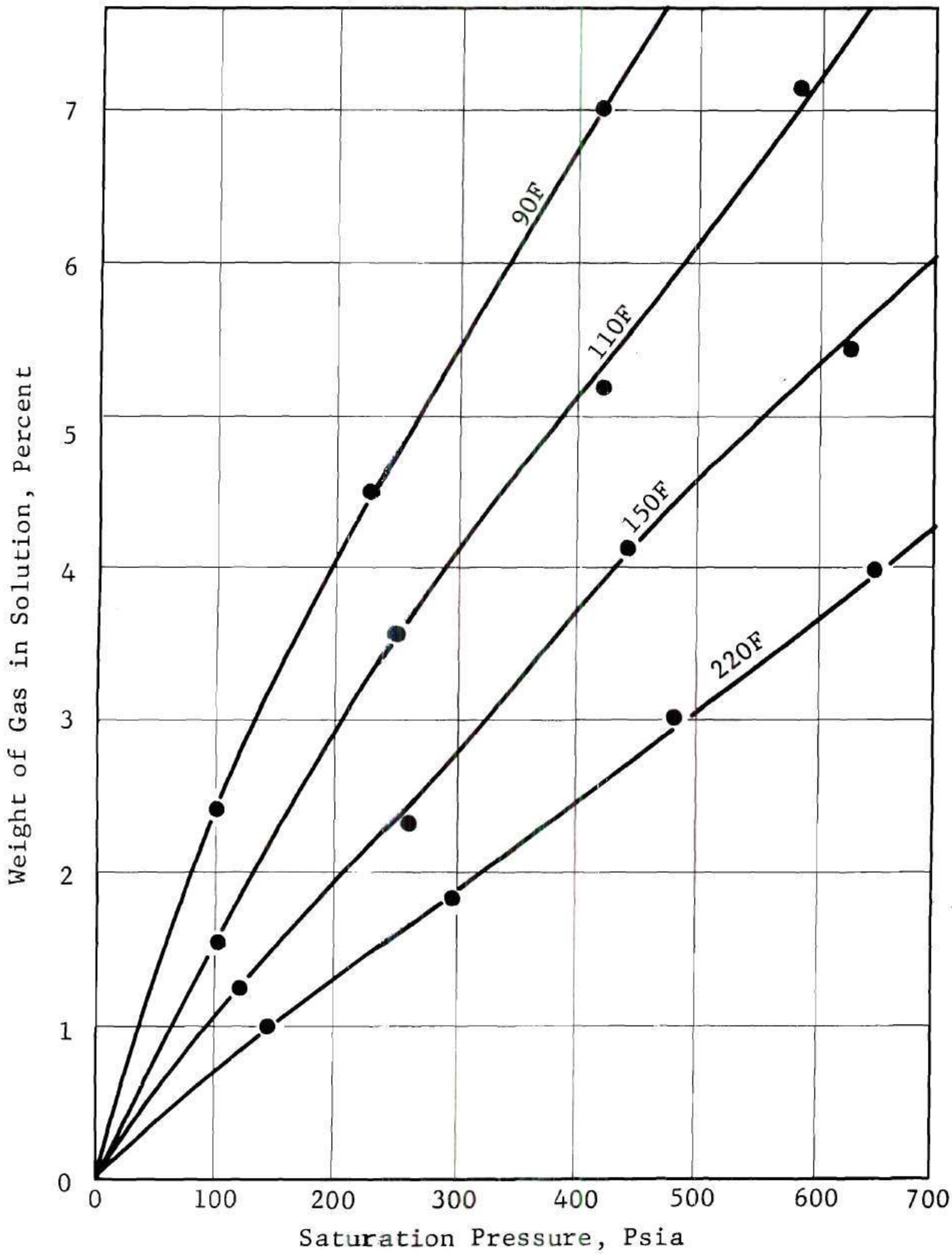

Figure 39. Gas Solubility in Oil Type B for Equilibrium Conditions with Carbon Dioxide

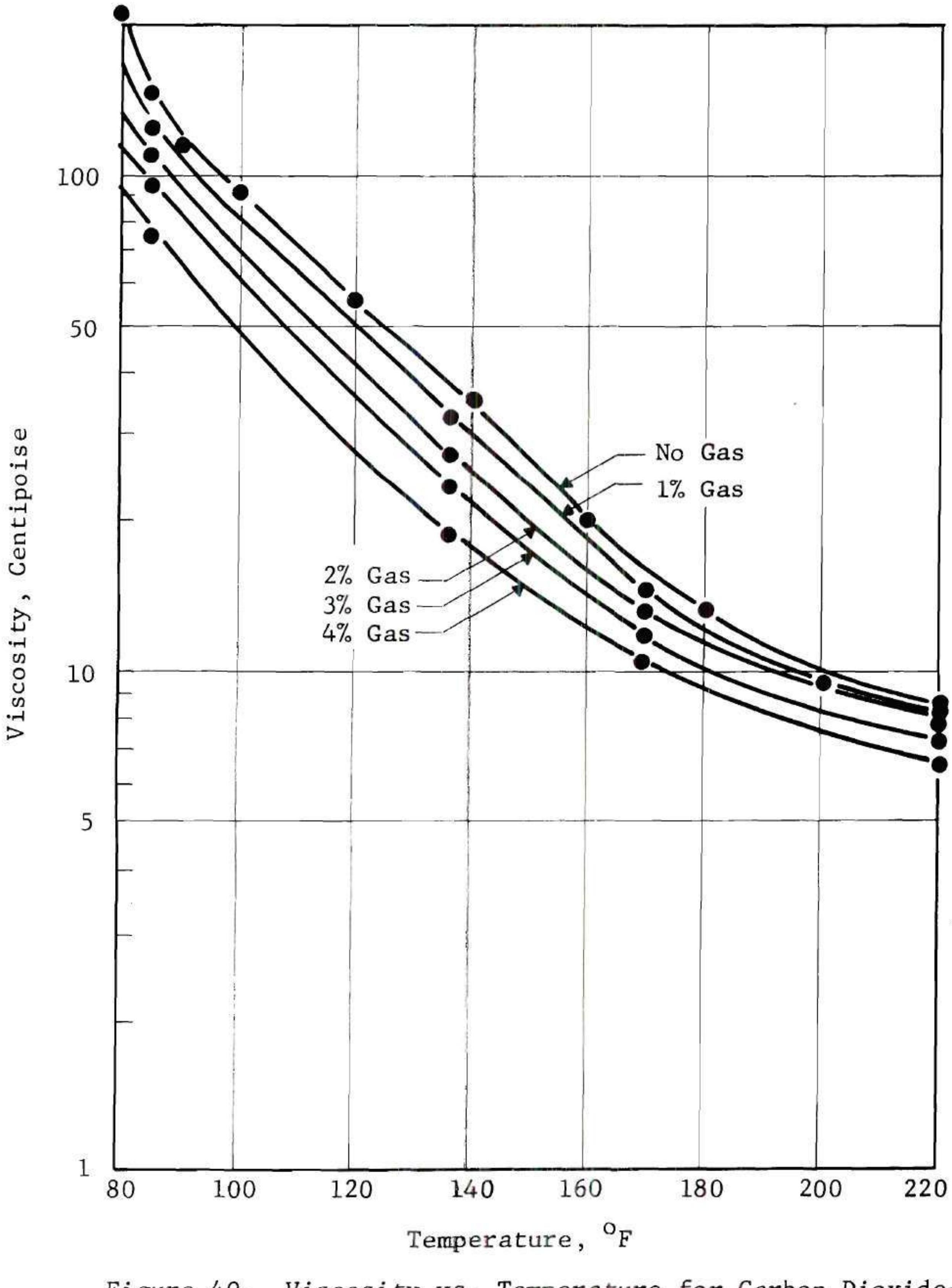

Figure 40. Viscosity vs. Temperature for Carbon Dioxide-Oil Type B System

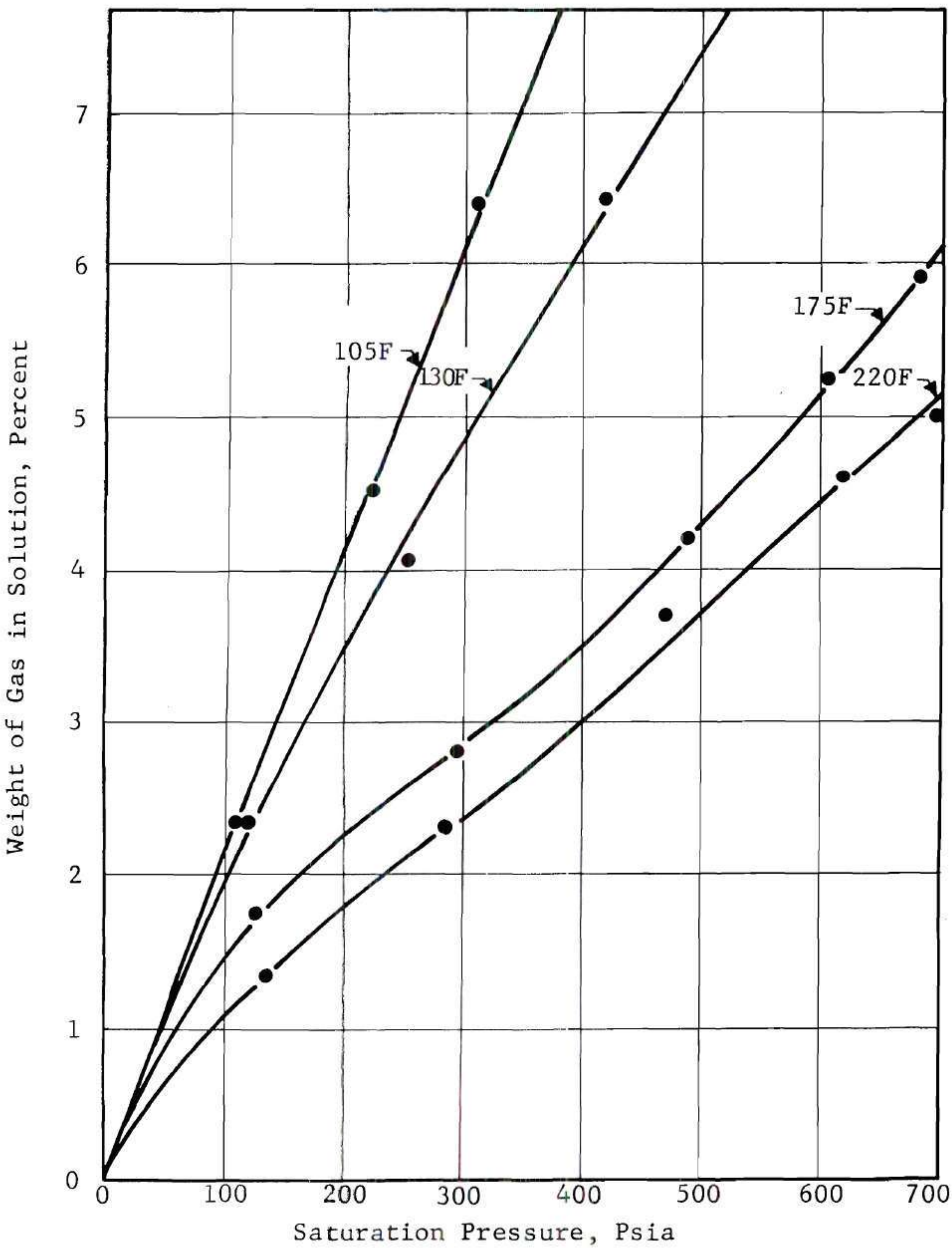

Figure 41. Gas Solubility in Oil Type C for Equilibrium Conditions with Carbon Dioxide

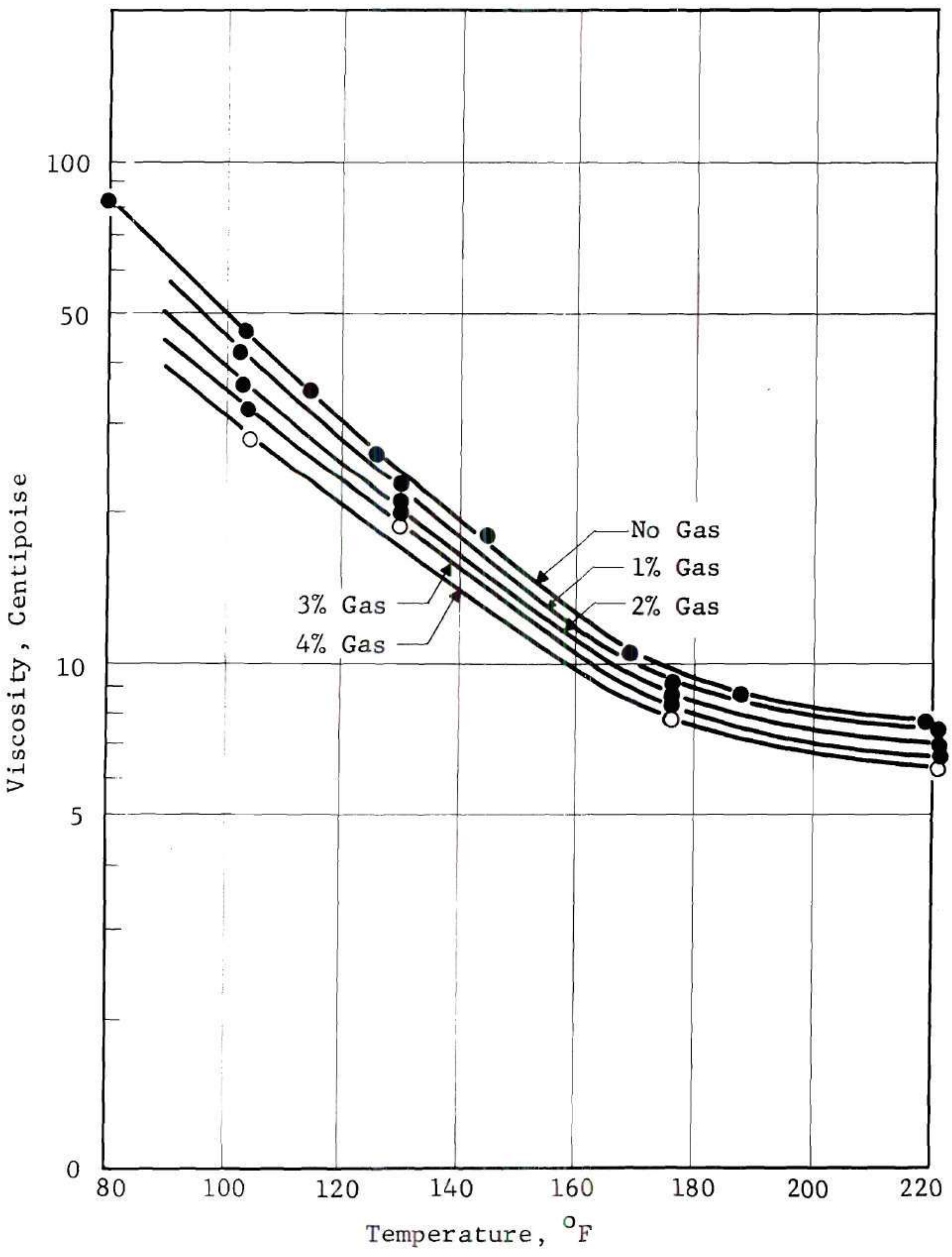

Figure 42. Viscosity vs. Temperature for Carbon Dioxide-Oil Type C System

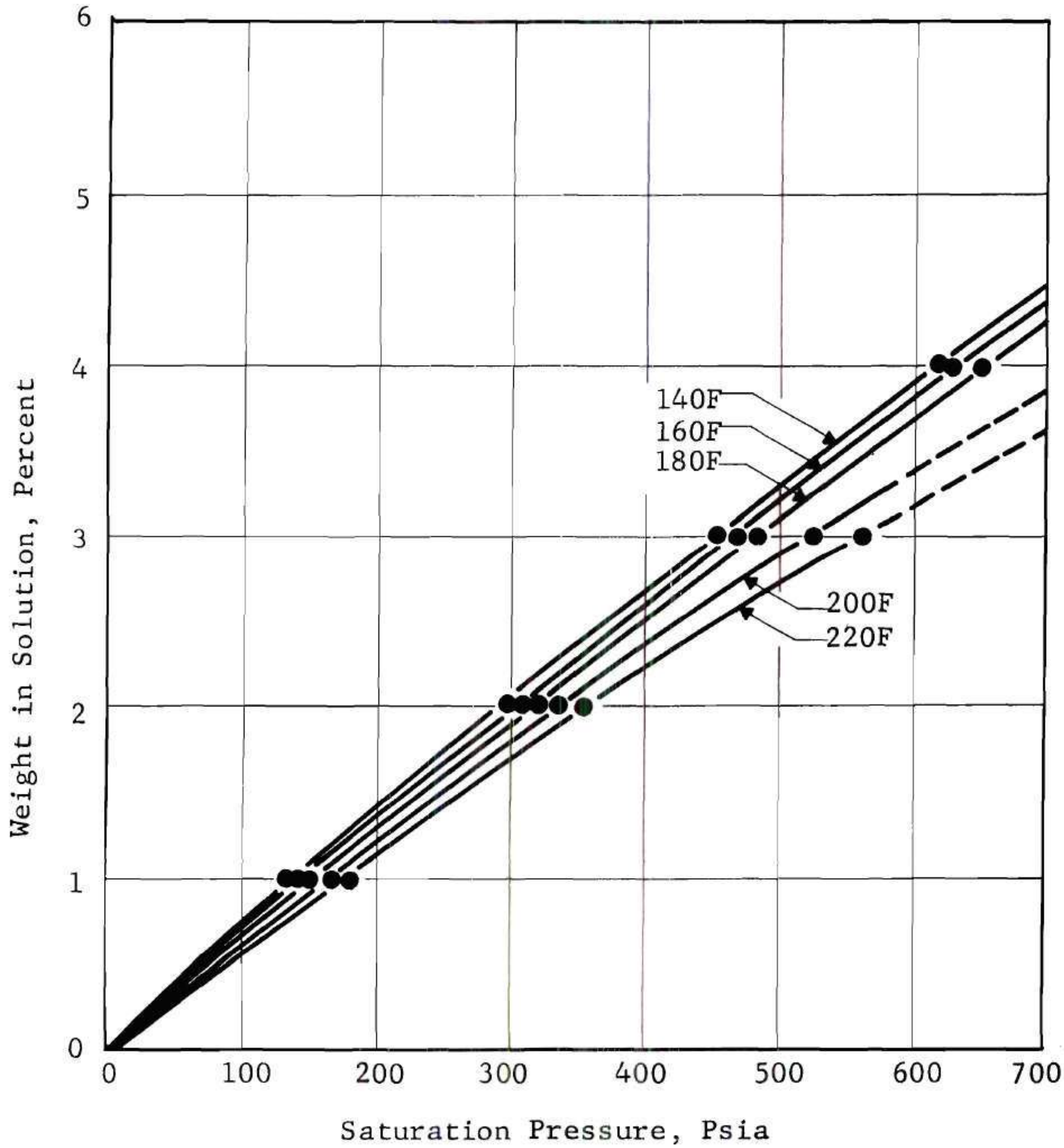

Figure 43. Gas Solubility in Polyphenyl Ether for Equilibrium Conditions with Carbon Dioxide

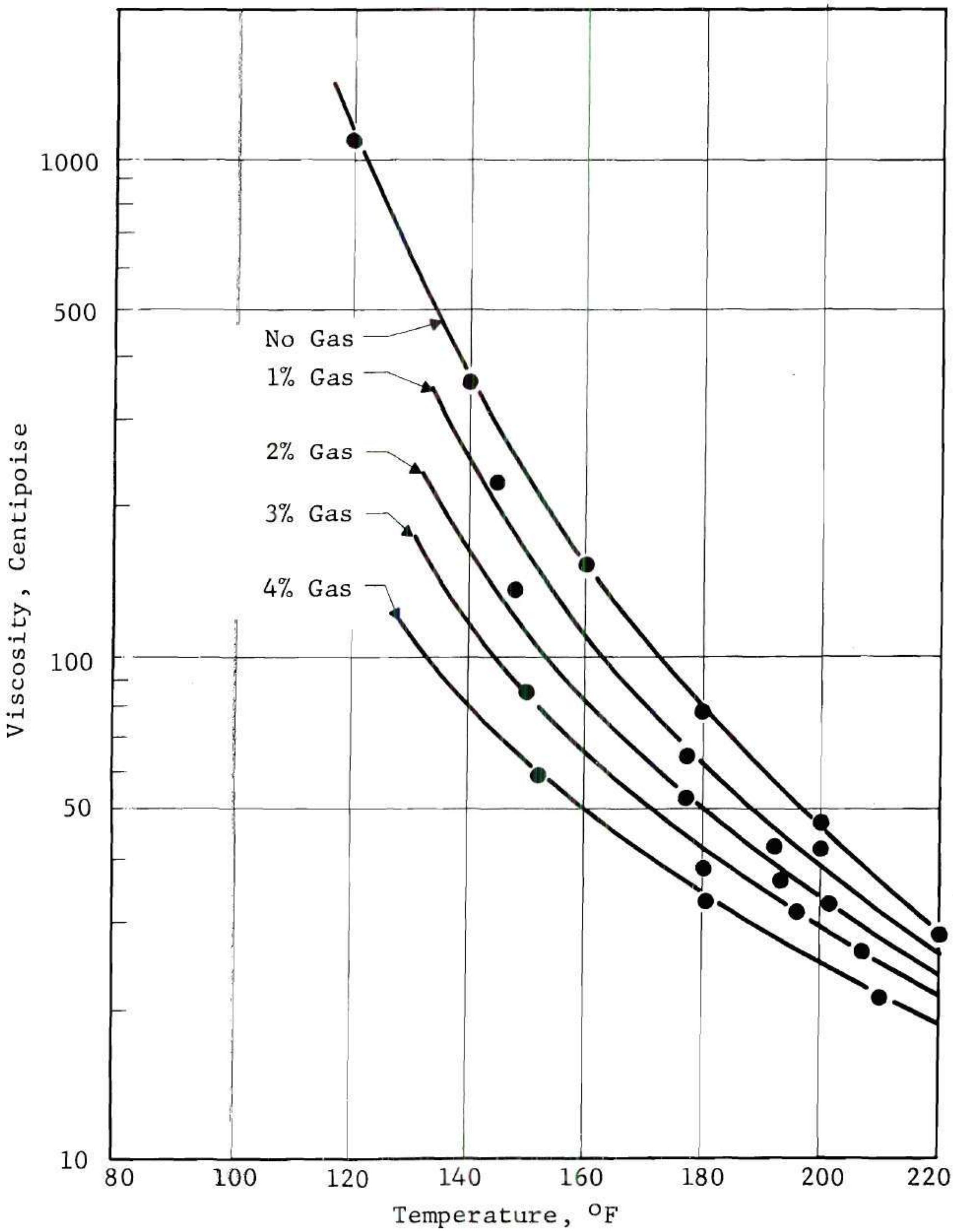

Figure 44. Viscosity vs. Temperature for Carbon Dioxide-Polyphenyl Ether System

APPENDIX C

COMPUTER SOLUTIONS AND SAMPLE OUTPUTS

1. Gas Absorption

(Computer program in FORTRAN language for CDC 1604 digital computer.)

Computer Nomenclature

BLKMDLA	Bulk modulus, psi
DL	Density of liquid, $\frac{gm}{cc}$
H	Height of liquid in sight glass, cm
HR	Reference mark height, cm
I	Charge number (1, initially; 2, first recharge;.....)
J	Run number (all of one data set has same run number)
K	State number (1, initially; 2, gas admitted; 3, saturated)
MM	Total number of runs
NN	Total number of times gas admitted per run
PC	Critical pressure, psia
PERCT	Percent gas absorbed by weight
PMA(I,J,K)	Absolute pressure in volume measurement cell, psia
PMG(I,J,K)	Gage pressure in volume measurement cell, psig
PR	Reduced pressure of volume measurement side, dimensionless.
PRV	Reduced pressure of visual cell, dimensionless
PVA(I,J,K)	Absolute pressure of visual cell, psia
PVG(I,J,K)	Gage pressure of volume measurement cell, psig
R	Gas constant, $\frac{ft\text{-}lb}{lb\text{-}^{o}R}$
TA(I,J,K)	Absolute temperature of system, ^{o}R

TC	Critical temperature, ^{o}R
VVC	Volume of visual cell side of system, cc
VVM	Volume of volume measurement side of system, cc
V12	Volume between valves 1 and 2, cc
Z(I,J,K)	Compressibility factor for volume measurement side of system, dimensionless
ZV(I,J,K)	Compressibility factor for visual cell, dimensionless

Density and Percent Gas Absorbed in Liquid

```
..GRADY RYLANDER      ME 030043
       PROGRAM GASABS
20     DIMENSION H(7,5,3),HR(7,5,3),T(7,5,3),PMG(7,5,3),PVG
         (7,5,3),
201    VVC(7,5,3),PMA(7,5,3),PVA(7,5,3),TA(7,5,3),Z(7,5,3)
         ZV(7,5,3)
30     COMMON H,HR,T,PMG,PVG,VVM,V12,R,PC,TC,MM,NN,LL,RT,TT,
         TM,VVC,PMA,
301    PVA,TA,A,B,C,TO,PO,WO,SS,PP,TR,PR,PRV,Z,ZV,DL
40     READ 12,A,B,C,VVM,V12
41     READ 12,PC,TC,TO, PO,WO
12     FORMAT (5E12.5)
       READ 10,SS,LL,MM,NN,PP
       DO 200 J=1,MM
10     FORMAT (5I10)
       SUM2=0.000
       WA1=0.000
       SUM1=0.000
       TERM9=0.000
       SUM4=0.000
42     READ 12,PMG(1,J,1),T(1,J,1),R,H(1,J,1),HR(1,J,1)
43     DO 300 I=2,NN
44     READ 12,PMG(I,J,2),PVG(I,J,2),T(I,J,2),H(I,J,2),HR
         (I,J,2)
45     READ 12,PMG(I,J,3),PVG(I,J,3),T(I,J,3),H(I,J,3),HR
         (I,J,3)
46     VVC(I,J,3)=71.90+(HR(I,J,3)-H(I,J,3))*(19.48+(0.269)*
         (T(I,J,3)-
461    100.0)/100.0
       PRINT 500
500    FORMAT (/ 10H DATA READ)
300    CONTINUE
```

```
      DO 100 I=1,NN
 50   DO 400 K=1,3
 51   PMA(I,J,K)=PMG(I,J,K)+14.7
 52   PVA(I,J,K)=PVG(I,J,K)+14.7
 53   TA(I,J,K)=T(I,J,K)+459.7
 54   PR=PMA(I,J,K)/PC
 55   PRV=PVA(I,J,K)/PC
 56   TR=TA(I,J,K)/TC
 57   TR2=TR**2
 58   TR4=TR**4
 62   TR7 = TR**7
 63   TR11 = TR**11
 64   IF (TR-1.06) 67,65,65
 65   IF (TR-1.08) 68,68,69
 67   FACTOR = 0.18764/TR-0.4758/TR2-0.05/TR4-0.0942/TR7
      GO TO 60
 68   FACTOR = 0.18764/TR-0.4758/TR2-0.05/TR4-0.0942/TR7+
        0.05/TR11
      GO TO 60
 69   FACTOR = 0.18764/TR-0.4758/TR2-0.05/TR4-0.0942/TR7+
        0.0749/TR11
 60   Z(I,J,K)=FACTOR*(PR)+1.0
 61   ZV(I,J,K)=FACTOR*(PRV)+1.0
 66   IF (PR-0.4) 400,125,127
127   IF (PR-0.6) 125,125,400
125   Z(I,J,K) = Z(I,J,K)*1.015
128   IF (PRV-0.4) 400,130,129
129   IF (PRV-0.6) 130,130,400
130   ZV(I,J,K) = ZV(I,J,K)*1.015
400   CONTINUE
      TEST=I-2
      IF (TEST) 70,34,34
 70   VL=159.63+(H(1,J,1)-HR(1,J,1))*(19.48)+(0.269)*(T(1,J,1)
        -100.0)/
 701  100.0
 71   DL = 0.856-0.000365*(T-84.0)
 72   WL=(DL)*(VL)
 34   IF (TEST) 33,75,75
 75   W2PHASE=WL+SUM2
 76   V2PHASE=159.63+(H(I,J,3)-HR(I,J,3))*(19.48)+(0.269)*
        (T(I,J,3)-100
 761  .0)/100.0
 77   D2PHASE=W2PHASE/V2PHASE
 33   IF (TEST) 31,32,35
 35   X = I-NN
 36   IF (X) 32,73,73
 31   BLKMDLS=((159.63+0.269*(T(1,J,1)-100.0)/100.0+((H(1,J,1)
        -HR(1,J,1
 311  ))*19.48))*(PVG(2,J,2)))/(((H(1,J,1)-HR(1,J,1)-
        H(2,J,2)+HR(2,J,2))
 312* 19.48)-0.011*PVG(2,J,2)/1000.0)
        IF (TEST) 73,32,32
```

```
32     BLKMDLS=((159.63+0.269*(T(I,J,3)-100.0)/100.0+((H
         (I,J,3)-HR(I,J,3)
321)*  19.48))*(PVG(I+1,J,2)-PVG(I,J,3)))/(((H(I,J,3)-HR
         (I,J,3)-H(I+1,J
322,2)+HR(I+1,J,2))*19.48)-0.011*PVG(I+1,J,2)/1000.0)
73     AN=I-2
       WA1=0.0
       WA2=0.0
       WA3=0.0
74     IF (AN) 110,80,88
80     TERM1=(PMA(1,J,1))*(VVM)/((Z(1,J,1))*(R)*(TA(1,J,1))*
         (196.68))
81     TERM2=(PMA(2,J,3))*(VVM)/((Z(2,J,3))*(R)*(TA(2,J,3))*
         (196.68))
82     TERM3=(PVA(2,J,3))*(V12)/((ZV(2,J,3))*(R)*(TA(2,J,3))*
         (196.68))
84     TERM4=(PVA(2,J,3))*(VVC(2,J,3))/((ZV(2,J,3))*(R)*
         (TA(2,J,3))*
841    (196.68))
85     SUM1=TERM4-TERM3
86     WA1=TERM1-TERM2+TERM3-TERM4
87     GO TO 110
88     IF (T(I,J,2)) 200,200,90
90     IF (PMG(I,J,2)) 91,91,37
91     TERM6=(PMA(I-1,J,3))*(VVM)/((Z(I-1,J,3))*(R)*(TA(I-1,
         J,3))*
911    (196.68))
92     TERM7=(PMA(I,J,3))*(VVM)/((Z(I,J,3))*(R)*(TA(I,J,3))*
         (196.68))
94     SUM4=SUM1-TERM8+TERM9
93     TERM8=(PVA(I,J,3))*(V12)/((ZV(I,J,3))*(R)*(TA(I,J,3))*
         (196.68))
95     TERM9=(PVA(I,J,3))*(VVC(I,J,3))/((ZV(I,J,3))*(R)*
         (TA(I,J,3))*
951    (196.68))
96     WA2=TERM6-TERM7+TERM8-TFRM9+SUM4
       WA1=0.000
       WA3=0.000
97     SUM1=0.000
       GO TO 110
37     IF (T(I,J,2)) 200,200,98
98     TER10=(PMA(I,J,2))*(VVM)/((Z(I,J,2))*(R)*(TA(I,J,2))*
         (196.68))
       TERM7=(PMA(I,J,3))*(VVM)/((Z(I,J,3))*(R)*(TA(I,J,3))*
         (196.68))
       SUM4 = TERM9-TERM8
       TERM8=(PVA(I,J,3))*(V12)/((ZV(I,J,3))*(R)*(TA(I,J,3))*
         (196.68))
       TERM9=(PVA(I,J,3))*(VVC(I,J,3))/((ZV(I,J,3))*(R)*
         (TA(I,J,3))*
```

```
    1     (196.68))
   99     WA3=TER10-TERM7+TERM8 TERM9+SUM4
          WA1=0.000
          WA2=0.000
  110     SUM2=SUM2+WA1+WA2+WA3
  111     PERCT=(SUM2/(WL))*(100.0)*(454.0)
          PRINT 1000
 1000     FORMAT (//38H CO2 ABSORBED IN USED SAE 30 PENNZOIL)
  112     PRINT 10,I,J,LL,MM,NN
  113     PRINT 12,T(I,J,3),PVG(I,J,3),SUM2,PERCT,DL
  114     PRINT 12,SUM1,WA1,WA2,WA3,SUM4
  115     PRINT 12,TERM1,TERM2,TERM3,TERM4,TERM6
  116     PRINT 12,TERM7,TERM8,TERM9,TER10,ZV(I,J,3)
  117     PRINT 12,PMA(I,J,2),PVA(I,J,3),TA(I,J,2),TR,TR2
  118     PRINT 12,TR4,FACTOR,Z(I,J,2),PR,PRV
  119     PRINT 12,BLKMDLS,W2PHASE,V2PHASE,D2PHASE,WA2
  100     CONTINUE
  200     CONTINUE
          END
          END
```

475.8E-03	1876.4E-04	0.5E-01	3248.9E-01	36.7E-01
107.4E+01	54.8E+01	00.0E+00	00.0E+00	00.0E+00
0	0	4	6	0
804.0E+00	101.5E+00	35.1E+00	77.582E+00	77.867E+00
0.0E+00	205.0E+00	101.4E+00	77.574E+00	77.867E+00
753.0E+00	92.0E+00	103.0E+00	77.659E+00	77.874E+00
0.0E+00	392.0E+00	103.0E+00	77.636E+00	77.870E+00
700.0E+00	213.0E+00	104.7E+00	77.774E+00	77.870E+00
0.0E+00	580.0E+00	104.7E+00	77.737E+00	77.870E+00
635.0E+00	392.0E+00	105.7E+00	77.885E+00	77.879E+00
812.0E+00	704.0E+00	104.3E+00	77.910E+00	77.838E+00
736.0E+00	545.0E+00	104.7E+00	78.082E+00	77.838E+00
816.0E+00	746.0E+00	104.3E+00	78.065E+00	77.838E+00
770.0E+00	638.0E+00	104.5E+00	78.207E+00	77.838E+00
815.0E+00	129.0E+00	35.1E+00	77.680E+00	77.875E+00
0.0E+00	222.0E+00	129.0E+00	77.644E+00	77.875E+00
747.0E+00	102.0E+00	129.3E+00	77.733E+00	77.880E+00
0.0E+00	392.0E+00	129.6E+00	77.725E+00	77.878E+00
680.0E+00	239.0E+00	129.6E+00	77.834E+00	77.880E+00
815.0E+00	587.0E+00	129.3E+00	77.827E+00	77.890E+00
739.0E+00	397.0E+00	128.7E+00	77.967E+00	77.890E+00
827.0E+00	727.0E+00	128.7E+00	77.957E+00	77.893E+00
769.0E+00	561.0E+00	128.7E+00	78.120E+00	77.895E+00
829.0E+00	743.0E+00	128.8E+00	78.120E+00	77.900E+00
780.0E+00	638.0E+00	129.3E+00	78.195E+00	77.898E+00
840.0E+00	173.5E+00	35.1E+00	77.735E+00	77.838E+00
0.0E+00	242.0E+00	173.7E+00	77.745E+00	77.838E+00
773.0E+00	111.0E+00	173.8E+00	77.822E+00	77.838E+00

848.0E+00	221.3E+00	35.1E+00	77.870E+00	77.860E+00
0.0E+00	230.0E+00	221.3E+00	77.808E+00	77.860E+00
784.0E+00	116.0E+00	221.6E+00	77.875E+00	77.840E+00
0.0E+00	417.0E+00	221.6E+00	77.865E+00	77.840E+00
719.0E+00	271.0E+00	221.6E+00	77.955E+00	77.870E+00
830.0E+00	620.0E+00	221.5E+00	77.945E+00	77.870E+00
755.0E+00	454.0E+00	221.6E+00	78.055E+00	77.860E+00
839.0E+00	722.0E+00	221.5E+00	78.028E+00	77.850E+00
784.0E+00	606.0E+00	221.3E+00	78.135E+00	77.850E+00
839.0E+00	753.0E+00	221.2E+00	78.128E+00	77.850E+00
814.0E+00	685.0E+00	221.0E+00	78.189E+00	77.850E+00
0.0E+00	428.0E+00	174.0E+00	77.812E+00	77.838E+00
713.0E+00	280.0E+00	174.7E+00	77.915E+00	77.838E+00
828.0E+00	643.0E+00	173.5E+00	77.885E+00	77.840E+00
759.0E+00	469.0E+00	174.2E+00	78.038E+00	77.838E+00
0.0E+00	694.0E+00	174.5E+00	78.022E+00	77.838E+00
712.0E+00	592.0E+00	174.6E+00	78.114E+00	77.838E+00
827.0E+00	721.0E+00	174.6E+00	78.125E+00	77.865E+00
799.0E+00	657.0E+00	174.6E+00	78.165E+00	77.840E+00

..GRADY RYLANDER ME 030043

DATA READ

DATA READ

DATA READ

DATA READ

DATA READ

CO2 ABSORBED IN USED SAE 30 PENNZOIL

1	1	0	4	6
.00000E+00	.00000E+00	.00000E+00	.00000E+00	.88666E+00
.00000E+00	.00000E+00	.00000E+00	.00000E+00	.00000E+00
.00000E+00	.00000E+00	.00000E+00	.00000E+00	.00000E+00
.00000E+00	.00000E+00	.00000E+00	.00000E+00	.98801E+00
.14700E+02	.14700E+02	.45970E+03	.83887E+00	.70370E+00
.49519E+00	-.87568E+00	.98801E+00	.13687E-01	.13687E-01
.20566E+06	.00000E+00	.00000E+00	.00000E+00	.00000E+00

CO2 ABSORBED IN USED SAE 30 PENNSOIL

2	1	0	4	6
.10300E+03	.92000E+02	.70534E-02	.23439E+01	.88666E+00
.20699E-02	.70534E-02	.00000E+00	.00000E+00	.00000E+00
.98305E-01	.89181E-01	.10489E-03	.21748E-02	.00000E+00
.00000E+00	.00000E+00	.00000E+00	.00000E+00	.96108E+00
.14700E+02	.10670E+03	.56110E+03	.10268E+01	.10544E+01
.11117E+01	-.39177E+00	.99458E+00	.71480E+00	.99348E-01
.12748E+06	.13662E+03	.15545E+03	.87886E+00	.00000E+00

CO2 ABSORBED IN USED SAE 30 PENNZOIL

3	1	0	4	6
.10470E+03	.21300E+03	.13544E-01	.45010E+01	.88666E+00
.00000E+00	.00000E+00	.64910E-02	.00000E+00	.20699E-02
.98305E-01	.89181E-01	.10489E-03	.21748E-02	.89181E-01
.80296E-01	.23367E-03	.46977E-02	.00000E+00	.91786E+00
.14700E+02	.22770E+03	.56270E+03	.10299E+01	.10607E+01
.11252E+01	-.38743E+00	.99464E+00	.66546E+00	.21201E+00
.81053E+05	.13663E+03	.15777E+03	.86597E+00	.64910E-02

CO2 ABSORBED IN USED SAE 30 PENNZOIL

4	1	0	4	6
.10570E+03	.39200E+03	.19502E-01	.64808E+01	.88666E+00
.00000E+00	.00000E+00	.59578E-02	.00000E+00	.44640E-02
.98305E-01	.89181E-01	.10489E-03	.21748E-02	.80296E-01
.70493E-01	.44765E-03	.87576E-02	.00000E+00	.85424E+00
.14700E+02	.40670E+03	.56440E+03	.10318E+01	.10645E+01
.11332E+01	-.38491E+00	.99470E+00	.60493E+00	.37868E+00
-.38538E+05	.13663E+03	.15976E+03	.85522E+00	.59578E-02

2. Bearing Performance

(Programs in FORTRAN language
for CDC 1604 digital computer.)

Computer Nomenclature

A	Viscosity coefficient, $\frac{\text{lb-sec}}{\text{in.}^2}$
ALF	Exponential viscosity coefficient for temperature, $\frac{1}{^{o}R}$
AN	Exponent for polytropic gas law, dimensionless
AMUAV	Average viscosity, $\frac{\text{lb-sec}}{\text{in.}^2}$
B	Viscosity coefficient, $\frac{\text{lb-sec}}{\text{in.}^2}$
BETA	Position of lubricant supply from load line, rad
C	Bearing clearance, in.
CAPU	Surface velocity, $\frac{\text{in.}}{\text{sec}}$
COF	Coefficient of friction, dimensionless
CRA,CRB,EPS,EPSIL,EPSILN,TEST,FINA	Convergence limits for program
CSTAR	Constant, in.
CV	Specific heat at constant volume, $\frac{\text{in.-lb}}{\text{lb-degR}}$
DX	Distance between grid stations in the x-direction, in.
DY	Distance between grid stations in the y-direction, in.
DZ	Distance between grid stations in the z-direction, in.
E	Shaft eccentricity, in.
ECC	Shaft eccentricity, in.
FK	Heat conductivity coefficient, $\frac{\text{in.-lb-in.}}{\text{in.-degR-sec}}$

FMU	Viscosity, $\frac{\text{lb-sec}}{\text{in.}^2}$
GAM	Exponential viscosity coefficient for pressure, $\frac{1}{\text{psia}}$
HK	Lubricant film thickness, in.
HP	Particle diameter, in.
HX	Slope, $\frac{\partial h}{\partial x}$ at position x, dimensionless
I	Index for x-station
J	Index for y-station
JJ	Number of grid stations in the y-direction, dimensionless
K	Index for z-station
L	Number of pressure stations in the x-direction
LL	Number of temperature stations in the x-direction
MM	Number of grid stations in the z-direction, dimensionless
N	Number of pressure stations in the y-direction
PHI	Angle between load line and a line through the bearing center and the point of minimum film thickness, rad
P(I,J)	Pressure, psia
PN	Particle concentration, weight percent
QOUT1	Side flow, $\frac{\text{lb}}{\text{sec}}$
QOUT2	Swept flow, $\frac{\text{lb}}{\text{sec}}$
QOUT3	Total flow, $\frac{\text{lb}}{\text{sec}}$

R	Bearing radius, in.
RP	Gas constant, $\frac{in.-lb}{lb-degR}$
RHO	Weight density, $\frac{lb}{in.^3}$
SFN	Sommerfeld, number, dimensionless
SUML	Load on bearing, lb
SUMT	Friction torque onshaft, in.-lb
SUMV	Side volume flow in y-direction, $in.^3/sec$
SUMV2	Swept volume flow in x-direction, $in.^3/sec$
SUMV3	Total volume flow, $in.^3/sec$
TAU	Shear stress on particles, psi
T(I,J,K)	Temperature, ^oR
U	Fluid velocity in the x-direction, $\frac{in.}{sec}$
V	Fluid velocity in the y-direction, $\frac{in.}{sec}$
X	Distance in the x-direction from inlet station, in.
Y	Distance in the y-direction from the bearing center line, in.
Z	Distance in the z-direction from shaft surface, in.

Bearing Performance For Oil D

```
..GRADY RYLANDER          ME030043         .001
      PROGRAM RYLAND
      CALL LIMIT (30)
20    DIMENSION FMU(70,8,8), P(70,8),  TEST(70,8,8),
 1    T(70,8,8),PRE(70,8)
      COMMON FMU,P,TEST,T,FINA,PRE
30    COMMON LL,JJ,MM,L,N,DX,DY,EPS,EPSIL,EPSILN,CV,FK,CAPU,
        A,B,ALF,
 1    GAM,CSTAR,AN ,R,BETA,C,E,RP,MMO,JMO,PHI,AK,TAU,PN,HP,
        CRA,CRB
      PRINT 1000
```

```
1000    FORMAT (13H OIL,E/C=.40)
        READ 10, LL,JJ,MM,L,N
  10    FORMAT (5I10)
        READ 12,DX,DY,EPS,EPSIL,EPSILN
  12    FORMAT (5E12.5)
        READ 12,CV,FK,CAPU,A,B
        READ 14,ALF,GAM,CSTAR,AN
  14    FORMAT (4E12.5)
        READ 12,R,BETA,C,E,RP
        READ 12,TAU,PN,HP,CRA,CRB
        MMO=MM-1
        JMO=JJ-1
        PHI = ACOSF (E/C)
        AK = 0.0
        FINA = 0.0
        DO 20 K=1,MM
        DO 20 J=1,JJ
        DO 20 I=1,LL
        T(I,J,K) = 600.0*(1.0+0.0005*( FLOATF(I-1)))
        P(I,J) = 15.0
        FINA = FINA + T(I,J,K)
  20    CONTINUE
        DO 26 J=2,JMO
        DO 26 I=1,LL
        P(1,J)=50.0
        P(I,7)=15.0
  26    CONTINUE
        CONVERG=1.0
 805    DO 806 I=1,LL
        DO 807 J=2,JMO
        DO 808 K=2,MMO
 808    CONTINUE
 807    CONTINUE
 806    CONTINUE
        CALL TEMPER
        CALL PRESSUR
        CALL TEMPER
        TSUM=0.0
        DO 810 I=1,LL
        DO 811 J=2,JMO
        DO 812 K=2,MMO
        TSUM=TSUM+T(I,J,K)
 812    CONTINUE
 811    CONTINUE
 810    CONTINUE
        CM=CONVERG
        TRY = ABSF(FINA-TSUM)
        TAVG = TSUM/FLOATF(LL*(JMO-1)*(MMO-1))
        CONVERG = TRY/TSUM
        FINA = TSUM
        PRINT 2002, CONVERG
2002    FORMAT (E20.5)
```

```
      IF(CONVERG - EPS)250,250,803
 803  IF (CM-CONVERG)250,250,805
 250  PRINT 10,LL,JJ,MM,L,N,MMO
      PRINT 12,DX,DY,EPS,EPSIL,EPSILN
      PRINT 12,CV,FK,CAPU,A,B
      PRINT 14,ALF,GAM,CSTAR,AN
      PRINT 12,R,BETA,C,E,RP
      PRINT 12,TAU,PN,HP,CRA,TAVG
      PRINT 2001
2001  FORMAT (// 22H PRESSURE DISTRIBUTION)
      DO 263 I=1,LL
      PRINT 18,( P(I,J), J=2,JMO)
  18  FORMAT(6F10.3)
 263  CONTINUE
      PRINT 2000
2000  FORMAT (// 25H TEMPERATURE DISTRIBUTION)
 103  DO 107 K=2,MMO
      PRINT 105,K
 105  FORMAT (/  3H Z=I1/)
      DO 109 I=1,LL
      PRINT 18,  (T(I,J,K), J=2,JMO)
 109  CONTINUE
 107  CONTINUE
      QOUT2 = 0.00
      SUMV2 = 0.00
      QOUT1 = 0.00
      SUMV = 0.00
 602  SUML = 0.00
 603  SUMMU = 0.00
 604  SUMT = 0.00
 601  PI = 3.1415927
 605  DO 690 I-3,LL
 606  JMA = JJ-1
 607  DO 690 J=3,JMA
 608  AI = I-1
 609  X = AK+(AI+0.5)*DX
 610  HK = C+E*COSF(X/R)
 611  PAV = 0.25*(P(I-1,J)+P(I,J)+P(I-1,J+1)+P(I,J+1))
      AMU = (FMU(I,J,3)+ FMU(I,J,4)+FMU(I,J,5)+FMU(I,J,6)
        +FMU(I,J,7))/5.0
      TAP = (PN*TAU)
      CLN = HK-HP
      IF (CLN) 621,621,613
 613  TAP = 0.0
 621  TAA = ((0.50*HK*(P(I,J)-P(I-1,J)))/DX)+(AMU*CAPU)/HK+TAP
 620  SUML = SUML+PAV*COSF(PI-(X/R+PHI))*DX*DY
 222  SUMT = SUMT+TAA*DX*DY*R
 623  SUMMU = SUMMU+AMU
      IN = J-6
      IF (IN) 637,624,637
 637  GO TO 689
```

```
 624   X1 = AK+AI*DX
 625   X2 = AK+(AI+1.0)*DX
 630   HK1 = C+E*COSF(X1/R)
 631   HK2 = C+E*COSF(X2/R)
 632   IF (AN) 635,636,635
 635   RHO = ((P(I,6)+P(I,7))/(CSTAR*2.0))**(1.0/AN)
       GO TO 640
 636   RHO = 0.0307-0.0000132*(T(I,J,3)-520.0)
 640   DVO = 0.0
       HAV = (HK1+HK2)/2.0
       IF (P(I,3)) 642,642,641
 641   DVO =-(2.0*P(I,7)-P(I-1,6)-P(I,6))*(HAV**3)*DX/(DY*AMU
         *24.0)
 642   SUMV = SUMV+DVO
 643   DQ = RHO*DVO
 644   QOUT1 = QOUT1+DQ
 645   HMIN = C-E
 646   DV2 = HMIN*FLOATF(N)*CAPU*DY/2.0
 647   QOUT2 = DV2*RHO
 648   SUMV2 = DV2
 649   QOUT3 = QOUT1+QOUT2
 650   SUMV3 = SUMV+SUMV2
 651   AMUAV = SUMMU/(FLOATF((LL-2)*(JMA-2)))
 652   COF = SUMT/(R*SUML)
 689   CONTINUE
 690   CONTINUE
       PRINT 3005
3005   FORMAT (/ 57H LOAD   TORQUE   SIDE VOL   SWEPT VOL  FLOW
   1   VOL)
       PRINT 12,SUML,SUMT,SUMV,SUMV2,SUMV3
       PRINT 3006
3006   FORMAT (/ 61H SIDE FLOW  SWEPT FLOW  TOT FLOW  VISCOSITY
   1     COEF FRICTION)
       PRINT 12,QOUT1,QOUT2,QOUT3,AMUAV,COF
       END
       SUBROUTINE TEMPER
  20   DIMENSION FMU (70,8,8),P(70,8),  TEST(70,8,8)
   1   T(70,8,8),PRE(70,8)
       COMMON FMU,P,TEST,T,FINA,PRE
  30   COMMON LL,JJ,MM,L,N,DX,DY,EPS,EPSIL,EPSILN,CV,FK,CAPU,A,
   1     B,ALF,CAM,CSTAR,AN,P,BETA,C,E,RP,MMO,JMO,PHI,AK,TAU,
         PN,HP,CRA,CRB
       JAY = 1
       IT = 0
       PRINT 999
 999   FORMAT(18H CHECK POINT TEMP)
 108   DO 110 K=2,MMO
       DO 110 I-1,LL
       T(I,1,K) = T(I,3,K)
       T(I,JJ,K) = T(I,JJ-2,K)
       P(I,1) = P(I,3)
```

```
      P(I,JJ)= P(I,JJ-1)
110   CONTINUE
      DO 115 I=1,LL
      DO 115 J=1,JJ
      T(I,J,1) = T(I,J,3)
      T(I,J,MM) = 620.0
115   CONTINUE
      DO 515 K=1,MM
      DO 515 J=1,JJ
      T(LL+1,J,K) = T(LL-1,J,K)
      T(LL,J,K) = T(LL-1,J,K)
      P(LL+1,J) = P(LL-1,J)
515   CONTINUE
      GO TO (516,106),JAY
516   DO 105 K=1,MM
      DO 105 J=1,JJ
      DO 105 I=1,LL
      FMU(I,J,K) = EXPF(GAM*P(I,J))*(A/EXPF(ALF*T(I,J,K))+B)
105   CONTINUE
      CMCONV = 10.0
106   GREAT = 0.0
      TSUM = 0.0
      DEVSUM = 0.0
      IT=IT+1
      DO 166 I = 2,LL
      X=FLOATF(I-1) * DX + AK
      H = C + E * COSF (X/R)
      DO 167 K=2,MMO
      DZ = H/FLOATF(MM-3)
      Z= DZ * FLOATF (K-2)-DZ/2.0
      DO 165 J=2,JMO
      Y=FLOATF (J-2) * DY
C     FIRST TERM
122   IF (AN) 125,126,125
125   RHO = (P(I,J)/CSTAR)**(1.0/AN)
      GO TO 127
126   RHO = 0.0307-0.0000132*(T(I,J,K)-520.0)
127   TWOMU = 2.0 * FMU(I,J,K)
      DPDX = (P(I+1,J) -P(I -1,J)) / (2.0*DX)
      DPDY = (P(I,J+1) -P(I,J-1)) / (2.0*DY)
      U = (1.0/TWOMU)*DPDX*(Z**2-Z*H) + CAPU*(H-Z)/H
      V = (1.0/TWOMU)* DPDY* (Z**2 - Z*H)
      DTDX = (T(I+1,J,K) - T(I-1,J,K)) / (2.0*DX)
      DTDY = (T(I,J+1,K) - T(I,J-1,K)) / (2.0*DY)
      FIRST = RHO *CV *(U*DTDX + V*DTDY)
C     SECOND TERM
      IF (AN) 136,140,136
136   PAREN = (CSTAR/P(I,J)) ** ((1.0+AN)/AN)
      FNCTOR = (-1.0/(AN*CSTAR))*PAREN
      DXRHIN = FNCTOR *DPDX
      DYRHIN = FNCTOR *DPDY
```

```
      SECOND = RHO * P(I,J)*(U*DXRHIN + V*DYRHIN)
      GO TO 143
140   SECOND = 0.0
C     THIRD TERM
143   DMUDZ = (FMU(I,J,K+1) - FMU(I,J,K-1)) / (2.0*DZ)
      FMUINV = 1.0 / FMU(I,J,K)
      FMUIN2 = FMUINV ** 2
      PARN = FMUINV * (2.0*Z-H) - (Z**2 - Z*H) * FMUIN2 * DMUDZ
      DUDZ = 0.5*DPDX*PARN-CAPU/H
      DVDZ = 0.5 * DPDY * PARN
C     TEMPERATURE
      DYDZ2 = (DY*DZ)**2
      DXDZ2 = (DX*DZ)**2
      DXDY2 = (DX*DY)**2
      ONE = T(I+1,J,K) + T(I-1,J,K)
      TWO = T(I,J+1,K) + T(I,J-1,K)
      THREE = T(I,J,K+1) + T(I,J,K-1)
      FACTOR = 0.5 / (DXDZ2 +DYDZ2 +DXDY2)
      PART 1 = DYDZ2 *ONE +DXDZ2 *TWO +DXDY2 *THREE
      TEMP = T(I,J,K)
      THIRD = -FMU(I,J,K)*(DUDZ**2+DVDZ** 2)
      DELSQ = (DX*DY*DZ)**2
      FOUR = RHO*CV*(U/DX+V/DY)
      PART 3 = 1.0+FOUR*DELSQ*FACTOR/FK
      FIVE = RHO*CV*U*T(I-1,J,K)/DX
      AI = I-1
      X = AK + AI*DX
      HK = C+E*COSF(X/R)
      CLN = HK-HP
      FOURTH = 0.0
      IF(CLN) 213,213,214
213   FOURTH = PN*TAU*ABSF(DUDZ)
214   SIX = RHO*CV*V*T(I,J-1,K)/DY
      IF (P(I,3)) 215,215,216
215   THIRD = 0.0
      SECOND = 0.0
216   PART 4 = (DELSQ/FK)*(SIX+FIVE-THIRD-SECOND +FOURTH)
      PART 5 = FACTOR*(PART1+PART4)
      T(I,J,K) = PART5/PART3
      OMG=1.0
      DEV = ABSF (T(I,J,K) - TEMP)
      TSUM = TSUM + T(I,J,K)
      DEVSUM = DEVSUM + DEV
      IF (GREAT - DEV) 172,173,173
172   GREAT = DEV
173   IF(10.0E+10 - GREAT) 248,248,165
165   CONTINUE
167   CONTINUE
166   CONTINUE
      CM=CMCONV
      CMCONV = DEVSUM / TSUM
```

```
      AVDEV = DEVSUM / FLOATF((LL-1)*(JJ-2)*(MM-2))
      PRINT 905, T(3,2,2),T(9,2,2),T(20,4,6),T(40,4,4),T(50,4,
    1 4), T(60,4,4), T(65,4,4)
905   FORMAT (7E12.5/)
304   IF(1.0E-03- CMCONV) 400,302,302
302   JAY=1
      IT=0
307   SM = 0.0
      DO 310 K=2,MMO
      DO 309 J=2,JMO
      DO 308 I=1,LL
      SM = SM + ABSF(TEST(I,J,K) - T(I,J,K))
308   CONTINUE
309   CONTINUE
310   CONTINUE
      CONV = SM/TSUM
      IF(1.0E-03 - CONV)315,312,312
312   PRINT 313
313   FORMAT (16H T HAS CONVERGED)
      GO TO 901
315   DO 319 K=2,MMO
      DO 318 J=2,JMO
      DO 317 I=1,LL
      TEST(I,J,K)=T(I,J,K)
317   CONTINUE
318   CONTINUE
319   CONTINUE
      PRINT 301
301   FORMAT (12H FMU CHANGED)
      GO TO 108
400   IF(IT-2)102,102,401
401   IF(CM - CMCONV) 402,402,102
402   GO TO 302
102   JAY = 2
      GO TO 108
248   PRINT 249
249   FORMAT (18H DEV OUT OF RANGE)
      STOP
901   CONTINUE
      END
      SUBROUTINE PRESSUR
   20 DIMENSION FMU(70,8,8), P(70,8), TEST (70,8,8),
    1 T(70,8,8), PRE(70,8)
      COMMON FMU,P,TEST,T,FINA,PRE
   30 COMMON LL,JJ,MM,L,N,DX,DY,EPS,EPSIL,EPSILN,CV,FK,CAPU,
        A,B,ALF,
    1  GAM,CSTAR,AN,R,BETA,C,E,RP,MMO,JMO,PHI,AK,TAU,PN,HP,CRA,
        CRB
      PRINT 998
998   FORMAT(18H CHECK POINT PRES)
202   M1 = L+1
```

```
      N1 = N+1
      M2 = L+2
      N2 = N+2
      DX2 = DX*DX
      DY2 = DY*DY
300   DIFS = 0.0
      SUMP = 0.0
      DO 233 M=2,N1
      DO 232 K=2,M1
      AI = K-1
      X = AK + AI*DX
      HK = C + E*COSF(X/R)
      HX = -(E/R) * SINF(X/R)
      TAB = 2.0/DX2 + 2.0/DY2
      AMU=(FMU(K,M,3)+FMU(K,M,4)+FMU(K,M,5)+FMU(K,M,6)+FMU(K,
        M,7))/5.0
      G1 = (P(K+1,M) + P(K-1,M))/DX2
      G2 = (P(K,M+1) + P(K,M-1))/DY2
      PMK = P(K+1,M) - P(K-1,M)
      G3 = (3.0*HX* PMK) / (DX*HK* 2.0)
      G = (G1+G2+G3 - (6.0* AMU* CAPU *HX)/(HK**3))/(2.0*TAB)
      PX = PMK/DX
      PX2 = PX*PX
      PY = (P(K,M+1) - P(K,M-1)) /DY
      PY2 = PY*PY
      IF (AN) 299,299,228
299   HMK = 0.0
      GO TO 229
228   HMK = ((3.0 *AMU *CAPU *PX)/(HK*HK)-(0.25*PX2)-(0.25*PY2))
       /(TAB*AN)
229   PMK = G +SQRTF(G*G-HMK)
      IF (PMK) 231,296,296
231   DO 297 K1=K,M2
297   P(K1,M) =0.0
      IF (M-3)233,701,233
701   DO 702 K1=K,M2
702   P(K1,M-2) = P(K1,M)
      GO TO 233
296   DIFS = ABSF (PMK-P(K,M))+DIFS
      SUMP = SUMP + PMK
      P(K,M) = PMK
      IF (M-3) 232,295,232
295   P(K,M-2) = PMK
232   CONTINUE
      P(K,M) = PMK
233   CONTINUE
      CONV = (DIFS/SUMP) - EPS
      IF (CONV)900,900,300
900   CONTINUE
      END
      END
```

69	8	8	68	5
0.1E+00	0.1E+00	.001E+00	.001E+00	.001E+00
4300.0E+00	0.0171E+00	397.0E+00	0.2600E+00	0.260E-06
0.0186E+00	4.36E-05	0.0E+00	0.0E+00	
1.084E+00	1.57079E+00	0.001E+00	0.00040E+00	639.6E+00
25.0E+00	0.05E+00	0.0E+00	0.0E+00	0.0E+00

Solution For Oil D, E/C=0.40
Bearing Wall Temperature=620R

..GRADY RYLANDER ME030043 .001
OIL,E/C=.40
CHECK POINT TEMP

.60079E+03	.60276E+03	.60684E+03	.61264E+03	.61549E+03
.60098E+03	.60333E+03	.61156E+03	.61360E+03	.61631E+03
.60109E+03	.60392E+03	.61416E+03	.61457E+03	.61716E+03
.60116E+03	.60448E+03	.61594E+03	.61609E+03	.61838E+03
.60120E+03	.60497E+03	.61729E+03	.61755E+03	.61956E+03
.60133E+03	.60592E+03	.61839E+03	.61892E+03	.62069E+03
.60141E+03	.60693E+03	.61934E+03	.62021E+03	.62175E+03
.60145E+03	.60778E+03	.62018E+03	.62141E+03	.62276E+03
.60147E+03	.60841E+03	.62094E+03	.62255E+03	.62372E+03
.60147E+03	.60884E+03	.62164E+03	.62361E+03	.62462E+03
.60148E+03	.60927E+03	.62283E+03	.62555E+03	.62628E+03
.60148E+03	.60927E+03	.62283E+03	.62555E+05	.62628E+03

FMU CHANGED

.60147E+03	.60930E+03	.62302E+03	.62621E+03	.62686E+03

T HAS CONVERGED
CHECK POINT PRES
CHECK POINT TEMP

.60156E+03	.60939E+03	.62316E+03	.62599E+03	.62658E+03

FMU CHANGED

.60162E+03	.60946E+03	.62332E+03	.62574E+03	.62625E+03

T HAS CONVERGED
.74384E+00
CHECK POINT TEMP

.60165E+03	.60951E+03	.62349E+03	.62547E+03	.62587E+03

T HAS CONVERGED
CHECK POINT PRES
CHECK POINT TEMP

.60165E+03	.60952E+03	.62363E+03	.62519E+03	.62546E+03

```
FMU CHANGED
.60165E+03    .60951E+03    .62374E+03    .62498E+03    .62507E+03
T HAS CONVERGED
         .15435E-03

    69            8             8           68            5
     7
.10000E+00    .10000E+00    .10000E-02    .10000E-02    .10000E-02
.43000E+04    .17100E-01    .39700E+03    .26000E+00    .26000E-06
.18600E-01    .43600E-04    .00000E+00    .00000E+00
.10840E+01    .15708E+01    .10000E-02    .40000E-03    .63960E+03
.00000E+00    .00000E+00    .00000E+00    .00000E+00    .62198E+03

PRESSURE DISTRIBUTION
  50.000     50.000     50.000     50.000     50.000    50.000
  55.157     54.346     51.708     46.517     36.597    15.000
  60.981     59.527     54.950     46.700     33.741    15.000
  67.861     65.914     59.906     49.567     34.575    15.000
  75.926     73.563     66.338     54.154     36.969    15.000
  85.172     82.411     73.997     59.909     40.186    15.000
  95.555     92.381     82.715     66.557     43.950    15.000
 107.045    103.427     92.404     73.973     48.157    15.000
 119.641    115.539    103.036     82.116     52.773    15.000
 133.374    128.744    114.629     90.994     57.801    15.000
 148.301    143.097    127.228    100.639     63.260    15.000
 164.496    158.667    140.896    111.101     69.181    15.000
 182.040    175.535    155.703    122.438     75.596    15.000
 201.008    193.771    171.715    134.701     82.538    15.000
 221.456    213.431    188.982    147.933     90.032    15.000
 243.399    234.530    207.520    162.149     98.090    15.000
 266.794    257.026    227.297    177.327    106.703    15.000
 291.506    280.794    248.204    193.389    115.830    15.000
 317.284    305.591    270.031    210.178    125.385    15.000
 343.719    331.027    292.439    227.437    135.226    15.000
 370.212    356.526    314.923    244.783    145.139    15.000
 395.937    381.295    336.788    261.681    154.821    15.000
 419.814    404.295    357.118    277.429    163.874    15.000
 440.498    424.232    374.771    291.145    171.794    15.000
 456.400    439.574    388.394    301.779    177.976    15.000
 465.749    448.611    396.471    308.154    181.738    15.000
 466.703    449.569    397.424    309.034    182.363    15.000
 457.541    440.780    389.766    303.252    179.163    15.000
 436.901    420.926    372.312    289.864    171.577    15.000
 404.082    389.323    344.436    268.355    159.283    15.000
 359.353    346.221    306.329    238.838    142.320    15.000
 304.218    293.060    259.240    202.245    121.191    15.000
 241.583    232.633    205.614    160.436     96.938    15.000
 175.755    169.091    149.112    116.224     71.151    15.000
 112.260    107.771     94.481     73.296     45.923    15.000
  57.456     54.855     47.310     36.073     23.766    15.000
  18.003     16.893     13.742      9.660      7.522    15.000
```

.000	.000	.000	.000	.000	15.000
.000	.000	.000	.000	.000	15.000
.000	.000	.000	.000	.000	15.000
.000	.000	.000	.000	.000	15.000
.000	.000	.000	.000	.000	15.000
.000	.000	.000	.000	.000	15.000
.000	.000	.000	.000	.000	15.000
.000	.000	.000	.000	.000	15.000
.000	.000	.000	.000	.000	15.000
.000	.000	.000	.000	.000	15.000
.000	.000	.000	.000	.000	15.000
.000	.000	.000	.000	.000	15.000
.000	.000	.000	.000	.000	15.000
.000	.000	.000	.000	.000	15.000
.000	.000	.000	.000	.000	15.000
.000	.000	.000	.000	.000	15.000
.000	.000	.000	.000	.000	15.000
.000	.000	.000	.000	.000	15.000
.000	.000	.000	.000	.000	15.000
.000	.000	.000	.000	.000	15.000
.000	.000	.000	.000	.000	15.000
.000	.000	.000	.000	.000	15.000
.000	.000	.000	.000	.000	15.000
.000	.000	.000	.000	.000	15.000
.000	.000	.000	.000	.000	15.000
.000	.000	.000	.000	.000	15.000
.000	.000	.000	.000	.000	15.000
.000	.000	.000	.000	.000	15.000
.000	.000	.000	.000	.000	15.000
.000	.000	.000	.000	.000	15.000
.000	.000	.000	.000	.000	15.000
.000	.000	.000	.000	.000	15.000

TEMPERATURE DISTRIBUTION

Z=2

600.000	600.000	600.000	600.000	600.000	600.000
600.745	600.739	600.722	600.692	600.649	600.580
601.651	601.642	601.614	601.568	601.513	601.455
602.717	602.706	602.671	602.617	602.555	602.484
603.920	603.907	603.868	603.808	603.738	603.647
605.228	605.214	605.172	605.106	605.028	604.911
606.611	606.596	606.551	606.481	606.395	606.250
608.043	608.028	607.981	607.908	607.815	607.640
609.507	609.491	609.443	609.367	609.270	609.063
610.988	610.972	610.924	610.847	610.746	610.506
612.475	612.459	612.412	612.336	612.235	611.959
613.961	613.946	613.900	613.825	613.727	613.414
615.436	615.421	615.378	615.307	615.213	614.862
616.890	616.876	616.836	616.770	616.683	616.294

618.310	618.298	618.261	618.202	618.125	617.697
619.680	619.669	619.637	619.587	619.521	619.056
620.982	620.972	620.946	620.905	620.853	620.354
622.194	622.186	622.166	622.136	622.100	621.570
623.295	623.291	623.277	623.259	623.241	622.686
624.270	624.267	624.262	624.256	624.257	623.686
625.105	625.105	625.107	625.115	625.136	624.559
625.796	625.799	625.809	625.831	625.872	625.302
626.348	626.353	626.372	626.408	626.470	625.921
626.773	626.781	626.808	626.859	626.941	626.427
627.090	227.100	627.135	627.199	627.300	626.837
627.317	627.330	627.373	627.373	627.449	627.170
627.476	627.492	627.541	627.629	627.765	627.441
627.585	627.603	627.658	627.757	627.907	627.667
627.661	627.680	627.740	627.847	628.009	627.857
627.716	627.737	627.801	627.913	628.084	628.021
627.764	627.785	627.851	627.968	628.145	628.164
627.815	627.836	627.903	628.020	628.199	628.291
267.877	627.898	627.964	628.080	628.257	628.407
627.961	627.981	628.044	628.155	628.326	628.513
628.074	628.093	628.151	628.253	628.410	628.612
628.226	628.242	628.293	628.380	628.514	628.705
628.423	628.437	628.479	628.548	628.641	628.794
627.025	627.032	627.052	627.086	627.131	627.205
626.223	626.227	626.236	626.251	626.771	626.305
625.870	625.871	625.875	628.882	625.890	625.905
625.753	625.754	625.755	625.758	625.761	625.768
625.742	625.743	625.743	625.744	625.746	625.748
625.774	625.774	625.774	625.775	625.775	625.776
625.820	625.820	625.820	625.820	625.821	625.821
625.870	625.870	625.870	625.870	625.870	625.871
625.920	625.920	625.920	625.920	625.920	625.920
625.967	625.967	625.967	625.967	625.967	625.967
626.012	626.012	626.012	626.012	626.012	626.012
626.054	626.055	626.055	626.055	626.055	626.055
626.095	626.095	626.095	626.095	626.095	626.095
626.133	626.133	626.133	626.133	626.133	626.133
626.169	626.169	626.169	626.169	626.169	626.169
626.203	626.203	626.203	626.203	626.203	626.203
626.236	626.236	626.236	626.236	626.236	626.236
626.267	626.267	626.267	626.267	626.267	626.267
626.297	626.296	626.297	626.297	626.297	626.297
626.326	626.326	626.326	626.326	626.326	626.326
626.354	626.354	626.354	626.354	626.354	626.354
626.381	626.381	626.381	626.381	626.381	626.381
626.408	626.408	626.408	626.408	626.408	626.408
626.434	626.434	626.434	626.434	626.434	626.434
626.460	626.460	626.460	626.460	626.460	626.460
626.486	626.486	626.486	626.486	626.486	626.486
626.511	626.511	626.511	626.511	626.511	626.511
626.537	626.537	626.537	626.537	626.537	626.537

626.563	626.563	626.563	626.563	626.563	626.563
626.589	626.589	626.589	626.589	626.589	626.589
626.616	262.616	626.616	626.616	626.616	626.616
626.631	626.631	626.631	626.631	626.631	626.631

Z=3

600.000	600.000	600.000	600.000	600.000	600.000
600.908	600.903	600.888	600.863	600.826	600.767
602.008	602.000	601.976	601.938	601.890	601.840
603.258	603.248	603.218	603.172	603.117	603.057
604.605	604.593	604.559	604.506	604.444	604.365
606.006	605.994	605.956	605.898	605.827	605.726
607.436	607.423	607.382	607.319	607.240	607.115
608.877	608.863	608.820	608.753	608.667	608.515
610.320	610.306	610.261	610.191	610.100	609.919
611.760	611.745	611.700	611.627	611.533	611.323
613.192	613.177	613.132	613.059	612.963	612.721
614.613	614.599	614.554	614.483	614.388	614.113
616.020	616.005	615.963	615.893	615.801	615.493
617.404	617.390	617.350	617.285	617.198	616.854
618.756	618.743	618.706	618.646	618.567	618.189
620.062	620.051	620.018	619.965	619.895	619.483
621.306	621.297	621.268	621.224	621.166	620.722
622.470	622.462	622.439	622.404	622.360	621.887
623.532	623.526	623.510	623.485	623.456	622.961
624.477	624.473	624.463	624.450	624.438	623.926
625.291	625.290	625.287	625.286	625.292	624.773
625.969	625.970	625.975	625.986	626.011	625.497
626.514	626.518	626.530	626.555	626.598	626.101
626.936	626.942	626.962	627.000	627.063	626.595
627.252	627.260	627.287	627.338	627.419	626.995
627.479	627.490	627.525	627.588	627.686	627.318
627.639	627.652	627.694	627.768	627.882	627.581
627.749	627.764	627.811	627.895	628.024	627.798
627.824	627.841	627.893	627.986	628.126	627.980
627.879	627.897	627.953	628.052	628.202	628.136
627.924	627.943	628.002	628.105	628.262	628.272
627.971	627.990	628.050	628.155	628.315	628.392
628.027	628.046	628.106	628.210	628.370	628.501
628.102	628.121	628.178	628.279	628.434	628.600
628.204	628.221	628.274	628.367	628.511	628.693
628.340	628.355	628.401	628.482	628.605	628.780
628.517	628.530	628.569	628.632	628.720	628.861
626.912	626.918	626.938	626.971	627.015	627.088
626.016	626.019	626.029	626.045	626.065	626.100
625.615	625.616	625.621	625.628	624.637	625.652
625.472	625.473	625.474	625.477	625.481	625.488
625.446	625.446	625.447	625.448	625.450	625.453
625.468	625.468	625.469	625.469	625.470	625.471
625.508	625.508	625.508	625.508	625.509	625.509

625.553	625.553	625.553	625.553	625.553	625.554
625.598	625.598	625.598	625.598	625.598	625.599
625.642	625.642	625.642	625.642	625.642	625.642
625.684	625.684	625.684	625.684	625.684	625.684
625.723	625.723	625.723	625.723	625.723	625.723
625.760	625.760	625.760	625.760	625.760	625.760
625.795	625.795	625.795	625.795	625.795	625.795
625.828	625.828	625.828	625.828	625.828	625.828
625.860	625.860	625.860	625.860	625.860	625.860
625.890	625.890	625.890	625.890	625.890	625.890
625.919	625.919	625.919	625.919	625.919	625.919
625.947	625.947	625.947	625.947	625.947	625.947
625.973	625.973	625.973	625.973	625.973	625.973
625.999	625.999	625.999	625.999	625.999	625.999
626.024	626.024	626.024	626.024	626.024	626.024
626.049	626.049	626.049	626.049	626.049	626.049
626.073	626.073	626.073	626.073	626.073	626.073
626.097	626.097	626.097	626.097	626.097	626.097
626.120	626.120	626.120	626.120	626.120	626.120
626.144	626.144	626.144	626.144	626.144	626.144
626.167	626.167	626.167	626.167	626.167	626.167
626.191	626.191	626.191	626.191	626.191	626.191
626.215	626.215	626.215	626.215	626.215	626.215
626.240	626.240	626.240	626.240	626.240	626.240
626.256	626.256	626.256	626.256	626.256	626.256

Z=4

600.000	600.000	600.000	600.000	600.000	600.000
601.435	601.433	601.424	601.408	601.386	601.350
603.124	603.119	603.105	603.081	603.052	603.021
604.843	604.836	604.817	604.787	604.752	604.713
606.492	606.484	606.462	606.427	606.385	606.332
608.048	608.040	608.104	607.974	607.925	607.856
609.518	609.509	609.481	609.436	609.381	609.294
610.918	610.908	610.878	610.829	610.769	610.662
612.263	612.253	612.221	612.170	612.106	611.979
613.568	613.557	613.524	613.472	613.405	613.256
614.841	614.830	614.797	614.744	614.676	614.503
616.088	616.077	616.045	615.993	615.925	615.728
617.311	617.300	617.269	617.219	617.153	616.931
618.508	618.498	618.469	618.422	618.360	618.111
619.674	619.665	619.639	619.596	619.539	619.264
620.800	620.792	620.768	620.730	620.681	620.380
621.872	621.865	621.845	621.813	621.772	621.446
622.875	622.869	622.853	622.828	622.798	622.450
623.793	623.789	623.777	623.760	623.741	623.374
624.613	624.610	624.603	624.594	624.587	624.206
625.322	625.321	625.320	625.320	625.326	624.937
625.918	625.919	625.922	625.931	625.950	625.562
626.401	626.404	626.412	626.430	626.463	626.084

626.781	626.785	626.799	626.826	626.871	626.512
627.070	627.076	627.095	627.131	627.189	626.859
627.286	627.293	627.317	627.361	627.430	627.140
627.443	627.452	627.480	627.531	627.611	627.369
627.556	627.566	627.599	627.656	627.745	627.557
627.639	627.650	627.686	627.749	627.846	627.716
627.702	627.714	627.752	627.819	627.922	627.852
627.754	627.767	627.806	627.877	627.984	627.970
627.803	627.816	627.857	627.928	628.038	628.075
627.856	627.869	627.909	627.981	628.090	628.169
627.919	627.932	627.971	628.040	628.147	628.255
627.999	628.011	628.047	628.112	628.212	628.335
628.101	628.112	628.144	628.201	628.288	628.410
628.231	628.240	628.268	628.314	628.378	628.480
626.312	626.317	626.333	626.359	626.394	626.451
625.368	625.370	625.378	625.391	625.409	625.438
624.970	624.972	624.975	624.981	624.989	625.003
624.831	624.832	624.833	624.836	624.839	624.845
624.803	624.803	624.804	624.805	624.806	624.809
624.820	624.820	624.820	624.821	624.821	624.822
624.853	624.853	624.853	624.853	624.854	624.854
624.891	624.891	624.891	624.892	624.892	624.892
624.930	624.930	624.930	624.930	624.930	624.930
624.968	624.968	624.968	624.968	624.968	624.968
625.003	625.003	625.003	625.003	625.003	625.003
625.037	625.037	625.037	625.037	625.037	625.037
625.069	625.069	625.069	625.069	625.069	625.069
625.099	625.099	625.099	625.099	625.099	625.099
625.128	625.128	625.128	625.128	625.128	625.128
625.155	625.155	625.155	625.155	625.155	625.155
625.181	625.181	625.181	625.181	625.181	625.181
625.206	625.206	625.206	625.206	625.206	625.206
625.230	625.230	625.230	625.230	625.230	625.230
625.253	625.253	625.253	625.253	625.253	625.253
625.275	625.275	625.275	625.275	625.275	625.275
625.297	625.297	625.297	625.297	625.297	625.297
625.318	625.318	625.318	625.318	625.318	625.318
625.338	625.338	625.338	625.338	625.338	625.338
625.359	625.359	625.359	625.359	625.359	625.359
625.379	625.379	625.379	625.379	625.379	625.379
625.399	625.399	625.399	625.399	625.399	625.399
625.419	625.419	625.419	625.419	625.419	625.419
625.440	625.440	625.440	625.440	625.440	625.440
625.461	625.461	625.461	625.461	625.461	625.461
625.482	625.482	625.482	625.482	625.482	625.482
625.496	625.496	625.496	625.496	625.496	625.496

Z=5

600.000	600.000	600.000	600.000	600.000	600.000
602.815	602.815	602.815	602.816	602.818	602.819

605.508	605.508	605.506	605.504	605.503	605.495
607.733	607.731	607.727	607.720	607.713	607.696
609.553	609.550	609.543	609.532	609.519	609.494
611.086	611.082	611.072	611.057	611.040	611.007
612.424	612.420	612.408	612.390	612.369	612.326
613.631	613.626	613.613	613.593	613.570	613.516
614.748	614.744	614.730	614.709	614.685	614.618
615.805	615.801	615.787	615.766	615.741	615.660
616.820	616.815	616.802	616.782	616.758	616.661
617.802	617.798	617.786	617.768	617.745	617.632
618.759	618.755	618.745	618.729	618.709	618.578
619.691	619.688	619.680	619.666	619.651	619.501
620.597	620.594	620.588	620.578	620.568	620.400
621.469	621.468	621.464	621.459	621.455	621.267
622.300	622.300	622.298	622.298	622.301	622.094
623.078	623.079	623.080	623.085	623.095	622.871
623.793	623.794	623.798	623.807	623.825	623.586
624.432	624.434	624.441	624.456	624.481	624.229
624.989	624.992	625.002	625.021	625.054	624.793
625.462	625.465	624.478	625.501	625.540	625.275
625.850	625.855	625.869	625.897	625.941	625.678
626.163	626.168	626.184	626.214	626.264	626.009
626.408	626.414	626.432	626.464	626.517	626.277
626.599	626.605	626.624	626.658	626.713	626.495
626.747	626.753	626.772	626.807	626.863	626.672
626.861	626.867	626.886	626.922	626.977	626.818
626.951	626.957	626.976	627.011	627.066	626.942
627.023	627.029	627.048	627.082	627.135	627.047
627.084	627.089	627.107	627.140	627.191	627.139
627.136	627.142	627.159	627.190	627.239	627.221
627.185	627.190	627.207	627.237	627.284	627.294
627.233	627.238	627.254	627.283	627.329	627.361
627.285	627.289	627.305	627.333	627.376	627.424
627.343	627.347	627.362	627.388	627.428	627.482
627.411	627.415	627.428	627.451	627.485	627.537
625.210	625.213	625.223	625.240	625.264	625.302
624.315	624.317	624.323	624.332	624.344	624.365
623.974	623.974	623.977	623.982	623.988	623.998
623.859	623.860	623.861	623.863	623.866	623.870
623.837	623.837	623.838	623.838	623.840	623.841
623.850	623.850	623.850	623.851	623.851	623.852
623.877	623.877	623.877	623.877	623.877	623.877
623.907	623.907	623.907	623.907	623.907	623.907
623.937	623.937	623.937	623.937	623.937	623.937
623.967	623.967	623.967	623.967	623.967	623.967
623.995	623.995	623.995	623.995	623.995	623.995
624.021	624.021	624.021	624.021	624.021	624.022
624.047	624.047	624.047	624.047	624.047	624.047
624.070	624.070	624.070	624.070	624.070	624.070
624.093	624.093	624.093	624.093	624.093	624.093
624.114	624.114	624.114	624.114	624.114	624.114

624.135	624.135	624.135	624.135	624.135	624.135
624.154	624.154	624.154	624.154	624.154	624.154
624.173	624.173	624.173	624.173	624.173	624.173
624.191	624.191	624.191	624.191	624.191	624.191
624.208	624.208	624.208	624.208	624.208	624.208
624.225	624.225	624.225	624.225	624.225	624.225
624.242	624.242	624.242	624.242	624.242	624.242
624.258	624.258	624.258	624.258	624.258	624.258
624.274	624.274	624.274	624.274	624.274	624.274
624.290	624.290	624.290	624.290	624.290	624.290
624.306	624.306	624.306	624.306	624.306	624.306
624.322	624.322	624.322	624.322	624.322	624.322
624.338	624.338	624.338	624.338	624.338	624.338
624.354	624.354	624.354	624.354	624.354	624.354
624.371	624.371	624.371	624.371	624.371	624.371
624.382	624.382	624.382	624.382	624.382	624.382
600.000	600.000	600.000	600.000	600.000	600.000
606.047	606.050	606.062	606.084	606.121	606.170
609.634	609.638	609.651	609.672	609.699	609.706
611.838	611.841	611.851	611.866	611.884	611.885
613.369	613.371	613.378	613.389	613.404	613.404
614.549	614.550	614.555	614.564	614.577	614.577
615.527	615.528	615.532	615.540	615.554	615.550
616.382	616.383	616.387	616.396	616.411	616.402
617.158	617.160	617.165	617.175	617.192	617.175
617.883	617.884	617.891	617.903	617.923	617.896
618.572	618.574	618.582	618.596	618.620	618.583
619.236	619.239	619.249	619.266	619.294	619.245
619.881	619.884	619.896	619.917	619.949	619.887
620.508	620.512	620.526	620.550	620.588	620.513
621.116	621.121	621.138	621.166	621.209	621.120
621.703	621.709	621.727	621.760	621.809	621.705
622.263	622.269	622.290	622.326	622.381	622.263
622.788	622.795	622.818	622.858	622.918	622.786
623.272	623.280	623.304	623.347	623.412	623.266
623.708	623.716	623.742	623.787	623.856	623.698
624.092	624.100	624.126	624.173	624.244	624.076
624.421	624.430	624.456	624.502	624.574	624.400
624.698	624.706	624.731	624.777	624.847	624.669
624.927	624.934	624.958	625.001	625.068	624.890
625.113	625.120	625.142	625.181	625.243	625.069
625.266	625.272	625.291	625.325	625.380	625.213
625.391	625.396	625.412	625.440	625.486	625.331
625.495	625.499	625.511	625.533	625.569	625.428
625.582	625.585	625.593	625.608	625.634	625.509
625.655	625.657	625.661	625.669	625.685	625.579
625.716	625.716	625.717	625.720	625.726	625.639
625.766	625.766	625.764	625.762	625.761	625.693
625.806	625.805	625.802	625.797	625.791	625.742
625.837	625.836	625.832	625.826	625.819	625.786
625.859	625.858	625.855	625.851	625.846	625.828

625.874	625.874	625.873	625.871	625.871	625.867
625.885	625.885	625.885	625.888	625.896	625.904
623.674	623.676	623.681	623.691	623.705	623.726
622.974	622.975	622.978	622.984	622.992	623.005
622.729	622.730	622.731	622.734	622.738	622.745
622.651	622.651	622.652	622.653	622.655	622.658
622.636	622.636	622.636	622.367	622.638	622.639
622.645	622.645	622.645	622.646	622.646	622.647
622.663	622.663	622.664	622.664	622.664	622.664
622.684	622.684	622.684	622.684	622.684	622.684
622.705	622.705	622.705	622.705	622.705	622.705
622.725	622.725	622.725	622.725	622.725	622.725
622.744	622.744	622.744	622.744	622.744	622.744
622.762	622.762	622.762	622.763	622.763	622.763
622.780	622.780	622.780	622.780	622.780	622.780
622.796	622.796	622.796	622.796	622.796	622.796
622.811	622.811	622.811	622.811	622.811	622.811
622.826	622.826	622.826	622.826	622.826	622.826
622.840	622.840	622.840	622.840	622.840	622.840
622.853	622.853	622.853	622.853	622.853	622.853
622.866	622.866	622.866	622.866	622.866	622.866
622.878	622.878	622.878	622.878	622.878	622.878
622.890	622.890	622.890	622.890	622.890	622.890
622.902	622.902	622.902	622.902	622.902	622.902
622.913	622.913	622.913	622.913	622.913	622.913
622.924	622.924	622.924	622.924	622.924	622.924
622.935	622.935	622.935	622.935	622.935	622.935
622.946	622.946	622.946	622.946	622.946	622.946
622.957	622.957	622.957	622.957	622.957	622.957
622.968	622.968	622.968	622.968	622.968	622.968
622.979	622.979	622.979	622.979	622.979	622.979
622.990	622.990	622.990	622.990	622.990	622.990
623.001	623.001	623.001	623.001	623.001	623.001
623.008	623.008	623.008	623.008	623.008	623.008

Z=7

600.000	600.000	600.000	600.000	600.000	600.000
612.178	612.184	612.203	612.238	612.298	612.378
615.016	615.022	615.040	615.069	615.105	615.107
616.280	616.285	616.300	616.323	616.349	616.355
617.084	617.089	617.101	617.122	617.147	617.159
617.686	617.690	617.702	617.722	617.750	617.765
618.179	618.183	618.195	618.216	618.247	618.261
618.606	618.610	618.624	618.647	618.681	618.692
618.993	618.997	619.012	619.037	619.075	619.082
619.352	619.358	619.374	619.402	619.444	619.445
619.694	619.700	619.718	619.749	619.796	619.789
620.024	620.030	620.050	620.085	620.136	620.121
620.343	620.351	620.373	620.411	620.467	620.444
620.655	620.663	620.687	620.728	620.789	620.757
620.958	620.966	620.992	621.037	621.103	621.062

621.251	621.260	621.288	621.336	621.407	621.355
621.532	621.541	621.571	621.621	621.696	621.635
621.797	621.807	621.837	621.890	621.969	621.898
622.043	622.053	622.084	622.139	622.219	622.139
622.267	622.277	622.308	622.363	622.445	622.356
622.467	622.477	622.508	622.562	622.643	622.546
622.641	622.651	622.680	622.733	622.811	622.708
622.792	622.801	622.828	622.877	622.951	622.843
622.920	622.928	622.953	622.997	623.064	622.953
623.029	623.036	623.057	623.095	623.154	623.041
623.122	623.128	623.145	623.176	623.224	623.112
623.203	623.207	623.219	623.242	623.279	623.169
623.274	623.276	623.283	623.297	623.321	623.216
623.335	623.336	623.338	623.343	623.353	623.254
623.388	623.387	623.385	623.382	623.379	623.287
623.433	623.430	623.424	623.413	623.399	623.315
623.467	623.464	623.454	623.438	623.415	623.340
623.492	623.488	623.476	623.456	623.429	623.363
623.505	623.501	623.489	623.468	623.439	623.384
623.506	623.502	623.492	623.474	623.447	623.404
623.495	623.492	623.484	623.471	623.453	623.424
623.474	623.472	623.467	623.460	623.455	623.442
621.872	621.873	621.876	621.880	621.887	621.897
621.495	621.496	621.498	621.501	621.505	621.512
621.368	621.368	621.369	621.370	621.372	621.376
621.326	621.326	621.327	621.328	621.328	621.330
621.318	621.318	621.318	621.319	621.319	621.320
621.323	621.323	621.323	621.323	621.323	621.323
621.331	621.331	621.331	621.332	621.332	621.332
621.342	621.342	621.342	621.342	621.342	621.342
621.352	621.352	621.352	621.352	621.352	621.352
621.362	621.362	621.362	621.362	621.362	621.362
621.372	621.372	621.372	621.372	621.372	621.372
621.381	621.381	621.381	621.381	621.381	621.381
621.389	621.389	621.389	621.389	621.389	621.389
621.397	621.398	621.398	621.398	621.398	621.398
621.405	621.405	621.405	621.405	621.405	621.405
621.412	621.412	621.412	621.412	621.412	621.412
621.419	621.419	621.419	621.419	621.419	621.419
621.426	621.426	621.426	621.426	621.426	621.426
621.432	621.432	621.432	621.432	621.432	621.432
621.439	621.439	621.439	621.439	621.439	621.439
621.445	621.445	621.445	621.445	621.445	621.445
621.450	621.450	621.450	621.450	621.450	621.450
621.456	621.456	621.456	621.456	621.456	621.456
621.462	621.462	621.462	621.462	621.462	621.462
621.467	621.467	621.467	621.467	621.467	621.467
621.472	621.472	621.472	621.472	621.472	621.472
621.478	621.478	621.478	621.478	621.478	621.478
621.483	621.483	621.483	621.483	621.483	621.483
621.489	621.489	621.489	621.489	621.489	621.489

TEMPERATURE DISTRIBUTION Cont'd.
Z-7

621.494	621.494	621.494	621.494	621.494	621.494
621.500	621.500	621.500	621.500	621.500	621.500
621.504	621.504	621.504	621.504	621.504	621.504

LOAD	TORQUE	SIDE VOL	SWEPT VOL	FLOW VOL
.16091E+03	.42572E+01	.63534E-01	.59550E-01	.12308E+00

SIDE FLOW	SWEPT FLOW	TOT FLOW	VISCOSITY	COEF FRICTI
.18668E-02	.17447E-02	.36115E-02	.27054E-05	.24352E-01

TIME, 13 MINUTES AND 7 SECONDS

TOTAL NUMBER OF PAGES 010

Program for Multiphase
Oil D-MoS_2
T = 600F

```
..GRADY RYLANDER            ME030043          .001
      PROGRAM RYLAND
      CALL LIMIT (30)
 20   DIMENSION FMU(70,8,8),P(70,8),  TEST (70,8,8),
  1    T(70,8,8),PRE(70,8)
      COMMON FMU,P,TEST,T,FINA,PRE
 30   COMMON LL,JJ,MM,L,N,DX,DY,EPS,EPSIL,EPSILN,CV,FK,
  1   CAPU,A,B,ALF, GAM,CSTAR,AN,R,BETA,C,E,RP,MMO,JMO,PHI,
      AK,TAU,PN,HP,CRA,CRB
      READ 10,LL,JJ,MM,L,N
10    FORMAT (5I10)
      READ 12,DX,DY,EPS,EPSIL,EPSILN
12    FORMAT (5E12.5)
      READ 12,CV,FK,CAPU,A,B
      READ 14,ALF,GAM,CSTAR,AN
14    FORMAT (4E12.5)
      READ 12,R,BETA,C,E,RP
      READ 12, TAU,PN,HP,CRA,CRB
      MMO=MM-1
      JMO=JJ-1
      AK = 0.0
      FINA = 0.0
      DO 20 K=1,MM
      DO 20 J=1,JJ
      DO 20 I=1,LL
        T(I,J,K) = 600.0
      P(I,J) = 15.0
      FMU(I,J,K) = EXPF(GAM*P(I,J))*(A/EXPF(ALF*T(I,J,K))+B)
      FINA = FINA + T(I,J,K)
20    CONTINUE
      DO 26 J=2,JMO
```

```
      DO 26 I=1,LL
      P(1,J)=18.0
      P(1,7)=15.0
 26   CONTINUE
 805  DO 806 I=1,LL
      DO 807 J=2,JMO
      DO 808 K=2,MMO
 808  CONTINUE
 807  CONTINUE
 806  CONTINUE
      DO 3009 KK=2,18
      E=(0.00005)*FLOATF(KK)
      ECC=E/C
      CONVERG=1.0
      PHI = ACOSF (E/C)
      CALL PRESSR
      TSUM=0.0
      DO 810 I=1,LL
      DO 811 J=2,JMO
      DO 812 K=2,MMO
      TSUM=TSUM+T(I,J,K)
 812  CONTINUE
 811  CONTINUE
 810  CONTINUE
      CM=CONVERG
      TRY = ABSF(FINA-TSUM)
      TAVG = TSUM/FLOATF(LL*(JMO-1)*(MMO-1))
      CONVERG=TRY/TSUM
      FINA = TSUM
      PRINT 2002,CONVERG
2002  FORMAT (E20.5)
      IF(CONVERG - EPS) 250,250,803
 803  IF (CM-CONVERG)250,250,805
 250  PRINT 10,LL,JJ,MM,L,N,MMO
       PRINT 12,DX,DY,EPS,EPSIL,EPSILN
      PRINT 12,CV,FK,CAPU,A,B
      PRINT 14,ALF,GAM,CSTAR,AN
      PRINT 12,R,BETA,C,E,RP
      PRINT 12,TAU,PN,HP,CRA,TAVG
      PRINT 2001
2001  FORMAT (// 22H PRESSURE DISTRIBUTION)
      DO 263 I=1,LL
      PRINT 18,( P(I,J), J=2,JMO)
 18   FORMAT(6F10.3)
 263  CONTINUE
 103  DO 107 K=2,MMO
 109  CONTINUE
 107  CONTINUE
      QOUT2 = 0.00
      SUMV2 = 0.00
      QOUT1 = 0.00
```

```
      SUMV = 0.00
 602  SUML = 0.00
 603  SUMMU = 0.00
 604  SUMT = 0.00
 601  PI = 3.1415927
 605  DO 690 I=3,LL
 606  JMA = JJ-1
 607  DO 690 J=3,JMA
 608  AI = I-1
 609  X = AK+(AI+0.5)*DX
 610  HK = C+E*COSF(X/R)
 611  PAV=0.25*(P(I-1,J)+P(I,J)+P(I-1,J+1)+P(I,J+1))
      AMU=(FMU(I,J,3)+FMU(I,J,4)+FMU(I,J,5)+FMU(I,J,6)+
        FMU(I,J,7))/5.0
      TAP = (PN*TAU)
      CLN = HK-HP
      IF (CLN) 621,621,613
 613  TAP= 0.0
 621  TAA = ((0.50*HK*(P(I,J)-P(I-1,J)))/DX)+(AMU*CAPU)/HK+TAP
 620  SUML = SUML+PAV*COSF(PI-(X/R+PHI))*DX*DY
 222  SUMT = SUMT+TAA*DX*DY*R
 623  SUMMU = SUMMU+AMU
      IN = J-6
      IF (IN) 637,624,637
 637  GO TO 689
 624  X1 = AK+AI*DX
 625  X2 = AK+(AI+1.0)*DX
 630  HK1 = C+E*COSF(X1/R)
 631  HK2 = C+E*COSF(X2/R)
 632  IF (AN) 635,636,635
 635  RHO = ((P(I,6)+P(I,7))/(CSTAR*2.0))**(1.0/AN)
      GO TO 640
 636  RHO = 0.0307-0.0000132*(T(I,J,3)-520.0)
 640  DVO = 0.0
 641  DVO = -(2.0*P(I,7)-P(I-1,6)-P(I,6))*(HAV**3)*DX/(DY*AMU
        *24.0)
 642  SUMV = SUMV+DVO
 643  DQ = RHO*DVO
 644  QOUT1 = QOUT1+DQ
 645  HMIN = C-E
 646  DV2 = HMIN*FLOATF(N)*CAPU*DY/2.0
 647  QOUT2 = DV2*RHO
 648  SUMV2 = DV2
 649  QOUT3 = QOUT1+QOUT2
 650  SUMV3 = SUMV+SUMV2
 651  AMUAV =SUMMU/(FLOATF((LL-2)*(JMA-2)))
 652  COF = SUMT/(R*SUML)
      SFN=(AMUAV/SUML)*(CAPU/(2.0*3.1416*R))*R*(R/C)**2
 689  CONTINUE
 690  CONTINUE
```

```
      PRINT 3005
3005  FORMAT (/ 57H LOAD   TORQUE   SIDE VOL   SWEPT   VOL
    1   FLOW VOL)
      PRINT 12,SUML,SUMT,SUMV,SUMV2,SUMV3
      PRINT 3006
3006  FORMAT (/ 61H SIDE FLOW SWEPT FLOW  TOT FLOW  VISCOSITY
    1   COE  F FRICTION )
      PRINT 12,QOUT1,QOUT2,QOUT3,AMUAV,COF
      PRINT 12,SFN,ECC,T(1,2,3),T(2,2MM),P(1,2)
3009  CONTINUE
      END
      SUBROUTINE PRESSUR
   20 DIMENSION FMU(70,8,8), P(70,8),  TEST(70,8,8),
    1 T(70,8,8),PRE(70,8)
      COMMON FMU,P,TEST,T,FINA,PRE
   30 COMMON LL,JJ,MM,L,N,DX,DY,EPS,EPSIL,EPSILN,CV,FK,
    1 CAPU,A,B,ALF, GAM,CSTAR,AN,R,BETA,C,E,RP,MMO,JMO,PHI,
      AK,TAU,PN,HP,CRA,CRB
      PRINT 998
 998  FORMAT(18H CHECK POINT PRES )
 202  M1 = L+1
      N1 = N+1
      M2 = L+2
      N2 = N+2
      DX2 = DX*DX
      DY2 = DY*DY
 300  DIFS = 0.0
      SUMP = 0.0
      DO 233 M=2,N1
      DO 232 K=2,M1
      AI = K-1
      X = AK + AI*DX
      HK = C + E*COSF(X/R)
      HX = -(E/R)* SINF(X/R)
      TAB = 2.0/DX2 + 2.0/DY2
      AMU=(FMU(K,M,3)+FMU(K,M,4)+FMU(K,M,5)+FMU(K,M,6)+
        FMU(K,M,7))/5.0
      G1 = (P(K+1,M) + P(K-1,M))/DX2
      G2 = (P(K,M+1) + P(K,M-1))/DY2
      PMK = P(K+1,M) - P(K-1,M)
      G3 = (3.0*HX* PMK) / (DX*HK* 2.0)
      G = (G1+G2+G3 - (6.0* AMU* CAPU *HX)/(HK**3))/(2.0*TAB)
      PX = PMK/DX
      PX2 = PX*PX
      PY = (P(K,M+1) - P(K,M-1)) /DY
      PY2 = PY*PY
      IF (AN) 299,299,228
 299  HMK = 0.0
      GO TO 229
 228  HMK = ((3.0*AMU *CAPU *PX)/(HK*HK)-(0.25*PX2)-(0.25*
        PY2))/(TAB*AN)
```

```
229     PMK = G + SQRTF(G*G-HMK)
        IF (PMK) 231,296,296
231     DO 297 K1=K,M2
297     P(K1,M) =0.0
        IF (M-3)233,701,233
701     DO 702 K1=K,M2
702     P(K1,M-2) = P(K1,M)
        GO TO 233
296     DIFS = ABSF (PMK-P(K,M))+DIFS
        SUMP = SUMP + PMK
        P(K,M) = PMK
        IF (M-3) 232,295,232
295     P(K,M-2) = PMK
232     CONTINUE
        P(K,M) = PMK
233     CONTINUE
        CONV = (DIFS/SUMP) - EPS
        IF (CONV)900,900,300
900     CONTINUE
        END
        END
```

69	8	8	68	5
0.1E+00	0.1E+00	.001E+00	.001E+00	.001E+00
4300.0E+00	0.0171E+00	397.0E+00	0.2600E+00	0.260E-06
0.0186E+00	4.36E-05	0.0E+00	0.0E+00	
1.084E+00	1.57079E+00	0.001E+00	0.00040E+00	639.6E+00
116.0E+00	0.01E+00	0.700E-03	0.0E+00	0.0E+00

Solution For Multiphase

Oil D - MoS_2

```
..GRADY RYLANDER            ME030043                .001
CHECK POINT PRES
        .77778E+00
CHECK POINT PRES
        .00000E+00
```

69	8	8	68	5
7				
.10000E+00	.10000E+00	.10000E-02	.10000E-02	.10000E-02
.43000E+04	.17100E-01	.17000E+03	.26000E+00	.26000E-06
.18600E-01	.43600E-04	.00000E+00	.00000E+00	
.10840E+01	.15708E+01	.10000E-02	.10000E-03	.63960E+03
.11600E+03	.10000E-01	.70000E-03	.00000E+00	.60000E+03

PRESSURE DISTRIBUTION

18.000	18.000	18.000	18.000	18.000	18.000
20.343	20.201	19.752	18.931	17.546	15.000
22.744	22.476	21.639	20.179	18.000	15.000
25.226	24.844	23.664	21.653	18.769	15.000

27.783	27.294	25.793	23.257	19.661	15.000
30.395	29.804	27.989	24.931	20.608	15.000
33.036	32.344	30.219	26.639	21.576	15.000
35.681	34.888	32.454	28.353	22.549	15.000
38.303	37.410	34.671	30.053	23.514	15.000
40.876	39.885	36.846	31.722	24.462	15.000
43.375	42.289	38.959	33.342	25.381	15.000
45.773	44.596	40.986	34.898	26.264	15.000
48.044	46.781	42.907	36.371	27.101	15.000
50.160	48.817	44.696	37.744	27.880	15.000
52.091	50.674	46.329	38.997	28.592	15.000
53.805	52.323	47.779	40.111	29.225	15.000
55.270	53.732	49.019	41.064	29.768	15.000
56.453	54.870	50.020	41.834	30.207	15.000
57.319	55.704	50.755	42.400	30.530	15.000
57.836	56.201	51.194	42.739	30.725	15.000
57.972	56.332	51.310	42.832	30.780	15.000
57.697	56.068	51.080	42.658	30.684	15.000
56.986	55.384	50.482	42.202	30.427	15.000
55.820	54.263	49.498	41.450	30.003	15.000
54.186	52.691	48.118	40.394	29.406	15.000
52.079	50.664	46.338	39.031	28.634	15.000
49.504	48.188	44.163	37.364	27.689	15.000
46.480	45.279	41.607	35.404	26.577	15.000
43.034	41.964	38.693	33.168	25.308	15.000
39.209	38.285	35.458	30.685	23.897	15.000
35.061	34.294	31.948	27.990	22.365	15.000
30.660	30.060	28.223	25.127	20.736	15.000
26.091	25.663	24.353	22.151	19.041	15.000
21.453	21.199	20.421	19.124	17.314	15.000
16.862	16.779	16.522	16.116	15.595	15.000
12.449	12.526	12.763	13.208	13.927	15.000
8.367	8.585	9.265	10.486	12.357	15.000
4.797	5.125	6.160	8.041	10.932	15.000
1.970	2.348	3.593	5.966	9.699	15.000
.202	.516	1.709	4.336	8.691	15.000
.000	.000	.592	3.177	7.919	15.000
.000	.000	.035	2.419	7.359	15.000
.000	.000	.000	1.981	6.969	15.000
.000	.000	.000	1.690	6.687	15.000
.000	.000	.000	1.479	6.478	15.000
.000	.000	.000	1.325	6.325	15.000
.000	.000	.000	1.220	6.220	15.000
.000	.000	.000	1.160	6.160	15.000
.000	.000	.000	1.140	6.140	15.000
.000	.000	.000	1.157	6.157	15.000
.000	.000	.000	1.210	6.210	15.000
.000	.000	.000	1.293	6.293	15.000
.000	.000	.000	1.405	6.405	15.000
.000	.000	.000	1.542	6.542	15.000
.000	.000	.000	1.701	6.701	15.000

.000	.000	.000	1.878	6.878	15.000
.000	.000	.000	2.071	7.071	15.000
.000	.000	.000	2.278	7.278	15.000
.000	.000	.000	2.496	7.496	15.000
.000	.000	.000	2.723	7.723	15.000
.000	.000	.000	2.958	7.958	15.000
.000	.000	.000	3.198	8.198	15.000
.000	.000	.000	3.440	8.440	15.000
.000	.000	.000	3.682	8.681	15.000
.000	.000	.000	3.915	8.910	15.000
.000	.000	.000	4.124	9.101	15.000
.000	.000	.000	4.279	9.169	15.000
.000	.000	.000	4.369	8.840	15.000
.000	.000	.000	4.642	7.113	15.000

LOAD	TORQUE	SIDE VOL	SWEPT VOL	FLOW VOL
.26019E+02	.24604E+01	.00000E+00	.38250E-01	.38250E-01

SIDE FLOW	SWEPT FLOW	TOT FLOW	VISCOSITY	COEF FRICTI
.00000E+00	.11339E-02	.11339E-02	.39511E-05	.86964E-01
.48261E+01	.10000E+00	.60000E+03	.60000E+03	.18000E+02

APPENDIX D

EXPERIMENTAL DATA

Table 2. Experimental Data for SAE 10 Oil in Air Compression

Shaft Speed = 888 rpm

Small Drop Size

Jacket Water Temperature = 160F

R_o	Cylinder Volume, Cubic Inches										n
	27.25	24.31	20.61	17.39	14.37	11.72	9.50	7.85	6.83	6.48	
2.18	23.8	29.2	36.4	46.6	60.0	79.9	108.5	145.0	182.6	203.0	1.42
2.18	24.4	29.7	36.8	46.8	60.5	81.6	110.4	148.4	184.9	203.3	1.42
5.98	22.5	26.9	34.1	44.2	57.5	77.0	113.0	137.0	169.0	183.8	1.46
8.05	22.8	28.4	35.8	46.1	60.8	83.2	112.2	151.2	195.3	213.5	1.46
8.05	21.5	26.9	34.8	44.9	60.0	82.1	113.2	153.0	198.7	225.5	1.50
10.91	22.4	28.0	35.9	46.5	62.4	85.2	118.2	162.0	217.3	247.8	1.53
10.91	22.3	28.0	35.4	46.7	63.3	87.3	121.7	166.2	222.5	254.0	1.62
12.90	21.8	26.5	34.1	45.0	61.8	86.5	121.0	170.1	235.2	270.0	1.67
12.90	19.2	24.2	32.0	42.7	59.0	82.7	116.1	160.9	220.0	255.3	1.70
	Absolute Cylinder Pressure, psia										

Table 3. Data for Clean Oil Friction

Oil -- Type B

$c = 0.0011$ inch

$r = 1.085$ inch

Torque Reading Scale X2

T', °F	$\mu x10^6$	Radial Load, Lb.	Journal Speed, rpm	Torque Reading, Scale 2	S_o	$f\frac{r}{c}$
140	2.75	61	500	14	0.771	14.9
140	2.75	61	1000	29	1.590	29.8
140	2.75	61	1500	45	2.36	46.3
140	2.75	61	2000	64	3.12	65.9
140	2.75	61	2500	80	3.94	81.5
140	2.75	61	3000	90	4.72	91.0
140	2.75	61	3500	101	5.51	10.3
140	2.75	360	500	22	0.134	3.77
140	2.75	360	1000	39	0.267	6.79
140	2.75	360	1500	58	0.402	9.98
140	2.75	360	2000	78	0.535	13.5

Table 4. Data for Oil-MoS_2 Friction

Oil -- Type B

MoS_2 -- Microsize Powder

Torque Reading Scale X2

c = 0.0013 inch

r = 1.085 inch

T', °F	$\mu x10^6$	Radial Load, Lb.	Journal Speed, rpm	Torque Reading, Scale 2	S_o	$f\frac{r}{c}$
139	2.79	360	500	23.1	0.0985	3.430
139	2.79	360	1000	43.4	0.197	6.00
139	2.79	360	1500	65.2	0.296	9.61
139	2.79	360	2000	89.7	0.396	13.2
139	2.79	360	2500	110.8	0.496	16.4
138	2.85	211	2500	104.0	0.837	26.0
138	2.85	211	3000	122.5	1.008	3.08
132	3.28	14	1000	24.2	5.96	92.7
132	3.28	14	500	14.5	2.98	55.2
132	3.28	28	500	8.0	1.45	32.5

Table 5. Data for Oil-Teflon

Oil -- Type B

c = 0.0011 inch

r = 1.085 inch

Torque Reading Scale X2

T', °F	$\mu \times 10^6$	Radial Load, Lb.	Journal Speed, rpm	Torque Reading, Scale 2	S_o	$f\frac{r}{c}$
140	2.75	131	500	30	0.370	13.9
140	2.75	131	1500	77	1.110	37.1
140	2.75	131	2000	111	1.480	52.6
140	2.75	131	3000	142	2.210	67.5
140	2.75	131	3500	165	2.580	78.5
138	2.85	360	500	27	0.138	4.68
138	2.85	360	1500	87	0.435	15.0
138	2.85	360	2000	104	0.558	18.0
138	2.85	360	2500	141	0.695	24.4
138	2.85	360	3000	168	0.835	29.0
204	0.90	61	3500	61.5	1.810	62.7

Table 6. Density of Liquid-Gas Mixtures

System Composition, Weight per cent Gas	80	100	130	160	200
Carbon Dioxide					
1	0.8641	0.8586	0.8503	0.8410	0.8278
2	0.8610	0.8550	0.8457	0.8410	0.8306
4	0.8587	0.8479	0.8343	0.8267	0.8256
Ethane					
1	0.8522	0.8486	0.8418	0.8383	0.8199
2	0.8435	0.8391	0.8320	0.8244	0.8145
4	0.8381	0.8314	0.8241	0.8164	0.8050
Methane					
0.935	0.8500	0.8466	0.8379	0.8201	0.8057
2	0.8506	0.8451	0.8325	0.8058	0.7952

APPENDIX E

CALIBRATION CURVES

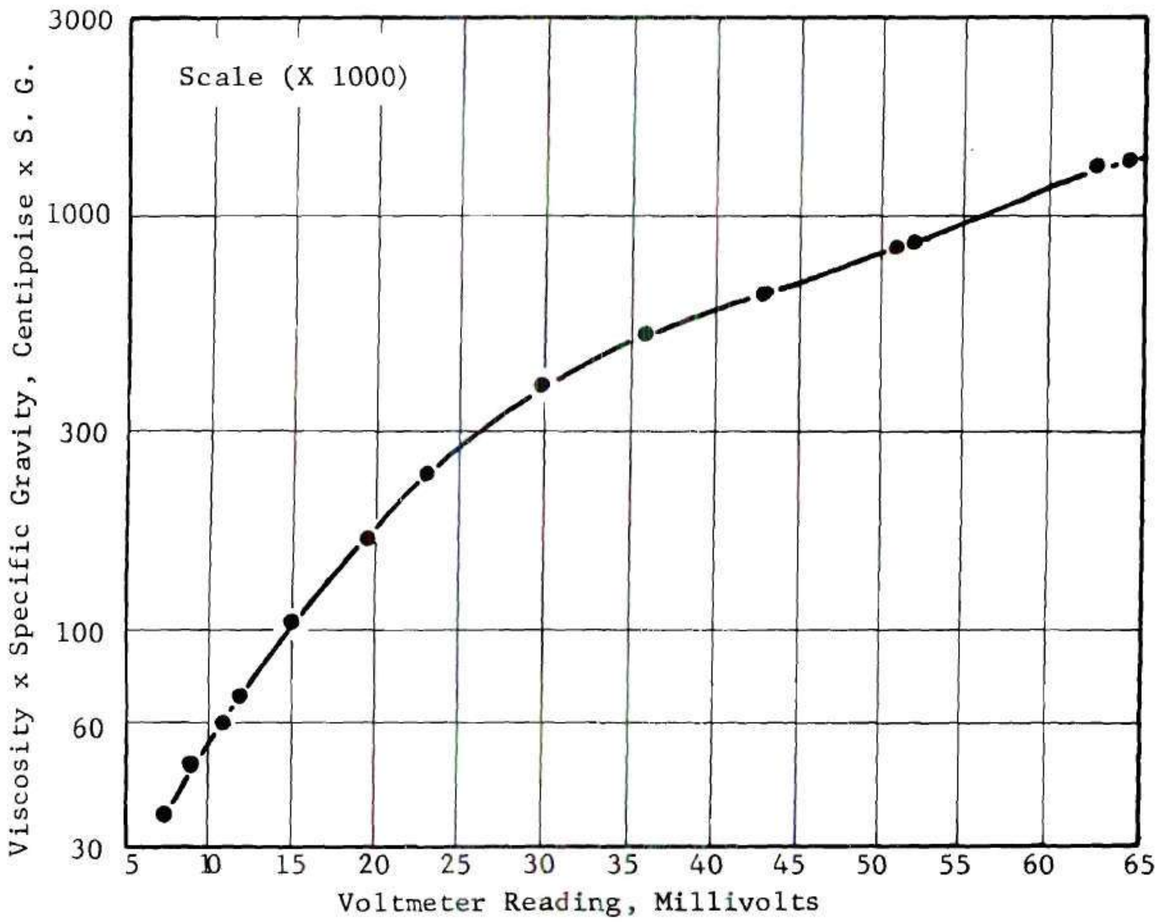

Figure 45. Viscosity Calibration of Bendix Ultraviscoson

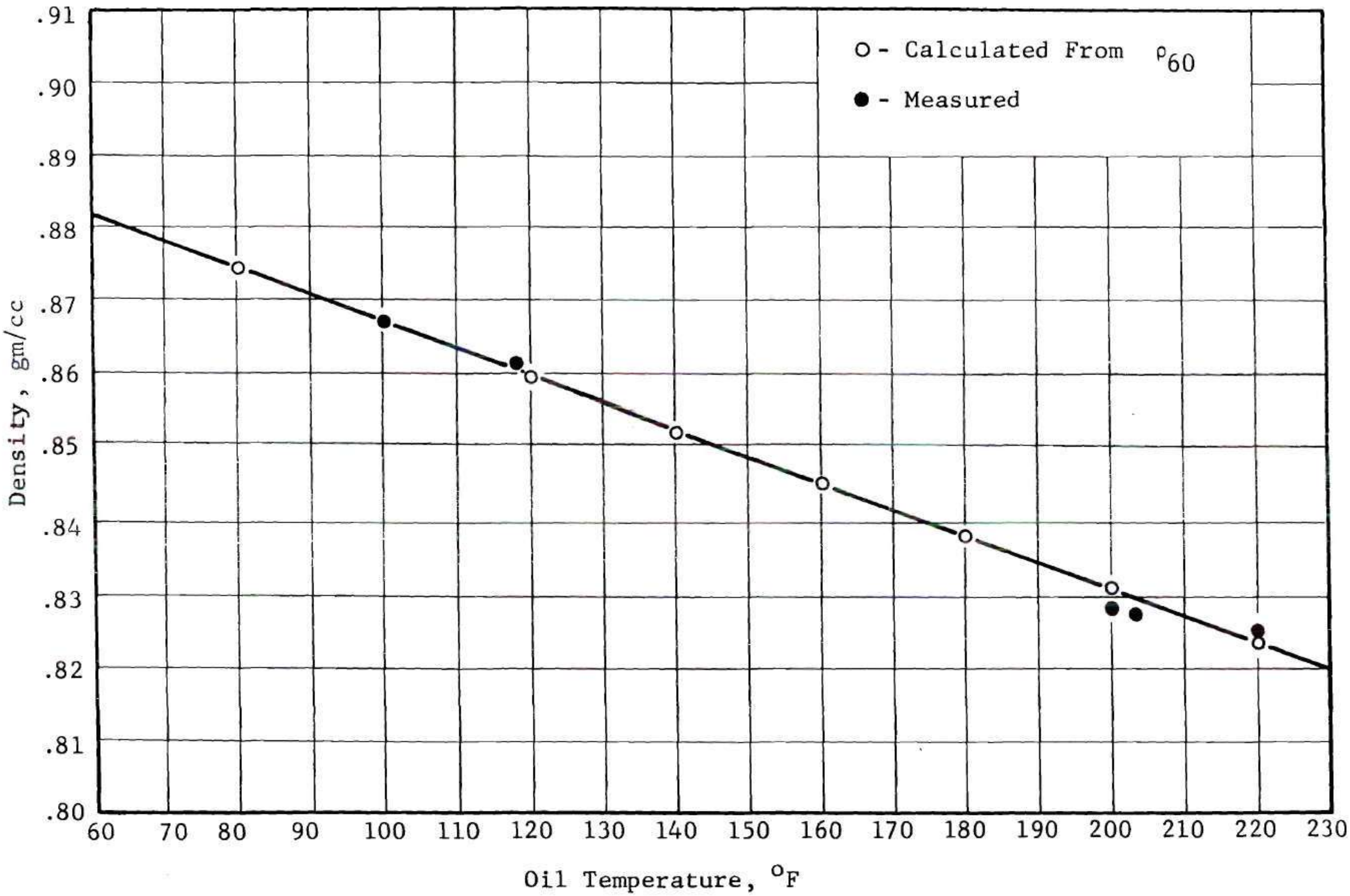

Figure 46. Density of Oil Type A as a Function of Temperature

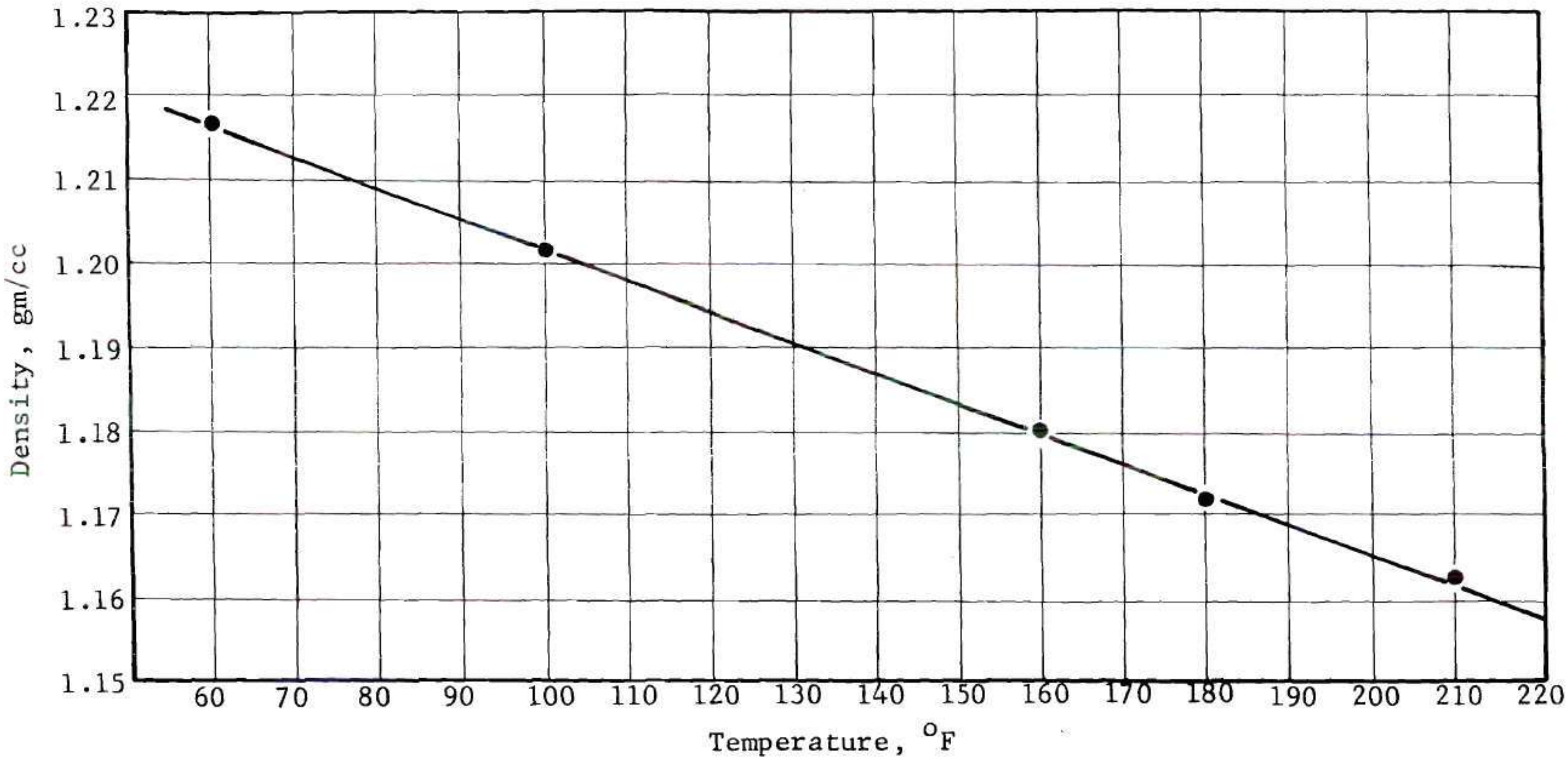

Figure 47. Density of Polyphenyl Ether as a Function of Temperature

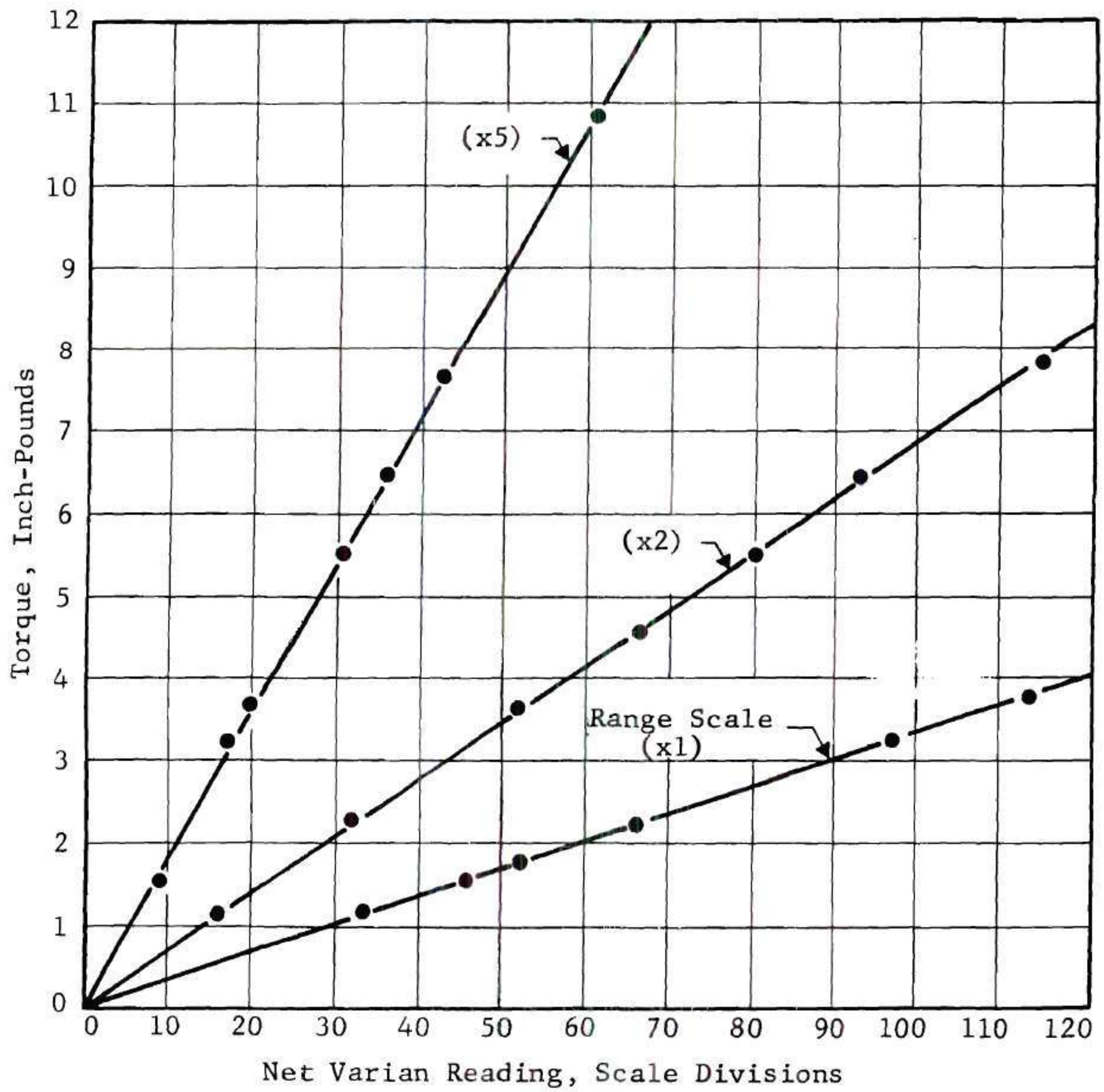

Figure 48. Friction Torque as a Function of Varian Reading

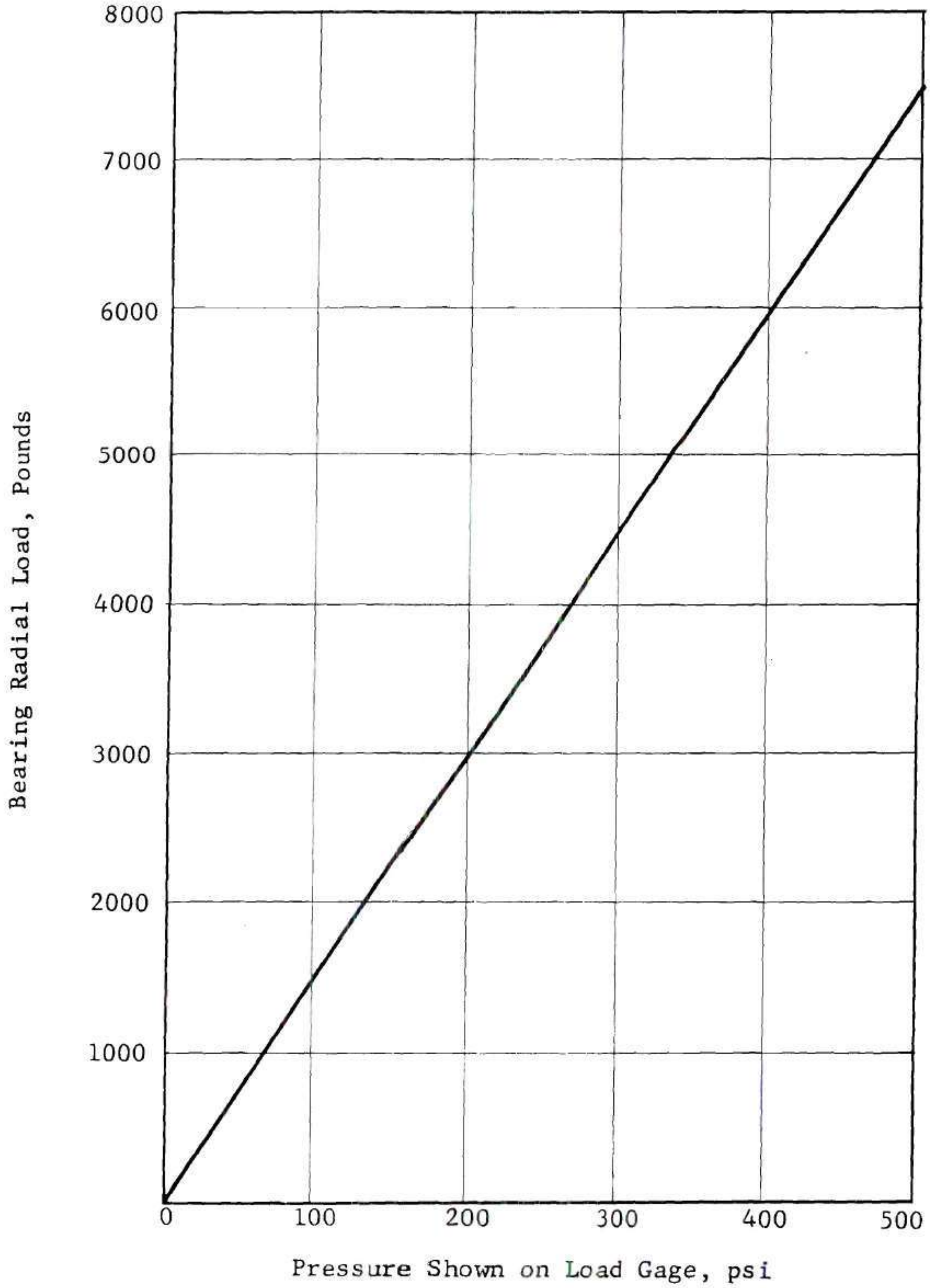

Figure 49. Bearing Radial Load as a Function of Load Pressure

BIBLIOGRAPHY

Literature Cited

1. Ausman, J.S., "The Fluid Dynamic Theory of Gas - Lubricated Bearings," Transactions of the ASME, Vol. 79, August, 1957, pp. 1218-1224.

2. Boyd, J., Lubrication Science and Technology, Vol. 1, New York, Pergamon Press, 1958.

3. Courant, R., Friedricks, K., and Lewy, H., "Über die Partiellen Differenzengleichungen der Mathematirchen Physik," Mathematische Annalen, Vol. 100, 1928.

4. Christropherson, D.G., "A New Mathematical Method for the Solution of Film Lubrication Problems," Proceedings of the Institute of Mechanical Engineers, 146, 1941, pp. 126-135.

5. Cope, W.T., "The Hydrodynamical Theory of Film Lubrication," Proceedings of the Royal Society of London, 197, Ser. A, June, 1949, pp. 201-217.

6. Gross, W.A., "A Gas Film Lubrication Study, Part I; Some Theoretical Analyses of Slider Bearings," IBM Journal Research and Development, 3, No. 3, July, 1959, pp. 237-255.

7. Li, K.Y., Performance of Solid-Film Lubricants in Boundary Lubricated Journal Bearings. Thesis, The University of Texas, Austin, Texas, January, 1960.

8. Michael, W.A., "A Gas Film Lubrication Study, Part II, Numerical Solutions of the Reynolds Equation for Finite Slider Bearings," IBM Journal Research and Development, Vol. 3, No. 3, July, 1959, pp. 256-259.

9. Milne, A.A., "A Theory of Rheodynamic Lubrication," Kolloid Zeit, Band 139, Heft 1/2, 1954, p. 6.

10. Milne, A.A., "A Theory of Grease Lubrication of a Slider Bearing," Proceedings of the Society of the International Congress of Rheology, 1958.

11. Milne, A.A., "Theory of Rheodynamic, Lubrication for a Maxwell Liquid," Conference on Lubrication and Wear, paper 41, London, 1947.

12. Osterle, F., Charnes, A., and Saibel, F., "Rheodynamic Squeeze Film," Lubrication Engineering, Vol. 12, No. 1, 1958, pp. 33-36.

13. Osterle, F., and Saibel, E., "The Rheostatic Thrust Bearing," ASME Paper No. 55-LUB-6, 1955.

14. Potts, P.S., "Hydrostatic Bearings Minimize Friction in Cradle Dynamometer," Machine Design, Vol. 24, 1950, pp. 180-184.

15. Pinkus, O., and Sternlicht, B., Theory of Hydrodynamic Lubrication, McGraw-Hill Book Co., New York, 1961.

16. Purvis, M.G., Meyer, W.E., and Benton, T.C., "Temperature Distribution in the Journal-Bearing Lubricant Film," Transactions of the ASME, Vol. 79, February, 1957, pp. 343-350.

17. Reynolds, O., "On the Theory of Lubrication and Its Application to Mr. Beauchamp Tower's Experiments, Including an Experimental Determination of the Viscosity of Olive Oil," Transactions of the Royal Society, pt. 1, No. 157, London, 1886.

18. Rylander, H.G., Dickerson, L.R., and Crawford, G.W., "Viscosity, Gas Absorption, and Density of Several Multiphase Lubricants," Transactions of the ASLE, Vol. 4, No. 2, November, 1961.

19. Rylander, H.G. and Li, K.Y., "The Performance of Solid-Film Lubricants Relative to Gas-Solid and Gas-Liquid Lubricants," ASME Paper No. 62-LUBS-13, 1962.

20. Schlichting, H., Boundary Layer Theory, McGraw-Hill Book Company, New York, 1955.

21. Shaw, M.C., and Macks, E.F., Analysis and Lubrication of Bearings, McGraw-Hill Book Company, New York, 1949, p. 332.

22. Silbar, A., and Paslay, P.R., "On the Theory of Grease Lubricated Thrust Bearings," ASME Paper No. 56-LUB-1, 1956.

23. Southwell, R.V., Relaxation Methods in Theoretical Physics, New York, Oxford University Press, 1946.

24. Tower, B., "First Report on Friction Experiments," Proceedings of the Institute of Mechanical Engineers, Vol. 34, No. 632, London, 1883.

Other References

1. Allan, A.J.G., "Plastics as Solid Lubricants and Bearings," Lubrication Engineering, Vol. 14, No. 5, May 1958, pp. 211-215.

2. Allen, D.N., Relaxation Methods, McGraw-Hill Book Company, New York, 1954.

3. Bell, T.G., and Sharp, L.H., "Develops Application of a Practical Viscosity Temperature Coefficient for Oil Products," The Oil and Gas Journal, Vol. 32, August, 1933, p. 12.

4. Berry, L., "Solid Lubricant Coatings," ASME Paper No. 58-AV-20, 1958.

5. Bisson, E.E. and Anderson, W.J., Advanced Bearing Technology, National Aeronautics and Space Administration, Washington, D. C., 1964.

6. Bondi, A., Physical Chemistry of Lubricating Oils, Reinhold Publishing Company, New York, 1951.

7. Bradbury, D., and Kleinschmidt, R.V., "Viscosity and Density of Lubricating Oils from 0 to 150,000 psig and 32 to 425 Deg. F.," Transactions of the ASME, Vol. 73, July, 1951, pp. 667-676.

8. Bureau of Standards, United States, Technical Paper, August 26, 1926, p. 77.

9. Campbell, W.E., "Solid Film Lubrication," Product Engineering, Vol. 9, No. 4, August 1953, pp. 195-200.

10. Charles, A., Osterle, F., and Saibel, E., "On the Energy Equation for Fluid-Film Lubrication," Product of the Royal Society of London, 214 Ser. A., August, 1952, pp. 133-136.

11. Charnes, A., Osterle, F., and Saibel, E., "On the Solution of the Reynolds Equation for Slider-Bearing Lubrication-IV, Effect of Temperature on the Viscosity," Transactions of the ASME, Vol. 75, August, 1953, pp. 1117-1123.

12. Chew, J.N., and Connally, C.A., "A Viscosity Correlation of Gas Saturated Crude Oils," Journal of Petroleum Technology, Technical Section, Vol. 11, Feb. 1959, p. 23.

13. Collins, F.C., "Activation Energy of the Eyring Theory of Liquid Viscosity and Diffusion," Journal of Chemistry and Physics, Vol. 26, February, 1957, p. 398.

14. Comings, E.W., Mayland, B.J., and Egly, R.S., "The Voscosity of Gases at High Pressures," University of Illionis Engineering Experiment Station Bulletin, Series No. 354. November 28, 1944.

15. Connally, C.A., "A Viscosity Correlation of Gas Saturated Crude Oils," Journal of Petroleum Technology, Vol. 11, 1959.

16. Cornelissen, J., and Waterman, H.I., "Temperature Dependence of the Viscosity of Liquids, Especially Lubricating Oils," Institute of Petroleum Journal, Vol. 42, February 1956, p. 62.

17. Crump. R.E., "Solid Film Lubrication," Product Engineering, Vol. 27, No. 2, February, 1946, p. 202.

18. Goodrich, S.M., Numerical Solution of a Certain Nonlinear Partial Differential Equation in Three Dimensions, Thesis, The University of Texas, Austin, Texas, January, 1963.

19. Gulinger, W.H., and Saibel, E., "The Effect of Heat Conductance on Slider-Bearing Characteristics," ASME Paper No. 57-IA-90, June, 1957.

20. Hermans, J.J., Flow Properties of Disperse Systems, North-Holland Publishing Co., Amsterdam, 1953.

21. Hersey, M.D., and Hopkins, R.F., "Viscosity of Lubricants Under Pressure (Coordinated Data from Twelve Investigations)," ASME Research Committee on Lubrication, New York, 1954.

22. Herzig, H.L., "Effect of Solid Additives on Fluid Lubricants," Lubrication Engineering, Vol. 15, No. 4, April, 1959.

23. Huschler, A.E., "Molecular Weight of Viscous Hydrocarbon Oils: Correlation of Density with Viscosity," Institute of Petroleum Journals, Vol. 32, March, 1946, p. 133.

24. Horowitz, H.H. and Steidler, F.E., "Calculated Performance of Non-Newtonian Lubricants in Finite Width Journal Bearings," Transactions of the ASLE, Vol. 4, No. 2, November, 1961.

25. Hughes, W.F., and Osterle, J., "On the Adiabatic Couette Flow of a Compressible Fluid," Transactions of the ASME, Vol. 79, August, 1957, pp. 1313-1316.

26. Hughes, W.F., and Osterle, J.F., "Temperature Effects in Journal Bearing Lubrication," Transactions of the ASLE, Vol. 1, No. 1, 1958, pp. 210-212.

27. Johnson, V.R., and Vaughn, W., "Investigation of the Mechanism of MoS_2 Lubrication in Vacuum," Journal of Applied Physics, Vol. 27, No. 10, October, 1956, p. 1173.

28. Kay, J.M., An Introduction to Fluid Mechanics and Heat Transfer, Cambridge University Press, 1957.

29. Kingsbury, A., "Heat Effects in Lubricating Films," Mechanical Engineering, Vol. 55, 1933, pp. 685-688.

30. Kreith, F., Principles of Heat Transfer, International Textbook Company, Scranton, 1958.

31. Kunz, K.S., Numerical Analysis, New York, McGraw-Hill Book Company, Inc., 1957.

32. Langer, R.E., Boundary Problems in Differential Equations, Madison, The University of Wisconsin Press, 1960.

33. Laub, J.H., "Hydrostatic Gas Bearings," Transactions of the ASME Journal Basic Engineering, Vol. 82, June, 1960, pp. 276-286.

34. Laub, J.H., "Externally Pressurized Journal Gas Bearings," ASLE Paper No. 60-LC-15, October, 1960.

35. McConnell, B.D., "Survey of Solid Film Lubricants," Proceedings of the Air Force-Navy-Industry Propulsion Systems Lubricants Conference, 1961, pp. 113-127.

36. Pinkus, O., and Sternlicht, B., "The Maximum Temperature Profile in Journal Bearings," Transactions of the ASME, Vol. 79, February, 1957, pp. 337-341.

37. Raimondi, A.A., "A Numerical Solution for the Gas Lubricated Full Journal Bearing of Finite Length," ASLE Paper No. 60-LC-14, October, 1960.

38. Raimondi, A.A., and Boyd, J., "A Solution for the Finite Journal Bearing and Its Application to Analysis and Design," Transactions of the ASLE, Vol. 1, No. 1, 1958, pp. 159-174.

39. Raimondi, A.A., and Boyd, J., "A Solution for the Finite Journal Bearing and Its Application to Analysis and Design Part II," Transactions of the ASLE, Vol. 1, No. 1, 1958, pp. 175-194.

40. Raimondi, A.A., and Boyd, J., "A Solution for the Finite Journal Bearing and Its Application to Analysis and Design, Part III," Transactions of the ASLE, Vol. 1, No. 1, 1958, pp. 194-209.

41. Reynolds, O., Scientific Papers, Vol. II. 1881-1900, Cambridge University Press, London, 1901.

42. Rounds, F.G., "Influence of Glycol Molecular Configuration on Friction," ASLE Paper No. 62-LC-16, 1962.

43. Rylander, H.G. and Moorman, C.T., "Analytical Study and Numerical Solutions for Journal Bearing Hydrodynamic Lubrication Using Gas, Oil, and Multiphase Lubricants," ASME Paper No. 62-LUBS-12, 1962.

44. Stupp, B.C., "Molybdenum Disulfide and Related Solid Lubricants," Lubrication Engineering, Vol. 14, No. 4, April, 1958, pp. 159-163.

45. Walther, C., "The Viscosity-Temperature Diagram," Petroleum Zeit, Vol. 26, 1930, p. 775.

46. Wildmann, M., "Experiments on Gas Lubricated Journal Bearings," ASME Paper No. 56-LUB-8, 1956.

VITA

Henry Grady Rylander, Jr. was born August 23, 1921, in Frio County near Pearsall, Texas. After graduation from the Pearsall High School, Pearsall, Texas, in May, 1939, he entered the University of San Antonio for two years of pre-engineering studies. In the fall of 1941 he entered The Universtiy of Texas and was graduated with the Degree of Bachelor of Science in Mechanical Engineering in June, 1943.

Following graduation, he worked with the Westinghouse Electric Corporation in their Steam and Aviation Gas Turbine Divisions as a student engineer and design engineer until June, 1947. In the summer of 1947, he joined the teaching staff of The University of Texas as Assistant Professor of Mechanical Engineering and entered the Graduate Division of The University of Texas in the fall of 1947. He received a Master of Science degree in Mechanical Engineering in January, 1952. In September, 1953, he was promoted to the position of Associate Professor of Mechanical Engineering.

He continued his teaching while working as a research and consulting engineer the summers of 1949 and 1950 for the Fargo Engineering Company, the summers of 1954, 1955, and 1957 for The University of Texas Defense Research Laboratory, and the summer of 1946 for the Magnolia Petroleum Co. He has been a consultant for TRACOR, Inc. from 1960 until the present time.

In September, 1961, he entered the Graduate Division at the Georgia Institute of Technology to pursue the Doctor of Philosophy in Mechanical Engineering. He returned to The University of Texas as Associate Professor of Mechanical Engineering in September, 1963.

He was married to Grace Elizabeth Zirkel on September 24, 1943, at Norwood, Pennsylvania, and is the father of two sons, Henry Grady, III, and Gary Ray, and two daughters, Betty Grace, and Martha Jane. They now reside at 3409 Foot-hills Terrace, Austin, Texas.